UNIVERSITY OF LONDON THESIS

Degree phD Year 2006 Name of Author AMZU HAMAGUCHI

MOLECULAR AND CELLULAR PHARMACOLOGY OF NOVEL PYRROLO [2,1-c] [1,4] DIAZEPINE-BASED ANTICANCER AGENTS

ANZU HAMAGUCHI

A thesis submitted for the Degree of Doctor of Philosophy

Department of Oncology
Royal Free and University College Medical School
University College London

2006

ProQuest LLC
789 East Eisenhower Parkway
P.O. Box 1346
Ann Arbor, MI 48106-1346

ABSTRACT

The pyrrolo[2,1-c][1,4]benzodiazepines (PBDs) are a family of naturally occurring antitumour antibiotics which includes anthramycin, DC-81, tomaymycin and sibiromycin. They exert their biological activity through covalent binding to the exocyclic N2 group of guanine in the minor groove of DNA and block transcription in a sequence-specific manner. These PBD monomers span three DNA base pairs and have a preference for binding to purine-G-purine triplets. The PBDs have been used as a scaffold to attach other moieties, leading to novel sequence-selective DNA minor groove alkylating agents. In addition, as part of a rational approach to producing more efficient and selective DNA interstrand crosslinking agents, two PBD monomers have been linked together to form PBD dimers. The research in this thesis is a study of the molecular and cellular pharmacology of several series of novel PBD-containing agents including novel PBD dimers with different linker lengths, PBD-nitrogen mustard conjugates, PBD-polyamide conjugates and C2-aryl PBD monomers. Cytotoxicity in human tumour cell lines, efficiency of DNA interstrand crosslinking in naked linear plasmid DNA, and DNA sequence specificity were assessed. DNA interstrand crosslink formation and repair in cells were also measured. Resulting from this work C2/C2'-*exo*-unsaturated PBD dimers have been characterised to be highly cytotoxic and efficient in producing interstrand crosslinks both in naked DNA and in cells that are not repaired up to 48 hours. Only two of the PBD-nitrogen mustard conjugates showed some interaction with DNA although several members of this group showed significant cytotoxicity. A PBD-tri-pyrrole conjugate was found to bind preferentially to the sequence 5'-AGATTATC. Novel C2-aryl PBD monomers were shown to bind selectively to 5'-purine-G-purine sequences and demonstrated significant cytotoxicity. In addition, a method utilizing fluorescently end-labelled oligonucleotides was developed and validated to screen libraries of PBD-containing molecules synthesised on beads by combinatorial chemistry. This method allowed the isolation and discrimination of beads containing compounds, which have a high affinity for specific DNA sequences.

ACKNOWLEDGEMENTS

First of all... I would like to thank Professor John Hartley for giving me support and guidance throughout the course of my PhD, both academically and psychologically, and for being so patient with me for so many years! This thesis would not have been completed without him.

Also, I would like to thank everyone in the lab and my close friends for their support, especially those who were there for me when I was going through a traumatic phase in my life. Having being around you certainly has kept me sane!

And last but not least, I would like to thank my mother for her unconditional love and constant encouragement (even though it might have bordered on nagging sometimes!). Mother, I finally did it!

I dedicate this thesis to my father in heaven...

TABLE OF CONTENTS

LIST OF FIGURES

LIST OF TABLES

ABBREVIATIONS

5-FU	5-Fluorouracil
ara-C	cytosine arabinoside
A	adenine
ASO(s)	antisense oligonucleotide(s)
ATase	*O6*-alkylguanine-DNA alkyltransferase
BCNU	carmustine
BER	base-excision repair
bp	base pair
C	cytosine
CCNU	lomustine
CPI	cyclopropylindole
dNTPs	deoxynucleoside triphosphates
DSBs	DNA double strand breaks
dTMP	thymidine monophosphate
dUMP	deoxyuridine monophosphate
G	guanine
GSH	glutathione
GST	glutathione-*S*-transferases
Hp	*N*-methyl-3-hydroxypyrrole
ICL(s)	DNA interstrand crosslink(s)
Im	imidazole
MDR	multidrug resistance
methyl-CCNU	semustine
MMR	mismatch repair
NER	nucleotide-excision repair
PBD(s)	pyrrolo [2,1-c][1,4] benzodiazepine(s)
Pgp	P-glycoprotein

Py	pyrrole
RNAi	RNA interference
T	thymine
TCR	transcription-coupled repair
TF	transcription factor
TFO(s)	triple-helix forming oligonucleotide(s)
topo I	topoisomearse I
topo II	topoisomearse II
VM-26	teniposide
VP-16	etoposide

CHAPTER 1

INTRODUCTION

1.1 Cancer and Chemotherapy

1.1.1 Cancer

Cancer is one of the leading causes of death in the UK and approximately one in three people will be diagnosed with cancer during their lifetime. In the UK 65 per cent of cases occur in those over 65 years of age, and this trend suggests that cancer will be of increasing importance throughout the world as the average life expectancy rises. More than 267,000 new cases of cancer were registered in the UK in 1999. There are around 200 different types of cancer but the four major types, lung, breast, prostate and colorectal, account for over half of all cases diagnosed. In the young, other cancers are more common *i.e.*, leukaemia in children and testicular cancer in young men ages 20-39 (Statistics obtained from the Cancer Research UK. http://www.cancerresearchuk.org).

Over the past 25 years, cancer research has seen tremendous development revealing a complex knowledge of cancer being a disease that involves dynamic changes in the genome (Hanahan and Weinberg, 2000). The progress of this knowledge is mainly due to breakthroughs in molecular biology that are focused on the characterisation, cloning and sequencing of various genes that account for the transformation of a normal cell to a malignant cell (Hill and Tannock, 1998).

Cancer is caused mainly by mutations in genes that normally regulate cell multiplication, collectively called oncogenes and tumour suppressor genes. The precise mutations vary depending on the type of cancer, but oncogenes are generally

mutated to have gain-of-function and tumour suppressor genes to have loss-of-function. Oncogenes in normal cells (proto-oncogenes) control some aspect of cell growth and regulate a normal function, and are under the control of regulator genes. Following mutation, the oncogene can lose this control and become over-expressed. This can cause abnormal cell functions such as excessive cell growth leading to unrestrained proliferation, then cancer.

Tumour suppressor genes, such as retinoblastoma (Rb) and p53, control key cellular functions such as DNA repair and apoptosis (Kreidberg and Natoli, 2001). Cells with mutated tumour suppressor genes can multiply in the absence of the growth-promoting factors required for proliferation of normal cells and are often resistant to signals that normally program cell death (apoptosis). The primary tumour cells may invade adjacent tissues and enter the vasculature or lymphatics system. This process is followed by the release of individual cells or small emboli, which can subsequently settle in the capillary beds of distant organs where secondary tumours (metastases) then grow. Metastasis is the most clinically significant behavioural trait of malignant cancer (Hart, 2001) and it is the cause of 90% of deaths from cancer (Hanahan and Weinberg, 2000).

It has been suggested that the majority, or perhaps even all types of cancer, share six common essential alterations in cell physiology that are required for malignant growth: 1) self-sufficiency in growth signals, 2) insensitivity to growth-inhibitory (antigrowth) signals, 3) evasion of apoptosis, 4) limitless replicative potential, 5) sustained angiogenesis, and 6) tissue invasion and metastasis (Hanahan and Weinberg, 2000).

1.1.2 Treatment of cancer

Surgery is the first treatment considered and is one of the main treatments for cancer. It is a local treatment to remove a primary tumour and also to remove a border of healthy tissue surrounding the tumour. After the surgery, chemotherapy and/or radiotherapy may be given to prevent any undetectable micrometastases (adjuvant treatment). Chemotherapy and/or radiotherapy are sometimes given before surgery to help shrink the cancer (neo-adjuvant treatment). However, when cancer has spread, other treatments such as chemotherapy, radiotherapy, immunotherapy or hormone therapy are given.

1.1.3 Principles and limitation of current chemotherapy

Chemotherapy has been used in cancer therapeutics for almost 60 years and is primarily used in three different aspects; 1) as the major curative therapy for several types of malignancies, such as Hodgkin's disease and other types of lymphomas, acute leukaemia in children, and testicular cancer in men; 2) as a palliative treatment for many types of advanced cancers; and 3) as an adjuvant treatment before, during, or after local treatment (surgery and/or radiotherapy) in order to both eradicate undetectable micrometastases and to control the primary tumour. Such treatments usually involve a combination of drugs. Two of the most important factors in successful combination chemotherapy are 1) the ability to combine drugs at close-to-maximum tolerated doses with additive effects against tumours and less than additive toxicities to normal tissues and 2) to include at least one drug to which the tumour is sensitive. Also, the drugs are sometimes combined

because of the synergic interaction among the drugs, either based on a theoretical or experimental expectation (Tannock and Goldenberg, 1998).

Despite advances in chemotherapy, cancer remains a life-threatening problem in our society because current treatments have clear limitations and unmet needs (Gibbs, 2000). One of the limiting factors with current chemotherapy is the poor 'therapeutic index' of many drugs, *i.e.* side-effects of the given dose can outweigh the benefits to the patient. This is because most anti-cancer drugs are antiproliferative in nature and they are not inherently selective to cancer cells (Workman, 2001). For example, myelosuppression is one of the most common complications of cancer chemotherapy, causing bone marrow to slow production of white blood cells, red blood cells and plasma cells leading to patients becoming more sensitive to infection. Another factor limiting the effectiveness of current antitumour agents is the ability of cancer cells to acquire resistance towards the drugs even though a response may have been seen during an initial treatment (Garrett and Workman, 1999; Workman, 2001). The mechanisms of drug resistance will be discussed in section 1.3.

While a small range of cancers can be cured by current chemotherapy, effective cures for the major solid cancers (e.g., lung, colon) appear to be difficult prospects for the near future (Garrett and Workman, 1999).

1.2 Anticancer drugs

1.2.1 Drug discovery and development

The modern process of preclinical anticancer drug discovery and development begins with a lead discovery, which results from serendipitous

observations, systematic screening, or drug design efforts. The process of systematic screening can include *in vivo* empirical screening, *in vitro* cytotoxicity screening and molecular-targeted screening. The latter two can make use of high-throughput screening technologies. Drug design efforts often revolve around chemical diversity created using synthetic combinatorial libraries, structural biology and molecular modelling. From lead discovery, the next step for preclinical drug development is lead optimisation. In this step, substantial chemical modification of the lead structure is undertaken in order to improve pharmaceutical properties, such as metabolic stability or tissue distribution. Following these modifications, extensive pharmacokinetic evaluations are made to determine the correct formulation. Once the formulation is accepted, formal pharmacokinetic and toxicology studies are performed to establish safe starting doses for clinical trials (Shoemaker and Sausville, 2001). The traditional steps for clinical development are; (1) Phase I clinical trial to define the maximum tolerated dose on a particular schedule of administration and to determine the toxic effects of the treatment, (2) Phase II clinical trial to establish efficacy (response rates) on regimen supported by the phase I results in various tumour types, and (3) Phase III clinical trial to optimise efficacy in specific application. This is followed by the filing of a new drug application (Shoemaker and Sausville, 2001).

1.2.2 History of the first anticancer drugs

The first approaches to chemotherapy started in the World War II era where alkylating agents were chosen for the treatment of lymphoma and leukaemia. They were developed from an original observation with sulphur mustard gas used as a

chemical weapon in World War I. This gas was observed to cause delayed myelosuppression and lymphotoxic symptoms in addition to the vesicant actions to the skin, conjuctiva and respiratory tract (Hartley, 2001). The disclosure of the clinical therapeutic activity of nitrogen mustards led to extensive research on alkylating agents and to the approval of several drugs in this class for use in chemotherapy in the late 1940s and early 1950s (Shoemaker and Sausville, 2001). Once insights into the biochemical mechanisms of action of antibacterial drugs such as sulphonamides were obtained, more research was performed using antimetabolites as potential antitumour drugs leading to the approval of methotrexate for clinical use in 1953 (Shoemaker and Sausville, 2001). In addition, the value of natural products as potential sources of new antitumour agents became apparent and plant products vinblastine and vincristine were approved for clinical use in 1961 and 1963, respectively (Shoemaker and Sausville, 2001). The details for these agents are discussed in Section 1.2.4.

1.2.3 Types of anticancer drugs

Anticancer drugs that are currently in clinical use can be divided into different general families according to their biochemical activities or their origins (Table 1.1). These main families are the alkylating agents, antimetabolites, and several types of natural products and their derivatives.

Alkylating agents	Nitrogen mustard (mechlorethamine)
(classical)	Chlorambucil
	Melphalan
	Cyclophosphamide
	Ifosfamide
	Busulfan
	Nitrosoureas : BCNU, CCNU, Methyl CCNU
	Cisplatin
(non-classical)	Carboplatin
	Tetrazines : Dacarbazine, Hexamethylmelamine,
	Temozolomide
Antimetabolites	Methotrexate
	5-Fluorouracil
	Cytosine Arabinoside
	6-Thioguanine
	6-Mercaptopurine
	Gemcitabine
Natural Products and their Derivatives	Anthracyclines: Doxorubicin, Daunorubicin, Epirubicin
	Mitoxantrone
	Mitomycin C
	Actinomycin D
	Bleomycin
	Vinca Alkaloids: Vinblastine, Vincristine, Vindesine, Vinorelbine
	Etoposide (VP-16)
	Camptothecins
	Taxanes: Paclitaxel, Docetaxel

Table 1.1 Classes of commonly used anticancer drugs (Adapted from Boyer andTannock, 1998)

When a new drug shows an anticancer activity, many closely-related analogues are synthesised and their biological activities are tested during the development process. A few alkylating agents that are currently used clinically were synthesised following the initial use of nitrogen mustard (mechlorethamine). Other drugs are heterogenous and include derivatives of naturally occurring species (antibiotics) and synthesised compounds (e.g., cisplatin) (Boyer and Tannock, 1998).

1.2.4 Alkylating agents

Alkylating agents are the oldest class of anticancer drugs and have toxicities that include myelosuppression, alopecia, pulmonary fibrosis, leukaemogenesis, infertility, teratogenesis, renal injury (with BCNU) and cardiac toxicity (cyclophosphamide) (Tew, Colvin and Chabner, 1996).

1.2.4.1 Nitrogen mustards

Nitrogen mustard (mechlorethamine) was the first clinically used anticancer drug. In 1946, Gilman and Philips reported that side effects of the nitrogen mustard, such as nausea, vomiting and myelosuppression, were probably due to toxicity in the specific organs with the high proliferative tissues (epithelia of gastrointestinal tract and bone marrow cells) (Gilman and Philips, 1946). Hence, nitrogen mustards were used to treat leukaemias, lymphomas and Hodgkin's disease, which also have high proliferative rates compared to most normal tissues. This was the beginning of cancer chemotherapy and led to numerous alkylating agents being synthesised and

evaluated in attempts to obtain more effective and selective agents with less side effects (Hartley, 2001; Moore and Erlichman, 1998).

The group of drugs that derives from the original nitrogen mustard (mechlorethamine) includes four of the most commonly used alkylating agents cyclophosphamide, ifosfamide, melphalan, and chlorambucil. The common functional group of these agents is the bis-chloroethyl amino group. Figure 1.1 shows the structures of these agents. The mechanism of action of the nitrogen mustards will be discussed in Section 1.5.2.

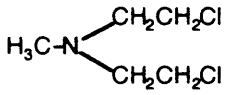

Mechlorethamine

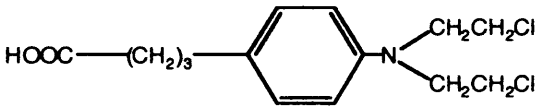

Chlorambucil

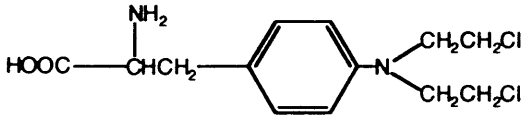

Melphalan

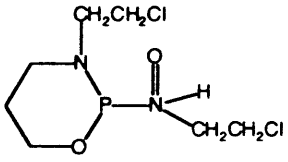

Ifosfamide

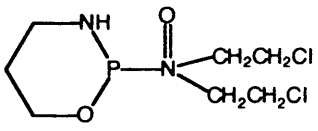

Cyclophosphamide

Figure 1.1 Structures of nitrogen mustards.

Mechlorethamine is still used clinically as part of the MOPP (Mechlorethamine, Vincristine, Procarbazine and Prednisone) treatment schedule for Hodgkin's disease but has been largely replaced by other nitrogen mustards for treatments of other cancers. The chemical reactivity of this drug is very high with a half-life of a few minutes.

Chlorambucil is the phenylbutyric acid derivative of mechlorethamine. It is relatively stable in aqueous solution and enters cells by simple diffusion. Administration can be achieved orally because chlorambucil is a well-absorbed and tolerated agent. It is used mainly against slowly progressive neoplasms such as low-grade lymphomas and chronic lymphocytic leukaemia (Hartley, 2001; Moore and Erlichman, 1998).

Melphalan (L-phenylalanine mustard) is the amino acid phenylalanine derivative of mechlorethamine. It is used for treating multiple myeloma and in some high-dose bone marrow or stem cell transplantation protocols for breast, ovarian and testicular cancers. This agent can be given both orally and intravenously and some patients have responded better to the drug given intravenously perhaps as absorption of this drug is low and highly variable after oral administration. Uptake of melphalan into cells is mediated by an active amino acid transport process and resistance may occur due to changes in this transport system (Hartley, 2001; Moore and Erlichman, 1998).

Cyclophosphamide is one of the most widely used alkylating agents and is part of the treatment protocols for many types of cancer (Tew, Colvin and Chabner, 1996). It is an inert prodrug which requires metabolic activation to become a

reactive nitrogen mustard. The mechanism of activation will be discussed in Section 1.5.2.

Ifosfamide is an analogue of cyclophosphamide with one of the 2-chloroethyl groups moved onto the nitrogen atom of the oxazaphosphorine ring. It is also a prodrug and used for treatment of testicular, sarcoma, and lung cancer. Neurotoxicity may occur with high doses of ifosfamide, a side-effect not seen with cyclophosphamide (Hartley, 2001; Moore and Erlichman, 1998).

1.2.4.2 Nitrosoureas and other classical alkylating agents

The chloroethylnitrosoureas (Figure 1.2) – BCNU (carmustine), CCNU (lomustine) and methyl-CCNU (semustine)- are lipid-soluble drugs that can decompose to form a number of reactive intermediates including the chloroethyldiazohydroxide species which can readily chloroethylate nucleophiles on DNA (Hartley, 2001; Moore and Erlichman, 1998). The mechanism of the breakdown is discussed in Section 1.5.2. BCNU is similar to the nitrogen mustards in that it has two chloroethyl groups, whereas CCNU and methyl-CCNU have a single chloroethyl group making them more lipophilic than BCNU. These drugs have limited clinical application because the concentration required to achieve cytotoxicity in cancer cells is too toxic for normal tissue. This class of drugs often cause prolonged myelosuppression, probably due to their direct effects on bone marrow stem cells.

Busulfan (Figure 1.2) is one of the alkylalkanesulphonate family of alkylating agents (Hartley, 2001; Moore and Erlichman, 1998). It has selective

effects on some blood-forming cells and is used for treating chronic myelogeneous leukaemia.

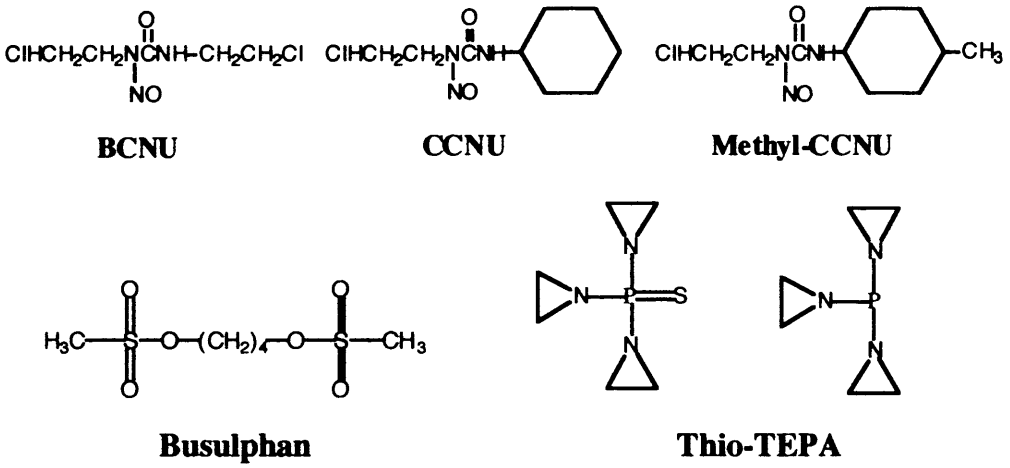

Figure 1.2 Structures of nitrosoureas, busulphan and thio-TEPA.

Thio-TEPA (Figure 1.2) belongs to the aziridine family whose structure resembles intermediates produced by nitrogen mustards, but is less reactive (Tew, Colvin and Chabner, 1996). This family has no unique advantages but thio-TEPA is occasionally used for treating breast cancer.

1.2.4.3 Non-Classical Alkylating Agents and Platinum Agents

This class of agents bind to DNA in a different manner from that of the classical alkylating agents. They include bioreductive prodrugs and platinum based drugs (Figure 1.3).

Dacarbazine (DTIC) was originally synthesised as an antimetabolite to inhibit purine biosynthesis (Friedman, Averbuch and Kurtzberg, 1996). It requires

metabolic activation in order to obtain monofunctional alkylating (methylating) properties. The active metabolite is produced by hepatic cytochrome P450 in the liver. It is mainly used for treatment of soft tissue sarcomas, Hodgkin's disease and melanoma. The drug is administered intravenously and its dose-limiting toxicity is myelosuppression.

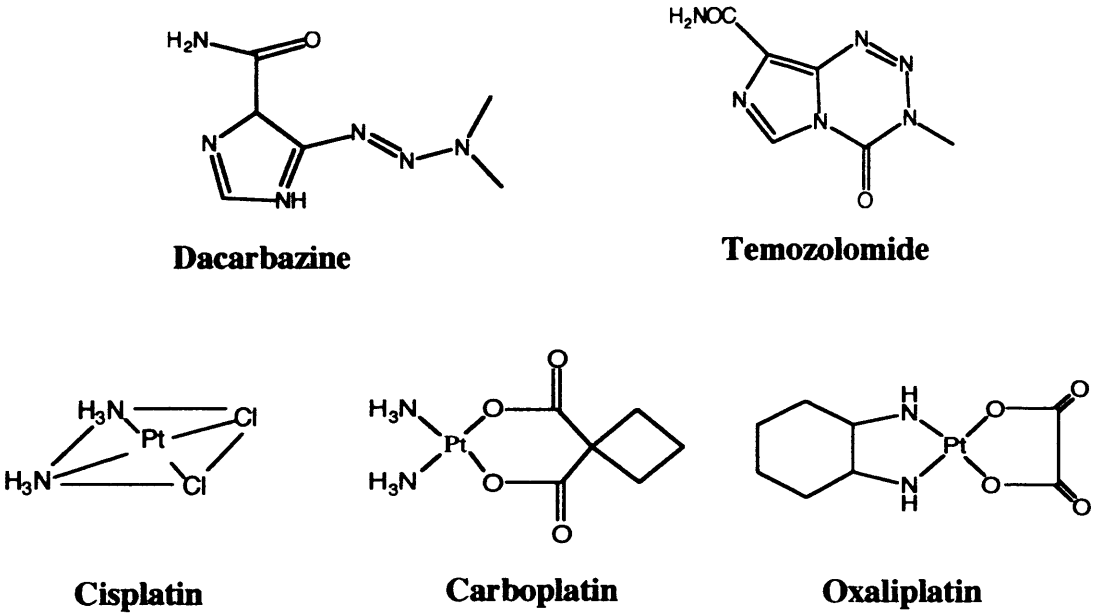

Figure 1.3 Structures of non-classical alkylating agents and platinum compounds.

Temozolomide also acts as a monofunctional alkylating agent. It was developed in the UK through the Cancer Research Campaign and generates the active metabolite of dacarbazine spontaneously so that it overcomes the relatively inefficient N-demethylation step in humans (Newlands *et al.*, 1997). This drug can be administered orally and has shown clinical efficacy in the treatment of a variety

of malignant tumours. It has recently been approved for treating malignant glioma and various trials are being investigated (Chang *et al.* 2003).

Cisplatin (cis-diamminedichloroplatinum II) was first developed from the observation that an electric current delivered via platinum electrodes led to inhibition of bacterial growth (Rosenberg, *et al.*, 1965). Cisplatin is one of the most commonly used anticancer agents with a very wide spectrum of activity (Judson and Kelland, 2001). It is used for testicular cancer and, in combination with other drugs for palliation of a variety of solid tumours. Its major dose-limiting toxicities include severe nausea and vomiting, damage to the kidneys, and loss of hearing and neurotoxicity after prolonged use. Many analogues of cisplatin have been synthesised in an attempt to retain the antitumour activity but decrease the side-effects. Of these only carboplatin and oxaliplatin are widely used clinically. The dose-limiting toxicity of carboplatin is myelosuppression (Judson and Kelland, 2001). The mechanisms of action of cisplatin will be discussed in section 1.5.2.

1.2.5 Antimetabolites

These drugs resemble normal metabolites and can compete as substrates for enzyme activity. They particularly affect the synthesis of DNA required for replication. Unlike the alkylating agents, these drugs do not cause the later problems of carcinogenesis as they interact indirectly with DNA. The structures of some of these drugs are shown in Figure 1.4.

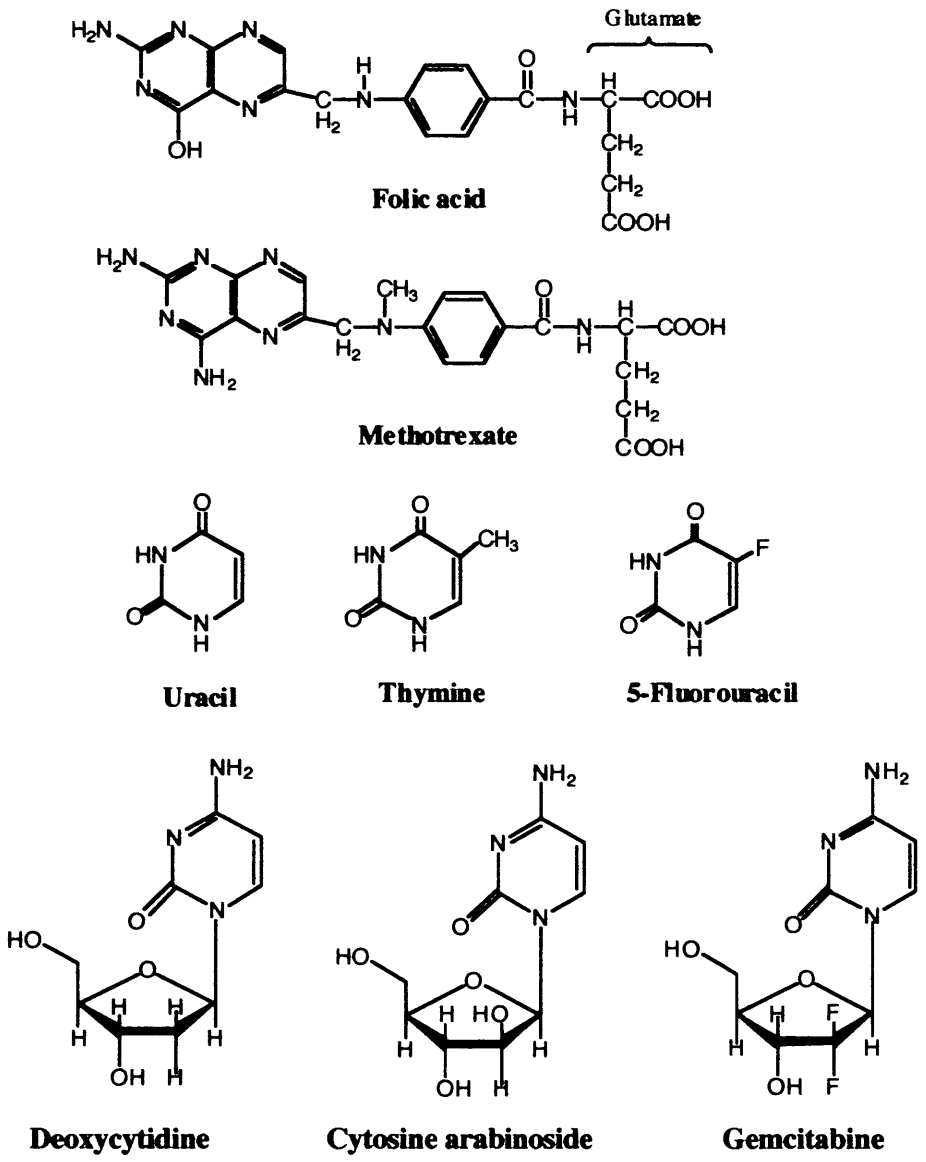

Figure 1.4 Structures of antimetabolites and their corresponding metabolites.

Many of the clinically used agents are analogues of purine (e.g., 6-thioguanine, 2-chlorodeoxyadenosine) or pyrimidine (e.g., 5-fluorouracil, cytosine arabinoside). There are also antifolates (e.g., methotrexate). Agents either inhibit the formation of the normal nucleotides or inhibit cell division processes. Since most antimetabolites are cell cycle-specific and affect cell proliferation, the cytotoxic

effect is primarily seen in high-rate proliferation cells such as bone marrow and gastrointestinal mucosa. With these types of drug, the duration of administration is often more important to inhibit an enzyme than the peak concentration, when given as a single administration (Peters and Jansen, 2001).

Antifolates are not nucleoside analogues, but act by inhibiting the formation of reduced folates that are required for the transfer of methyl groups in the biosynthesis of purines and in the conversion of deoxyuridine monophosphate (dUMP) to thymidine monophosphate (dTMP), a reaction catalysed by thymidylate synthase (TS). Methotrexate is an analogue of the vitamin folic acid and is a competitive substrate inhibitor of the enzyme dihydrofolate reductase (DHFR). This inhibition leads to cell death due to nonavailability of dTMP and / or purines (Chu and Allegra, 1996).

5-Fluorouracil (5-FU) resembles the pyrimidine bases uracil (RNA component) and thymine (DNA component) (Grem, 1996; Longley *et al.*, 2003). It penetrates rapidly into cells where it is metabolised to nucleoside forms in reactions catalysed by enzymes that normally act on uracil and thymine. Phosphorylation then yields the active fluorinated nucleotides 5-FUTP and 5-FdUMP. 5-FUTP inhibits nuclear processing of ribosomal and messenger RNA and may cause other errors of base pairing during transcription of RNA. 5-FdUMP inhibits irreversibly the enzyme thymidylate synthase, leading to depletion of dTMP, which is required for DNA synthesis. 5-Fluorouracil is commonly used for treatment of breast and gastrointestinal cancers.

Cytosine arabinoside (ara-C) resembles the nucleoside deoxycytidine with an arabinose sugar moiety replacing a deoxyribose (Chabner, 1996). Ara-C enters cells

rapidly by a carrier-mediated process usually reserved for deoxycytidine. It is phosphorylated in cells to ara-CTP, which is a competitive inhibitor of DNA polymerase, the crucial enzyme required for DNA synthesis, as it has a similar affinity for this enzyme as the normal substrate, dCTP. When ara-CTP binds DNA polymerase, DNA synthesis is arrested and cells are left in S-phase and subsequently die. Incorporation of ara-C into DNA is also a feature and may contribute to cytotoxic effects, possibly because of defective ligation or incomplete synthesis of DNA fragments.

Gemcitabine (2'2'-difluorodeoxycytidine) is another deoxycytidine analogue with proven activity in different solid malignancies (Sehouli, 2005). Its cytotoxic action is associated with a specific inhibition of DNA synthesis that requires intracellular phosphorylation to its triphosphate derivative dFdCTP (Heinemann *et al.*, 1988; Huang *et al.*, 1995). Other intracellular effects of gemcitabine include inhibition of ribonucleotide reductase, stimulation of deoxycytidine kinase which is the enzyme responsible for its activation, and inhibition of cytidine deaminase which is the primary enzyme responsible for its degradation (Huang *et al.*, 1991). Gemcitabine is primarily used to treat lung (non-small cell), pancreatic, bladder, and breast cancers (http://www.cancerbackup.org.uk/Treatments/Chemotherapy/Individualdrugs/Gemcitabine).

1.2.6 Natural products

These agents (Figure 1.5) have a variety of mechanisms of action. They are either compounds isolated from plants, fungi, or bacteria or derivatives of such compounds.

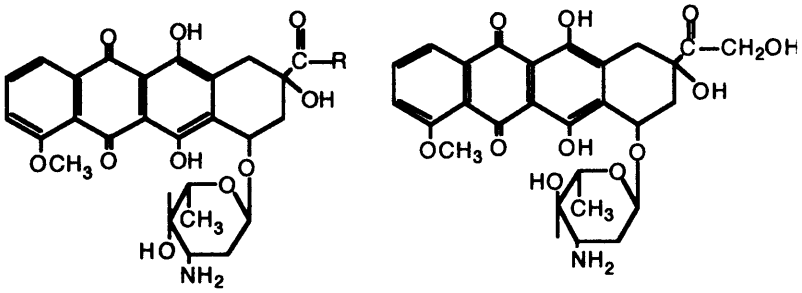

R = CH_2OH, Doxorubicin
= CH_3, Daunorubicin

Epirubicin

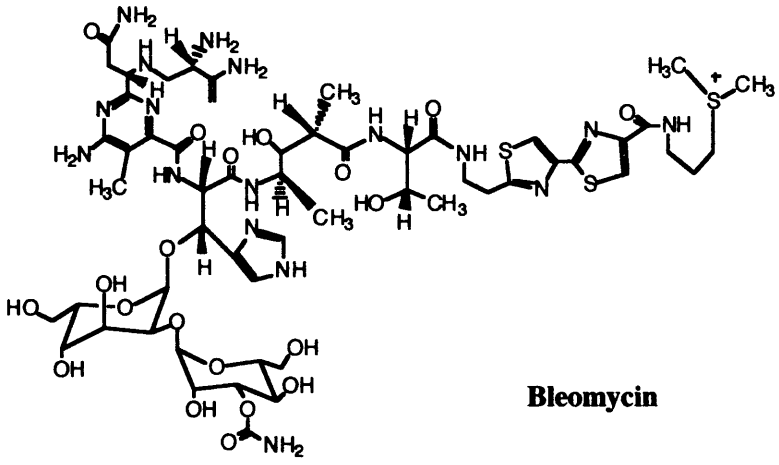

Bleomycin

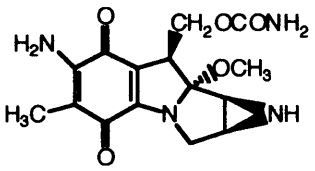

Mitomycin C

Figure 1.5 Structures of antitumour antibiotics

1.2.6.1 Antitumour antibiotics

Doxorubicin (adriamycin) is one of the most active anticancer drugs in current chemotherapy and belongs to the anthracycline family that intercalate into DNA (Doroshow, 1996). Doxorubicin has greater activity against many solid

tumours than its parent drug, daunorubicin, which is a product of a *Streptomyces* species originally isolated from an Italian soil sample in 1958. Daunorubicin has high activity against acute leukemia and is used in many current protocols (Moore and Erlichman, 1998). The dose-limiting toxicity of doxorubicin is cardiotoxicity (Mohamed *et al.*, 2004).

The success of doxorubicin has led to the synthesis and testing of hundreds of analogues, but only two are currently widely used, idarubicin and epirubicin. Idarubicin is an orally absorbed daunorubicin analogue which has a similar effect against acute leukaemia as doxorubicin. Epirubicin differs from doxorubicin in its three-dimensional configuration and has equivalent activity but with possibly less toxicity (Doroshow, 1996).

Bleomycin is a large complex structure consisting of a glycopeptide group and a DNA intercalating component (Lazo and Chabner, 1996). It is used mainly in combination chemotherapy for the treatment of testicular cancer and lymphomas. It has relatively little toxicity to bone marrow but with repeated dosing it may cause serious toxicity to lung tissues.

Mitomycin C is a quinone-containing compound that requires activation by a reductive mechanism to an alkylating metabolite. It is used in the clinical treatment of several malignancies, and its cytotoxicity to tumours is due to its interstrand crosslinking ability. It causes delayed myelosuppression and pulmonary toxicity (Tomasz, 1993). The mechanism of mitomycin C will be discussed in Section 1.6.

1.2.6.2 Plant derivatives

The vinca alkaloid family (Figure 1.6) contain naturally occurring and semi-synthetic compounds derived from the periwinkle plant. The family includes vinblastine, vincristine and vinorelbine. These compounds bind to the tubulin protein and inhibit its polymerisation thus preventing the formation of microtubules. Microtubules are crucial for cellular functions such as the formation of the mitotic spindle responsible for the separation of chromosomes, and the structural and transport functions in axons of nerves. Although they are similar in structures, these drugs have different clinical activities and toxicities (Rowinsky and Donehower, 1996).

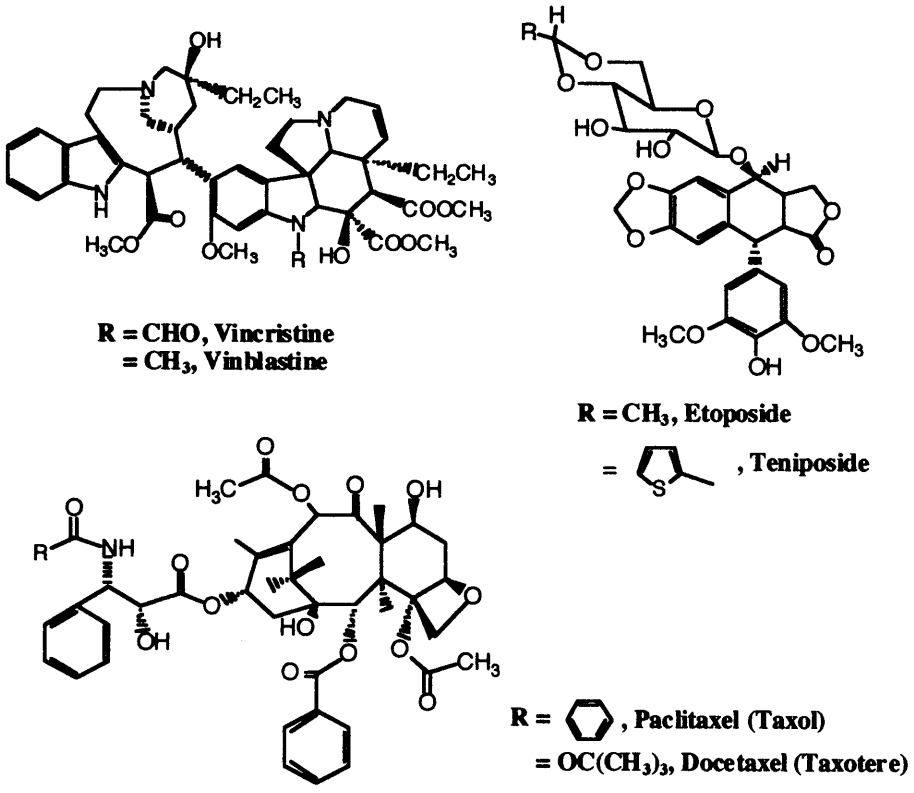

Figure 1.6 Structures of plant derivatives.

The taxanes paclitaxel (Taxol) and docetaxel (Taxotere) are plant alkaloids extracted from the bark and needles of the western yew tree. Taxanes, like vinca alkaloids, are antimicrotubular agents but bind to tubulin at a different site. Unlike the vinca alkaloids, taxanes inhibit microtubular depolymerisation leading to the prevention of normal cell growth by preventing the breakdown of microtubules, and hence inhibiting cell division (Rowinsky and Donehower, 1995; D'Incalci, 2001). They are active in particular against ovarian, breast and lung cancers. The dose-limiting toxicity of taxanes is a noncumulative myelosuppression, mainly neutropenia.

The epipodophyllotoxins VP-16 (etoposide) and VM-26 (teniposide) are semi-synthetic glycoside derivatives of the antimitotic agent podophyllotoxin, itself derived from the mandrake plant. Although podophyllotoxin binds to tubulin and inhibits polymerisation, VP-16 and VM-26 have been found to inhibit a different enzyme, topoisomerase II (Van Mannen *et al*, 1988). VP-16 is widely used while VM-26 has a more limited role in childhood hematological cancer (Moore and Erlichman, 1998). Topoisomearse II (topo II) is an enzyme that is indispensable for its ability to modify DNA tertiary structure without changing the primary structure. The enzyme catalyzes a transient breakage and reunion of double-stranded DNA during transcription and replication, and is also responsible for chromosome dysfunction during mitosis (Cuvier and Hirano, 2003, Valkov and Sullivan, 2003). There are two isozymes of topo II with molecular weights of 170 and 180 kDa, called topo IIα and topo IIβ, respectively (Stacey *et al.*, 2000). Although the biochemical activities of the two proteins are closely related, their cellular distribution and expression characteristics differ greatly. Topo II inhibiting drugs are

used clinically against a wide range of tumours (Hande, 1998) and target both isotypes of topo II, although a broad range of evidence indicates that topo IIα is the primary target (Burden and Osheroff, 1998).

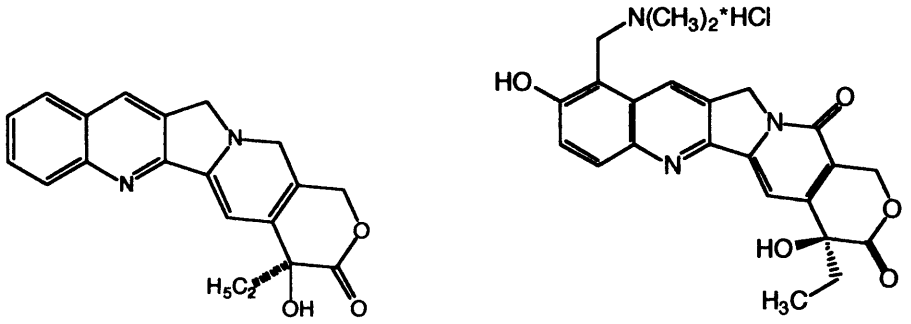

Camptothecin **Topotecan**

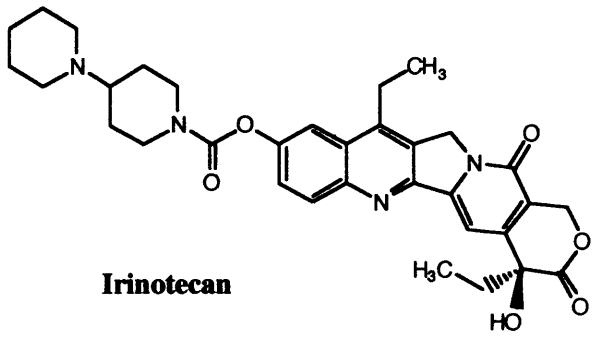

Irinotecan

Figure 1.7 Structures of the camptothecin family.

Camptothecin (Figure 1.7) is an extract of the tree *Campotheca accuminata* that exerts its antitumour activity through inhibition of topoisomerase I (topo I) (Rothenberg, 1997). Topo I is an enzyme that catalyses transient cleavage and resealing on a single strand of DNA during transcription and replication (Wang, 1991). A number of water-soluble camptothecin semisynthetic derivatives have undergone extensive evaluation and have demonstrated significant clinical activity,

and these include topotecan and irinotecan (CPT-11) (Rothenburg, 1997). The camptothecin family (Figure 1.7) acts as an uncompetitive inhibitor and structure-activity relationships have been demonstrated (Staker *et al.*, 2002). Topotecan and irinotecan have well-established antitumour activities against various primary tumours (Wong and Berkenblit, 2004; Timur *et al.*, 2005; Ajani, 2005).

1.3 Drug Resistance

Drug resistance is a central problem that is restricting progress of cancer treatment by chemotherapy. Resistance may be either intrinsic, where the tumour cells do not respond to drugs even in the initial treatment, and acquired, where a tumour responds initially but becomes resistant during / after the treatment (Jong *et al.*, 2001). There is a wide range of metabolic or structural properties of cells that may lead to drug resistance (Tannock and Goldenberg, 1998), and elucidating the mechanisms of the drug resistance may allow the effectiveness of currently used drugs to be improved until better drugs are developed (Middleton and Margison, 2003).

A summary of the major mechanisms of drug resistance to anticancer drugs that have been shown *in vitro* is shown in Table 1.2. These mechanisms include decreased cellular uptake, decreased drug activation, detoxification (e.g., formation of sulfhydryl-drug conjugates such as glutathione conjugates), and alterations to target enzymes (e.g., topoisomerase II). The relevance of many of these mechanisms in the clinical situation remains to be established.

Mechanism	Drugs
Decreased Uptake	Methotrexate, nitrogen mustard, melphalan, cisplatin
Increased efflux	Anthracyclines, Vinca alkaloids, etoposide, taxanes
Decrease in drug activation	Many antimetabolites
Increase in drug catabolism	Many antimetabolites
Increase/decrease in levels of target enzyme	Methotrexate, topoisomerase inhibitors
Alterations in target enzyme	Methotrexate, other antimetabolites, topoisomerase inhibitors
Inactivation by binding to sulfhydryls (e.g., glutathione)	Alkylating agents, cisplatin, anthracyclines
Increased DNA repair	Alkylating agents, cisplatin, anthracyclines, etoposide
Decreased ability to undergo Apoptosis	Alkylating agents, cisplatin, anthracyclines, etoposide

Table 1.2 General Mechanisms Associated with Resistance to Anticancer Drugs (Adapted from Tannock and Goldenberg, 1998)

Simultaneous resistance to various structurally and functionally unrelated chemotherapeutic drugs is termed multidrug resistance (MDR) (Gottesman *et al.*, 2002). MDR can result from changes that limit accumulation of drugs in cells by reducing uptake, enhancing efflux or affecting membrane lipids such as ceramide (Liu *et al.*, 2001). These changes inhibit apoptosis that is activated by most anticancer drugs, activation of general response mechanisms that detoxify drugs and repair damage to DNA, and alterations in the cell cycle and checkpoints that make cells relatively resistant to the cytotoxic effects of drugs on cancer cells (Synold *et al.*, 2001; Ambudkar *et al.*, 1999; Borst *et al.*, 2000). One of the major mechanisms of MDR has been shown *in vitro* to be due to over-expression of an energy-

dependent drug efflux pump, known as P-glycoprotein (Pgp) or the multidrug transporter (Juliano & Ling, 1976, Kartner *et al.*, 1983; Gerlach *et al.*, 1986; Ueda *et al.*, 1987; Gottesman, 1994). Pgp is a surface-membrane, ATP-dependent transport protein that can increase the efflux of many natural products and derivatives including many drugs from the cell, thus reducing the effective intracellular concentration at the target, and hence, inducing drug resistance. Pgp is the product of the MDR1 gene in the human (Chen *et al.*, 1986), and is expressed in about 50% of human cancers at levels thought to be physiologically significant. Because tissues such as the colon, adrenal cortex, kidney, and liver normally express detectable quantities of Pgp, tumours from these organs often show inherent resistance to a range of anticancer drugs (Goldstein *et al.*, 1989).

1.3.1 Specific resistance mechanisms to alkylating agents and cisplatin

Although the exact resistance mechanisms evoked in response to DNA damaging agents have not yet been fully elucidated, a number of mechanisms of cellular resistance have been observed by various *in vitro* experiments (Jong *et al.*, 2001).

- Decreased drug uptake. This is one of the mechanisms of resistance to many alkylating agents that do not enter cells via passive diffusion and is due to reduced binding affinities of drug transport carriers resulting in decreased net cellular uptake of drugs (Tannock and Goldenberg, 1998; Hartley, 2001). For example, either altered or mutated active transport carriers such as amino acid and choline transporters have been observed in the cells resistant *in vitro* to either melphalan or mechlorethamine, respectively (Moscow, *et al.*, 1993).

- Decreased drug activation. This involves glutathione-mediated detoxification pathways and occurs when glutathione binds to the drug and prevents the formation of drug-DNA adducts. As an example, it is known that elevated glutathione levels correlate with cisplatin resistance (Green *et al.*, 1993). The formation of a glutathione-drug conjugate can occur by direct reaction or is catalysed by specific glutathione-*S*-transferases (GST), a group of detoxifying enzymes (Green *et al.*, 1993). However, overexpression of appropriate glutathione-*S*-transferase does not consistently induce resistance to cisplatin (Jong *et al.*, 2001).
- DNA repair pathways have also been shown to be involved in the development of drug resistance. Such pathways can be characterised by elevated levels of p53 protein, increased DNA nucleotide/base excision repair and decreased DNA mismatch repair. Decreased DNA mismatch repair may also lead to increased tolerance of DNA damage.
- *O6*-alkylguanine-DNA alkyltransferase (or ATase) is the DNA repair protein that plays an important role in a resistance mechanism against agents that alkylate at the *O6* position of guanine, such as nitrosoureas. ATase directly removes drug-DNA adducts and it has been shown that the inactivation of this protein reverses the resistance to many *O6*-alkylating agents. Interestingly, drugs that inactivate ATase are now under-going clinical trials (Middleton and Margison, 2003). The alkylation mechanism of these agents will be discussed in section 1.5.
- Dysregulation of apoptosis. Suppression of drug-induced apoptosis is also a means of acquiring drug resistance. This could be mediated by the

overexpression of Bcl-2 protein, which inhibits apoptosis, and/or inactivating mutations of p53 protein, which is involved in regulation of cell-cycle checkpoints (Reed, 1999). Mutations of these proteins can be found in the gene and may influence the sensitivity of tumour cells to cytotoxic drugs, resulting in drug resistance (Huang *et al.*, 2005).

1.4 DNA as a Target in Cancer Chemotherapy

1.4.1 DNA structure

Ever since its discovery by Watson and Crick over 50 years ago, the three-dimensional structure of DNA has been considered to be one of nature's most magnificent constructions. Its critical role in heredity is responsible for the transfer of genetically determined characteristics from one generation to the next (Green *et al.*, 1993).

DNA stores all the information required to construct the cells and tissues of an organism. It consists of two long helical strands coiled around a common axis to form a double helix. Each strand is composed of four different nucleotides. In protein-coding DNA these nucleotides are encoded to specify the amino acid sequence.

Each strand of a double helix presents a sugar-phosphate backbone on the outside of the helix and projects bases (purines and pyrimidines) into the interior. The adjoining bases in each strand stack on top of one another in parallel planes via phosphodiester bonds (Figure 1.8). Each DNA strand has a chemical orientation of 5' to 3' and the synthesis of DNA proceeds in this direction. Purines (A and G) are larger than pyrimidines (C and T) and in order to maintain the geometry of the

double helix structure, purines must pair with pyrimidines. The two strands are held by a regular base-pairing, with Adenine (A) pairing to Thymine (T) and Guanine (G) pairing to Cytosine (C) and are paired through two and three hydrogen bonds, respectively. As well as the presence of thousands of such hydrogen bonds in a DNA molecule, hydrophobic bonds and van der Waals interactions between stacked adjacent base pairs stabilise the double helix (Lodish *et al.*, 1999).

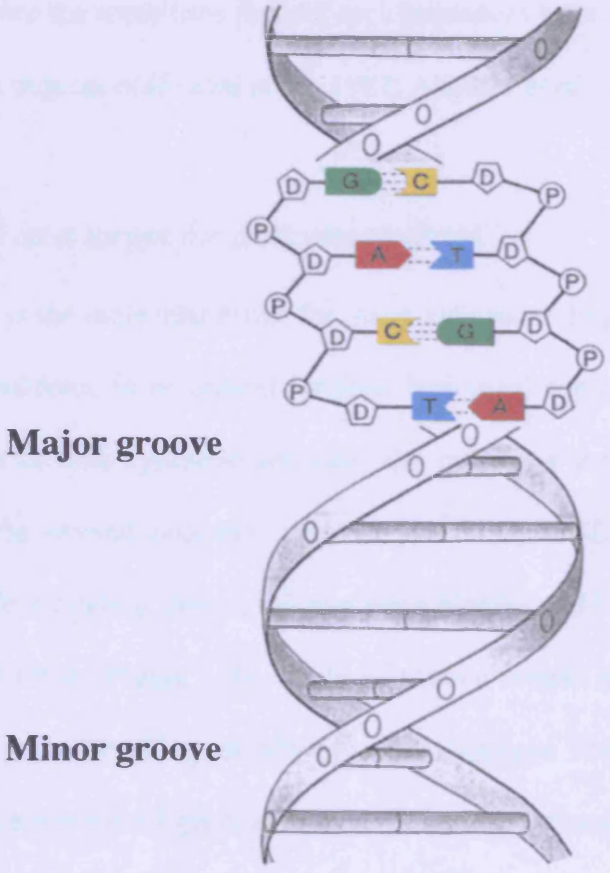

Figure 1.8 Structure of DNA.

DNA can exist in at least four forms but is normally present in its B-form, a right-handed double helix. Other forms include A-DNA, Z-DNA, a triple- and a quadruple- stranded DNA. On the outside of B-form DNA, there are two helical grooves of different widths known as the major groove (≈ 12Å) and the minor groove (≈ 6Å).

The helix makes a complete turn every 3.4 nm, which is about every 10 base pairs with the stacked bases regularly spaced 0.34 nm apart along the helix axis (Lodish, 1999). The base sequence can, however, influence the structure. Indeed it has been known for some time that AT-rich sequences have narrower minor grooves than GC-rich sequences (Fratini *et al.*, 1982; Alexeev *et al.*, 1987).

1.4.2 DNA as a target for anticancer drugs

DNA is the molecular target for many anticancer drugs, and interactions with DNA are considered to be critical for their biological and clinical activities. There are a number of both synthetic and naturally occurring small ligands that interact with DNA via several potential mechanisms of ligand-DNA interaction. These include covalent binding, non-covalent groove binding and intercalation between the base pairs of DNA (Figure 1.9). While alkylation results in binding covalently to DNA, non-covalent binding usually involves hydrogen bonding or van der Waals interactions between the ligand and DNA. Such interactions take place either in the major or minor groove of DNA, with some agents found to have preference for specific sequences. Detailed mechanisms of binding for different types of anticancer drugs will be discussed in the next section.

DNA is full of potential targets for reactive ligands. Although the atoms involved in hydrogen bonding between base pairs are occupied in B-form of DNA, there are other hydrogen bond accepting and donating groups specific to each base, both in the major and minor grooves of the helix. In the major groove, the C6 amino group of adenine or C4 amino group of cytosine can act as hydrogen bond donating groups while the adenine N7, thymine O4, guanine N7 and O6 can act as accepting groups. The thymine methyl is a hydrophobic site. In the minor groove, the adenine N3, thymine O2, guanine N3, and the cytosine O2 can act as hydrogen bond acceptors while the C2 amino group of guanine can act as a donating group. Therefore both grooves have potential hydrogen bond atoms that can be used as targets in the design of sequence specific DNA binding compounds (Turner and Denny, 2000). Selectivity of such binding sites will be discussed in section 1.5.

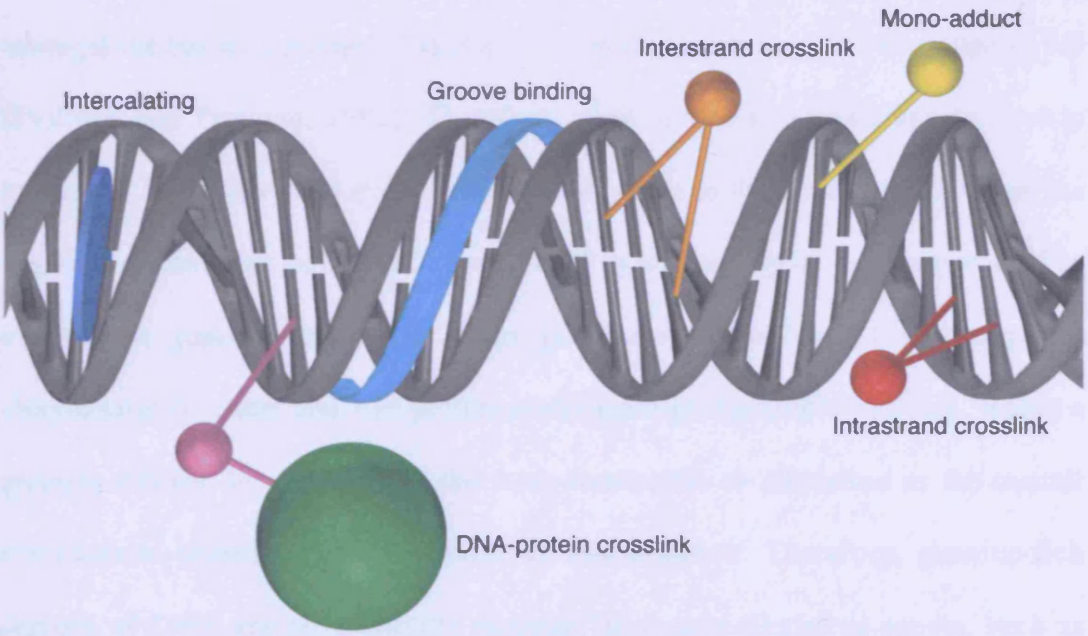

Figure 1.9 Modes of binding to DNA (Adapted from McHugh *et al.*, 2001).

1.5 Mechanism of Action of Alkylating Agents

1.5.1 Base selectivity of alkylating agents

Almost all biological molecules contain electron-rich nucleophilic sites that are potential targets for alkylation. Drug molecules that do not react with water or with thiols (which protect cells from alkylation-induced damage), can damage biological macromolecules such as proteins and nucleic acids. The alkylation targets for DNA-reactive compounds are the oxygen and nitrogen atoms in the DNA bases and in the phosphodiester bonds between the bases.

The most frequent alkylation sites for simple alkylating agents are the N7 and O6 positions of guanine and the N3 position of adenine. Guanine N7 and O6 sites lie in the major groove and adenine N3 is found in the minor groove of DNA. The fact that these sites are most frequently alkylated is explained by the calculation that the regions of guanine N7 and adenine N3 show the most negative potentials amongst the bases. Guanine N7 is also considerably more negative than adenine N3 (Pullman and Pullman, 1981). Therefore, most simple alkylating agents bind to guanine N7. However, not every guanine is alkylated to the same extent because the negative electrostatic potential of guanine N7 is affected by its local sequence. For example, a guanine flanked by other guanine residues has a highly negative electrostatic potential and will preferentially undergo electrophilic attack, whilst a guanine flanked by cytosines is the least susceptible to alkylation as the overall electrostatic potential of the guanine is less negative. Therefore, guanine-rich regions of DNA are preferentially targeted by simple alkylating agents, such as mechlorethamine, that form highly electrophilic carbocation intermediates (Mattes *et al.*, 1988). Figure 1.10 shows the main alkylation sites in the DNA base pairs.

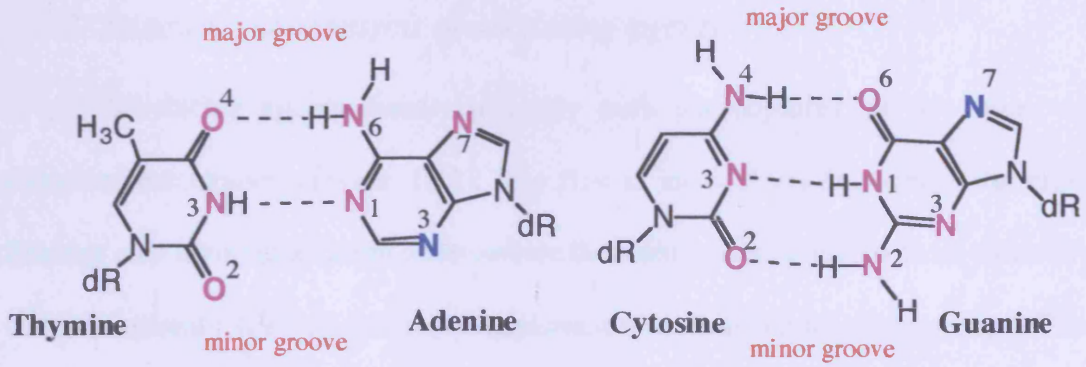

Figure 1.10 Alkylation sites in DNA base pairs. The regions with the most negative potentials are indicated in blue.

There are several types of alkylating agent and they are classified by the way they alkylate DNA. Table 1.3 shows a list of alkylating agents with their most cytotoxic lesions in DNA (Hartley, 2001; Middleton and Margison, 2003).

Class of agent	Examples of drugs	Mechanism
Bischloroethylamines	Cyclophosphamide, melphalan, chlorambucil, ifosfamide	N7-G / N7-G' interstrand crosslinking
Aziridines	ThioTEPA, mitomycin C	N7-G or N2-G alkylation, N2-G / N2-G' crosslinking
2-Chloroethyl Nitrosoureas	BCNU, CCNU	O6-G / N1-C crosslinking
Tetrazines	Dacarbazine, temozolomide	O6-G methylation
Alkyl alkanesulfonates	Busulphan	N7-G / N7-G' crosslinking
Platinum compounds	Cisplatin, carboplatin, oxaliplatin	N7-G / N7-A intrastrand crosslinking N7-G / N7-G' intra- and inter- strand crosslinking

Table 1.3 Classes of alkylating agents and their principal toxic lesion in DNA (Adapted from Middleton and Margison, 2003)

1.5.2 Reaction mechanisms of alkylating agents

Alkylating agents react covalently with nucleophiles by two types of chemical mechanism (Figure 1.11). The first is an S_N1 reaction where the rate-limiting step involves a cation intermediate that then reacts rapidly with an electron-rich nucleophile (*i.e.* an amino, phosphate, sulfhydryl, or hydroxy group). The reaction rate is therefore dependent on the concentration of the alkylating agent. The second reaction is an S_N2 reaction, where an intermediate transition state involves two species so that the attack of a nucleophile on the atom displaces the leaving group of the atom (Loudon, 1995).

Alkylating agents containing a single alkylating group are categorised as monofunctional. Agents such as nitrogen mustards are bifunctional alkylating agents as they contain two alkylating groups and hence have the ability to alkylate twice (Hartley, 2001).

$$RX \longrightarrow R^+ + X^- \xrightarrow{+Y^-} RY + X^-$$

S_N1

$$RX + Y^- \longrightarrow [X\text{--}R\text{---}Y\ ] \longrightarrow X^- + RY$$

S_N2

Figure 1.11 S_N1 and S_N2 reaction mechanisms.

1.5.2.1 Nitrogen mustards

Nitrogen mustards alkylate via a chloroethyl arm by an S_N2 mechanism (Figure 1.12) that involves the formation of a highly reactive aziridinium cation by the loss of a chloride ion. This cation can then attack an electron-rich nucleophile.

The same reaction may be repeated with the other chloroethyl arm of the agent attacking a second nucleophile (Boyer and Tannock, 1998; Hartley, 2001). In place of the methyl group present in mechlorethamine, melphalan and chlorambucil have aromatic substituents that act as electron withdrawing groups. These slow down the loss of chlorine atoms and subsequently the aziridinium cation forms less readily making the agents chemically less reactive. Such agents are therefore more stable and easier to handle and may be administered orally (Hartley, 2001).

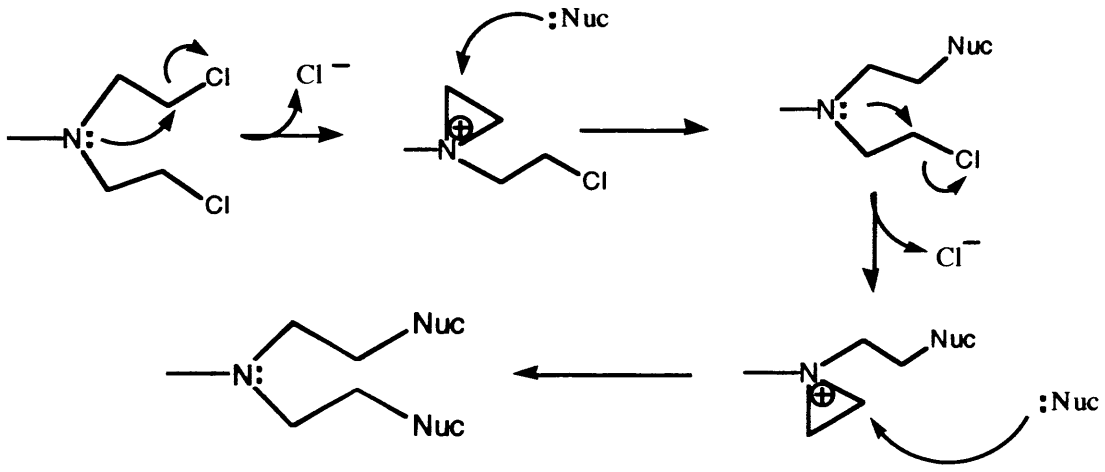

Figure 1.12 Alkylation mechanism of nitrogen mustards.

Additionally, some nitrogen mustards are administered as prodrugs eg. cyclophosphamide (Colvin, 2001). Cyclophosphamide is metabolised by hepatic microsomal enzymes into 4-hydroxycyclophosphamide, which exists in equilibrium with its acyclic isomer aldophosphamide. 4-hydroxycyclophosphamide enters cells and spontaneously decomposes to form phosphoramide mustard and a by-product, acrolein. Alternatively, 4-hydroxycyclophosphamide is detoxified by aldehyde dehydrogenase to form nor-nitrogen mustard. It is now apparent that the route of

activation is not via the originally proposed mechanism but it is in the liver where enzymes cause primary activation rather than within tumours. Figure 1.13 shows the metabolism of cyclophosphamide.

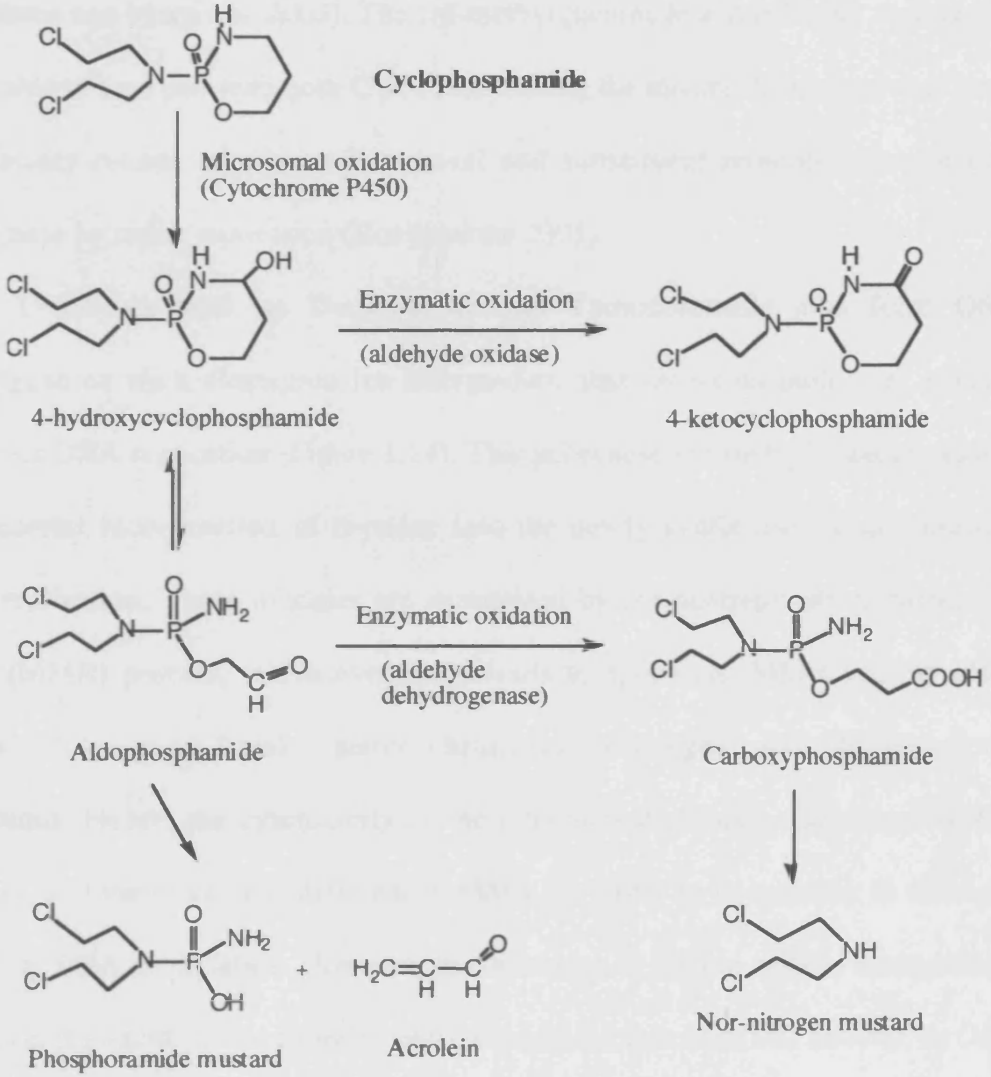

Figure 1.13 Activation mechanism of cyclophosphamide (adapted from Hartley, 2001).

1.5.2.2 O6-alkylating agents

This class of agents have a different mechanism of action from most bifunctional alkylating agents. The cytotoxicity of these agents is related to their ability to alkylate at the O6 position of guanine to produce *O6*-alkylguanine (Middleton and Margison, 2003). The *O6*-methylguanine lesion is highly mutagenic and is able to base pair with both C or T, misleading the mismatch repair system into unnecessary rounds of mismatch removal and subsequent reincoporation of the wrong base by repair replication (Hoeijmakers 2001).

Tetrazines such as Dacarbazine and Temozolomide also form O6-methylguanine via a diazonium ion intermediate that shows its biological effects only after DNA replication (Figure 1.14). This is because *O6*-methylguanine causes the incorrect incorporation of thymine into the newly synthesised strand during DNA replication. These mispairs are recognised by the postreplication mismatch repair (MMR) process, which eventually leads to apoptosis. MMR activity also causes DNA strand breaks, sister chromatid exchanges, and chromosomal aberrations. Hence, the cytotoxicity of the tetrazines depends on an intact MMR pathway, and therefore cells deficient in MMR are likely to be resistant to damage caused by DNA methylation. However, the resistance of tumour cells to methylating *O6*-alkylating agents is not entirely contributed by the loss of MMR activity, as *O6*-alkylguanine-DNA-alkyltransferase (ATase) is also an important factor. ATase recognises and removes alkyl adducts from potentially cytotoxic *O6*-alkylguanine lesions. The alkyl group is transferred to a cysteine residue within the active site of the enzyme. This stoichiometric reaction inactivates the protein, which is then

ubiquitinated and digested by proteasomes (Ayi *et al.* 1992; Humbert *et al.*, 1999; Middleton and Margison 2003).

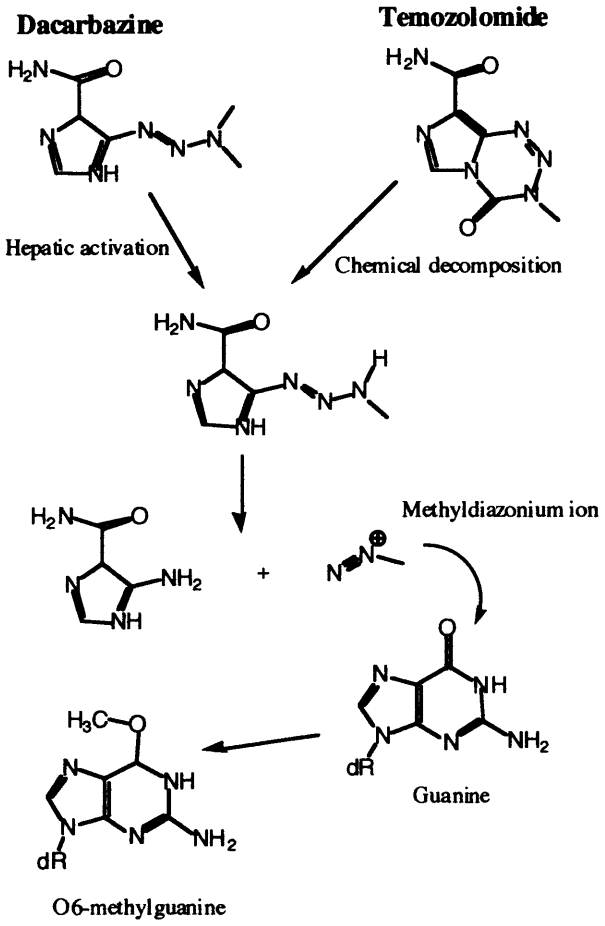

Figure 1.14 Metabolic activation (dacarbazine) or spontaneous degradation (temozolomide) mechanisms leading to DNA damage by formation of *O6*-guanine (Modified from Middleton and Margison, 2003).

The methylating agent, *N*-methyl-*N'*-nitro-*N*-nitrosoguanidine (MNNG) was originally found to be active in the mouse L1210 leukaemia in 1960 at the National Cancer Institute before a new drug *N*-methyl-*N*-nitrosourea was found to have better activity (Middleton and Margison 2003). Several chloroethylnitrosoureas were developed from this original structure because the substitution of a chloroethyl

group showed increased activity. They have proved effective against both solid and intracranially implanted tumours in animals (Schabel 1963). *N*, *N'*-bis(2-chloroethyl)-*N*-nitrosourea (carmustine), *N*-(2-chloroethyl)-*N'*-cyclohexyl-*N'*-nitrosourea (lomustine), and *N*-(2-chloroethyl)-*N'*-(diethyl)ethylphosphonate-*N*-nitrosourea (fotemustine) are some of the agents used clinically (Middleton and Margison 2003) (Figure 1.15).

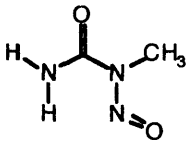

***N*-methyl-*N*-nitrosurea**

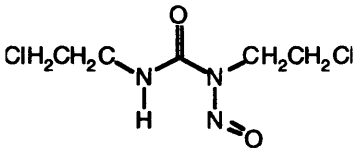

Carmustine

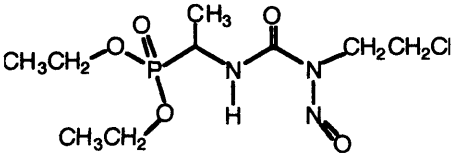

Fotemustine

Figure 1.15 *Structures of N-methyl-N-nitrosourea and O6-alkylating agents in common clinical use.*

Nitrosoureas decompose in aqueous solution to give various reactive compounds including isocyanates and diazonium ions, the latter being crucial to their cytotoxicity.

Chloroethylnitrosoureas cause the formation of crosslinks between guanine and cytosine residues on opposite strands of DNA. The chloroethyl group initially attacks the guanine O6 to form the *O6*-chloroethylguanine intermediate which can

cyclyse to become the 1-*O6*-ethanoguanine intermediate, which then reacts with the cytosine N3 to form the crosslink (Figure 1.16) (Tong *et al.*, 1982).

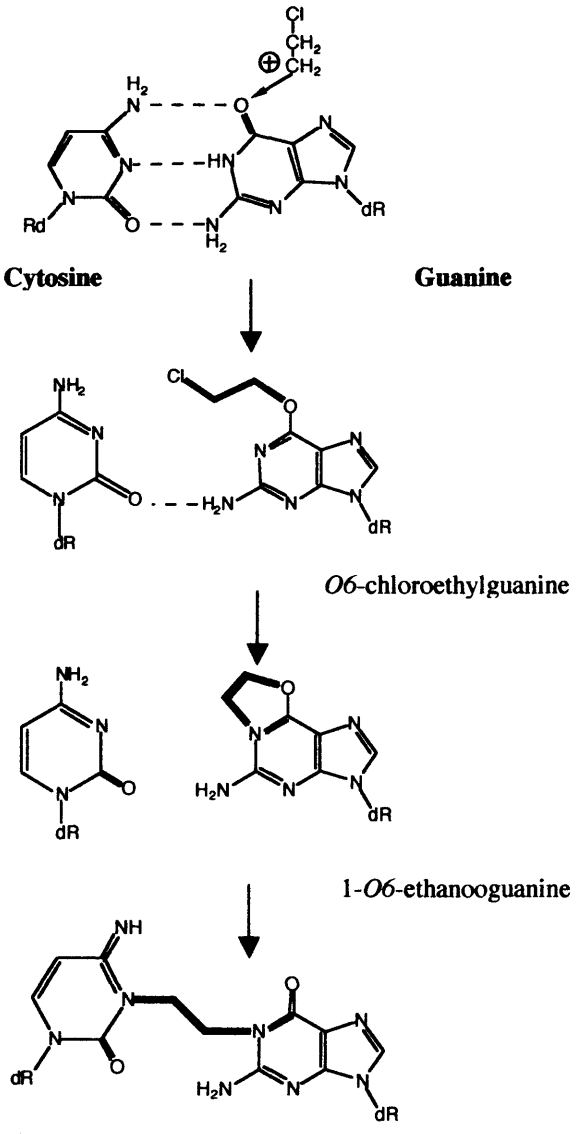

Figure 1.16 Mechanism of DNA interstrand crosslink formation after chloroethylation of guanine in DNA. dR: deoxyribose residue (Adapted from Middleton and Margison, 2003).

1.5.2.3 Cisplatin

Although cisplatin and its analogues are not alkylating agents *per se*, they form DNA adducts and there are several steps involved. The first step, which is the rate-limiting step for DNA binding, is the hydrolysis of a chloride ligand that takes place once the drug passes through the cell membrane, forming *cis*-$[Pt(NH_3)_2Cl(H_2O)]^+$. The second step sees the aquated cisplatin binding to guanine N7 in DNA, displacing the cisplatin-water molecule in a relatively fast reaction step, forming a mono-adduct. This is followed by a third step where the formation of a bifunctional adduct occurs due to hydrolysis of the second chloride ligand, where the re-aquated cisplatin binds another purine N7 (Figure 1.17) (Jamieson and Lippard, 1999).

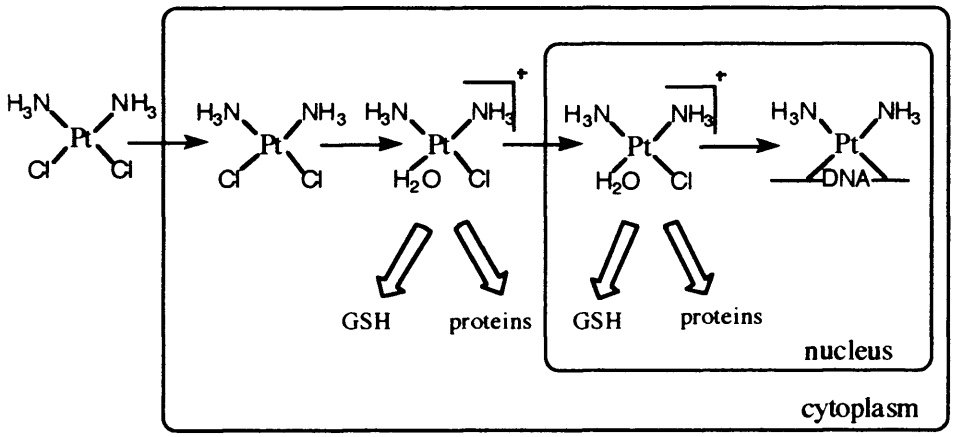

Figure 1.17 Intracellular chemistry of cisplatin (GSH = glutathione) (Adapted from Comess and Lippard, 1993).

1.5.3 DNA crosslinks and cytotoxic effects of alkylating agents

Alkylation of DNA bases is considered to be the major mechanism involved in the cytotoxicity of alkylating agents. This is mainly due to either the formation of crosslinks in DNA by bifunctional agents, or single-strand breaks or damaged bases resulting from monofunctional agents. Most of the alkylating agents in current clinical use are bifunctional. The crosslink formation requires an initial alkylation to form a monoadduct followed by a second alkylation, which is often slow. Additionally, not all monoadducts go on to form cross-links and in many cases, the ratio of monoadducts to crosslinks is at least 20:1 and often higher (Brendel and Ruhland 1984). Such monoadducts are considered to be mutagenic and/or carcinogenic. There are three possible types of crosslink involving DNA; crosslinks on the same strand of DNA (intrastrand), between the two strands of DNA (interstrand), or between a base on DNA and a reactive group on a protein (DNA-protein).

DNA interstrand crosslinks and DNA-protein crosslinks can be detected in mammalian cells at pharmacologically relevant doses of bifunctional alkylating agents by the technique of alkaline elution developed by Kohn (Kohn *et al.* 1981). DNA intrastrand crosslinks have been measured indirectly (Chun *et al.* 1969). Although it is difficult to quantitate directly intrastrand crosslinks, among the three modes of crosslink formation, interstrand crosslinks are considered to be the critical cytotoxic lesion. For example, nitrogen mustards generally show a good correlation between the extent of interstrand crosslinking and the cytotoxicity of the drug (O'Connor and Kohn 1990). In the case of melphalan, chlorambucil and benzoic acid mustard, although the order of chemical reactivity, based on hydrolysis rate, is

chlorambucil > melphalan > benzoic acid mustard, the order of cytotoxicity against human tumour cells *in vitro* was found to be melphalan > chlorambucil > benzoic acid mustard. This is the same order as the interstrand crosslinking efficiency of the compounds in the cells, or in naked DNA (Sunters *et al*, 1993).

Cisplatin has been shown to produce several adducts with DNA that each cause a distortion of the DNA (Jamieson and Lippard, 1999; Judson and Kelland, 2001). The most common adducts identified are 1,2-intrastrand crosslinks between two adjacent guanines (*cis*-GG) (60 to 65 per cent) or between an adjacent adenine and guanine (*cis*-AG) (20 to 25 per cent). Other identified adducts include 1,3-intrastrand crosslinks involving non-adjacent purines (*cis*-GNG and *cis*-ANG), monofunctional adducts, DNA-protein crosslinks and G-G interstrand crosslinks. In all cases, platinum binds to the N7 atom of purine bases. Although there still remains debate as to which of the above adducts on DNA are most efficient for killing tumour cells, different studies have supported both the predominant 1,2-intrastrand crosslink adduct and the interstrand crosslink adduct (Judson and Kelland, 2001). Support for the predominant 1,2- intrastrand crosslink comes from findings that the much less cytotoxic *trans*-isomer of cisplatin cannot form these adducts because of steric hindrance. Also, these adducts are relatively stable on DNA compared with 1,3-intrastrand and monofunctional adducts (Judson and Kelland, 2001). The other theory supporting the importance of interstrand crosslinks has been shown by studies showing relationships between cell killing to numbers of, or repair of, interstrand crosslinks (Comess and Lippard, 1993).

1.5.4 Cellular responses to alkylating agents

One way in which cells respond to DNA damage is by activating DNA repair systems. The repair of alkylation damage is complex and heterogeneous within the genome, and different repair mechanisms can apply to different DNA adducts formed by the same drug (Hartley, 2001). The exact mechanism that causes apoptosis in tumours is still not fully understood in detail but several experiments have shown that the expression of p53 is critical to apoptosis in response to DNA damage by alkylating agents (Guchelaar *et al.*, 1997; Zhou and Elledge, 2000). The inability to activate apoptosis by the p53-dependent pathway confers to mutant p53-containing cells a mechanism of drug resistance, however, it is difficult to definitively link p53 mutations in tumours and clinical resistance to antitumour agents (Valkov and Sullivan, 2003). Interestingly, when the anti-apoptotic gene bcl-2 is expressed, decreased sensitivity to chemotherapeutic alkylating agents may be seen (Reed *et al.*, 1994).

Monoadducts on DNA cause different types of structural alteration to DNA resulting in blocking of DNA polymerisation and base ring openings. DNA single strand breaks can occur via depurination and when they are not repaired correctly further damage, such as base deletions or the formation of DNA double strand breaks (DSBs) as the result of endonuclease attack, can be produced (Friedberg *et al.*, 1995). If this is allowed to persist, it can cause chromosomal rearrangements. *In vitro* experiments have demonstrated that the bulky DNA monoadducts and unrepaired DNA crosslinks, in particular, inhibit DNA replication and transcription by blocking DNA and RNA polymerases (Hartley, 2001).

Unrepaired DNA interstrand crosslinks (ICLs) are known to be among the most toxic forms of DNA damage. As well as ICLs, DSBs induce cell-cycle arrest to allow DNA repair and prevent genetic instability (Dronkert and Kanaar, 2001). If DSBs are unrepaired and persist, they can cause chromosome fragmentation, loss of translocation, and possibly carcinogenesis (Kanaar *et al.*, 1998; Khanna and Jackson, 2001). Because most alkylating agents are not cell-cycle specific, both fast and slow growing cells can be killed, although it is generally rapidly proliferating cells that are more sensitive.

1.5.4.1 DNA repair mechanisms

There are a number of important DNA damage repair pathways that commonly operate in mammals (Hoeijmakers, 2001). They include 1) nucleotide-excision repair (NER), 2) base-excision repair (BER), 3) mismatch repair (MMR), 4) homologous recombination, 5) non-homologous end joining, 6) transcription-coupled repair (TCR) and 7) direct reversal of damage (*e.g.* O6-methylguanine methyltransferase).

BER deals with small chemical alterations of mismatched bases but does not necessarily obstruct transcription and replication. Its reaction is initiated by specific DNA glycosylases which excise the damaged base. NER is the most versatile in terms of lesion recognition and is commonly involved with repairing helix-distorting lesions that interfere with base pairing and generally obstruct transcription and normal replication. Lesions repaired by NER and BER affect only one DNA strand where a damaged lesion is removed and the resulting single-stranded gap is filled in using the intact complementary strand as template.

Although the repair of DNA interstrand cross-links is not understood fully in mammalian cells, it is considered to require components of both nucleotide excision repair (in particular XPF and ERCC1) and homologous recombination (De Silva *et al.*, 2000; McHugh *et al.*, 2001). A first model of ICL repair in *E.Coli* was proposed by Cole (1973). Further models have since been reported in higher organisms, such as yeast and some mammals (McHugh *et al.*, 2001).

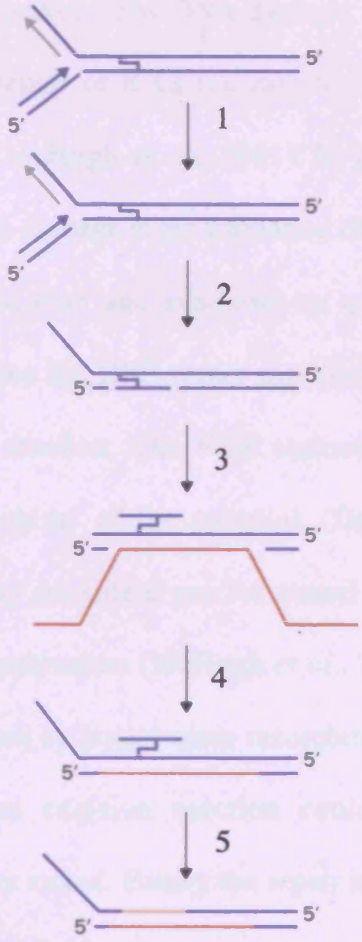

Figure 1.18 Proposed model of ICL repair in S-phase human cells. 1) DSB formation at stalled formation fork. 2) Unhooking mediated by XPF-ERCC1. 3) Gap resection and recombination. 4) Resolution of recombination. 5) Second excision and resynthesis. (Adapted from McHugh *et al.*, 2001)

Homologous recombination and non-homologous end joining processes repair DSBs. TCR focuses on DNA damage that blocks elongating RNA polymerases, and *O6*-methylguanine methyltransferase removes non-native methyl or higher alkyl groups, such as chloroethyl, from guanine residues and transfers them from DNA to an internal cysteine of the enzyme. MMR removes nucleotides mispaired by DNA polymerases and insertion/deletion loops (ranging from one to ten or more bases) that result from slippage during replication of repetitive sequences, during recombination or by DNA damage.

A model for the repair of ICLs relevant to S-phase human cells has been proposed (Figure 1.18) (McHugh *et al.*, 2001). In proliferating cells, one of the consequences of ICL DNA damage is the formation of DSB. DSB formation may be caused during DNA replication and synthesis by a stalled replication fork. This formation of DSBs initiates the DSB repair mechanism. The first step is a NER-dependent dual incision reaction. The NER endonuclease heterodimer, ERCC1-XPF, leads to the 'unhooking' of the crosslink (De Silva *et al.*, 2000). Further nucleolytic processing may provide a gap for strand invasion, which is the initial step for homologous recombination (McHugh *et al.*, 2001). This allows a template to replace the excision patch by homologous recombination repair, and resolution of recombination. A second excision reaction could then occur removing the crosslinked complementary strand. Finally the repair is completed by gap filling and ligation.

1.6 Molecular Recognition of DNA by Small Molecules

It has been recognised that numerous synthetic and natural products that affect DNA chemically or structurally have precise functions determined by their mode of binding. This observation has driven recent interest in understanding the association of small molecules with duplex DNA. Such small molecules include intercalators, non-covalent and covalent major / minor groove binders.

Intercalators are noncovalent DNA binding agents. They bind by inserting a planar aromatic chromophore between adjacent DNA base pairs (Chaires, 1998). Such compounds are hydrophobic and effectively fill the space between base pairs formed when the helix is locally elongated and partially unwound. The interaction between intercalators and adjacent base pairs is primarily through van der Waals interactions and electrostatic stabilisation. Therefore, it is considered that polarisable compounds intercalate preferentially at GC rich regions as their dipole moment is greater than that of AT rich regions (Reynisson *et al.*, 2003). Daunorubicin (Daunomycin) and doxorubicin (Adriamycin) are anthracycline antibiotics, which are among the most potent and clinically useful agents used in chemotherapy (section 1.2.3). Extensive studies of daunorubicin and its DNA interaction have become a foundation for the rational design of new anthracyclines targeted toward DNA (Chaires, *et al.*, 1997).

Drugs such as cisplatin, chlorambucil and melphalan that are important clinical anticancer agents, induce interstrand crosslinks in the major groove of duplex DNA. Further research to find better agents that act by this mode of action still continues. Azinomycins (Figure 1.19) are natural products that fall into this group. Azinomycins are potent antiumour antibiotics that are able to form

interstrand crosslinks between N7 of purines at 5-GXC or 5'-GXT sequences (Armstrong *et al.*, 1992). However, due to the lack of stability and poor bioavailability, the natural products are unlikely to progress as therapeutic agents (Coleman *et al.*, 2002). Therefore, extensive research has been focused on the design, synthesis and evaluation of novel analogous compounds that may potentially be more useful in clinical use (Casely-Hayford *et al.*, 2005; LePla *et al*, 2005; Alcaro *et al.* 2005).

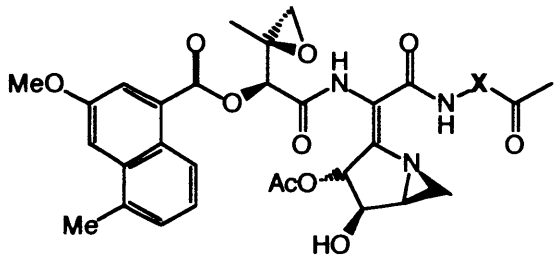

Azinomycin A: X = CH_2
Azinomycin B: X = C=CHOH

Figure 1.19 Structures of azinomycins.

Sequence-selective triple helix formation that occurs in the major groove is another approach. Triple-helix forming oligonucleotides (TFOs) bind as third strands to duplex DNA to form triplex DNA in a sequence specific manner (Figure 1.20) (Frank-Kamenetskii and Mirkin, 1995). Triplex DNA contains the third strand in the major groove of duplex DNA containing polypurine / polypyrimidine tracts, and is stabilised by two Hoogsteen hydrogen bonds between the third strand bases and the purines in the duplex (Radhakrishnan and Patel, 1994; Fossella *et al.*, 1993). The third strand may consist of pyrimidines (parallel triplex), or purines (antiparallel triplex), depending on the nature of the target sequences (Seidman and Glazer,

2003). In the pyrimidine motif, a homopyrimidine oligonucleotide binds in a direction parallel to the purine strand in the duplex with canonical base triplets of T-A:T and C-G:C. In the alternate purine motif, a homopurine strand binds antiparallel to the purine strand with base triplets of A-A:T and G-G:C (Letai, *et al.*, 1988). Due to their stable binding characteristics and sequence specificity, TFOs have vast potential in gene modification, such as inhibition of gene expression, inhibition of replication, and induction of site-specific mutagenesis (Nagatsugi and Sasaki, 2004).

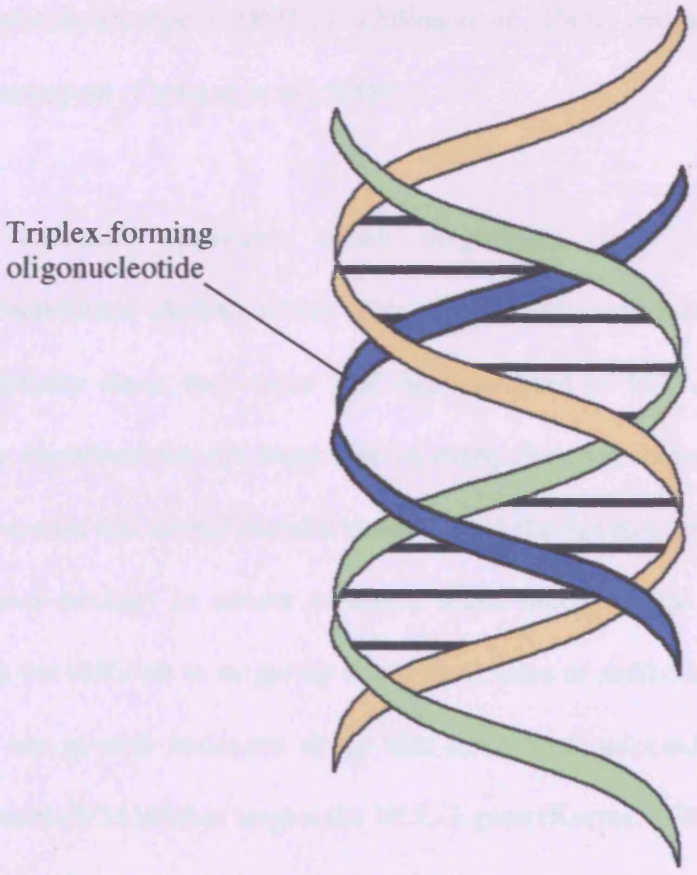

Figure 1.20 A diagram of a DNA triple helix with the third strand binding in the major groove (adapted from Seidman and Glazer, 2003).

However, a number of cellular barriers still limit the ability of TFOs to inhibit target gene expression in living cells. These barriers include removal of the TFO by the DNA repair machinery or by DNA helicases (Brosh *et al.*, 2001; Ziemba *et al.*, 2003), insufficient nuclear accumulation and limited accessibility of the target site (Carbone *et al.*, 2004). To overcome these problems DNA-interacting agents have been conjugated to TFOs so that it would potentially improve the stability of triplex formation within cells (Kutyavin *et al.*, 1993; Zhilina *et al.*, 2004). These DNA-reactive agents include minor groove binders such as pyrrolobenzodiazepines (PBDs) (Zhilina *et al.*, 2004) and intercalating agents such as daunomycin (Carbone *et al.*, 2004).

Another approach using oligonucleotides is that of antisense oligonucleotides (ASOs) which target RNA. Antisense therapeutics have evolved significantly since they were first demonstrated in 1977. ASOs are now being widely evaluated for the treatment of many diseases including genetic disorders, hypertension and cardiovascular disease, and the development of ASOs remains an attractive strategy in cancer medicine since many critical targets driving cancer growth are difficult to target by small molecules or antibodies (Vidal *et al.*, 2005). There are several antisense drugs that have been selected for clinical trials, *eg.* Genasense (G3139) that targets the BCL-2 gene (Kurreck, 2003).

ASOs are single strands of short deoxynucleotide sequence (usually around 18-20 oligomers) that cause targeted transcript destruction by binding to the mRNA of a particular gene by Watson-Crick hybridisation. Once the oligonucleotide binds to the target RNA, multiple mechanisms can be exploited to inhibit the function of

the RNA. Following the destruction of its mRNA, transcription of the corresponding protein cannot occur, resulting in cells becoming depleted of that protein (Crooke, 1999; 2000). The best characterised antisense mechanism results in activation of endogenous cellular mucleases, such as RNase H, which are deployed to cleave the RNA and release the specific oligonucleotide (Dean and Bennett, 2003).

The important mechanisms for gene regulation include small double stranded RNA molecules that induce RNA degradation via a natural gene-silencing process called RNA interference (RNAi) (Meister and Tuschl, 2004). RNAi has become the most widely used approach for gene knockdown because of its potency (Dallas and Vlassov, 2006). Some ASOs exhibit non-catalytic antisense effects, such as the occupancy of target RNA causing translational arrest or the modulation of RNA splicing (Crooke, 1999).

Some of the major challenges for using ASOs *in vivo* are poor cellular uptake and delivery. Advances to improve stability and cellular uptake of ASOs have been made by covalent attachment or complexing with natural cell-penetrating peptide sequences (Pardridge and Boado, 1991; Oehlke *et al.*, 2002)

Amongst the antitumour agents, minor groove binders have recently become one of the most widely studied classes. Increased interest in this group of compounds stems from their ability to interact in a sequence-selective fashion with relatively long stretches of DNA, and to discriminate binding sites that have mutations (Dervan, 1986). Minor groove binding often causes only small changes in DNA conformation, and DNA remains essentially in the native form (Neidle, 2001).

1.6.1 Non-covalent minor groove binders

1.6.1.1 Netropsin and distamycin

Netropsin and its close relative distamycin are antiviral antitumour antibiotics isolated from *Streptomyces* species (Figure 1.21). Distamycin differs from netropsin by having an extra pyrrole ring and only one cationic guanidinium group.

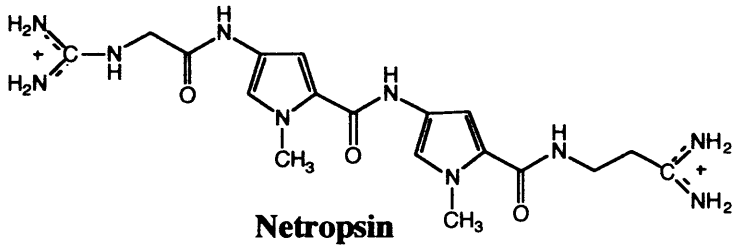

Netropsin

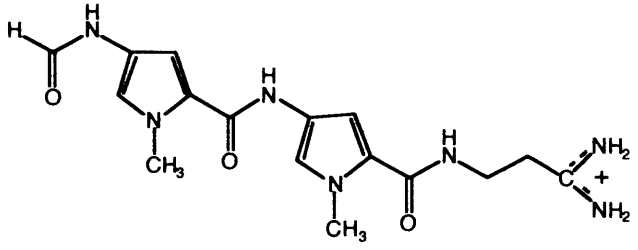

Distamycin

Figure 1.21 Structures of the natural products, netropsin and distamycin.

Although they are not used clinically, they have both been used as paradigms for extensive studies of base-specific, non-intercalative DNA-binding molecules. They interfere with both replication and transcription of DNA by binding tightly to DNA (Kopka *et al.* 1985a, b). They can bind reversibly within the minor groove of B-form DNA via van der Waals reactions with the groove walls and via hydrogen bonding to base groups such as the exposed adenine N3 and thymine O2 (Coll *et al.*,

1987). It was originally discovered that these molecules bind DNA with a preference for AT-rich sequences (Kopka *et al.* 1985a). Furthermore, the DNA binding affinity is higher at continuous runs of A or T rather than alternating A/T sequences (Marky and Breslauer, 1987). The minor groove of B-DNA in AT-rich regions, being narrow, allows the drug molecule to sit squarely in the centre of the groove, with each of its pyrrole rings approximately parallel to the walls of the groove.

NMR study showed that distamycin could bind to DNA as a 1:1 or 2:1 complex within the minor groove (Pelton and Wemmer, 1989). The 2:1 complex requires higher concentration of the drug and it is where the two molecules fit antiparallel within the minor groove. However, netropsin favoured a 1:1 complex and did not form a 2:1 complex, this may be due to the positive charges at both ends of the molecule. Figure 1.22 shows models for 1:1 netropsin-DNA and 2:1 distamycin-DNA complexes.

In the case of netropsin, the two cationic ends of the drug are centred at the bottom of the minor groove each associated with an adenine N3 on the outer-most base pair of four. Additionally, an extensive set of hydrogen bonds to base edges at the bottom of the minor groove provides selectivity for AT-rich sequences (Neidle 2001). The nitrogen atom of each amide group points into the groove, and each participates in a bifurcated arrangement with two consecutive AT base pairs (Neidle 2001).

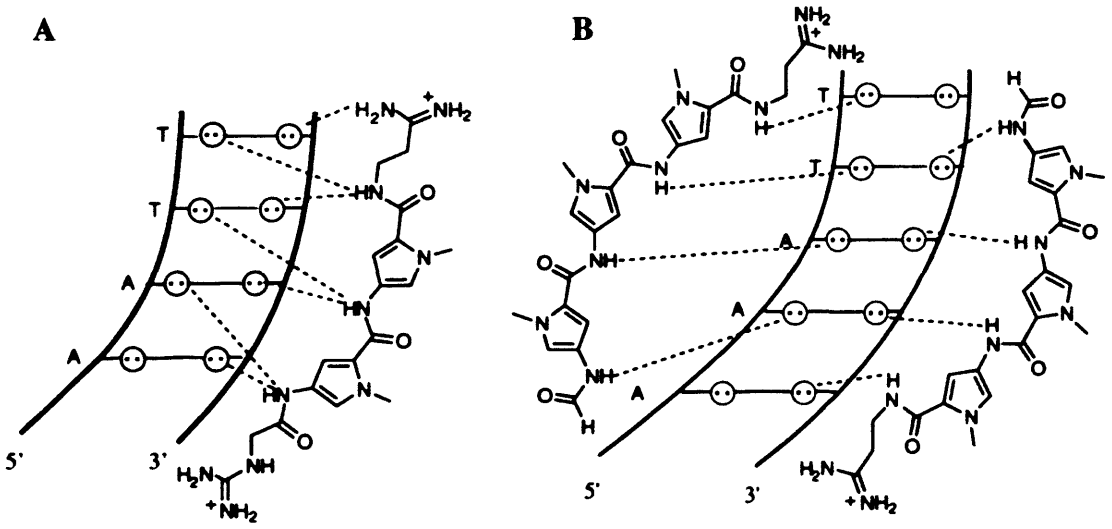

Figure 1.22 Structures for 1:1 netropsin-DNA complex (A) and 2:1 distamycin-DNA complex (B) (Taken from Dervan, 2001).

The discovery of base recognition by netropsin and distamycin has led to further research to discover molecules that can recognise the four base pairs of DNA. From such compounds it should be potentially possible to rationally design molecules that have sequence selectivity. Such compounds will be discussed in Section 1.8.

1.6.1.2 Hoechst 33258

Hoechst 33258 (Figure 1.23) is a bisbenzimidazole in which two benzimidazoles are linked head to tail and is similar to netropsin and distamycin in terms of the crescent shape and positioning of hydrogen bond donating groups (Reddy *et al.*, 1999). It has showed some antitumour activity but is not generally used clinically due to its toxicity. It is primarily used as a fluorescent DNA stain (Neidle, 2001). It is readily taken into cells (Bontemps *et al.*, 1975) and binds to

DNA extremely tightly (Loontiens *et al.*, 1990). The mechanism of cytotoxicity is not known, those suggested include inhibition of topoisomerase (Chen *et al.*, 1993) and DNA helicase (Soderlind *et al.*, 1999). Hoechst 33258 has been shown to have a strong preference for AT-rich sequences with a binding site size of 4-5 base pairs (Harshman and Dervan, 1985). X-ray crystallographic studies of Hoechst 33258 located in the central AATT region of the minor groove have shown that a general preference for AT regions is conferred by electrostatic charge within the minor groove and by narrowing of the walls of the groove (Quinta *et al.*, 1991). Also the binding preference for AT base pairs by the drug is the result of the close contact between the Hoechst molecule and the C2 hydrogen atoms of adenine. The nature of these contacts precludes the binding of the drug to GC pairs due to the presence of the 2-NH_2 groups of guanines in the minor groove.

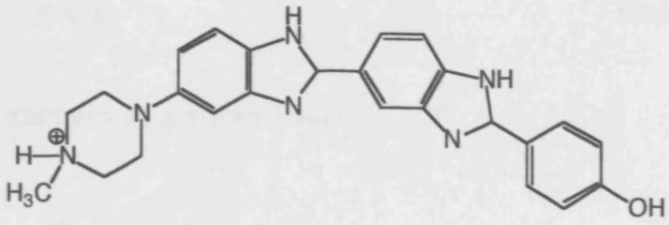

Figure 1.23 Structure of Hoechst 33258

1.6.1.3 Diarylamidines

This group of compounds (Figure 1.24) are known to be effective as antiparasitic agents, and a large number of derivatives have been synthesised.

DAPI is a strong trypanocide but its clinical use has been limited due to its undesireable side effects. Hence, DAPI has become used mainly as a DNA probe or a staining agent since it causes fluorescence upon binding to DNA (Reddy *et al.*, 1999). A series of studies concluded that DAPI binds strongly to AT-rich sequences in the minor groove of DNA, and preferentially at three or four consecutive AT base pairs.

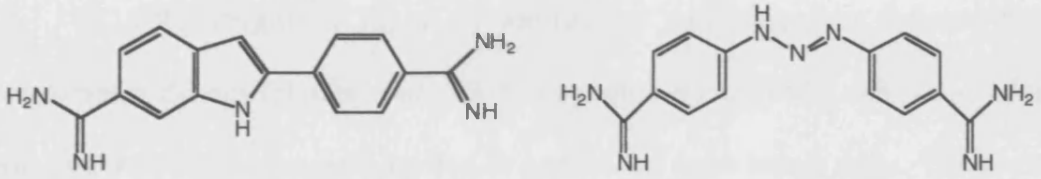

Figure 1.24 Structures of diarylamidines.

Berenil is an aromatic diamidine and is an antitrypanosomal agent. It has charged terminal amino groups and hence the possibility of electrostatic and hydrogen bonding interactions with DNA was suggested (Portugal & Waring, 1987). Also, as berenil-DNA complexes are stable in high ionic-strength solutions, other types of binding may be involved. Berenil binds preferentially to AT-rich DNA sequences, where the binding site is a three base pair sequence (ATT) in the 5'-PuPuATTPy-3' sequence (Yoshida *et al.*, 1990).

1.6.2 Covalent minor groove binders

1.6.2.1 CC-1065 and analogous agents

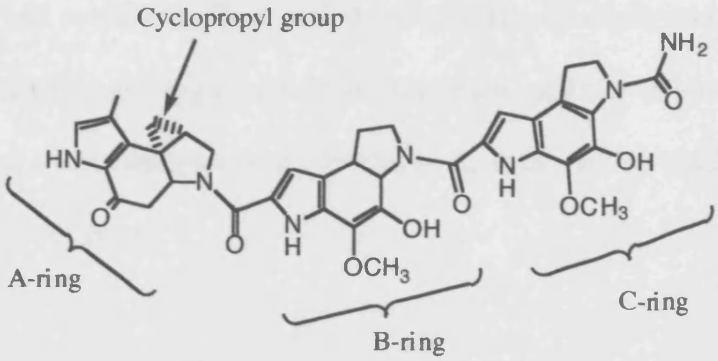

Figure 1.25 Structure of (+)-CC-1065

CC-1065 (Figure 1.25) is an antitumour antibiotic first isolated from *Streptomyces Zelenis* (Hanka *et al.*, 1978; Reynolds *et al.*, 1985), and is one of the most potent antitumour agents known. It consists of three indole units. The A-ring cyclopropylindole (CPI) subunit alkylates DNA, and the other subunits enhance the DNA-binding affinity and selectivity (Wang, *et al.*, 2003). It was found to exert its biological activity through selective alkylation of adenine N3 in the minor groove of B-form DNA. The N3-adenine-CC-1065 adduct was isolated and identified by NMR studies, and also X-ray crystallographic studies. Both showed that CC-1065 has a right-handed twist that can snugly fit into the DNA minor groove (Hurley *et al.*, 1984; Needham-VanDevanter *et al.*, 1984). The drug inhibits gene transcription by interfering with binding of the TATA box binding protein to its target DNA (Chiang *et al.*, 1994). Molecular modelling studies predict CC-1065 to span about five base pairs. The molecule was shown to have sequence specificity for 5'-AAAAA and 5'-

PuNTTA (alkylated bases are underlined) (Reynolds *et al.*, 1985). However, CC-1065 is too toxic to be used clinically as it causes delayed death in mice (McGovren *et al.*, 1984). Therefore various analogues with an improved therapeutic index have been synthesised and evaluated. They include adozelesin, bizelesin and carzelesin (Figure 1.26), which all have highly effective antitumour activity *in vivo* and have under gone clinical trials (Bhuyan *et al.*, 1992a, b; Li *et al.*, 1991, 1992; Carter *et al.*, 1996; Baraldi *et al.*, 2001).

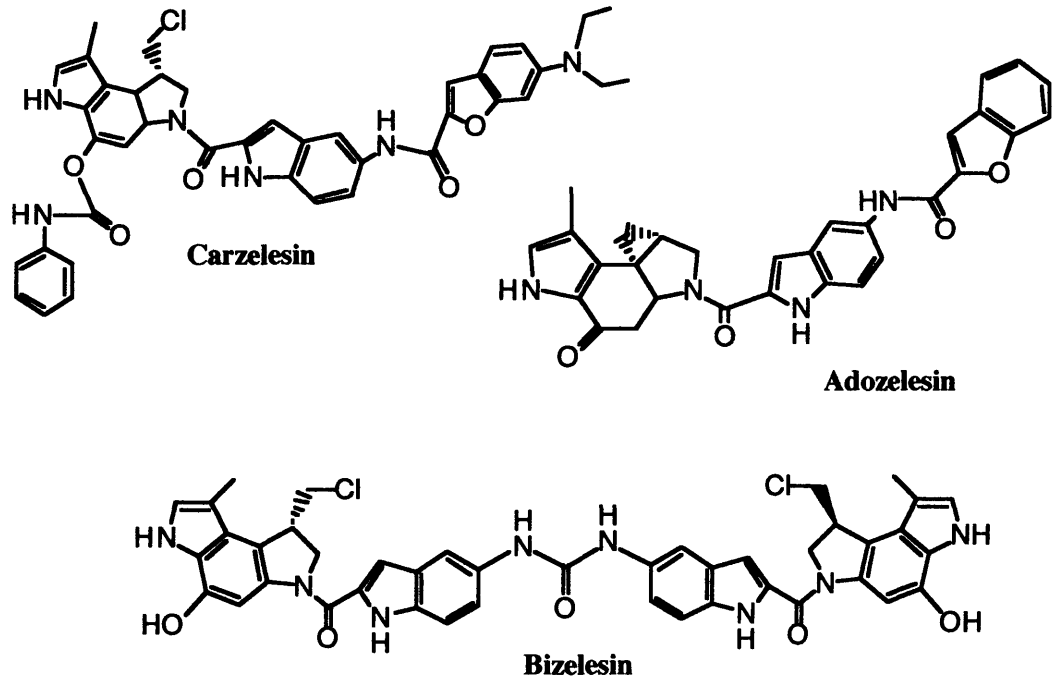

Figure 1.26 Structures of CPI analogues of CC-1065.

Bizelesin is a bifunctional alkylating agent, which shows more antitumour efficacy both *in vitro* and *in vivo*, and is generally 20- to 30- fold more toxic than the monofunctional adozelesin (D'Incalci and Sessa, 1997). Bizelesin produces interstrand crosslinks between two N3 groups of adenines, spanning six to seven base pairs (Sun and Hurley, 1993), and was also found to produce region-specific damage to AT islands in tumour cells. Region-specific targeting implies not only the ability to damage a desired critical target that may have distinct structural and/or functional properties, but also could potentially cause limited collateral damage elsewhere in the genome (Woynarowski, 2002).

1.6.2.2 Duocarmycins

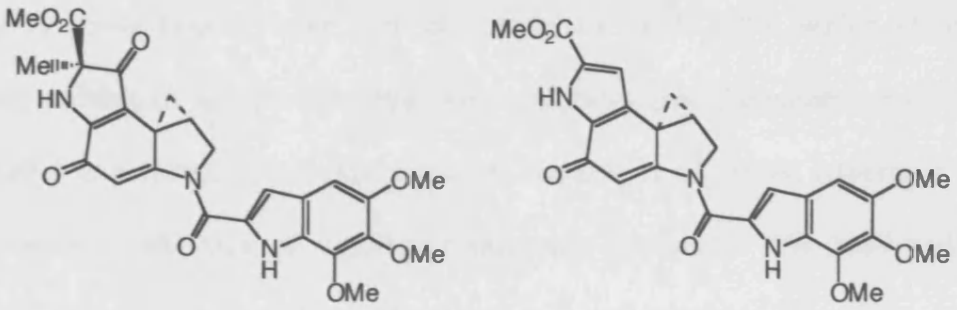

(+)-duocarmycin A

(+)-duocarmycin SA

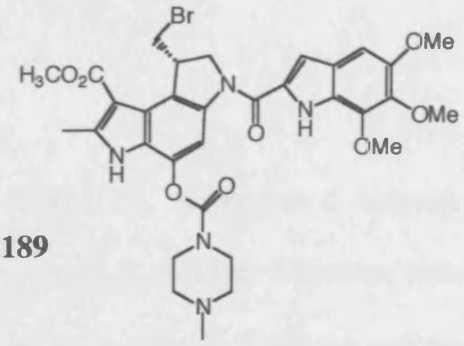

KW-2189

Figure 1.27 Structures of natural products duocarmycins and a synthetic derivative, KW-2189.

(+)-duocarmycin A and (+)-duocarmycin SA (Figure 1.27) are also exceptionally potent antitumour antibiotics that derive their biological effects through a reversible, stereochemically controlled sequence selective adenine N3 alkylation of DNA (Asai *et al.*, 1994). The alkylation occurs at the least substituted carbon of the activated cyclopropane (Boger *et al.*, 1994). Duocarmycins show high sequence selectivity for AT-regions with preferred sequences constituted by three base pairs in the order of 5'-AAA > 5'-TTA > 5'-TAA > 5'-ATA (alkylated bases are underlined) (Boger and Johnson, 1995). Boger and coworkers have studied a series of natural and unnatural agents that contained structural modifications in the alkylation subunit, and established the steric and electronic factors influencing the reactivity (Boger *et al.*, 1997; 2001). This has led to extensive investigation on a series of heterocyclic analogues of duocarmycins that showed increased biological activity in some cases. These compounds include KW-2189, which showed improved antitumour activity and better water solubility than the parent compound. KW-2189 was selected for clinical trials (Kobayashi *et al.*, 1994; Alberts *et al.*, 1998). However, the lack of significant antitumor activity of KW-2189 and its associated toxicity suggested that further testing is not warranted (Markovic *et al.*, 2002).

1.6.2.3 Mitomycin C

As described in Section 1.2.3, mitomycin C belongs to a class of potent antitumour antibiotics. Mitomycin C requires reductive activation in cells and it covalently binds to N7 and N2 of guanine in the major and minor grooves of DNA, respectively. It forms either monoadducts or crosslinks (Tomasz *et al.*, 1987; Basu *et*

al., 1993). Interstrand crosslink selectively occurs at a 5'-CG-3' sequence and intrastrand crosslinking at a 5'-GG-3' sequence (Warren and Hamilton, 2001). Interstrand crosslinks constitute 5-13% of all adducts (Warren *et al.*, 1998). While the interstrand crosslinking does not cause significant perturbation in the DNA (Tomasz *et al.*, 1995), intrastrand crosslinks result in distortion (Kumar *et al.*, 1992).

1.6.2.4 Distamycin and netropsin analogues

Tallimustine (Figure 1.28) is a benzoyl nitrogen mustard derivative of distamycin A, and shows high sequence specificity for alkylation to some AT-rich sequences, in particular 5'-TTTTGA sequence. This represents the highest sequence specific interaction observed for a small molecule interacting with DNA. Although it has a benzoyl nitrogen mustard group, tallimustine showed alkylation at adenine-N3 in the minor groove, instead of producing guanine-N7 alkylation, and binding was found to 5'-TTTTGA-3' (alkylated base is underlined) (Broggini *et al.*, 1995). Tallimustine has progressed into clinical trial (Cozzi, 2003).

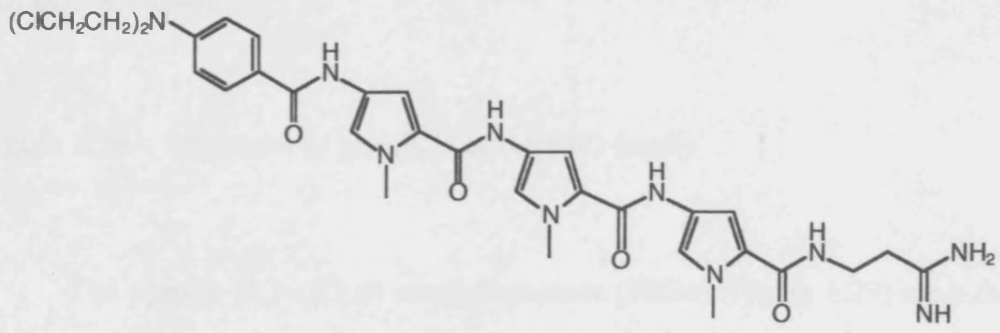

Figure 1.28 Structure of Tallimustine

1.6.2.5 Pyrrolo [2,1-c][1,4] benzodiazepines (PBDs)

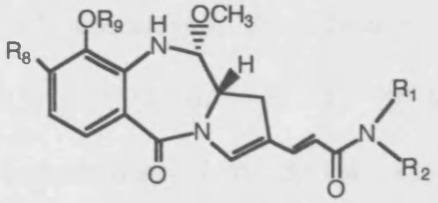

Anthramycin: $R_8=CH_3$, $R_9=R_1=R_2=H$
Mazethramycin: $R_8=R_1=CH_3$, $R_9=R_2=H$
Porothramycin B: $R_8=H$, $R_9=R_1=R_2=CH_3$

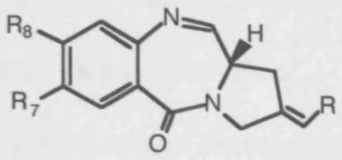

Tomaymycin: $R_7=CH_3O$, $R_8=OH$, $R=CH_3$
Prothracarcin: $R_7=R_8=H$, $R=CH_3$
Sibanomicin: $R_8=H$, R_7=sibirosamine pyranoside as in Sibiromycin, R=Et

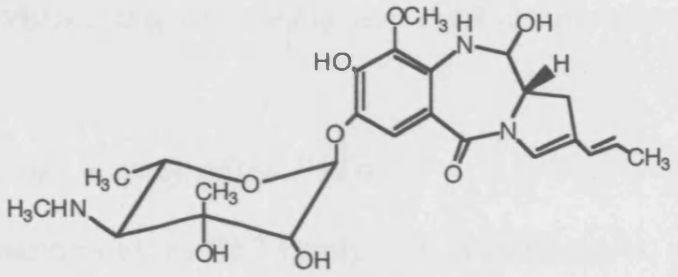

Sibiromycin

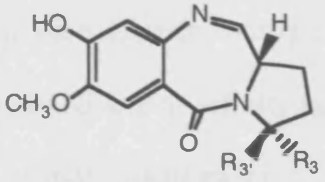

Neothramycin A: $R_3=H$, $R_{3'}=OH$
B: $R_3=OH$, $R_{3'}=H$
DC-81 : $R_3=R_{3'}=H$

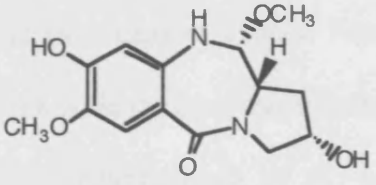

Chicamycin A

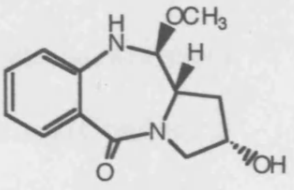

Abbeymycin

Figure 1.29 Structures of members of the PBD family

The pyrrolo [2,1-c][1,4] benzodiazepines (PBDs) (Figure 1.29) are a family of naturally occurring antitumour antibiotics produced by various *Streptomyces* species and their precise mode of interaction with DNA has been extensively studied. The first member of the family was discovered in 1965 when Leimgruber

and co-workers isolated anthramycin from *Streptomyces refuineus* (Leimgruber *et al.*, 1965a,b). Other members of the family include abbeymycin (Hochlowski *et al.*, 1987), chicamycin (Konishi *et al.*, 1984), DC-81 (Japanese Patent, 1983; Thurston *et al.*, 1990; Bose et al., 1992a), mazethramycin (Kunimoto et al., 1980), neothramycins A and B (Takeuchi *et al.*, 1976), porothramycin (Tsunakawa *et al.*, 1988), prothracarcin (Shimizu *et al.*, 1982), sibanomicin (DC-102) (Hara *et al.*, 1988; Itoh *et al.*, 1988), sibiromycin (Leber *et al.*, 1988) and tomaymycin (Arima *et al.*, 1972). The PBDs will be described in more detail in the next section.

1.6.3 Antitumour activity of the PBDs

Many members of the PBD family such as anthramycin, neothramycins A and B, sibiromycin and tomaymycin have significant cytotoxicity *in vitro* and have been used experimentally in the treatment of cancer. For example, anthramycin shows antitumour activity against a wide range of transplanted tumours (Grunberg *et al.*, 1966; Nishioka *et al.*, 1972; Brazhnikova *et al.*, 1972; Takeuchi, 1976). Anthramycin, sibiromycin and neothramycin have all reached various stages of clinical trials, but have failed due to their dose-limiting cardiotoxicity, and in the case of anthramycin and sibiromycin, tissue necrosis at the site of injection. Neothramycins A and B, although showing no cardiotoxicity, lacked efficacy (Hurley, 1977; Thurston and Bose, 1994).

1.6.4 Structure and mechanism of action of PBDs

The different PBD molecules vary in the number, type and position of substituents on both the aromatic A ring and the pyrrolo C ring (Figure 1.30). The C

ring can also have a degree of saturation that can be either fully saturated or unsaturated at either C2-C3 (endocyclic) or C2 (exocyclic).

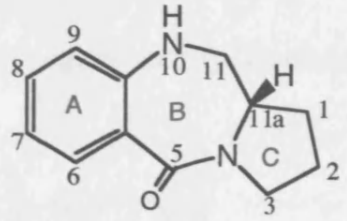

Figure 1.30 The PBD ring system.

The potent activity of PBDs is considered to be due to the possession of either an amine or a carbinolamine methyl ether at the N10-C11 position that acts as an electrophilic centre in the DNA alkylation reaction (Lown and Joshua, 1979). This N10-C11 moiety may exist, depending on the structure of the compound and the method of isolation or synthetic work-up, in the hydrated carbinolamine or carbinolamine methyl ether form (Figure 1.31). For example, DC-81 and anthramycin exist in the imine form and carbinolamine methyl ether form as solids or oils, respectively (Thurston, 1993). The carbinolamine form is rarely isolated (Leimgruber et al., 1965b) although NMR experiments show that it exists when dissolved in aqueous solution (Miyamoto et al., 1977).

All of the natural compounds are able to produce a snug fit when binding into the minor groove of B-form DNA without detectable distortion of the DNA because of their (S)-configuration at the chiral C11a position. This gives the molecule a right-handed twist and a three dimensional shape for isohelicity when viewed from the C-ring towards the A-ring (Hurley and Petrusek, 1979). Stereochemistry at the C11a position of the PBDs influences their DNA binding

affinity and biological activity. A synthetic PBD with (R)-configuration at C11a has been found to lack both DNA binding affinity and *in vitro* cytotoxicity. In this case, DC-81 with (R)-configuration showed no binding to DNA whereas the (S)-isomer showed significant binding and biological activity (Hurley *et al.*, 1988).

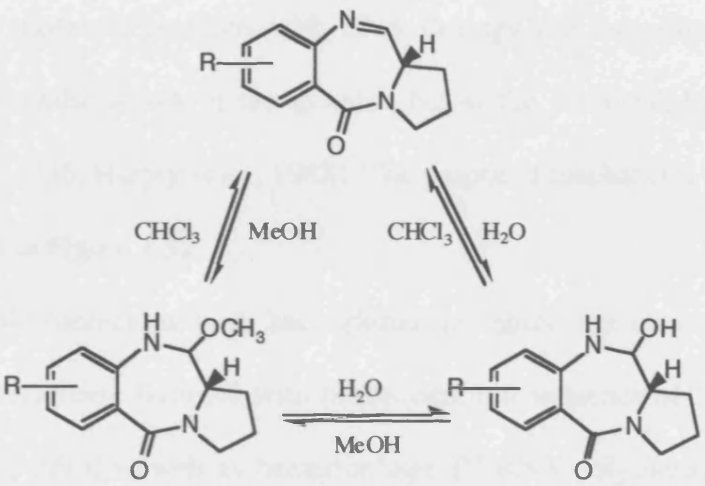

Figure 1.31 Three interconvertible forms of a PBD molecule.

With all PBD compounds, the biological potency is generally attributed to their ability to bond covalently to DNA (Kohn, *et al.*, 1974; Petrusek, *et al.*, 1981). PBD molecules have shown specificity towards guanine in double stranded DNA, and do not show any reaction with RNA or protein (Kohn and Spears, 1970; Hurley *et al.*, 1977). These early studies examined the formation of anthramycin–DNA adducts by using indirect techniques such as UV spectroscopy, thermal denaturation, dialysis, gel filtration and alcohol precipitation, but later the employment of fluorescence spectroscopy (Maruyama *et al.*, 1981; Barkley *et al.*, 1986, 1991; Cheatham *et al.*, 1988; Boyd *et al.*, 1990b), high-field NMR (Graves *et al.*, 1984,

1985; Cheatham *et al.*, 1988; Krugh *et al.*, 1989; Boyd *et al.*, 1990a, b) and molecular modelling (Barkley *et al.*, 1986, 1991; Rao *et al.*, 1986; Remers *et al.*, 1986; Zakrzewaka and Pullman, 1986; Cheatham *et al.*, 1988; Boyd *et al.*, 1990a, b; Rao and Remers, 1990) has led to a more detailed analysis. NMR experiments confirmed the mechanism of covalent adduct formation (Graves *et al.*, 1984). In this case, the PBD molecule interacts with DNA through the formation of an aminal bond by nucleophilic attack of the guanine N2 at the electrophilic C11 position (Barkley *et al.*, 1986; Hurley *et al.*, 1988). The proposed mechanism of action of the PBDs is shown in Figure 1.32.

The PBD molecules have been shown to inhibit the cleavage activity of restriction endonuclease Bam H1 with the recognition sequence of 5'-GGATCC-3' (Puvvada *et al.*, 1993) as well as bacteriophage T7 RNA polymerase transcription (Puvvada *et al.*, 1997).

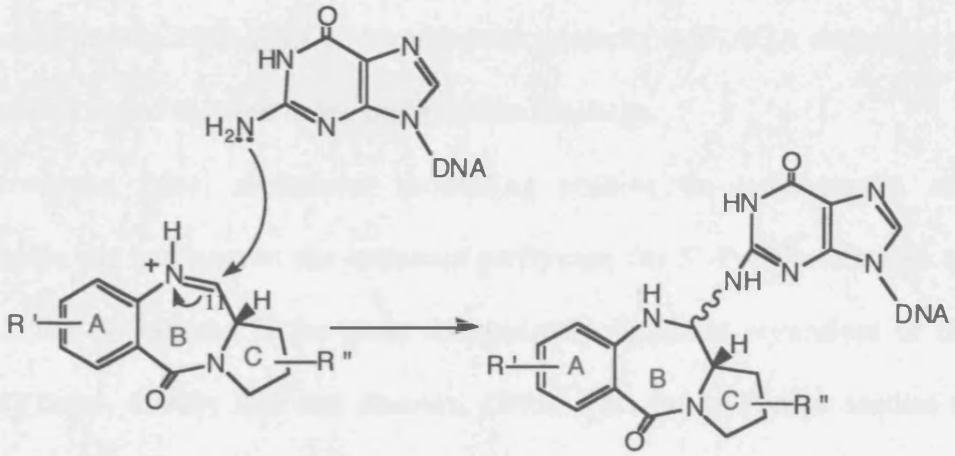

Figure 1.32 Mechanism of formation of an aminal bond between a PBD molecule and the N2 position of guanine.

1.6.5 Sequence selectivity of PBDs

From the numerous NMR studies on the PBD-DNA adducts, anthramycin was found to bind exclusively with C11 in the (*S*)-configuration, and with a preference for orientation of the aromatic A ring towards the 3' end of the strand to which the drug is bonded (*S*3' adduct) (Thurston, 1993). This was supported by molecular modelling suggesting that the *S*3' adduct is more energetically favourable than *S*5'. It was also demonstrated by footprinting experiments that the preferred binding sequence is 5'-PuGPu over 5'-PyGPu ~ 5'-PuGPy > 5'-PyGPy (where Pu = purine and Py = pyrimidine) (Hertzberg *et al.*, 1986; Hurley *et al.*, 1988), and for a 5'-GGG sequence *S*5' and (R)-adducts are highly disfavourable over *S*3' adducts (Zakrzewska and Pullman, 1986). Another study that supported the sequence preference is a concentration-dependent inhibitory effect of the PBDs on *in vitro* transcription. This study aimed to identify the DNA sequences that may be responsible for blockage of transcription (Puvvada *et al.*, 1997). The results demonstrated that the PBD-DNA adducts formed primarily at 5'-AGA sequences on the transcribed strand resulted in the transcription blockage.

However, other molecular modelling studies on tomaymycin and neothramycin did not support the sequence preference for 5'-PuGPu although all agree that the *S*3' adduct is the most energetically favoured regardless of the sequence (Boyd, 1990b; Rao and Remers, 1990). This led to further studies to elucidate the relationship between the individual structure of the drug and its influence on the binding site sequence. In order to investigate the non-covalent interaction of PBD molecule with DNA, Thurston and co-workers studied a series of pyrrolo[1,2-c][1,4]benzodiazepine-5,10-diones (dilactams) (Figure 1.33) that do not

have the N10-C11 imine moiety (or its equivalent) responsible for covalent bonding as described above (Jones *et al.*, 1990). Only two compounds out of 15 dilactams showed any significant binding to DNA.

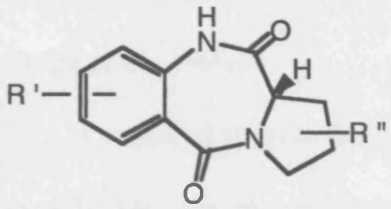

Figure 1.33 Example of a dilactam molecule.

From these results it was concluded that the C2-OH and the A-ring substituents are important in the binding process and that, apart from the N10-C11 carbinolamine moiety, other features such as the A- and C-ring substituents only participate in non-covalent interactions with DNA bases. One of the compounds in which the C8-OH was replaced by a benzyl substituent did not show any binding. This indicated that either the proton of C8-OH may be involved in a hydrogen bond or that any bulky substituent placed here may cause an undesireable steric hindrance for binding. Similarly, free-hydroxy groups at C2- and C8- positions are also required for binding. A further requirement is the (*R*)-configuration at C2 because it is able to stabilise the hydroxy group hydrogen bonding.

1.6.6 Structure-activity relationship (SAR) of PBD molecules

Based on previously published reviews and data, the most significant structure-activity information on PBD molecules has been summarised.

1 An imine, carbinolamine or carbinolamine methyl ether at N10-C11 position is essential for biological activity (Thurston and Hurley, 1983). However, there are compounds without this moiety that show biological activity (e.g., dilactams) possibly due to a completely different mechanism of action, and metabolism could be also involved (Jones *et al.*, 1990).

2 (*S*)-configuration at C11a is required to give the molecule the correct three-dimensional shape to snug fit into the minor groove of DNA (Hurley *et al.*, 1988).

3 Endocyclic or exocyclic unsaturation at C2 enhances DNA binding affinity, cytotoxicity and *in vivo* antitumour activity. A fully saturated C-ring leads to complete loss of DNA-binding and cytotoxicity (Hurley *et al.*, 1988).

4 Only small substituents, such as a hydroxy group at the C3 position of neothramycin, are tolerated to retain DNA-binding affinity, cytotoxicity and *in vivo* activity (Thurston 1993).

5 The sugar moiety at C7 of sibiromycin appears to enhance DNA-binding affinity compared to similar structure compounds without the sugar moiety (such as anthramycin) (Thurston 1993).

6 Electron donating substituents on the A-ring influence DNA binding affinity and cytotoxicity, although they are not a prerequisite for DNA binding (Hurley *et al.*, 1988). Additionally, the C7-methoxy / C8-hydroxy pattern of substituents show optimal fit into the DNA minor groove due to flexibility within the compounds (Thurston 1993).

7 Bulky substituents at N10 inhibit binding to DNA and abolish biological activity (Thurston and Hurley, 1983).

1.7 Development of Novel DNA Interacting Agents

The knowledge of the pathophysiology of different forms of cancer at the molecular level (i.e., cell signalling, cell-cycle regulation, apoptosis, telomere biology and angiogenesis) has grown considerably over the past 20 years and continues to do so at an ever-increasing rate (Hanahan and Weinberg, 2000). As a result of this, the approach to drug development has recently been shifted from the employment of random screening methods to a target-based approach in order to develop drugs that specifically block the pathogenic mechanisms which account for malignant transformation with the aim of producing an improved efficacy, reduction of toxicities and prevention of drug resistance (Fox *et al*, 2002; Gibbs, 2000).

1.7.1 DNA as a target of small molecules

Through improved understanding of established DNA-binding agents, a large number of novel compounds with higher sequence selectivity and DNA binding affinity have been synthesised (Chaires, 1998).

1.7.1.1 Base recognition of small molecules

As mentioned in Section 1.6, the discovery of the base recognition ability in netropsin and distamycin led researchers to explore analogues in an attempt to alter the A/T binding specificity of these compounds (Dervan, 2001). Distamycin has three pyrrole (Py) rings linked by carboxyamides, of which the amines point toward the minor groove floor of the DNA making hydrogen bonds with the AT and TA base pairs (N3 of A and O2 of T) as 1:1 and 2:1 ligand-DNA complexes (Kopka *et al.*, 1985; Pelton and Wemmer, 1989).

Lexitropsins are analogues of netropsin and distamycin that were synthesised and evaluated in order to achieve added recognition of G/C base pairs. Modification of netropsin or distamycin by replacing a pyrrole ring with N-methylimidazole gives the potential to recognise the exocyclic N2 atom of guanine in the minor groove (Kopka *et al.*, 1985). A series of lexitropsins were synthesised containing imidazoles (Lown, *et al.*, 1986; Krowicki & Lown, 1987), thiazoles (Rao *et al.*, 1990), furans (Lee *et al.*, 1989), and triazoles (Rao *et al.*, 1991). Figure 1.34 shows the model of a lexitropsin in comparison with netropsin.

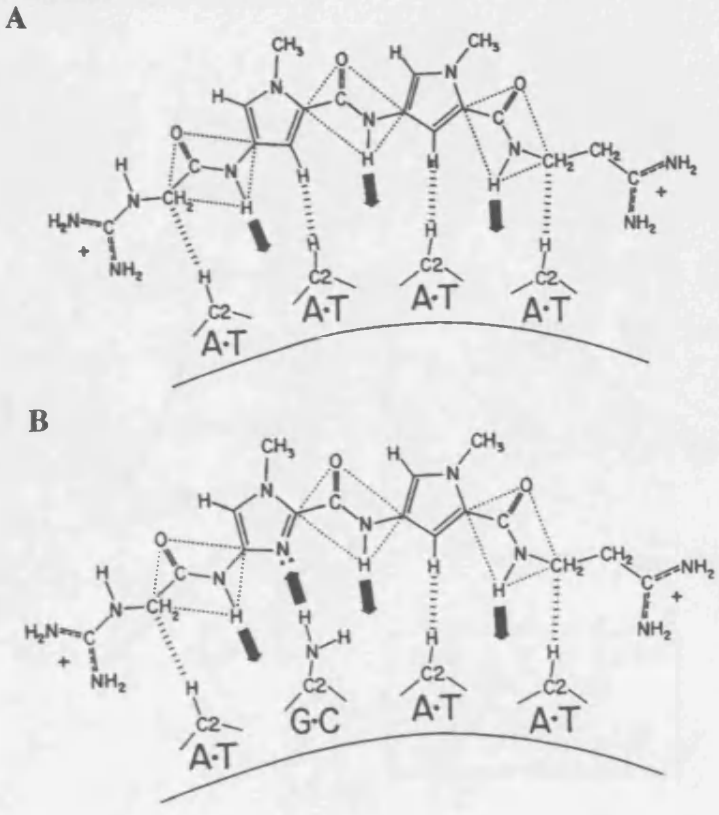

Figure 1.34 Models for netropsin recognising AT base pairs (**A**) and a lexitropsin containing an imidazole in place of a pyrrole to give added recognition of G/C base pairs (**B**) (taken from Dervan, 2001).

The novel polyamide ImPyPy when one of the pyrrole (Py) is replaced with imidazole (Im), has been shown to bind to the sequence of 5'-(W)G(W)C(W)-3' (where W=A or T) instead of the 5'-WGWWW-3' sequence, which would be expected for a 1:1 polyamide-DNA complex (Dervan, 2001). In addition, in terms of the formation of a 2:1 polyamide-DNA complex (Figure 1.35), it was subsequently rationalised, and verified by NMR (Mrksich *et al.*, 1992), that ImPyPy can bind as an antiparallel dimer with pairs of Im/Py recognising G•C, Py/Im recognising C•G and Py/Py recognising A•T or T•A (Wade *et al.*, 1992). This discovery gave a new paradigm of unsymmetrical ring pairs for the specific recognition of the DNA minor groove (Dervan and Edelson, 2003).

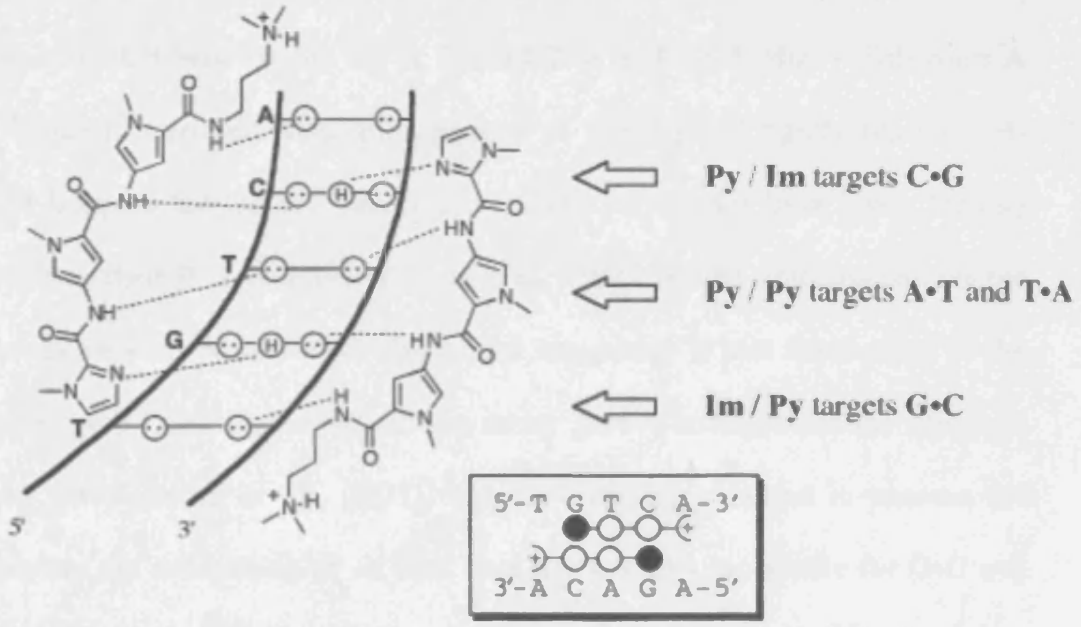

Figure 1.35 Model for antiparallel dimer ImPyPy binding 5'-TGTCA-3'. Unsymmetrical pair Im/Py distinguishes GC from CG and both from AT and TA (taken from Dervan, 2001).

Extensive studies on the Im/Py pair have confirmed the existence of a hydrogen bond between the Im nitrogen and the exocyclic amine of G. Also, energetic preference for a linear hydrogen bond, coupled with the unfavourable angle to an Im over the cytosine side of the base pair, provides a basis for the ability of an Im/Py pair to discriminate specifically G•C from C•G (Kielkopf *et al.*, 1998a).

Furthermore, the *N*-methyl-3-hydroxypyrrole (Hp) monomer was designed as a thymine-selective recognition element when paired across from Py (White *et al.*, 1998). High-resolution crystallographic data has determined two different Hp-containing polyamides as 2:1 complexes with DNA (Kielkopf *et al.* 1998b; 2000). Hp was chosen for reasons of size and the possibility to form two hydrogen bonds between the hydroxyl and the O2 of T, along with shape-selective recognition of an asymmetric cleft between the O2 of T and C2 of A. Indeed, Hp/Py disfavours A over T due to steric destabilisation against A, also Hp-OH tightly fits the cleft formed between the O2 of T and C2 of A. Hp polyamides have lower binding affinity than their Py counterparts (White *et al.*, 1998), but the structural basis of the difference remains to be found. One recent suggestion is that desolvation of the hydroxyl group upon insertion into the minor groove accounts for the energetic penalty (Wellenzohn *et al.*, 2003). This nevertheless resulted in success for completing the recognition of all four base pairs; Im/Py is specific for G•C and Hp/Py for T•A. These interactions can be conveniently described as 'pairing rules' (Table 1.4) (Kielkopf *et al.* 1998b; Dervan and Edelson, 2003).

Pair	G•C	C•G	T•A	A•T
Im/Py	+	-	-	-
Py/Im	-	+	-	-
Hp/Py	-	-	+	-
Py/Hp	-	-	-	+

Table 1.4 Pairing code for minor groove recognition. Favoured (+), disfavoured (-).

1.7.2 Affinity and specificity

In order to achieve increased affinity and specificity, Dervan and coworkers linked the antiparallel dimers covalently (Mrksich and Dervan, 1994). The standard motif is the eight-ring hairpin (Figure 1.36), in which a γ-aminobutyric acid (γ-turn) linker connects the carboxylic terminus of one polyamide to the amino terminus of another. Hairpin polyamides containing eight heterocyclic groups bind 6 bp and show approximately 100-fold higher affinity compared to the unlinked homodimers. The γ-turn demonstrates selectivity for A, T over G, C base pairs and it is suggested to be due to the steric hindrance with the exocyclic amine of G (Mrksich *et al.* 1994).

Other types of linked polyamides are H-pin and U-pin polyamides. They are linked via the ring nitrogens with an alkyl spacer that projects away from the minor groove (Mrksich and Dervan, 1994; Mrksich *et al.*, 1994). The H-pin motif is where the antiparallel heterodimers were coupled with a short methylene linker across the back bone, and the U-pin motif is where the dimers were coupled at the amino- and carboxy- termini through an aliphatic amino acid (γ). The U-pin motif has higher binding affinity and specificity towards the minor groove compared with the H-pin

motif. From this finding, an ImImPyPy dimer was synthesised to recognise a GGCC core sequence (Kielkopf *et al.*, 1998b). High resolution X-ray analysis of the 2:1 $(ImImPyPy)_2$-DNA complex revealed that the Im/Py pair makes three specific hydrogen bonds to a G•C base pair. Furthermore, there was an energetic penalty due to the polyamides being overcurved. To eliminate the problem, the (γ)-amino acid linkage was replaced by (ß)-alanine because of its flexibility allowing the crescent-shaped ligand to match the curvature of the DNA helix (Kelly *et al.*, 1996; Keilkopf *et al.*, 1998b; Trauger *et al.*, 1996). Tandem hairpin polyamides, linked either turn-to-turn or turn-to-tail (Weyermann and Dervan, 2002; Herman *et al.*, 1999), can recognise large DNA sequences (up to 10 base pairs) with good specificity and excellent binding affinity (Weyermann and Dervan, 2002; Kers and Dervan, 2002).

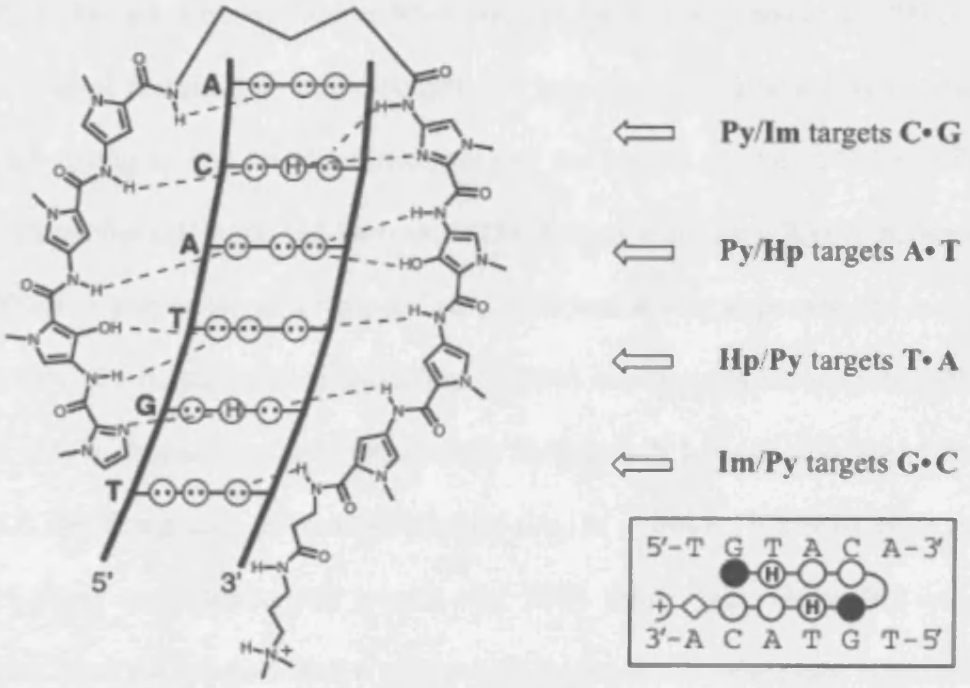

Figure 1.36 The hairpin motif. The amino and carboxy terminus of the antiparallel dimers are connected by γ-aminobutyric acid (taken from Dervan, 2001).

As a result of this breakthrough, a major effort has been undertaken to use the hairpin polyamides to effect the expression of specific genes. One of the approaches to modify gene expression involves inhibition of key transcription factor (TF)-DNA complexes in a designated promoter so that it interferes with the recruitment of RNA polymerases. As there are significantly fewer oncogenic TFs than potentially oncogenic signaling proteins, TF inhibition represents a uniquely promising approach to cancer treatment (Darnell, 2002). As a first target, the transcription factor TFIIIA was selected because it regulates a small number of genes and also the contacts between the nine zinc finger protein and the minor groove had been established. A polyamide bound in the recognition site of TFIIIA suppressed transcription of 5S RNA genes by RNA polymerase III *in vitro* and in cultured *Xenopus* kidney cells (Gottesfeld *et al.*, 1997). Polyamides were also used to target viral genes transcribed by RNA polymerase II (Dickinson *et al.*, 1998).

Novel hairpin polyamide-conjugates have been synthesised by combining with alkylating agents based on analogues of the natural product CC-1065, PBDs and chlorambucil (Wurtz and Dervan, 2000; Kumar and Lown 2003a, b; Wang *et al.*, 2003). A polyamide-chlorambucil conjugate was shown to possess the sequence selectivity of a polyamide and the enhanced DNA reactivity of chlorambucil (Wang *et al.*, 2003). It was demonstrated that the conjugate binds and alkylates DNA *in vitro* at the designated polyamide-binding site. In addition, it arrests cells in the G2/M phase and inhibits cell growth and DNA replication. Gottesfeld and co-workers have established that a polyamide-chlorambucil conjugate significantly downregulated a key component of chromatin, the histone H4c gene, however, the

downregulation did not lead to large global changes in gene expression (Dickinson *et al.*, 2004).

1.7.3 Limitations

Because of the sequence-dependent microstructure of double helical DNA, the pairing code will not allow targeting all 524,800 ten base-pair sequences of DNA with the criteria of high affinity and good specificity. However, having synthesised and characterised more than 250 polyamides, Dervan estimated that it is now possible to target as much as 50% of the DNA sites on any promoter which will be sufficient to target most important transcription factors (Dervan, 2001).

The size of binding site may be critical for biological application because longer sequences would be expected to occur less frequently in the genome. The number of base pairs that has been effectively recognised is up to 11 base pairs so far (Dervan and Edelson, 2003). Even both types of tandem polyamides that can recognise large DNA sequences with high affinity, specificity (expressed in terms of affinity for a match site over single base pair mismatch sites) is often poor and remains a challenge (Dervan and Edelson, 2003).

Another key concern is the accessibility of the DNA minor groove in chromatin. "The development of chemical approaches for the regulation of gene expression in cell culture requires that sequence-specific DNA binding small molecules be cell permeable, transit to the nucleus, and access specific target sites in chromatin" (Dudouet *et al.*, 2003). Several gene regulation studies using polyamides in cell culture provided both indirect and direct evidences for access to nuclear chromatin (Gottesfeld *et al.*, 1997; Dickinson *et al.*, 1998; Dudouet *et al.*, 2003).

These studies include the examination of the cellular uptake and localisation of polyamide-dye conjugates in a variety of living cells, in which the conjugates localised mainly in the cytoplasm and not in the nucleus with the exception of certain T-cell lines (Belitsky *et al.*, 2002). Another study using polyamide-fluorescein conjugates reported that the conjugate was shown to accumulate in the nuclei of HCT-116 colon cancer cells, suggesting that the fluorophore itself might play a role in cellular uptake (Crowley *et al.*, 2003). Based on this finding, a set of polyamide-fluorophore conjugates was synthesised and their nuclear uptake profiles in 13 live mammalian cell lines was tested (Best *et al.*, 2003). The results concluded that nuclear uptake does not correlate with molecular weight or with the number of imidazole residues of polyamide, although the positions of imidazole residues affect nuclear access properties significantly.

However, it is still unclear how the sequence-specific binding of polyamides is affected by both higher-order chromatin structures and the large excess of competing genomic DNA sites in the cell nucleus. Also the mechanism of inhibiting gene expression in cells is to be fully elucidated. "It will be of particular interest to understand why some genes can be switched off by polyamide treatment, while the expression of other genes that also bear the polyamide binding site are not affected" (Ebbinghaus, 2003).

1.8 Rational Design of Novel PBD Compounds

1.8.1 Biological activity of PBD based DNA crosslinking agents

In an attempt to enhance DNA-binding affinity, sequence selectivity and antitumor activity of the PBD molecules, a series of linked PBD agents have been

synthesised and evaluated. Among these are included C7- (Farmer *et al.*, 1988, 1991) or C8- (Bose *et al.*, 1992a, 1992b; Thurston *et al.*, 1996) linked PBD dimers and mixed imine-amide PBD dimers (Kamal *et al.*, 2004a). According to molecular modelling and NMR techniques C8-linked PBD dimers have greater isohelicity with the minor groove of DNA compared to C7-linked PBD dimers (Jenkins *et al.*, 1994).

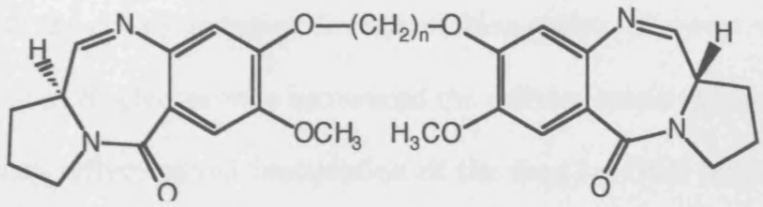

Figure 1.37 C8-linked dimer based on DC-81, DBS-120 (n = 3).

Thurston and co-workers synthesised a series of C8-linked dimers with linkers of various lengths (e.g., n = 3 – 6) (Figure 1.37), that comprises two DC-81 molecules linked through their C8 positions via a flexible inert alkyldioxy linker, and demonstrated a direct correlation between DNA interstrand cross-linking efficiency and cytotoxicity across a number of cell lines (Bose *et al.*, 1992a, b; Jenkins *et al.*, 1994; Thurston *et al.*, 1996). All four dimers showed significant cytotoxicity against three murine and one human tumour cell line *in vitro* (Bose *et al.*, 1992b). DSB-120 showed the highest DNA crosslinking efficiency, followed by n = 5 > 6 > 4 which correlates the order of cytotoxicity in several cell lines (Bose *et al.*, 1992b). It also showed enhanced DNA-binding affinity and sequence-specificity compared to the monomer DC-81 compound (Bose *et al.*, 1992b). The efficient and irreversible interstrand crosslinking ability of this dimer accounts for the improved

biological activity (Thurston *et al.*, 1999). It is approximately 50- and 300-fold more efficient in crosslinking than cisplatin and melphalan, respectively (Smellie *et al.*, 1994). The cellular pharmacology of this series of dimers was examined in a range of human tumour cell lines (Smellie *et al.*, 1994). The results revealed (i) rapid and highly efficient formation of interstrand DNA crosslinking with no evidence of single-strand breaks, (ii) poorly repaired crosslinks, and (iii) drug-induced arrest at the G2/M phase of the cell cycle typical for crosslinking agents. However, the levels of glutathione and p170 glycoprotein influenced the cellular sensitivity, suggesting that resistance may reflect partial inactivation of the drug by GSH binding or by increased activation of drug efflux, respectively. DSB-120 lacked significant antitumour activity against human tumour xenographs *in vivo* (Walton *et al.*, 1996).

1.8.2 PBD conjugates

As well as PBD dimers, a large number of PBD conjugates have been synthesised and evaluated (Figure 1.38). They include PBD-oligopyrrole hybrids (Baraldi *et al.*, 1999), C8-alkylamino-PBD (Kamal *et al.*, 2002a), C8-linked PBD naphthalimide hybrids (Kamal *et al.*, 2002b), chrysene-linked PBD hybrids (Kamal *et al.*, 2003), C8-linked PBD-benzimidazole conjugates (Kamal *et al.*, 2004c) and PBD C8 cyclic amine conjugates (Masterson *et al.*, 2004).

In the C8-alkylamino substituted DC-81s, the propane linkage was selected to enhance lipophilicity. The results indicate that the incorporation of an amino functionality appears to improve water solubility profile of the compound. They exhibit cytotoxic activity in some cancer cell lines and further studies are undergoing (Kamal *et al.*, 2002a). In the case of PBD-oligopyrrole hybrids, all hybrids exhibited

different DNA-binding activity with respect to the parent compounds distamycin A and DC-81. Also it was found that the higher number of pyrrole rings (up to n = 4) present in the hybrids led to an increase of *in vitro* cytotoxicity (Baraldi *et al.*, 1999). In addition, bis-PBD-pyrrole and imidazole polyamide conjugates have been synthesised and evaluated, which will be described in chapter 4 (Kumar and Lown, 2005).

Among the PBD C8 cyclic amine conjugates, although all the compounds were significantly cytotoxic *in vitro*, the isoindoline analogue (Figure 1.38; R_4) was the most cytotoxic and had the highest DNA-binding affinity with promising antitumour activity (Masterson *et al.*, 2004). Mixed imine-amine PBD dimers do not produce crosslinks, however, they exhibited significant DNA minor groove binding ability with promising *in vitro* antitumour activity in a number of human cancer cell lines (Kamal *et al.*, 2004a). Some of the C8-linked PBD naphthalimide hybrids (Kamal *et al.*, 2002b) and PBD benzimidazole conjugates (Kamal *et al.*, 2004c) have also shown significant DNA binding affinity as well as *in vitro* cytotoxicity.

Other PBD conjugates synthesised and evaluated by Kamal and coworkers include C8-linked PBD-acridone/acridine hybrids (Kamal *et al.*, 2004e), fluoroquinolone-PBD conjugates (Kamal *et al.*, 2005), C2-*exo*-fluorounsaturated PBD dimers (Kamal *et al.*, 2004d), alkoxyamido-linked PBD dimers (Kamal *et al.*, 2004f), PBD-anthraquinone conjugates (Kamal *et al.*, 2004b) and piperazine-linked PBD dimers (Kamal *et al.*, 2006). All of these compounds exhibited significant DNA binding affinity and promising anticancer activity *in vitro*.

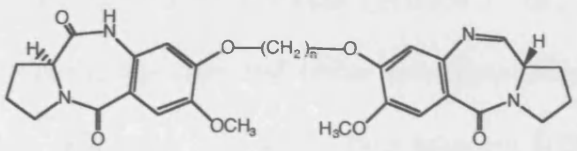

n = 3, 5, 8

Mixed imine-amide PBD

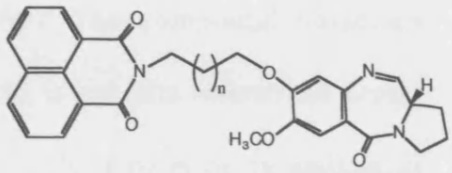

n = 1-3, 6, 8

Naphthalimide PBD

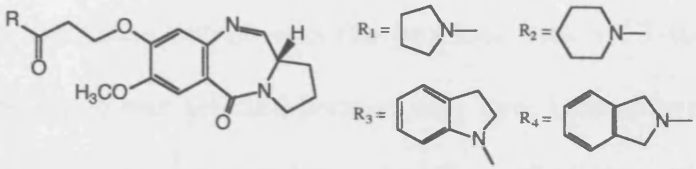

Cyclic amine PBD

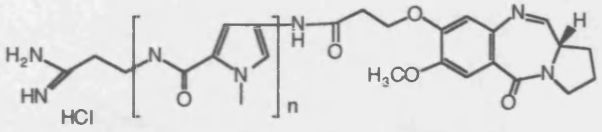

Oligopyrrole PBD n = 1- 4

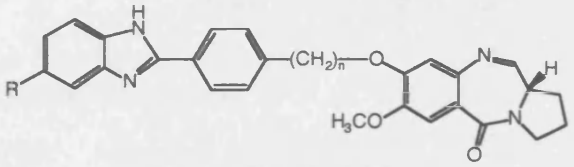

n = 3-5
R = H
= N-methylpiperazine

Benzimidazole PBD

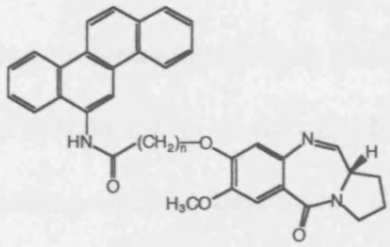

n = 3-4

Chrysene PBD

Figure 1.38 Structures of PBD conjugates.

A C8-linked DC-81 epoxide (Figure 1.39) was also designed and synthesised by Thurston and co-workers (Wilson *et al.*, 1999). The compound possesses electrophilic epoxide and imine functionalities, and it exhibits interstrand cross-linking efficiency and spans two adjacent [(GC) / (CG)] pairs or an analogous arrangement with a further spanned base pair [(GC) / N / (CG)]. The compound alkylates guanine residues on opposite strands. The C8-substituted epoxide overcame the problem of steric hindrance, which was the problem with a C7-substituted compound. An epoxide group was selected because they have been shown to have base selectivity for guanines, interacting at either the N7 or C2-NH2 position in the major or minor grooves, respectively.

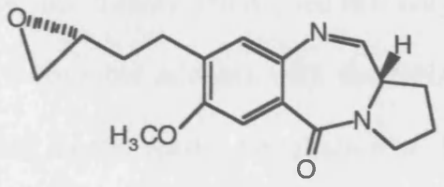

Figure 1.39 C8-linked DC-81 epoxide.

1.8.3 Sequence selectivity of PBD dimers

NMR spectroscopy and molecular modelling studies showed that DSB-120 forms a symmetric interstrand crosslink with double-stranded DNA involving a four base pair bonding site but spanning six DNA base pairs overall with a preference for 5'- PuGATCPy or 5'-PyGATCPu sequences with minimal distortion of the helix, and that it actively recognises the embedded $d(GATC)_2$ motif (Figure 1.40) (Bose *et al.*, 1992a; Jenkins *et al.*, 1994).

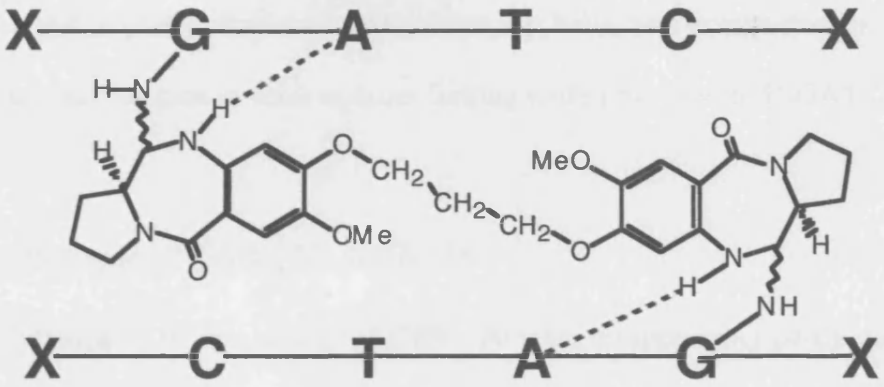

Figure 1.40 Proposed sequence selectivity of DSB-120.

Sequence selectivity studies confirmed, within the homologous PBD dimer series (n = 3 – 6), that the n = 3 and 5 (*i.e.*, odd n) homologoues are the most efficient crosslinking agents (Smellie *et al.*, 2003). The interaction energies for the interstrand crosslinking of the four dimers determined that only the dimers with n = 3 and 5 form energetically favourable adducts with the DNA hosts, and that the reactivity is inherently dictated by the spatial distribution of the PBD subunits. On the other hand, the dimers with n = 4 and 6 have poor geometry in the diether linkage which mitigate effective crosslinking of the guanines. This causes distortion to the host DNA and a poor conformation adopted by the ligand molecules, hence unfavoured in energy. The dimer with n =3 cannot tolerate an additional base pair between the two separate guanines on opposite strands (*i.e.*, 5'-GATC), whereas the extended PBD dimer with the n = 5 can crosslink a longer 5'-GATTC tract. This n = 5 compound can also crosslink, although not as efficiently, the shorter 5'-GATC sequence (Smellie *et al.*, 2003). With the dimer n = 5, the diether linkage group is snugly fit into the hydrophobic walls of the DNA minor groove in the case of 5'-

GATTC, but is partly displaced away from the helix and compacted by internal conformational rotation to achieve cross-linking within the shorter 5'-GATC tract.

1.8.4 Analogue of DSB-120: SJG-136

Subsequent *in vivo* studies of DSB-120 were disappointing partly due to the reaction of the molecule with cellular thiol-containing molecules before reaching the tumour site (Walton *et al.*, 1996). As a result, a series of derivatives with either different C2/C2' substitutions and / or unsaturation in the C-rings have since been synthesised and evaluated (Gregson *et al.*, 2001a). The unsaturation at the C2 of the ring is thought to be important for PBD monomers to be more biologically potent than molecules with C2-saturated c-rings. This can be explained by the fact that C2-unsaturation can lower the electrophilicity at the N10-C11 position, giving the agent greater availability to the target DNA sequence without reacting with thiol containing proteins. For example, tomaymycin is considerably more cytotoxic than DC-81 and binds more efficiently to DNA although it is less electrophilic overall (Morris *et al.*, 1990; Gregson *et al.*, 2001a). For this reason, a novel C2-*exo*-methylene PBD dimer, SJG-136, with unsaturation at the C2/C2' positions was synthesised (Figure 1.41) (Gregson *et al.*, 1999).

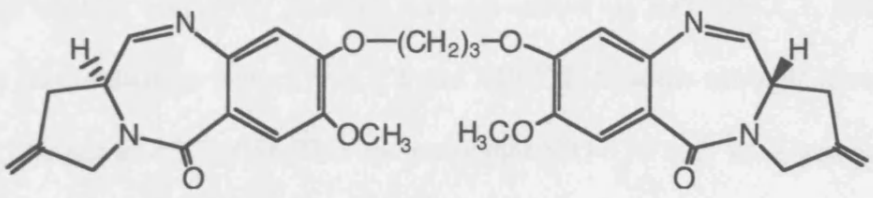

Figure 1.41 Structure of SJG-136.

SJG-136 is a more efficient crosslinking agent to naked DNA than DSB-120 and is 440-fold more efficient than the major groove cross-linking agent melphalan under identical conditions (Gregson 2001a). Molecular modelling of SJG-136 interstrand crosslinks revealed that they are relatively nondistorting for the DNA helix (Gregson *et al.*, 2001b). *In vitro* cytotoxicity assays in various human tumour cell lines have shown that SJG-136 is significantly more potent than either DSB-120 or the clinically used antitumor agent cisplatin (Gregson *et al.*, 1999, 2001b).

SJG-136 also showed significant *in vivo* activity and it has been selected for clinical trials (Hartley *et al.*, 2004, Alley *et al.*, 2004, Pepper *et al.*, 2004). The mean bar graph profiles of SJG-136 were compared by pattern recognition analysis (COMPARE) with 60,000 compounds tested in the NCI 60 cell line screen and it indicated that the SJG-136 has some similarity to other DNA binding agents. However, SJG-136 had a different activity pattern to three PBD monomers, and also the mean graph activity pattern of the agent did not fit within the clusters of any known chemotherapeutic agents. These results suggest that SJG-136 may possess a biologically distinct mechanism(s) of action (Hartley *et al.*, 2004).

SJG-136 forms interstrand crosslinks rapidly which persist in human tumour cells *in vitro*, compared with those produced by conventional DNA crosslinking agents such as the nitrogen mustards (Hartley *et al.*, 2004). However, in the case of SJG-136, the cellular sensitivity is much less dependent on XPF-ERCC1, and the homologous recombination factors XRCC2 and XRCC3, than the nitrogen mustard, melphalan (Clingen *et al.*, 2005). This indicates that SJG-136 may have activity in tumours that are resistant to conventional DNA crosslinking agents.

In conclusion, SJG-136 is the initial lead clinical candidate in a novel class of compounds that produce unique sequence selective G-G crosslinks in the minor groove of DNA and it is currently undergoing clinical trials in the UK and USA (Hartley *et al.*, 2004).

1.9 Aims of the Experimental Work

The aims of this study were to elucidate the molecular and cellular pharmacology of a series of novel PBD-based agents, which consisted of PBD dimers and PBD conjugates. The DNA interstrand crosslinking ability of PBD dimers, both in naked DNA and in cells, and their cytotoxicity were compared. The repair of ICLs induced by these agents was also investigated. For all the compounds, sequence selectivity was tested using DNA sequencing-based assays.

Methods for screening combinatorial libraries of PBD-containing compounds were also developed and studied. The methods allow solid phase 'multi-bead per compound' or 'one-bead per compound' libraries to be screened against target sequences of DNA using an appropriately labelled synthetic oligonucleotide, and hence the compound that bound to DNA could be selected. Some of the novel PBD conjugates that had been tested in the solution phase, were synthesised in the solid phase and screened against target DNA sequences for comparative determinations.

CHAPTER 2

MATERIALS AND METHODS

2.1 General Materials

2.1.1 Investigational compounds

Compounds were kindly provided by Professor David Thurston, School of Pharmacy, University of London, UK. Each compound was dissolved in methanol at a 10mM stock concentration and stored at -20°C until use. Dilutions were freshly prepared for each experiment in distilled water.

2.1.2 Plasmid DNA

pBR322 and pUC18 plasmid DNAs were obtained from Northumbria Biologicals (NBL) and was stored in 10mM Tris-HCL (pH 7.8), 1mM EDTA at -20°C.

2.1.3 Radioisotope

[γ-^{32}P]-ATP (5000 Ci/mmol, 10 mCi/ml) was purchased from GE Healthcare, Amersham, UK.

2.1.4 Cell culture

The cell lines, K562, A2780 and U937, were purchased from ECACC. Medium, foetal calf serum (FCS) and glutamine were purchased from Autogen Bioclear, Calne, UK. The human chronic myeloid leukaemia K562 and the human Caucasian

histocytic lymphoma cell lines U937 were grown as a suspension in RPMI 1640 medium, the human ovarian carcinoma cell line A2780 was grown as a monolayer in DMEM medium. Media was supplemented with 10% foetal calf serum (FCS) and 2 mM glutamine (Gln). The cells were incubated at 37°C in a 5% CO_2 atmosphere in the dark and maintained at a concentration of between 5×10^4 and 1×10^6 cells/ml, within log phase growth. Cells were passaged using conventional procedures and screened regularly for mycoplasma.

2.2 MTT Cytotoxicity Assay

2.2.1 Materials

Chemicals

Thiazolyl blue tetrazolium bromide (MTT) and phosphate buffered saline (PBS) were purchased from Sigma. Dimethyl sulfoxide (DMSO) was purchased from BDH.

2.2.2 Methods

This assay was previously described by Twentyman & Luscombe (1987). The assay is based on the ability of viable cells to reduce a yellow-coloured MTT solution into an insoluble purple coloured formazan precipitate. Following centrifugation at 270g for 5 mins, the cells were resuspended in the appropriate amount of medium (20 ml per experiment) to give 5×10^4 cells/ml. Cells were divided into 10 tubes (2 ml each), 8 drug treated and 2 controls, and incubated for 1 h at 37°C in a 5% CO_2 atmosphere in the dark. Cells were then centrifuged at 270g for 5 min at 4°C and the

supernatant discarded. Cells were resuspended in 2 ml drug-free medium and plated out in a transparent 96-well plate (round bottom for suspension cell lines and flat bottom for adherent cell lines), 8 wells per sample, 200 µl per well. The plates were then incubated for 4 days at 37°C in a 5% CO_2 atmosphere in the dark. After the incubation, 20 µl of 5 mg/ml solution of MTT in sterile PBS was added to each well and then the plates were incubated at 37°C in a 5% CO_2 atmosphere in the dark for further 5 h. The plates were centrifuged at 270g for 5 min at 4°C to pellet the cells at the bottom of the well. The medium was removed with care being taken not to disturb the pellet, leaving 10 to 20 µl in the well. 200µl of DMSO was added per well and the pellet was carefully dissolved, so as not to introduce air bubbles in to the wells. The absorption spectra of the wells were collected at a wavelength of 540 nm on a Tecan plate reader. The absorbance readings, an average of the 8 wells per sample, were then plotted as percentage of control untreated cells to determine the IC_{50} for each drug where IC_{50}= dose causing 50% inhibition of cell growth in treated cultures relative to untreated controls.

2.3 Detection of DNA Interstrand Crosslinking in Cells Using the Single Cell Gel Electrophoresis (Comet) Assay

This method was previously described by Spanswick *et al.* (1999). All procedures were carried out on ice and in subdued lighting.

2.3.1 Materials

Chemicals

Tris-hydroxymethyl-methylamine (Tris), tris-hydroxymethyl-methylamine hydrochloride salt (Tris-HCL), ethylenediaminetetraacetic acid disodium salt (Na_2EDTA), sodium chloride (NaCl), sodium hydroxide (NaOH), propidium iodide dye, Triton X-100, Type 1-A agarose and LGT agarose were purchased from Sigma.

Buffers

Lysis buffer: 100 mM Na_2EDTA, 2.5 M NaCl, 10 mM Tris-HCl, pH 10.5

Alkaline buffer: 50 mM NaOH, 1 mM Na_2EDTA, pH 12.5

Neutralisation buffer: 0.5 M Tris-HCl, pH 7.5

2.3.2 Methods

Exponentially growing K562 cells (5×10^4 cells/ml) were incubated in medium with drug at various concentrations (total volume of 2 ml per sample) for 1 h at 37°C in a 5% CO_2 atmosphere in the dark. Following the drug incubation, the samples were centrifuged at 270g at 4°C and washed twice with cold medium. Cells were then diluted to a density of 2.5×10^4 cells/ml and kept on ice. Immediately before analysis, drug treated samples and one control were irradiated with 12.5 Gy X-ray to deliver a fixed number of random DNA strand breaks. Another control remained

unirradiated. Following irradiation, 0.5 ml of sample was mixed with 1 ml of molten 1% type-VII agarose (kept at 37°C) and spread over a precoated microscope slide and a cover slip was placed on top until the agarose was set. All the slides were prepared in duplicate per dose. Cover slips were removed and slides were incubated in ice-cold lysis buffer containing 1% triton X-100, added immediately before use, for 1 h in the dark. Slides were then washed every 15 min in ice-cold distilled water for 1 h. The slides were then transferred to an electrophoresis tank containing ice-cold alkaline buffer and incubated for 45 min in the dark followed by electrophoresis in the same buffer for 25 min at 18 V (0.6 V/cm), 250mA. Slides were rinsed with neutralisation buffer for 10 min then PBS and allowed to dry overnight at room temperature. Slides were stained with 2.5 μg/ml of propidium iodide for 30 min, and rinsed with water and dried. Images were visualised using a Nikon DIAPHOT TDM inverted epi-fluorescent microscope (consisting of a high pressure mercury-vapour light source, a 580 nm dichromic mirror, 510-560 nm excitation filter and 590 nm barrier filter) at 20 x magnification. 25 cells were analysed per slide using Komet Assay Software version 4.0.2 (Kinetic Imaging, Liverpool, UK). The tail moment for each image was calculated by using the Komet Analysis software as the product of the percentage DNA in the comet tail and the distance between the means of the head and tail distributions, based on the definition of Olive *et al.* (1990).

The degree of DNA interstrand crosslinking present in a drug treated sample was determined by comparing the tail moment of the irradiated drug treated samples with irradiated untreated samples and unirradiated untreated samples. The level of DNA interstrand crosslinking is proportional to the decrease in tail moment in the

irradiated drug treated sample compared to the irradiated untreated control. The percentage decrease in tail moment was calculated using the following formula:

% decrease in tail moment = [1 - (TMdi - TMcu) / (TMci - TMcu)] x 100

where TMdi; tail moment of drug treated irradiated sample; TMcu; tail moment of untreated unirradiated control; and Tmci; tail moment of untreated irradiated control.

2.4 Detection of DNA Interstrand Crosslinking in plasmid DNA

This method was previously described by Hartley *et al.* (1991). The agarose gel electrophoresis assay was carried out using pUC18 or pBR322 plasmid DNA.

2.4.1 Materials

Chemicals

Concentrated hydrochloric acid (HCl, 12M), acetic acid were purchased from VWR International Ltd. Ultrapure agarose was purchased from Bethesda Research Laboratories (BRL). Triethanolamine, chloroform/isoamyl alcohol, sodium acetate (NaOAc), tRNA, bromophenol blue, sucrose and xylene cyanole 25:24:1 phenol:chloroform:isoamyl alcohol were purchased from Sigma. X-Omat Kodak film was purchased from Anachem.

Buffers

10x buffer: 6mM Tris-HCl (pH 7.5), 6mM $MgCl_2$, 100mM NaCl.

BAP (5x) buffer: 50mM Tris-HCl (pH 8.0), 600mM NaCl.

Forward reaction (5x) buffer: 200mM Tris-HCl (pH 8.0), 75mM 2-mercaptoethanol, 50 mM $MgCl_2$, 1.65μM ATP.

Stop Solution: 0.6M NaOAc, 20mM Na_2EDTA, 100μg/ml tRNA.

TEOA buffer: 25mM triethanolamine, 1mM Na_2EDTA, pH 7.2.

TAE agarose gel electrophoresis buffer: 40mM Tris, 20mM acetic acid, 2mM Na_2EDTA, pH 8.1.

Strand separation buffer: 30% DMSO, 1mM Na_2EDTA, 0.04% bromophenol blue and 0.04% xylene cyanol in distilled and deionised water.

Sucrose loading buffer: 0.6% sucrose, 0.04% bromophenol blue and 0.04% xylene cyanol in distilled and deionised water.

Enzymes

Hind III: 10 U/μl in in 50mM Tris-HCl (pH 7.5), 200mM KCl, 0.5mM EDTA, 1mM DTT, 0.5mg/ml BSA, 50% (v/v) glycerol, 0.1% (w/v) Triton X-100. Purchased from BRL.

Bam HI: 10 U/μl in in 50mM Tris-HCl (pH 7.5), 200mM KCl, 0.5mM EDTA, 1mM DTT, 0.5mg/ml BSA, 50% (v/v) glycerol, 0.1% (w/v) Triton X-100. Purchased from BRL.

Bacterial alkaline phosphatase (BAP): 100 U/μl in 10mM Tris-HCl (pH8.0), 0.12 M NaCl, 50% v / v glycerol. Purchased from InVitrogen.

T4 polynucleotide kinase (PNK): 5 U/μl in 50mM Tris-HCl (pH 7.5), 25mM KCl, 5mM DTT, 0.1 μl ATP, 50% v / v glycerol, 0.2 mg/ml BSA. Purchased from InVitrogen.

2.4.2 Linearisation of plasmid DNA

20 μg of the closed circular plasmid pUC18 DNA or pBR322 DNA was incubated with 10 x aqueous buffer, *HindIII* (30 units) or *Bam HI* (30 units), respectively, and distilled water (30 μl final volume) at 37°C for 1h. One tenths volume of aqueous

NaOAc (3M) and 3 volumes of EtOH (95%) were added and chilled in dry ice bath for 10 min and then centrifuged for 10 min at 1200g in a microfuge at 4°C. After centrifugation, the supernatant was removed and the DNA pellet was lyophilised to remove all ethanol. The lyophilised sample was then resuspended in 40 μl of distilled water ready for dephosphorylation.

2.4.3 Dephosphorylation of Linearised DNA

5 μg of the linearised DNA was incubated with BAP buffer, BAP (75 units) and distilled water (100 μl final volume) at 65°C for 1 h. Following the incubation, 1 volume of chloroform/isoamyl alcohol was added, vortexed thoroughly and centrifuged for 5 min at 1200g in a microfuge at 4°C. The organic layer was removed, and the aqueous layer was washed twice with 100 μl aliquots of 25:24:1 phenol:chloroform:isoamyl alcohol. The organic layers were back extracted with a 50 μl aliquot of distilled water, the aqueous layers containing DNA were combined. One tenths volume of aqueous NaOAc (3M) and 3 volumes of EtOH (95%) were added to the DNA and chilled in dry ice bath for 10 min and then centrifuged for 10 min at 1200g in a microfuge at 4°C. After centrifugation, the supernatant was removed and the DNA pellet was lyophilised to remove all ethanol. The DNA was resuspended in 40 μl of distilled water.

2.4.4 5'-End Labelling of the dephosphorylated DNA with [γ-^{32}P]-ATP

5 μg of the dephosphorylated DNA was incubated with 5x forward reaction buffer, [γ-^{32}P]-ATP (40 μCi) and T4 polynucleotide kinase (10 units) and distilled water (20

μl final volume) at 37°C for 45 min. 1 volume of aqueous NH_4OAc (7.5M) and 3 volumes of EtOH (95%) were then added and the mixture was chilled, centrifuged as described in section 2.4.3. The supernatant was removed and the DNA pellet was resuspended in 50 μl of distilled water. One tenths volume of aqueous NaOAc (3M) and 3 volumes of EtOH (95%) were added to the DNA and chilled, centrifuged and lyophilised as described in section 2.4.3. The DNA was resuspended in double distilled water at a concentration of 1μg / 8μl.

2.4.5 Reaction protocols

Approximately 100 ng of 5'-end labelled DNA was used for each experimental point. Reactions were performed with each compound at various concentrations (50 μl final volume) in 25mM triethanolamine/1mM EDTA at pH 7.2 and 37°C. After 2hr, the reactions were terminated by the addition of 50 μl of stop solution. After precipitation with 3 volumes of EtOH (95%), the samples were chilled and centrifuged, supernatant removed as described in section 2.4.3, and 75 μl of EtOH (70%) was added. The samples were centrifuged for another 10 min, supernatant removed and the DNA pellet was lyophilised as described in section 2.4.3. Samples to be denatured were resuspended in 10 μl of strand separation buffer, then denatured at 95°C for 3 min, and chilled immediately on ice prior to loading. The non-denatured control was dissolved in 10 μl of sucrose loading buffer and loaded directly.

2.4.6 Electrophoresis and Autoradiography

The samples were loaded onto a 20 cm horizontal submerged 0.8% agarose gel (25 x 20 x 1 cm) and electrophoresis was performed at 20V for 16 hr using 1 x TAE gel running buffer. After electrophoresis the gel was placed onto a layer of Whatman 3mm filter paper and a layer of DE81 anion exchange paper and dried using a Bio-Rad model 583 gel dryer connected to a vacuum. Autoradiography was performed with X-Omat Kodak film for 8 h at room temperature using a DuPont-Cronex lightingplus intensifying screen. Densitometry was carried out on a BioRad GS-670 densitometer infrared with a 7100/60 PowerPC.

2.5 Detection of DNA Interstrand Crosslinking in Synthetic Oligonucleotides

This method was previously described by Hartley *et al.* (1993).

2.5.1 Materials

Chemicals

Tetramethylenediamene (TEMED), acetonitrile were purchased from Sigma. Formamide and methanol were purchased from VWR International Ltd. The polyacrylamide gel used was the SequaGel™ Sequencing System from National Diagnostics. This was supplied as a three part ready to use system: SequaGel Concentrate (19:1 acrylamide: bisacrylamide, 8.3 M urea), SequaGel Diluent (8.3 M urea) and SequaGel Buffer (10 x TBE, 8.3 M urea, pH 8).

Chromatography Columns

Sephadex spin columns (biogel-P6: 5 base pair exclusion limit) consisted of 0.8 ml of P-6 polyacylamide were purchased from Biorad and stored in SSC, pH 7.0 (0.15 M sodium chloride, 17.5 mM sodium citrate, 0.2% sodium azide). Fluoro-impregnated silica gel coated TLC plates and Sep-Pak™ C18 desalting cartridges were purchased from Waters.

Buffers

TBE (polyacrylamide gel running buffer): 90 mM Tris, 90 mM boric acid and 2 mM EDTA, pH 8.3.

Gel slice elution buffer: 150 mM NaCl, 10 mM Tris (pH 8.0), and 1 mM EDTA.

Formamide dye buffer: 90% formamaide, 0.04% xylene cyanol, 0.04% bromophenol-blue, 0.1 mM EDTA.

2.5.2 Oligonucleotides

Synthetic oligonucleotides, synthesised on a 2 μM scale, were purchased from MWG biotech dissolved in distilled water and stored at -20°C.

Oligo-1: 5'- TATAGATCTATA -3'

3'- ATATCTAGATAT -5'

Oligo-2: 5'- TATAGATTCTATA –3'

3'- ATATCTAAGATAT –5'

Oigo-3: 5'- TACITAGATCTACITA -3'

3'- ATICATCTAGATICAT –5'

Oligo-4: 5'- TACITAGATTCTACITA -3'

3'- ATICATCTAAGATICAT -5' (where I=Inosine)

2.5.3 Purification of DNA duplexes

100 μg of each oligonucleotide per lane were purified through denaturing polyacrylamide gel electrophoresis (20%, 19:1 acrylamide: bisacrylamide. 8.3 M urea, 1.5 mm thick, 52 x 18 cm). Gels were prepared by mixing the appropriate amounts of ready-to-use gel casting solutions and then 0.8 ml 10% (w/v) ammonium persulphate and 40 μl TEMED for every 100 ml of gel casting solution to catalyse polymerisation.

Each oligonucleotide was dissolved in 10 μl formamide buffer and loaded on to denaturing polyacrylamide gels. Electrophoresis was performed for 1 h prior to loading the samples. Gels were run at approximately 3000 V using a BioRad model 3000xi power supply for approximately 3 hr. The gel was then transferred from the glass plate to cling film and placed on a fluoro-impregnated silica gel coated TLC plate. DNA was visualised by UV shadowing using a short wave UV lamp (254 nm model UVGII 215250V from Ultra-Violet Products). Full-length bands were extracted with a razor blade, crushed and soaked in 1 ml TE buffer overnight at 37°C. The samples were then desalted by flushing through Sep-Pak ™ C18 cartridges, which were in prior washed with 10 ml acetonitrile followed by 10 ml ultra-pure water, and eluted as 1.5 ml fractions with 60% methanol and lyophilised.

2.5.4 DNA measurement

The concentration of each sample was measured by fluorimetry with a Perkin-Elmer LS-2B fluorimeter. A standard curve was generated over a concentration range of 0 to 10 μg of salmon sperm DNA in 1x SSC (15 mM sodium citrate pH 7.0, 150 mM

NaCl) labelled with the DNA binding agent Hoechst 33258 (10 μg/ml) for 10 min at room temperature, in a final volume of 3 ml. Aliquots of sample were resuspended in 1x SSC and labelled with Hoechst 33258 (10 μg/ml). Fluorescence was measured at 360 nm excitation and 450 nm emission. Following the measurement, the final concentration of the sample was calculated and then solutions were lyophilised and resuspended in TEOA at 0.5 μg/μl and stored at -20°C until use.

2.5.5 5'-end labelling of DNA duplexes

5 μg self-complementary DNA was 5'-end labelled with γ^{32}P ATP using T4 polynucleotide kinase as described in section 2.4.4. Unincorporated ATP was removed from samples by centrifugation at 270g at 4°C through a Biospin column. The BioSpin columns were prepared just prior to use by spinning at 270 g twice with distilled water for 5 minutes to wash and once without for 5 min to pack the column. The samples were loaded onto the column and spun for 5 min to collect the primer in the eluent.

For non-complementary DNA duplexes, 2.5 μg single strand was 5'-end labelled in the same way prior to annealing with 2.5 μg of the complementary strand by heating to 90°C for 2 min and allowing to cool slowly to room temperature.

2.5.6 Reaction protocol and electrophoresis

0.5 μg radiolabelled dupex DNA was treated with drug in a final volume of 50 μl 1x TEOA buffer. The samples were incubated at 37°C for 2 h. DNA was recovered by ethanol precipitaion, washed with 70% ethanol, lyophilised to dryness and taken up

in 7 μl formamide dye buffer. The samples were denatured at 90°C for 2 min and chilled on ice prior to denaturing PAGE (10% gel, 19:1 acrylamide: bisacrylamide, 8.2M urea, 0.35 mm thick 52 x 18 cm) under the same condition as for duplex purification above. Gels were dried and autoradiography was performed as described in Section 2.4.6.

2.6 Measurement of Sequence Specific Covalent Binding Using *Taq* Polymerase Stop Assay

This method was previously described by Ponti *et al.* (1991).

2.6.1 Materials

Chemicals

Ammonium persulphate (APS), piperidine and boric acid were purchased from Sigma. SequaGel Sequencing system was purchased from National Diagnostics: SequaGel Concentrate (19:1 acrylamide: bisacrylamide, 8.3M urea), SequaGel Diluent (8.3M urea) and SequaGel Buffer (10x TBE, 8.3M urea, pH 8). Deoxynucleoside triphosphates (dNTPs): Ultrapure 100 mM solutions of the dNTPs were purchased from GE Healthcare.

Enzymes

Taq polymerase: 5 U/μl in 50 mM Tris-HCl (pH 8.0), 100 mM NaCl, 0.1 mM EDTA, 1 mM DTT, 50% glycerol and 1% Triton X-100. Purchased from Promega.

Buffers

Taq DNA polymerase 10x buffer: 50 mM KCl, 10 mM Tris-HCl (pH9.0), 1.5 mM $MgCl_2$ and 0.1% Triton X-100. Purchased from Promega.

Thermophilic DNA polymerase 10x buffer (Magnesium Free): 10 mM Tris-HCl (pH 9.0), 50 mM KCl and 0.1% Triton X-100. Purchased from Promega.

TBE polyacrylamide gel running buffer: 90 mM Tris, 90 mM boric acid and 2 mM EDTA, pH 8.3.

Synthetic oligonucleotide primers

The synthetic oligonucleotides were purchased from MWG. The synthetic primer, 5'-CTCACTCAAAGGCGGTAATAC, identified as pUC1, binds to the complementary strand at position 749-769 and was used to examine alkylation on the bottom strand of pUC18 plasmid DNA.

The synthetic primer, 5'-GCAGCAGATTACGCGCAGAA, identified as SCA, binds to the sequence 3090-3109 and was used to examine alkylation on the bottom strand of pBr322 plasmid DNA.

2.6.2 Linearisation of DNA plasmid

Described in section 2.4.2. The DNA pellet was resuspended in 400 μl of distilled water.

2.6.3 Drug reaction protocol

Approximately 100 ng of the linearised DNA was used for each sample. The labelled DNA was incubated with varying drug concentrations (50 μl final volume) in 25mM triethanolamine/1mM EDTA at pH 7.2 and 37°C. After 2 h, the reactions were terminated by the addition of 10 μl of NaOAC (3 M) and 40 μl of distilled water. 3 volumes of EtOH (95%) was added to the samples, chilled and centrifuged, supernatant removed as described in section 2.4.3. The samples were washed twice

with EtOH (70%) and centrifuged, supernatant removed and the DNA pellet was lyophilised as described in section 2.4.3. Samples were resuspended in 50 μl of distilled water.

2.6.4 5'-end labelling of oligonucleotide primer

An appropriate primer was 5'-end labelled with γ^{32}P ATP using T4 polynucleotide kinase as described in section 2.4.4, in a final volume of 25 μl. Unincorporated ATP was removed from the sample by centrifugation at 270g at 4°C through a pre-washed Biospin column. The BioSpin columns were prepared just prior to use by spinning at 270 g twice with distilled water for 5 minutes to wash and once without for 5 min to pack the column. The samples were loaded onto the column and spun for 5 min to collect the primer in the eluent.

2.6.5 Primer extension and electrophoresis

The drug treated DNA was combined with *Taq* DNA polymerase (1 unit), ^{32}P-5'-end-labeled oligonucleotide primer (5pmol), dideoxynucleoside triphosphate mixture (62.5nM), gelatin (0.2%), $(NH_4)_2SO_4$ (20μM), and $MgCl_2$ (2.5μM) in reaction buffer (10μl, Tris [pH 9, 75μM] / Tween 20 [0.01%]) to give a total volume of 100 μl. Thermal cycling was then carried out as follows: 94°C for 1 min (denaturation), 58°C for 1 min (annealing), and 72°C for 1 min (primer extension); this cycle was repeated for a total of 30 cycles, with the annealing step being extended by 1 s for each new cycle. The products were then precipitated with 3 volumes of EtOH (95%), washed twice with 100 μl EtOH (70%), and lyophilised as

described in section 2.4.3. Products were separated on 0.4mm thick 6% denaturing polyacrylamide at 1500V and 55°C for approximately 3 h using 1 x TBE gel running buffer. Autoradiography was carried out as described in section 2.4.6.

2.7 Measurement of Sequence Specific Binding Using a DNase I Footprinting Assay

This method was previously described by Schmitz *et al.* (1979). It was carried out using pUC18 or pBR322 and DNase I enzyme.

2.7.1 Materials

Chemicals

Ethidium bromide was purchased from Sigma.

DNA size marker

1 kb DNA ladder (1 mg/ml) in 10 mM Tris-HCl pH 7.5, 50 mM NaCl and 1mM EDTA was purchased from Invitrogen.

Kit

A Bio101 GENECLEAN II kit containing 6M sodium iodide, 'glassmilk' silica matrix and New Wash concentrate (NaCl, Tris, EDTA) was purchased from Anachem.

Enzyme

DNase I: 1 U/µl. Purchased from Promega.

Buffers

2x footprinting buffer: 10mM Tris pH 7.0, 1mM EDTA, 50mM KCl, 1mM $MgCl_2$, 0.5mM DTT and 20mM Hepes.

DNase I stop solution: 200mM NaCl, 30mM EDTA (pH8.0), 1% SDS.

Synthetic oligonucleotide primers

The synthetic oligonucleotides were purchased from MWG. The synthetic primer, 5'-TTTGGGCTGTC, identified as pUC5, binds to the sequence 930-940 of pUC18 plasmid DNA. The synthetic primer, 5'-GCATTGGTAACTGTCAGACC, identified as SRM binds to the sequence 3284-3303 of pBr322 plasmid DNA.

2.7.2 Primer labelling

An appropriate synthetic primer pUC5 (for pUC18 plasmid DNA) or SRM (for pBR322 plasmid DNA) was used as a reverse primer and was labelled using T4 polynucleotide kinase and [γ-^{32}P]ATP, as described in section 2.4.4.

2.7.3 PCR reaction

The labelled primer was combined with a forward primer pUC1 (for pUC18 plasmid DNA) or SCA (for pBR322 plasmid DNA), Taq DNA polymerase (unit 1), dideoxynucleoside triphosphate mixture (62.5nM), $(NH_4)_2SO_4$ (20μM), and MgCl2 (2.5μM) in reaction buffer (10μl, Tris [pH 9, 75μM] / Tween 20 [0.01%]) to give a total volume of 50 μl. Thermal cycling was carried out as follows: 94°C for 1 min (denaturation), 58°C for 1 min (annealing), and 72°C for 1 min (primer extension); this cycle was repeated for a total of 30 cycles, with the annealing step being extended by 1 s for each new cycle.

2.7.4 Purification of the double stranded single-end labelled fragment

Following amplification of the reverse primer, the unbound [γ-^{32}P]ATP were removed by running the sample through a BioSpin column as described in section 2.6.5. Then the sample was loaded in 2 x 25 μl aliquots onto a 2% agarose gel containing 10μl of ethidium bromide with TAE buffer and run with a 1μg of a 1kb DNA marker at 80 V for 2 hr. After the electrophoresis, the gel was viewed under UV light and the DNA bands showing the fragment (201 base pairs for pUC18 and 210 base pairs for pBR322) were cut out. Then the samples were purified using GENE clean kit using the manufacturer's standard protocol.

2.7.5 Reaction protocol and electrophoresis

The purified DNA sample was incubated with varying drug concentrations at 37°C for 2 h in 2 x footprinting buffer in a total volume of 50 µl. Then the samples were added to 0.1 units of DNase I diluted in ice-cold 10 mM Tris pH 7.0 from a stock solution (1 unit/µl) and a 1:1 solution of 250 mM $MgCl_2/CaCl_2$ mixture. The reactions were performed at room temperature for 3 min followed by precipitaion with 50 µl of stop solution. The samples were mixed with an equivolume of phenol:chloroform:isoamyl alcohol and centrifuged for 5 min at 1200g in microfuge at 4°C and the cleaved products in the upper layer were extrtacted into a fresh Eppendorf tube. This was then precipitated with EtOH (95%) in the presence of 1 µg glycogen, washed once with 70% EtOH, followed by lyophilisation as described in section 2.4.3. The dried samples were resuspended in 5 μl of formamide dye, heat

denatured at 90°C for 5 min, then placed on ice prior to loading onto the polyacrylamide gel. Electrophoresis was performed as described in section 2.6.6. Autoradiography was carried out as described in section 2.4.6.

2.7.6 Maxam-Gilbert Sequencing lanes

A purine-specific marker lane was generated using 5' single-end labelled DNA. 7 μl of labelled DNA was incubated at room temperature for 5 min in 50 μl of 70% formic acid, 10 μl distilled water. Following incubation, samples were snap frozen with a dry ice/ethanol bath and dried by lyophilisation. The DNA pellet was resuspended in 65 μl of a freshly diluted and chilled 10% piperidine solution and incubated at 90°C for 30 min. The DNA was then precipitated with one tenths volume of NaOAC (3 M) and 2 volumes of EtOH (95%), washed twice with EtOH (70%) and lyophlised. Samples were taken up in 4 μl formamide loading dye, heat denatured at 90°C for 5 min, then placed on ice prior to loading onto the polyacrylamide gel, which is loaded with other samples.

CHAPTER 3

EVALUATION OF NOVEL PYRROLO [2,1-c] [1,4] BENZODIAZEPINE (PBD) DIMERS: THE EFFECT OF LINKER LENGTH AND C2/C2' SUBSTITUENTS

3.1 Introduction

As discussed in Chapter 1, in an attempt to enhance the sequence selectivity and antitumour potency of the PBD molecules, C7- (Farmer, *et al.*, 1988) and C8-linked dimers (Bose *et al.*, 1992) have been synthesised. According to molecular modelling C8-linked dimers have greater isohelicity with the minor groove of DNA compared to the C7-linked dimers (Jenkins *et al.*, 1994). The first C8/C8'-linked dimer to be synthesised was DSB-120 (Figure 3.1) (Bose *et al.*, 1992) which comprises two DC-81 molecules linked through their C8 positions via a flexible diether linkage.

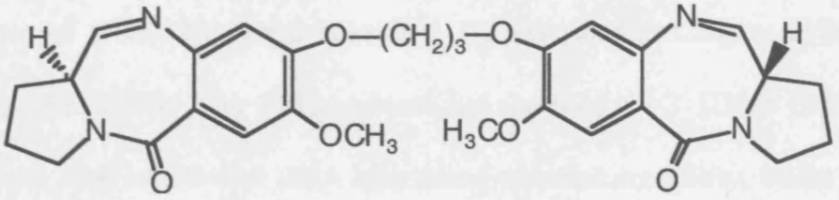

Figure 3.1. Structure of DSB-120.

DSB-120 exhibits potent *in vitro* cytotoxicity and enhanced DNA-binding affinity and sequence-specificity compared to DC-81 (Smellie *et al.*, 1994). The potent, irreversible interstrand cross-linking ability of the PBD dimers accounts for their

improved biological activity (Thurston *et al.*, 1999). NMR spectroscopy and molecular modelling studies showed that DSB-120 spans six DNA base pairs, actively recognising a 5'-GATC-3' sequence with minimal distortion of the helix (Bose *et al.*, 1992a; Jenkins *et al.*, 1994). However, the subsequent *in vivo* studies of DSB-120 were disappointing partly due to the reaction with cellular thiol-containing molecules (Walton *et al.*, 1996).

The unsaturation at the C2 of the C-ring is thought to be important for PBD monomers to be more biologically potent than molecules with C2-saturated C-rings. This can be explained by the fact that C2-unsaturation can lower the electrophilicity at the N10-C11 position (Morris *et al.*, 1990), giving the agent greater availability to the target DNA sequence without reacting with thiol-containing proteins. For example, the less electrophilic tomaymycin is considerably more cytotoxic than DC-81, and binds more efficiently to DNA (Morris *et al.*, 1990; Gregson *et al.*, 2001a).

In an attempt to produce PBD dimers with improved *in vivo* antitumour activity, several analogues of DSB-120 were synthesised. As described in Chapter 1, the fully saturated C-ring PBD dimers with odd numbered linkage (*i.e.*, n = 3- (DSB-120) and 5-methylene groups) showed efficient DNA interstrand crosslinking ability, whilst dimers with even numbered linkages (n = 4, 6) crosslinked much less efficiently (Smellie *et al.*, 2003). Therefore, analogues of DSB-120 that have C2/C2'-*exo*-unsaturation and containing either 3 and 5 methylene linkers were synthesised.

SJG-136 and DRG-16 (Figure 3.2) contain two C2-exo-methylene-substituted DC-81 subunits tethered through their C8 positions of the A-ring via an inert

propanedioxy (n = 3) and pentanedioxy (n = 5) linker, respectively (Gregson *et al.*, 2001). AT-150 and ELB-21 (figure 3.2) contain two tomaymycin subunits tethered via a propanedioxy (n = 3) and pentanedioxy (n = 5) linker, respectively.

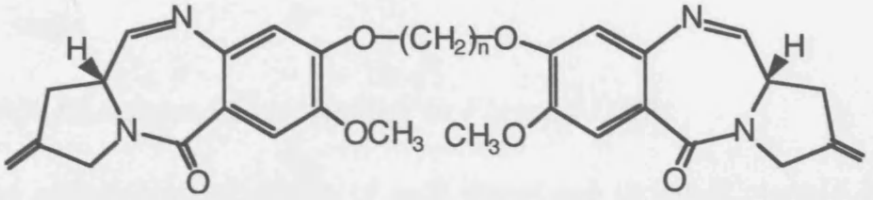

SJG-136 (n=3)

DRG-16 (n=5)

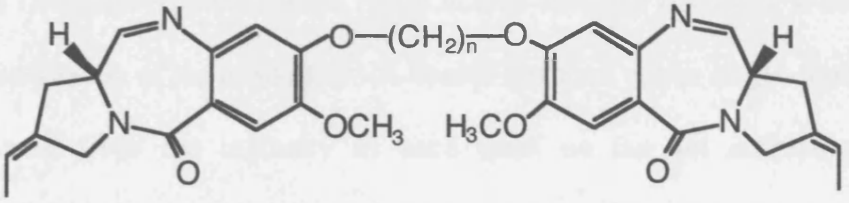

AT-150 (n=3)

ELB-21 (n=5)

Figure 3.2. Structures of novel PBD dimers containing C2/C2'-exo-unsaturation.

The aim of this study was to evaluate and compare the *in vitro* biological activity of these four novel PBD dimers. The study included measurement of cytotoxicity *in vitro*, ability of the dimers to produce DNA interstrand crosslinking both in naked DNA and cells, and measurement of sequence selectivity.

3.2 Results

3.2.1 DNA Interstrand Crosslinking in Plasmid DNA

The crosslinking efficiency of each compound in naked plasmid DNA was investigated using an agarose gel-based electrophoresis crosslink assay as described in Chapter 2. The formation of an interstrand crosslink between the two complementary DNA strands prevents the separation of the two strands when denatured. Such crosslinked DNA molecules therefore run as double-stranded DNA in a neutral agarose gel. The quantitation of the amount of the double-stranded versus single-stranded DNA was measured from the intensity of each band on the gel autoradiograph by densitometry and the % crosslinking in a given DNA sample is calculated. As an example of the assay, the known interstrand crosslinking agent, cisplatin, was tested. Figure 3.3 shows the autoradiograph of a crosslinking gel for cisplatin and the quantitation shown graphically in Figure 3.4. The result showed 50% interstrand crosslinking (XL_{50}) at a concentration of 2.3μM confirming previously reported data (Hartley *et al.*, 1991).

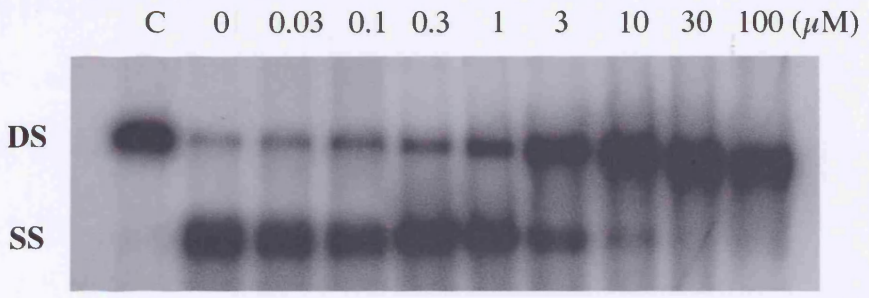

Figure 3.3 Autoradiograph of an agarose gel showing DNA interstrand crosslinking by cisplatin, in linear pUC18 plasmid DNA. Drug treatment was for 2 hours at 37°C at the concentrations shown above. C is a non-denatured control. DS = double stranded, SS = single stranded.

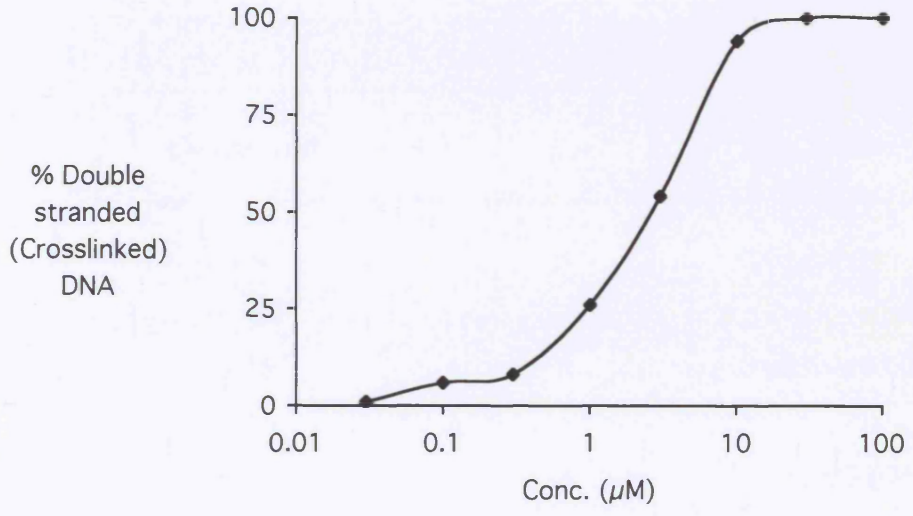

Figure 3.4 Dose response graph corresponding to the single experiment shown in Figure 3.3. Double- (DS) and single- (SS) stranded DNA were quantified by laser densitometry and a dose response curve derived.

The autoradiographs in Figure 3.5 are example gels showing the dose dependent crosslinking efficiency of SJG-136 and DRG-16. In each case an increase of crosslinked DNA with increasing concentration of agent is observed. The graph derived from the gel comparing the crosslinking ability between SJG-136 and DRG-16 is shown in Figure 3.6. The concentrations required for the four compounds to produce 50% interstrand crosslinking (XL_{50}) derived from several independent experiments in plasmid DNA are summarised in Table 3.1.

Table 3.1 50% DNA Interstrand Crosslinking Data for SJG-136, DRG-16, AT-150 and ELB-21 after 2 hr incubation at 37°C with pUC18 plasmid DNA. Data are the mean +/- standard error from at least three independent experiments.

Compound	n =	XL_{50} (μM)
SJG-136	3	0.03 ± 0.01
DRG-16	5	0.0039 ± 0.002
AT-150	3	0.045 ± 0.006
ELB-21	5	0.0027 ± 0.0016

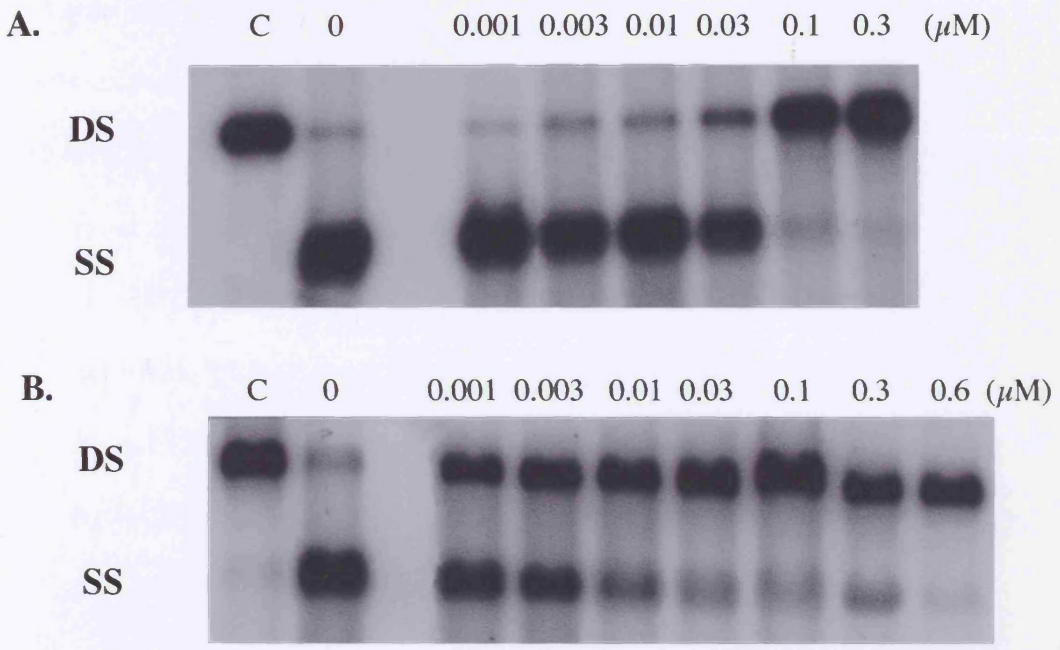

Figure 3.5 Autoradiographs of an agarose gel showing DNA interstrand crosslinking by **A**: SJG-136 and **B**: DRG-16, in linear pUC18 plasmid DNA. Drug treatments were for 2 hours at 37°C at the concentrations shown above. C is a non-denatured control. DS = double stranded, SS = single stranded.

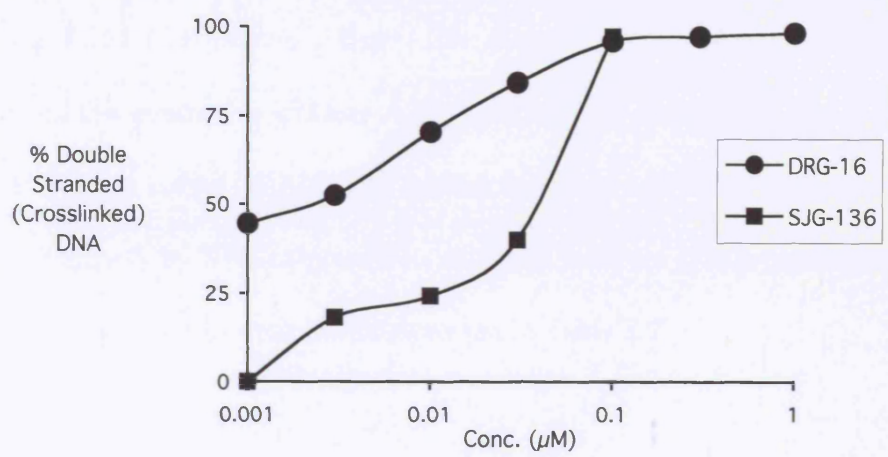

Figure 3.6 Dose response graph corresponding to the single experiments shown in Figure 3.5. Double- (DS) and single- (SS) stranded DNA were quantified by laser densitometry.

Under the conditions employed DRG-16 was found to be approximately 8-fold more efficient at producing interstrand crosslinking compared to SJG-136. Similarly, ELB-21 was 17-fold more efficient at producing interstrand crosslinking compared to AT-150. From these results it can be concluded that the compounds with the longer linker length (DRG-16 and ELB-21) are more efficient crosslinking agents.

AT-150 and ELB-21 have the extra methyl group on the C2 position compared to SJG-136 and DRG-16. This was found not to have a significant influence on the crosslinking ability of the agents since the values of XL_{50} for AT-150 and ELB-21 were similar to those for SJG-136 and DRG-16, respectively.

3.2.2 In Vitro Cytotoxicity Studies

The *in vitro* cytotoxicity of each compound against three human cancer cell lines was determined using the MTT assay. The cell lines used were the chronic myeloid leukaemia K562 (suspension culture), the histocytic lymphoma U937 (suspension culture) and the ovarian carcinoma A2780 (monolayer culture). Figure 3.7 shows the growth inhibition curves of SJG-136 against the three cell lines. The dose required to inhibit cell growth by 50% compared to untreated controls is expressed as IC_{50} and the values for the four compounds are summarised in Table 3.2.

Table 3.2 *In Vitro* Cytotoxicity Data for the PBD dimer compounds in K562, A2780 and U937 cell lines. Drug treatments were for one hour at 37°C. Data are the mean +/- standard error from at least three independent experiments.

Compound	n =	IC_{50} (μM)		
		K562	**A2780**	**U937**
SJG-136	3	0.025 ± 0.0087	0.056 ± 0.027	0.03 ± 0.001
DRG-16	5	< 0.001	0.063 ± 0.0025	< 0.001
AT-150	3	0.0034 ± 0.0021	0.045 ± 0.0012	< 0.001
ELB-21	5	< 0.001	< 0.001	< 0.001

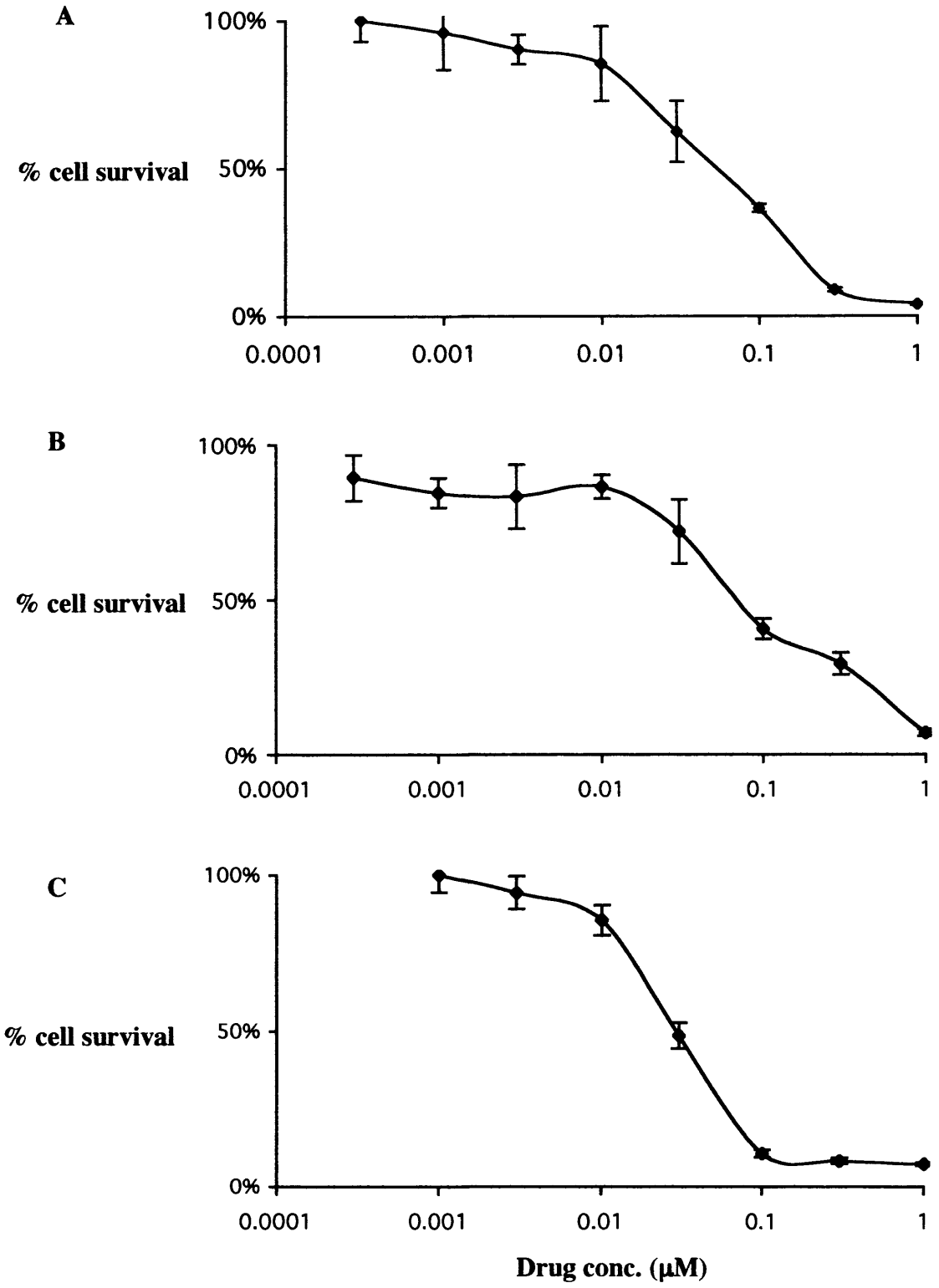

Figure 3.7. Cytotoxicity assays for SJG-136 in A: K562, B: A2780 and C: U937 cell lines. Drug treatments were for one hour at 37°C. Data are the mean +/- standard error from a single experiment.

All the compounds were found to be highly cytotoxic to the cell lines with IC_{50} values in the nanomolar, and in some cases the sub-nanomolar range. Where >50% growth inhibition was observed below 1nM accurate IC_{50} values were not determined. Between the C2/C2'-*exo*-methylene dimers, the n = 5 linked compound DRG-16 was much more cytotoxic than the n = 3 linked SJG-136 in the K562 and U937 cell lines (>25-fold and >30-fold, respectively), however in the A2780 cell line both of the agents showed similar cytotoxicity. Between the C2/C2'-*exo*-ethylene dimers, the n = 5 linked ELB-21 was more cytotoxic than the n = 3 linked AT-150 in all the cell lines. The cytotoxicity of the longer linked dimers therefore correlated with their higher efficiency of interstrand crosslinking in naked DNA.

The n = 3 linked dimer AT-150 containing the extra methyl group on the C2 position was more cytotoxic than SJG-136 against the K562 and U937 cell lines (7.4-fold and >30- fold, respectively), but no significant difference was observed in the A2780 cell line.

3.2.3 Determination of DNA Interstrand Crosslinking in Cells

The ability of the compounds to form DNA interstrand crosslinks in human K562 cells was investigated using a modification of the single cell electrophoresis (Comet) assay. Examples of typical comet images are shown in Figure 3.8. In control untreated, unirradiated K562 cells no DNA damage was detected, and the high-molecular-weight supercoiled DNA remained intact as shown in Figure 3.8A. When untreated cells are irradiated with 12.5Gy to introduce a fixed amount of random DNA

strand breaks, distinct comet tails are evident (Figure 3.8B). DNA interstrand crosslinks impede the migration of genomic DNA fragments during electrophoresis. When the cells were treated with 1nM DRG-16 for 1 h, comet tails were visible following irradiation but with reduced length and intensity compared to the irradiated control due to the presence of DNA ICLs (Figure 3.8C). With 10nM DRG-16 treated cells no comet tails were visible due to extensive ICLs (Figure 3.8D). The tail moment of the cells were measured and crosslinking expressed as % decrease in tail moment compared to irradiated controls. Figure 3.9 shows the curve for each compound showing the interstrand crosslinking efficiency against drug concentration following a 1hr incubation at 37°C. The concentration values to produce 50% interstrand crosslinking in cells for the four compounds are summarised in Table 3.3.

Table 3.3. DNA Interstrand Crosslinking Data in K562 cells after 1 hr incubation at 37°C. The data are the mean ± standard error of cells analysed from at least 3 independent experiments.

Compound	**n =**	**ICL_{50} (μM)**
SJG-136	3	0.017 ± 0.02
DRG-16	5	0.0011 ± 0.003
AT-150	3	0.0085 ± 0.001
ELB-21	5	0.0013 ± 0.003

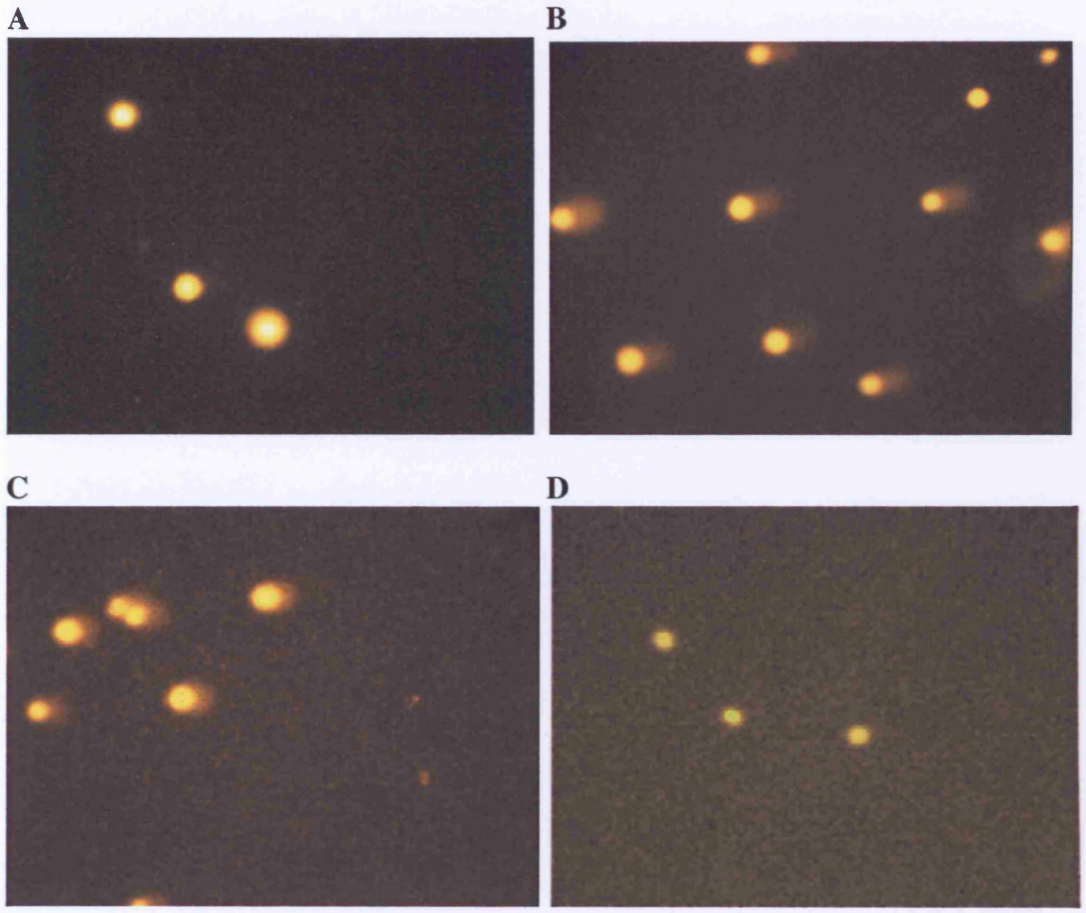

Figure 3.8 Typical Comet images of K562 cells treated with DRG-16. The drug treatment was for 1 hr. Untreated unirradiated control (A); untreated irradiated control (B); 1nM DRG-16 treated irradiated cells (C); 10nM DRG-16 treated irradiated cells (D). All images stained with propidium iodide. Original magnification, x20.

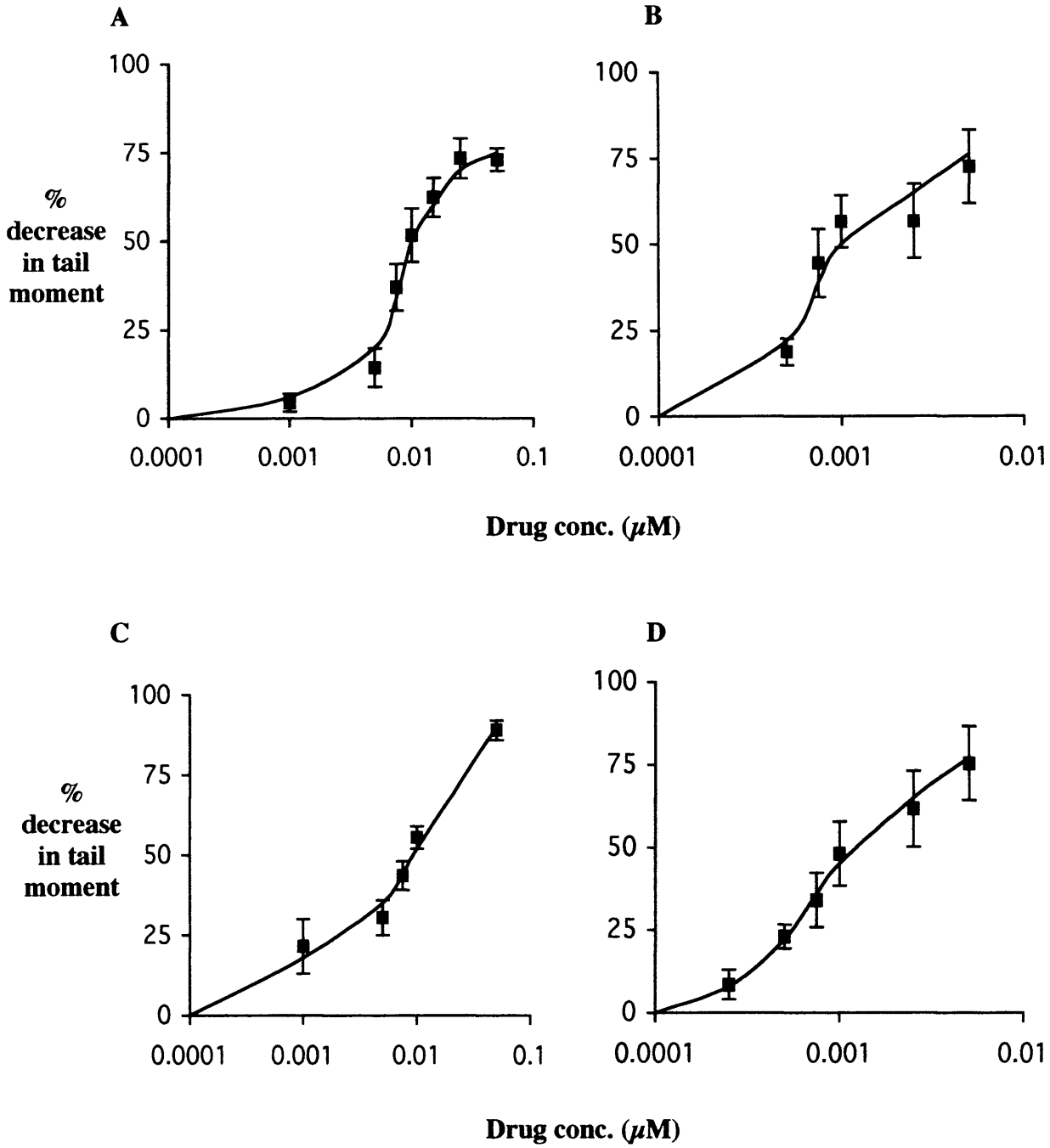

Figure 3.9. Dose dependent drug induced DNA interstrand crosslinking efficiency in K562 cells after 1 hr incubation at 37 °C. The data are the mean ± standard error of cells analysed from at least 3 independent experiments. A: SJG-136, B: DRG-16, C: AT-150 and D: ELB-21.

DRG-16 showed approximately 16-fold higher interstrand crosslinking efficiency than SJG-136 under identical treatment condition. ELB-21 showed approximately 7-fold higher interstrand crosslinking efficiency than AT-150. In addition, the compounds with the same linker length showed similar interstrand crosslinking efficiency with the longer linked pair (DRG-16 / ELB-21) being more efficient. This result correlates with their ability to produce DNA interstrand crosslinking in plasmid DNA and with their increased cytotoxicity against human tumour cells *in vitro*.

The time course of crosslink formation was studied for the four agents in K562 cells. Cells were treated for one hour at the approximate ICL_{50} value as determined from Figure 3.9. Cells were then post-incubated in drug-free medium for times up to 48 hours and samples analysed for crosslinking using the comet assay. The crosslink time course graphs are shown in Figure 3.10. For each of the agents tested crosslinks have formed in K562 cells during the 1 hour treatment, and continue to form during the post-incubation in drug-free medium. For SJG-136, the peak of crosslinks was observed by 4 hours post- incubation, and for the other three agents, the peak was observed by 2 hours post-incubation. For all four agents crosslinks persisted over a 48 hour period with no evidence of repair or unhooking.

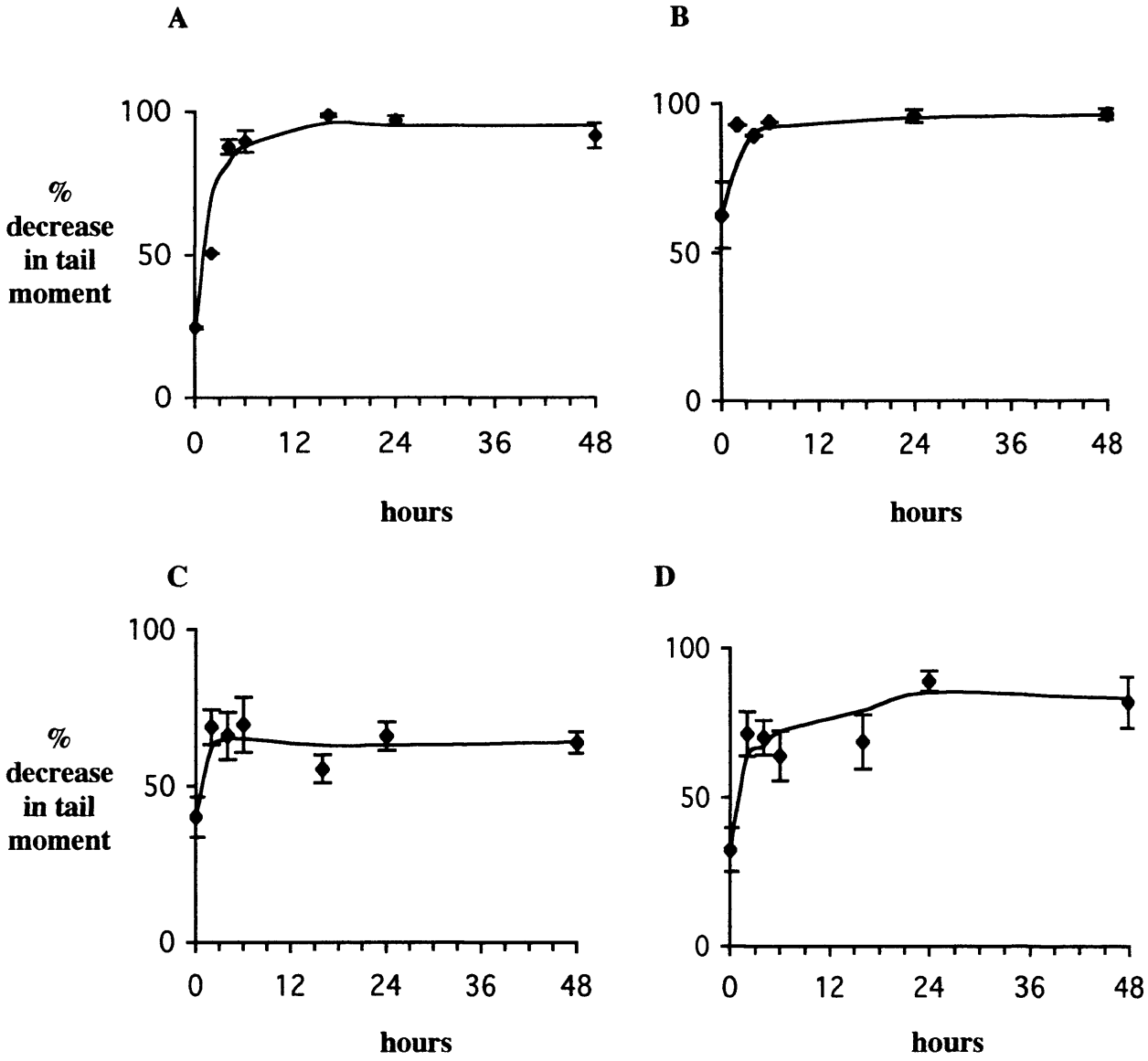

Figure 3.10. Time course of DNA interstrand crosslinking in K562 cells following a 1 hour drug exposure at 37°C. The data are the mean ± standard error of cells analysed from at least 3 independent experiments.

A: SJG-136 at 0.01μM
B: DRG-16 at 0.001μM
C: AT-150 at 0.01μM
D: ELB-21 at 0.001μM

3.3 Sequence Specificity of Alkylation

Based on the findings that DSB-120 could span six base pairs with a core sequence preference for 5'-GATC as described in chapter 1, three different sequence specificity evaluations with naked DNA were undertaken to determine whether the two propanedioxy-linked dimers, SJG-136 and AT-150, would also show the same sequence preference. In addition, the longer analogues DRG-16 and ELB-21 were studied to determine whether they could span more than 6 base pairs and exhibit a different sequence preference.

3.3.1 Determination of DNA Interstrand Crosslinking in Oligonucleotides

A pair of synthetic oligonucleotides were designed and synthesised, each containing an identical $(A/T)_4$ flanking sequence but one containing the core 5'-GATC sequence (Oligo-1) and the other containing the core 5'-GATTC sequence (Oligo-2) as shown in Table 3.4. The oligonucleotides were purified using non-denaturing polyacrylamide gel electrophoresis. The purified oligonucleotides were singly end-labelled with ^{32}P and annealed, then incubated with the four dimer compounds at 37 °C for 2 hours. The samples were then run on denaturing polyacrylamide electrophoresis gels. The method is described in detail in Chapter 2.

Experiments with Oligo-1 and -2 did not produce clear results. This may be due to the small size and low melting temperature of the duplex DNAs. As a result, longer DNA sequences, Oligo-3 and -4 (Table 3.4) were used. These oligonucleotides contained longer flanking sequences with the addition of two

inosine /cytosine base pairs. Inosine, which does not contain an exocyclic amino group and therefore cannot be covalently bound by a PBD, was used in place of guanine. Typical autoradiographs of DNA crosslinking in Oligo-3 and -4 for all four compounds are shown in Figure 3.11.

Table 3.4 The synthetic oligonucleotides used

Oligo-1:	5'- TATA**GATC**TATA -3'
	3'- ATAT**CTAG**ATAT -5'
Oligo-2:	5'- TATA**GATTC**TATA –3'
	3'- ATAT**CTAAG**ATAT –5'
Oigo-3:	5'- TACITA**GATC**TACITA -3'
	3'- ATICAT**CTAG**ATICAT –5'
Oligo-4:	5'- TACITA**GATTC**TACITA -3'
	3'- ATICAT**CTAAG**ATICAT -5' (where I=Inosine)

With the shorter oligonucleotide containing the 5'-GATC-3' core sequence (Figure 3.11A) crosslinking (measured as double stranded oligonucleotide) is observed with all four PBD dimers. At the conditions used, however, the level of crosslinking is low with <5% crosslinks observed. With SJG-136 crosslinking is observed at both 1μM and 10μM but with the other dimers significant crosslinking is only observed at 10μM. No double stranded oligonucleotide is observed in the control, denatured sample (lane a). With the longer oligonucleotide containing the 5'-GATTC-3' core sequence (Figure

3.11B) significant crosslinking is only observed with SJG-136 and AT-150 at the higher drug concentration. Evidence of drug interaction, but not crosslinking, is observed with DRG-16 and ELB-21 at 10μM by the presence of a band migrating more slowly than the single stranded oligonucleotide, suggestive of mono-alkylation (indicated by MA on the autoradiograph).

3.3.2 Determination of the sequence specificity of covalent interaction using the Taq Polymerase Assay

This technique was used in an attempt to identify the sequence specificity of covalent interaction of the compounds with naked pUC18 plasmid DNA. The principle employed is that the enzyme extends the DNA in the complex from the end of the strand and progress until it encounters the site of covalent attachment of the ligand. The method is described in Chapter 2.

The autoradiograph in Figure 3.12 shows the covalent binding sites of DRG-16 and ELB-21 in a region of pUC18 plasmid following treatment at 37°C for 2 hours. A number of premature stop sites for *Taq* polymerase in the control sample (lane a) are observed. In this assay, cisplatin was used as a control compound since the sequence selectivity of covalent interaction for cisplatin is well established. Clear evidence of dose-dependent covalent binding of cisplatin is seen in lanes j and k with sequence specificity primarily at runs of contiguous guanines as indicated. This confirms previous data with cisplatin using this assay (Ponti *et al.*, 1991).

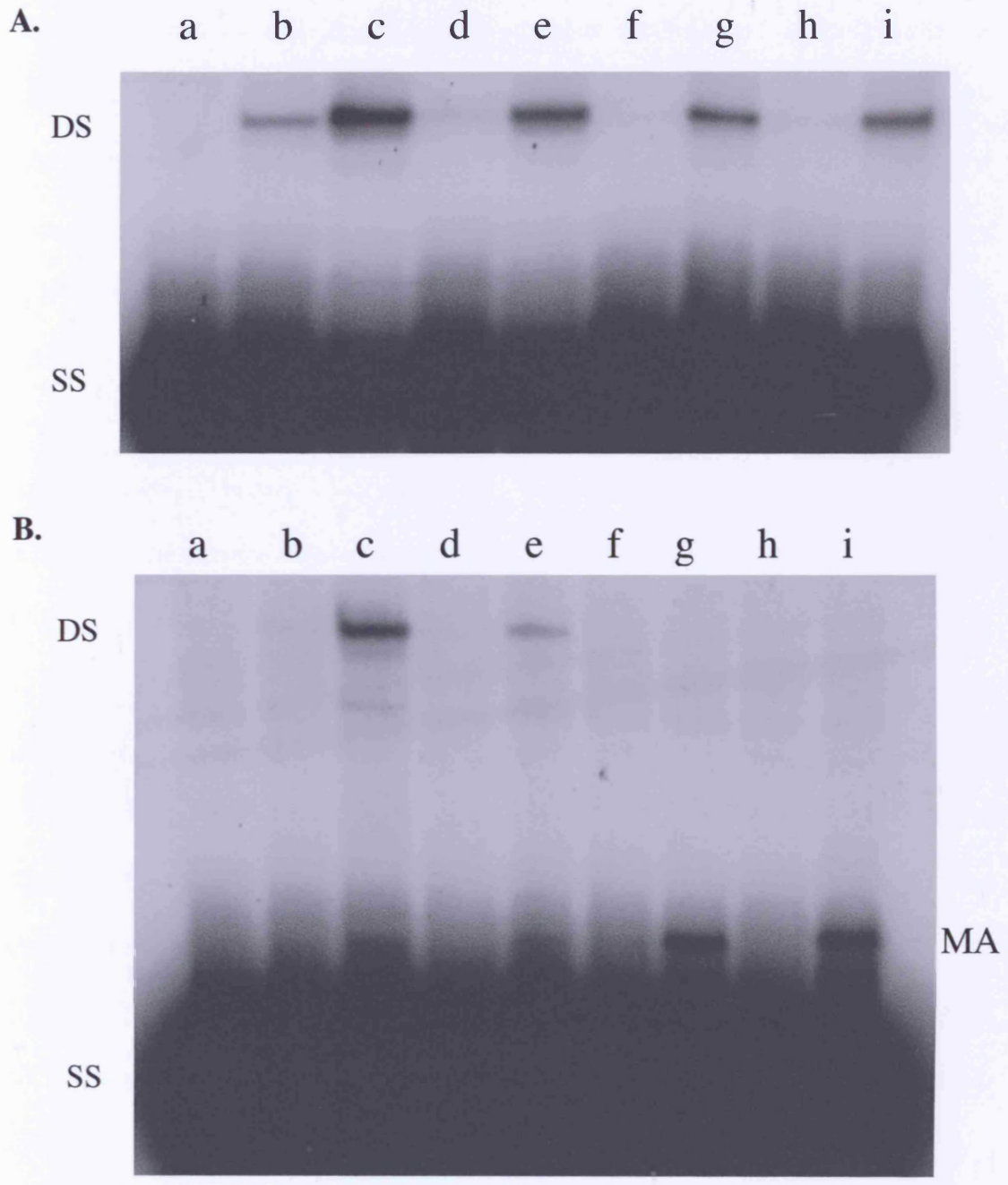

Figure 3.11. Autoradiographs of a gel showing the DNA interstrand crosslinking in oligonucleotide containing the core sequence of A: 5'- **GATC** and B: 5'-**GATTC.** Drug treatments were for 2 hours at 37°C. DS: double-stranded, SS: single-stranded, MA: mono-alkylated.

a: control
b-c: 1 μM, 10 μM (SJG-136)
d-e: 1 μM, 10 μM (AT-150)
f-g: 1 μM, 10 μM (DRG-16)
h-i: 1 μM, 10 μM (ELB-21)

There was very little evidence of sequence specific DNA interaction with the PBD dimers. DRG-16 was found to cause complete inhibition of *Taq* polymerase at concentrations of 1 and 3μM, which results in no bands (lanes d and e). However, weak evidence of covalent binding was observed at the lower concentration of 0.1 and 0.3 μM (lanes b and c). In particular, two bands that are not present in the control lane are observed as indicated by arrows. These stop sites corresponded to the sequences 5'-^{950}GATAC^{954}-3' and 5'-^{960}GTTTC^{964}-3' and were clearly at sites that were different to those for cisplatin. ELB-21 was found to give a similar result to DRG-16, binding at the same two sites. This was observed at 0.1, 0.3 and 1μM (lanes f-h) and complete inhibition of the enzyme was only observed at 3μM.

The autoradiograph in Figure 3.13 shows the covalent binding sites of DRG-16 and SJG-136 in the same region of pUC18 plasmid DNA. Again two weak bands at the same binding sites are observed with DRG-16 but these are not observed with SJG-136 at 1-3μM. Furthermore, some blocks to the polymerase by SJG-136 were seen but at different sites to those of DRG-16. SJG-136 caused inhibition of the enzyme at the concentration of 10μM. Sites of interaction of SJG-136 correspond to the sequences 5'-GTGC-3', 5'-GTTC-3' and 5'-GTCC-3'. Figure 3.14 shows the DNA sequence of pUC18 plasmid DNA corresponding to the highlighted region in the autoradiograph Figure 3.13. The binding sites of cisplatin, DRG-16 and SJG-136 are indicated.

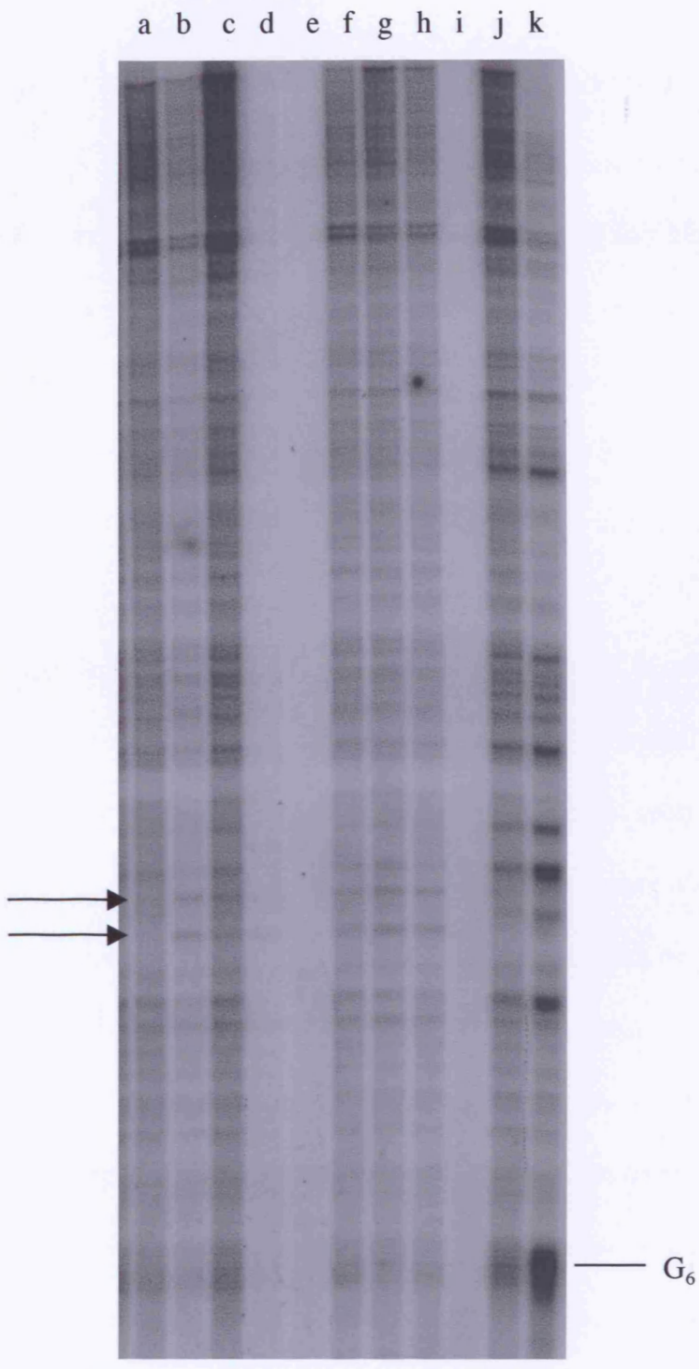

Figure 3.12 Autoradiograph of a gel showing the result of *Taq* Polymerase Stop assay for DRG-16 / ELB-21/ Cisplatin in pUC18 plasmid DNA. Drug treatments were for two hours at 37 °C. The main blocks to the polymerase by DRG-16 and ELB-21 are indicated by arrows. Sites of runs of guanines which form adducts with cisplatin are also indicated.

a: control
b-e: DRG-16 (0.1, 0.3, 1, 3μM)
f-i: ELB-21 (0.1, 0.3, 1, 3μM)
j-k: Cisplatin (0.1, 1μM)

3.3.3 Determination of Binding Sites using DNase I Footprinting

DNase I footprinting was used in an attempt to determine the sequence specificity for both covalent and non-covalent interactions of the PBD dimers with naked DNA. The experiments were carried out over a small concentration range to facilitate comparison of DNA binding of the four dimers. Areas of DNase I protection due to drug binding, or footprints, were assigned by eye as discrete regions of diminishing band intensity across all the lanes, where the intensity at these sites decreased with increasing drug concentration.

Where protection extended over a large number of base pairs at high concentrations, the primary site was assigned from the area protected at the onset of footprinting. Extended areas of protected DNA sequence seen at high drug concentrations only were not assigned as footprints, but as a non-specific binding due to drug saturation. Experiments were carried out on a GC-rich region of pUC18 plasmid DNA and an AT-rich region of pBR322 plasmid DNA. Footprinted sequences were identified by comparison with the corresponding region in GA sequencing lanes run alongside the footprinting reactions on each gel. In addition, sites of enhanced cleavage by DNase I, resulting from specific drug binding, were observed. In some cases it was difficult to assign specific recognition sites due to large areas of DNase I protection. This may be the result of overlapping binding sites or lack of cleavage by DNase I in control samples.

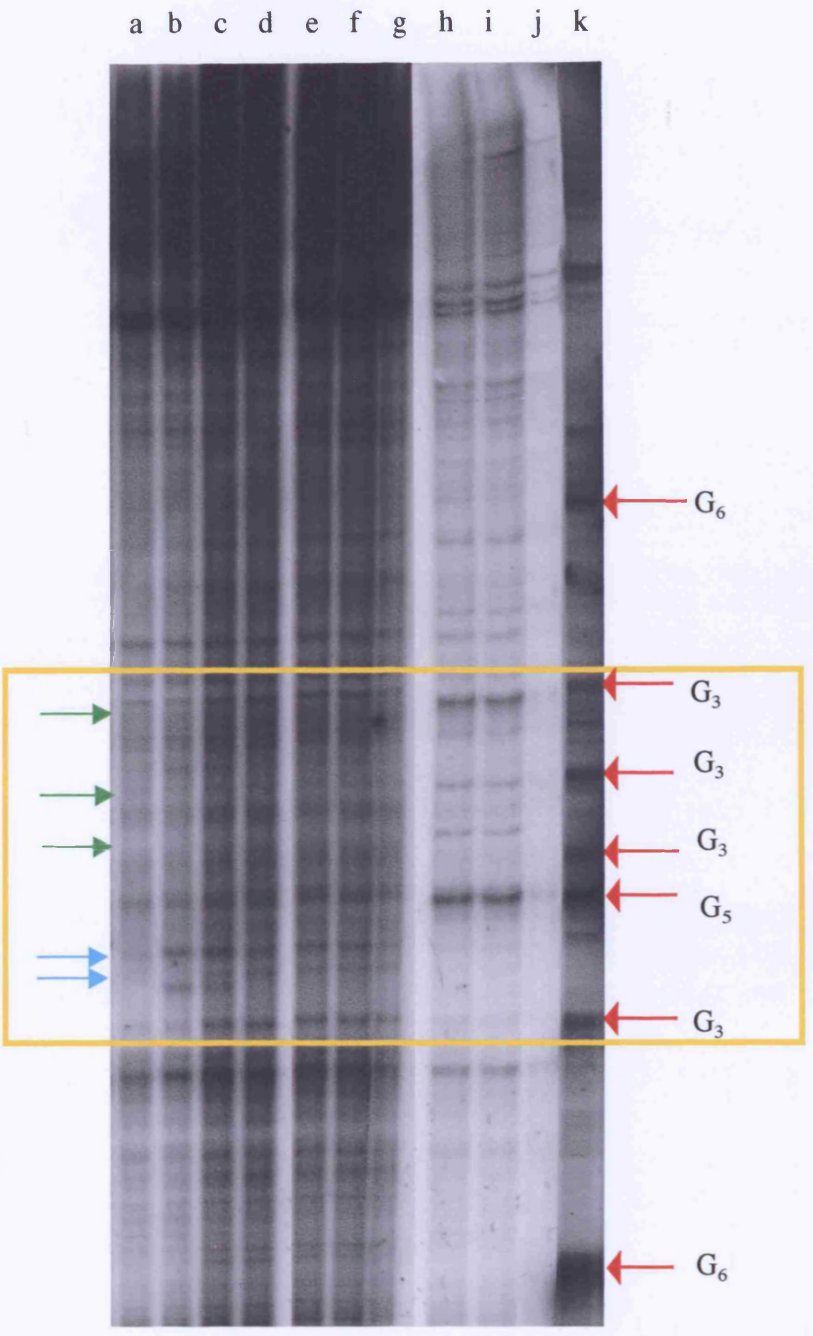

Figure 3.13 Autoradiograph of a gel showing the result of *Taq* Polymerase Stop assay for DRG-16, SJG-136 and Cisplatin in pUC18 plasmid DNA. Drug treatments were for two hours at 37 °C. The main blocks to the polymerase by DRG-16 (blue) and SJG-136 (green) are indicated by arrows. Sites of runs of guanines which form adducts with cisplatin are also indicated (red).

a: control
b-e: DRG-16 (0.05, 0.075, 0.1, 0.3, 0.5, 0.75μM)
f-i: SJG-136 (1, 3, 10μM)
j-k: Cisplatin (1μM)

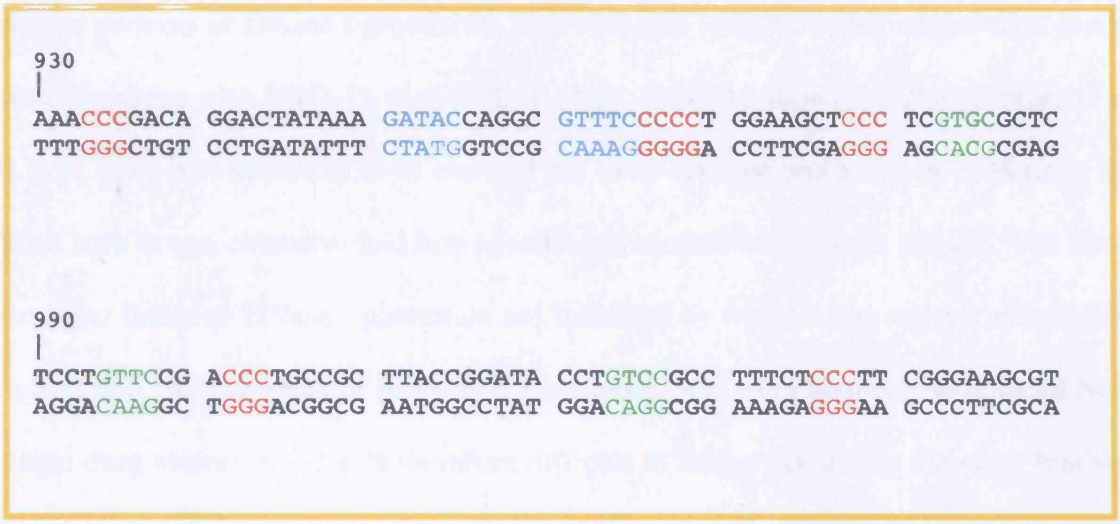

Figure 3.14. DNA sequence of region in pUC18 plasmid DNA highlighted in Figure 3.13 showing the sites of interaction for cisplatin (green), and potential alkylation sites of DRG-16/ ELB-21 (red) and SJG-136 (blue).

Cisplatin

DRG-16/ELB-21

SJG-136

The autoradiograph in Figure 3.15 shows the footprinting sites of DRG-16 and ELB-21 in a GC-rich region from pUC18. DRG-16 and ELB-21 both showed very similar patterns of DNase I protection. However, the footprints were observed at lower concentrations with DRG-16 than with ELB-21. DRG-16 showed distinct footprints at 0.3μM (lane b) whereas ELB-21 showed the same level of protection at 1μM (lane h). With both drugs, extensive and non-specific interaction was evident at 5μM. The three strongest bands of DNase I protection are indicated by white boxes and are also shown in Figure 3.16. The areas of protection span more base pairs than can be covered by a single drug molecule and it is therefore difficult to assign accurately the exact binding sites. No clear consensus binding sites are evident.

Figure 3.16 shows the autoradiograph of the binding sites of SJG-136, DRG-16 and ELB-21 in the same pUC18 fragment. DRG-16 and ELB-21 produced the same sites of interaction as shown in Figure 3.15 (indicated by boxes) and again DRG-16 produced footprints at a lower concentration. SJG-136 showed fewer and smaller footprints in this same fragment compared to DRG-16 and ELB-21, which are only observed at 3μM. Two sites, indicated by shaded boxes are shown in Figure 3.16. In addition, several drug-enhanced cleavage sites are observed with SJG-136, which are not observed with DRG-16 and ELB-21 (two are indicated by arrows).

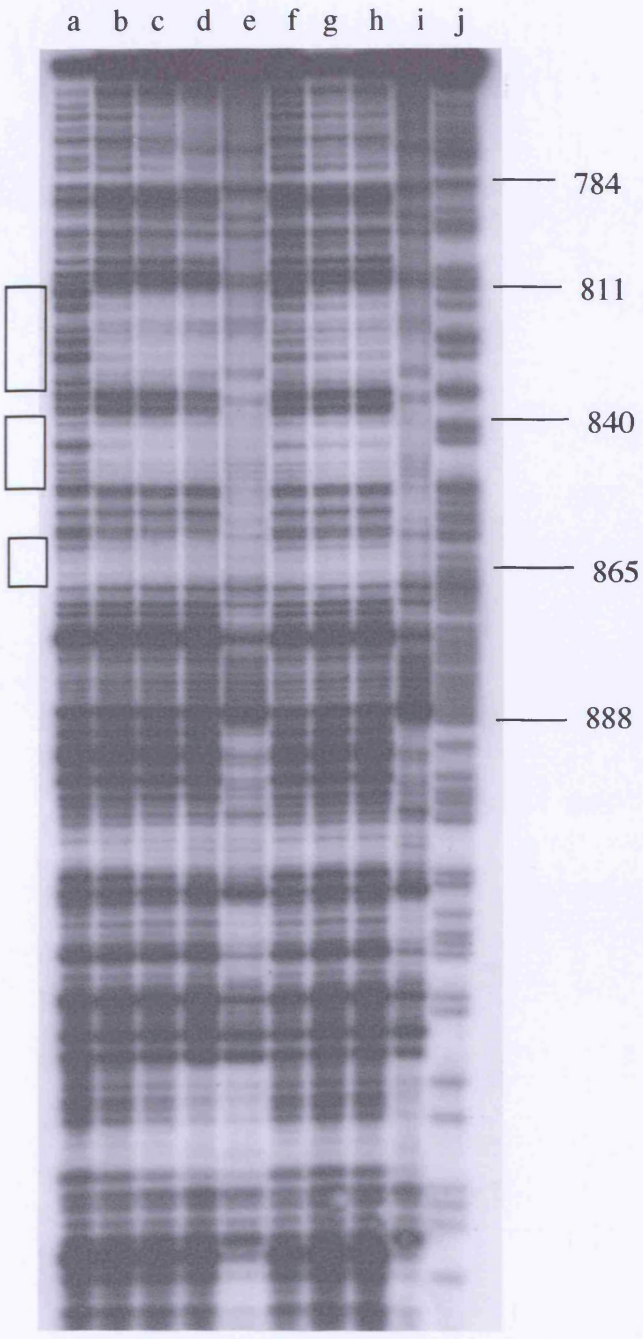

Figure 3.15 Autoradiograph of a gel showing the footprinting results for DRG-16 and ELB-21 in pUC18 plasmid DNA, showing multiple binding sites. Footprints observed at the lower concentrations are indicated by boxes.

a. Control (cleaved)
b-e. DRG-16 (0.3, 0.5, 1, 5μM)
f-i. ELB-21 (0.3, 0.5, 1, 5μM)
j. G+A marker lane

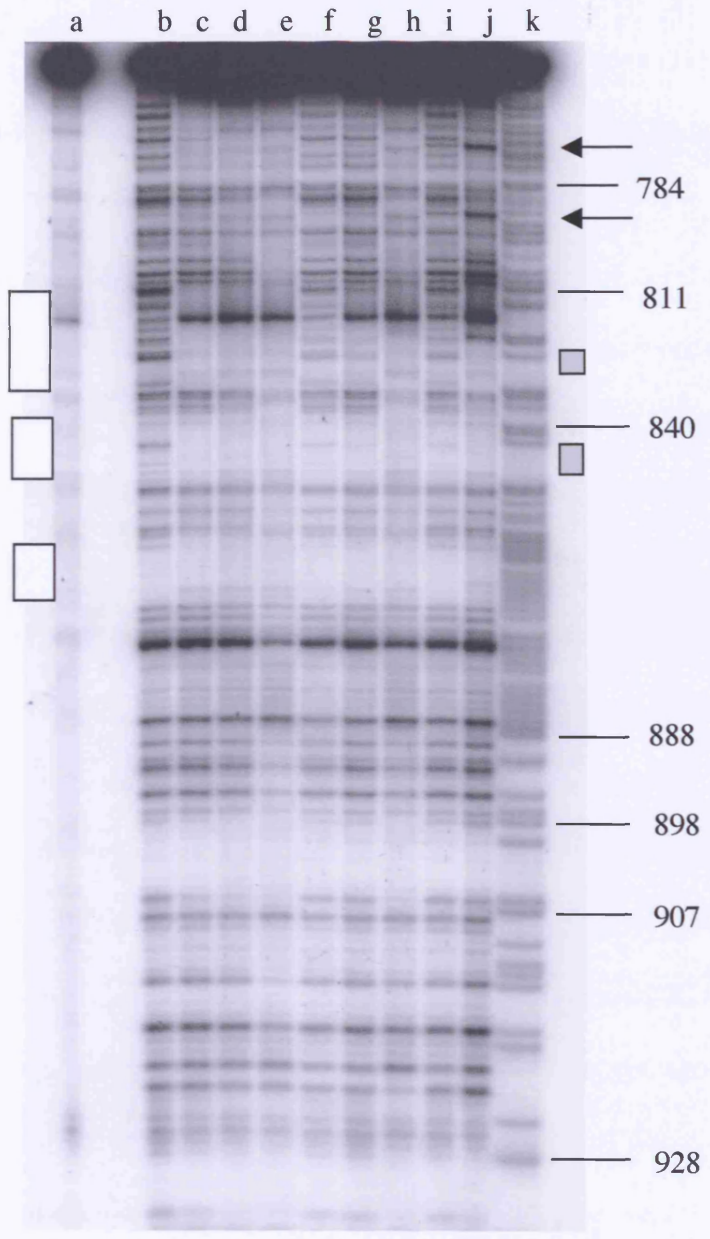

Figure 3.16 Autoradiograph of a gel showing the footprinting results for DRG-16, ELB-21 and SJG-136 in pUC18 plasmid DNA, showing multiple binding sites. Footprints observed at the lower concentrations for DRG-16 and ELB-21 are indicated by boxes. Footprints observed at the higher concentration for SJG-136 are also indicated by shaded boxes. Enhanced cleavages observed at the higher concentrations are indicated by arrows.

a. control (uncleaved)
b. control (cleaved)
c-e. DRG-16 (0.3, 1, 3μM)
f-h. ELB-21 (0.3, 1, 3μM)
i-j. SJG-136 (1, 3μM)
k. G+A marker lane

Enhanced cleavage is a clear evidence of drug interaction with the DNA causing DNA distortion and hence the enzyme to cleave at different sites. Box diagrams showing the multiple binding sites of DRG-16, ELB-21 and SJG-136 at the higher concentrations in pUC18 plasmid DNA are shown in Figure 3.17.

Figure 3.18 shows the autoradiograph of the binding sites of AT-150, DRG-16 and ELB-21 in an AT-rich region of pBR322. Higher concentrations were required for all three dimers to protect from DNase I cleavage compared to the GC-rich pUC18 fragment. Three compounds showed similar regions of protection (indicated by boxes) and are shown by box diagrams in Figure 3.19. With DRG-16 and ELB-21 weak footprints were observed at 1μM and more extensive protection at 10μM. Footprints were only observed at 10μM with AT-150. Similarly to SJG-136, enhanced cleavage was observed with AT-150 at the highest dose, which is not observed with DRG-16 or ELB-21 (indicated by arrows), again indicating a different interaction with the DNA.

Figure 3.20 shows the autoradiograph of the footprinting gel of AT-150, DRG-16, ELB-21 (as shown in Figure 3.18) and including a monofunctional PBD compound, GWL-6 (see Chapter 4). This figure includes the top portion of the gel, above the band of full length fragment (indicated by closed arrow). At the highest doses of the PBD dimer compounds, bands of high molecular weight DNA are observed above the full length fragment (indicated by open arrow). This may be due to DNA interstrand crosslinking by the dimer compounds.

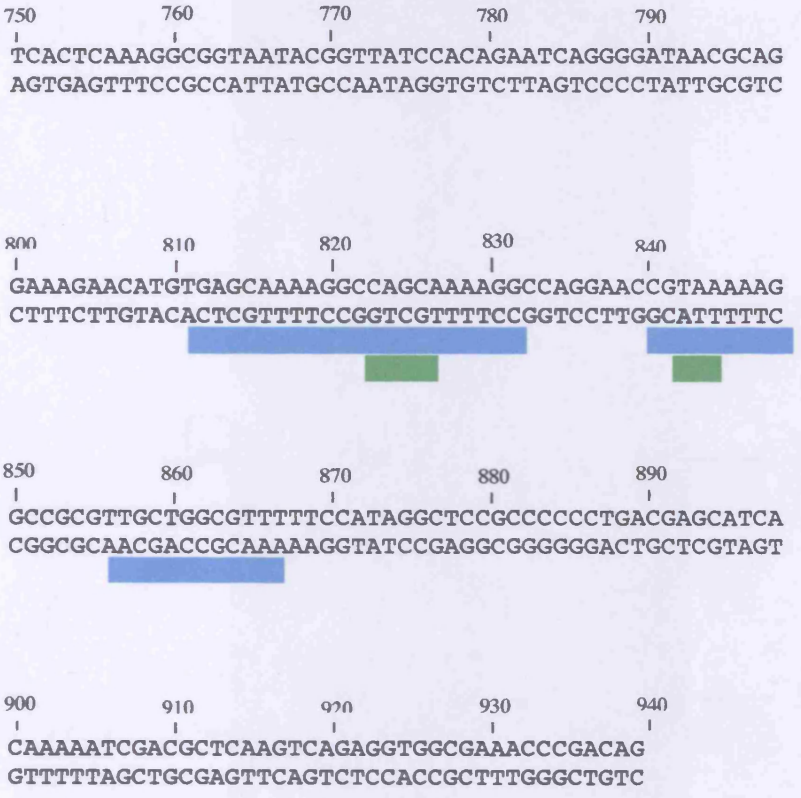

Figure 3.17. Box diagrams showing the multiple binding sites of DRG-16, ELB-21 and SJG-136 at the higher concentrations in pUC18 plasmid DNA.

DRG-16 and ELB-21

SJG-136

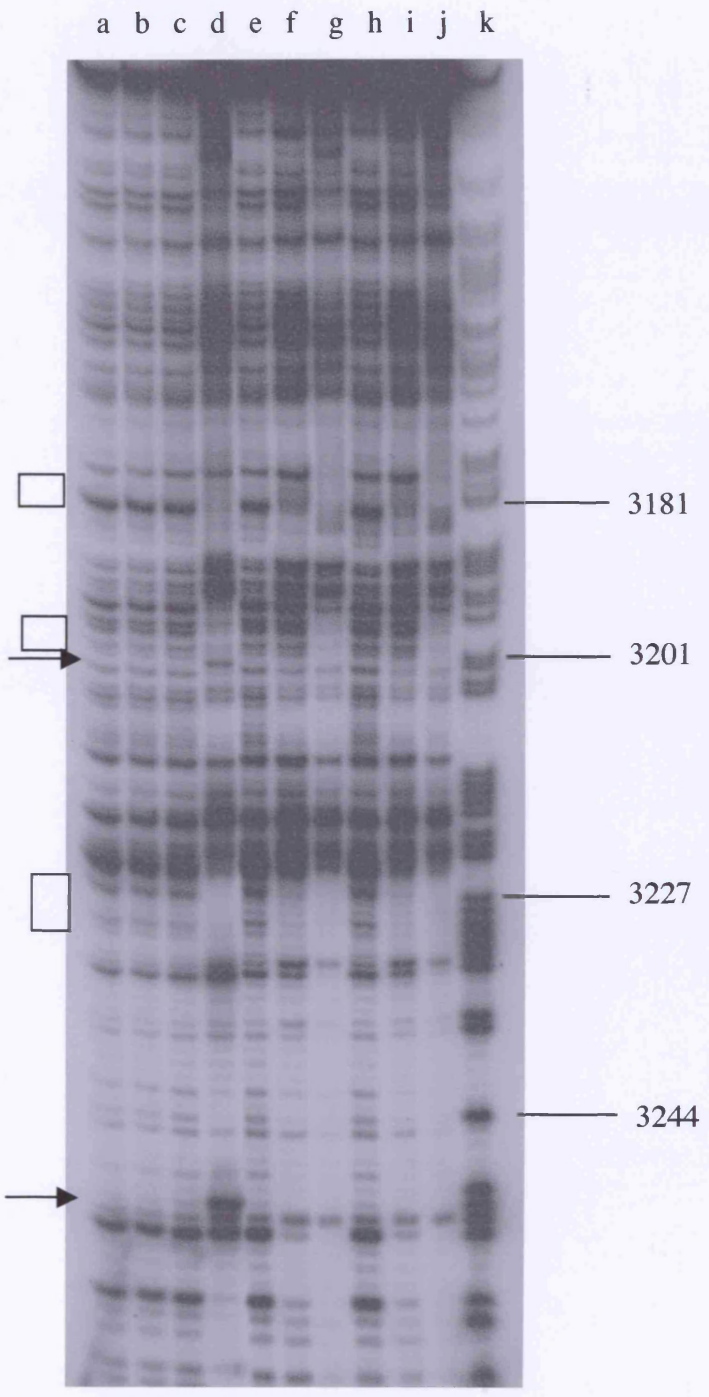

Figure 3.18 Autoradiograph of a gel showing the footprinting results for AT-150, DRG-16 and ELB-21 in pBR322 plasmid DNA, showing multiple binding sites. Enhanced cleavage observed at the higher concentration of AT-150 is indicated by arrows.

a. control
b-d. AT-150 (0.1, 1, 10 μM)
e-g. DRG-16 (0.1, 1, 10 μM)
h-j. ELB-21 (0.1, 1, 10 μM)
k. G+A marker lane

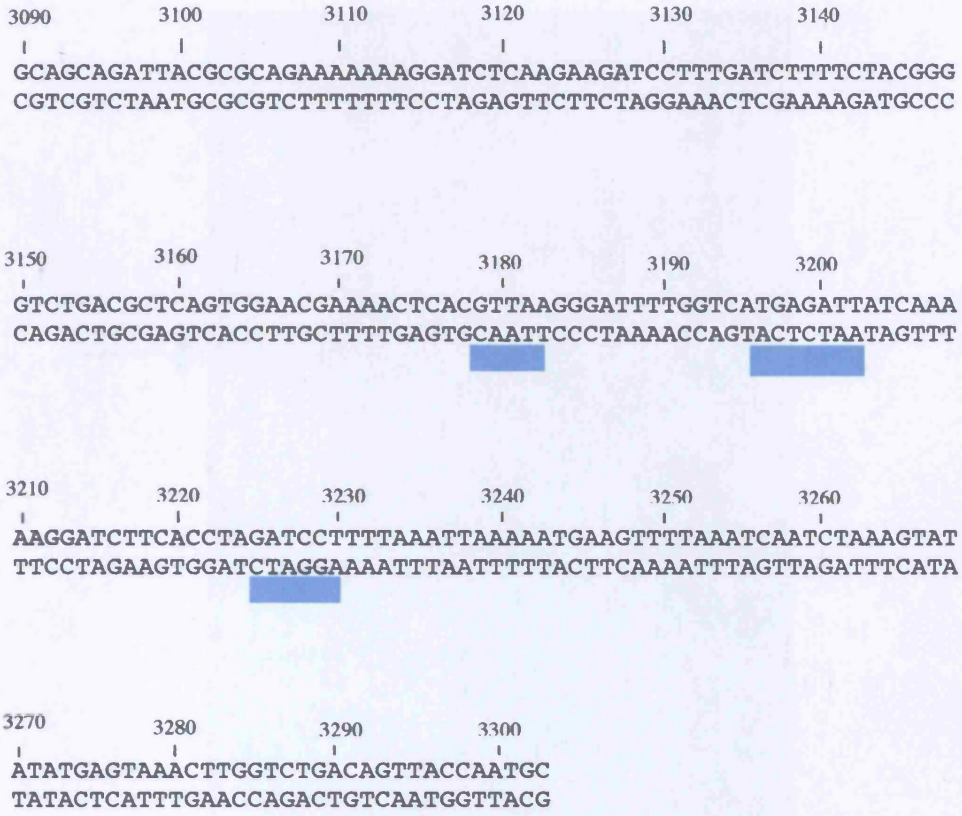

Figure 3.19 Box diagrams showing the multiple binding sites of DRG-16, ELB-21 and AT-150 at the higher concentrations in plasmid pBR322 DNA.

DRG-16, ELB-21, AT-150

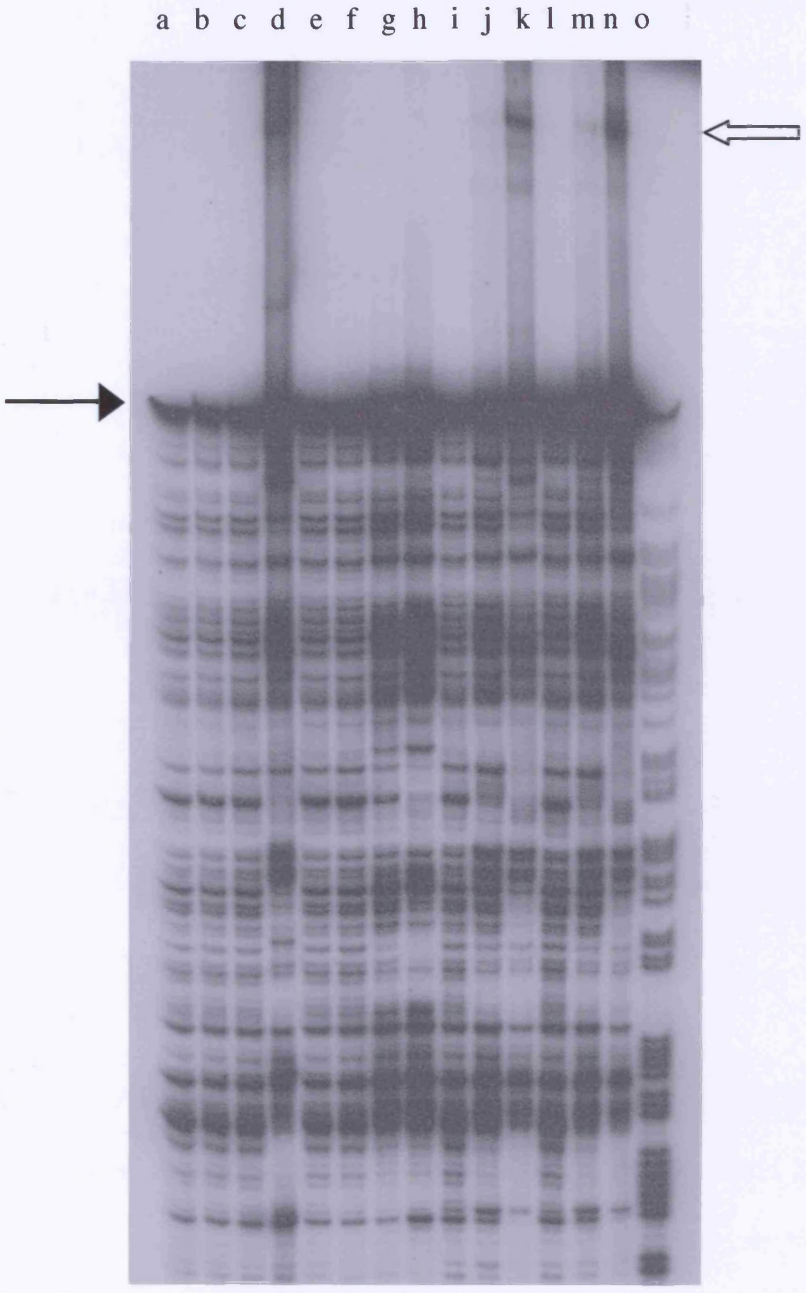

Figure 3.20 Autoradiograph of a gel showing the footprinting results for AT-150, GWL-6, DRG-16 and ELB-21 in pBR322 plasmid DNA, showing multiple binding sites. The high molecular weight of the crosslinked adducts of AT150, DRG-16 and ELB-21 are observed at the top.

a. control
b-d. AT-150 (0.1, 1, 10 μM)
e-h. GWL-6 (0.1, 1, 10, 100 μM)
i-k. DRG-16 (0.1, 1, 10 μM)
l-n. ELB-21 (0.1, 1, 10 μM)
o. G+A marker lane

In the case of GWL-6 (lanes e-h), although clear evidence of sequence selective binding is observed, no high molecular weight bands are evident, even at 100μM. This compound, containing only a single PBD moiety cannot form DNA interstrand crosslinks.

3.4 Discussion

Between the pair of C2/C2'-*exo*-methylene PBD dimers, SJG-136 and DRG-16, which contain a diether linkage (C8-O-$(CH2)_n$-O-C8' where n = 3 and 5, respectively), DRG-16 exhibited a higher crosslinking efficiency than SJG-136 by approximately 8-fold. Within the pair of C2/C2'-*exo*-ethylene PBD dimers, AT-150 and ELB-21, enhanced crosslinking activity by approximately 16-fold was observed with the increased linker length. This was in contrast to the parent dimer pair, DSB-120 and its longer analogue AT-286 (n = 5), which was previously shown to have a similar level of crosslinking (Bose *et al.*, 1992a, b; Smellie *et al.*, 2003).

DNA interstrand crosslinks in K562 cells evaluated using the comet assay also showed more efficient crosslinking activity of the 5 methylene linked compounds, DRG-16 and ELB-21, compared to their 3 linked analogues, SJG-136 and AT-150, respectively. These results demonstrate that the DNA interstrand crosslinking ability in cells follows that observed in naked DNA. Time course results of the same assay showed that in all cases crosslinks form rapidly in cells and that no repair of DNA interstrand crosslinking induced by the four PBD dimers is evident up to 48 hours.

These latter results are supported by the molecular modelling of SJG-136 and its analogues being relatively non-distorting for the DNA helix (Gregson *et al.*, 2001b) suggesting that these crosslinks on DNA will not be recognised easily by the repair mechanisms. Molecular modelling shows that the interstrand crosslinking adduct of DRG-16 is more favoured compared to the formation of an SJG-136 adduct (Gregson *et al.*, 2004). In contrast, extension of DSB-120 to AT-286 is disfavoured in overall energy for the equivalent crosslinked adducts (Smellie *et al.*, 2003). Such energetic differences may be explained in terms of superior accommodation of the C2-*exo*-PBD rings within the minor groove cavity of the host DNA molecule. Steric hindrance between the groove walls and the ring C2-hydrogens of DSB-120/AT-286 is avoided in the case of SJG-136/DRG-16/AT-150/ELB-21 (Gregson *et al.*, 2004). Importantly, the C2-*exo*-unsaturated C-ring (of SJG-136/DRG-16/AT-150/ELB-21) provides a more isohelical fit within the minor groove and hence facilitates improved groove penetration for ligand accommodation. This is why crosslinking by SJG-136 and DRG-16 is favoured compared to that of DSB-120 and AT-286, due to snug shape complementarity and avoidance of groove perturbation. In the case of the C2-saturated dimers (*i.e.*, DSB-120), localised wall distortions induced by the two C-rings are spread out within the spanned site to prevent a full isohelical drug fit of the PBD units and the tethering diether linkage (Gregson *et al.*, 2004). This perturbation is effectively excluded with the C2-*exo*-unsaturated dimers (SJG-136/DRG-16/AT-150/ELB-21).

The DNA interstrand crosslinking results of the four drugs in naked DNA and in cells follow the same general trend as their *in vitro* cytotoxicity. DRG-16 was more potent by at least 25-fold compared to SJG-136 in K562 cells following a 1 hour exposure. Similarly, ELB-21 was at least 7-fold more cytotoxic compared to AT-150. In the n = 3 linked compounds AT-150 was more potent than SJG-136. The IC50 values obtained were considerably lower than those of DSB-120 (n = 3) and AT-286 (n = 5) that had IC_{50} = 0.2 and 0.5 μM, respectively, in the K562 cell line following a 1 hour exposure (Smellie *et al.*, 1994). Interestingly, in this pair the n = 5 compound was slightly less cytotoxic than the n = 3 compound.

DRG-16 was found to be significantly more potent than SJG-136 in the NCI 60 cell line panel confirming the results found here (Gregson *et al.*, 2004). The GI_{50} values of DRG-16 ranged from 0.001 to 7.94nM (mean = 0.12nM) following continuous exposure compared to a range of 0.14 to 324nM (mean = 7.41nM) for SJG-136. Enhancement of cytotoxicity of DRG-16 compared to SJG-136 in individual cell lines ranged from a factor of ~30-fold for UACC-257 (melanoma) to >3000-fold for IGROV1 (ovarian) (Gregson *et al.*, 2004). The cytotoxicity results for the novel dimers therefore support the original theory that the unsaturation at C2/C2'- positions of the four novel dimers, which subsequently reduce the electrophilicity of the molecule compared to DSB-120 that has a saturated C2/C2', results in the improved accommodation within the minor groove of DNA. This then provides an efficient interstrand crosslinking opportunity, which results in the enhanced cytotoxicity of the

drugs. The activity *in vitro* also translates, in the case of SJG-136, into potent *in vivo* activity and has resulted in SJG-136 entering clinical trials (Hartley *et al.*, 2004; Alley *et al*, 2004). DRG-16 has also been shown recently to have significant antitumour activity *in vivo* (J. Hartley, personal communication).

Efficiency of crosslinking in naked DNA was reflected in efficient crosslinking in cells. Therefore, the gel assay (to detect crosslinking in naked DNA) is a good indicator of crosslinking in cells for PBD dimers as has been shown for major groove crosslinking agents such as the nitrogen mustards (Sunters *et al.*, 1992). The values of 50% crosslinking in naked DNA (XL_{50}) are similar to those in cells (ICL_{50}) suggesting that the dimers are able to get into cells/nuclei efficiently. Also, since the IC_{50} values correlate with the XL_{50} values in most cases, this suggests that interstrand crosslinking is the cytotoxic lesion produced by these molecules.

Thermal denaturation studies using calf thymus (CT) DNA as a host DNA duplex has been used to rank the reactivity of the PBD dimers (Gregson *et al.*, 2004). Among the DSB-120 homologues (n = 1 - 4), DSB-120 (n = 3) and AT-286 (n = 5) previously showed much better DNA reactivity than n = 2 and 4 compounds (Bose *et al.*, 1992a, b; Thurston *et al.*, 1996). In terms of induced ΔTm shift, SJG-136 and DRG-16 were similarly more effective than DSB-120 and AT-286 [*i.e.*, ~8-fold higher for DRG-16 versus DSB-120 homologue without DNA-drug incubation (t = 0 h)], but also showed this effect faster. Therefore, while DSB-120 and AT-286 gave 68 and 35% of

their maximum (*i.e.*, at t = 18 h) effect without prolonged DNA-drug contact (*i.e.*, at t = 0 h), this level increases to 76 and 97% for SJG-136 and DRG-16, respectively. From this it was concluded that DRG-16 is an unusually rapid and efficient modifier of duplex DNA. This may explain the results of the time course for interstrand crosslinking in cells of the four novel dimers. After a 1 hour of exposure of K562 cells, the peaks of crosslinks induced by all four dimers were reached in under 4 hours. In contrast, the peak of crosslinking observed after a 1 hour exposure of the same cells to the conventional major groove crosslinking agent melphalan was found to be ~16 hours, and clear evidence of loss of crosslinks was observed at 48 hours (Hartley *et al.*, 2004).

Restriction endonuclease inhibition studies have been utilised to find the relative binding affinity of DNA-interactive small molecule ligands (Balcarova *et al.*, 1992; Brabec *et al.*, 1993). Anthramycin was the first PBD molecule to be shown to have the ability to inhibit restriction endonucleases (Sumner and Bennett, 1981). More recently a quantitative restriction enzyme digest (RED100) assay was developed in which the inhibition of DNA cleavage by *Bam*H1 was used to probe the DNA binding behaviour of PBD monomers (Puvvada *et al.*, 1993). This technique was also used to study the covalent interaction of PBD dimers while clearly discriminating between the monomers and dimers. *Bam*HI was used as an endonuclease as its sequence preference for cleavage contains the 5'-GATC motif, which is favoured by DSB-120 and SJG-136 (Gregson *et al.*, 2004). The total percentage of cut DNA produced from restriction endonuclease digestion decreased as the concentration of the PBD molecule increased. It was shown that DRG-16 was the most effective of three dimers examined followed

by SJG-136 then DSB-120, while the monomer anthramycin was significantly less active. This study also correlates the results of DNA interstrand crosslinking and the *in vitro* cytotoxicity of these dimers. Furthermore, anthramycin was found to bind to DNA more rapidly compared to the dimers in a time course experiment. It was suggested that the greater sequence selectivity of binding of the dimers may lead to a kinetically limiting requirement to find a suitable binding site, and that a longer time interval may be required to target and bind to such sites since there are fewer appropriate DNA binding sites available for dimers compared to monomers (Gregson *et al.*, 2004). Nevertheless the PBD dimers form crosslinks much more rapidly than many conventional major groove crosslinking agents.

It was shown in previous studies that the PBD dimers DSB-120 (n = 3) and AT286 (n = 5), span 5'-Pu-**G**ATC-Py and 5'-Pu-**G**A(A/T)TC-Py, respectively, through interstrand crosslinking with a high degree of selectivity, with AT-286 showing some binding also in the shorter site 5'-Pu-**G**ATC-Py (Smellie *et al.*, 2003). Also molecular modelling studies of SJG-136 and DRG-16 for the same interstrand DNA crosslinking sites indicated that DRG-16 is a superior ligand compared to SJG-136 (Gregson *et al.*, 2004). It was suggested that this is partly due to the longer length of DRG-16 compared to SJG-136 and the greater opportunities for contact with the walls of the minor groove. Therefore, it was expected that SJG-136 / AT-150 pair and DRG-16 / ELB-21 pair would form interstrand crosslinks at 5'-Pu-**G**ATC-Py and 5'-Pu-**G**ATTC-Py, respectively, with the longer linker pair potentially forming crosslinks also in the shorter

5'-GATC. The molecular modelling showed that the linker group of the longer dimer is snugly held by the hydrophobic walls of the DNA minor groove in the case of 5'-GATTC, but is partly displaced away from the helix and compacted by internal conformational rotation to achieve crosslinking within the shorter 5'-GATC tract. However, the results obtained in short synthetic oligonucleotides were not as expected. SJG-136 and AT-150 showed formation of interstrand crosslinking in both sequences, 5'-GATC and 5'-GATTC with AT-150 crosslinking much less intensely in the 5'-GATTC sequence. On the other hand, the longer dimers, DRG-16 and ELB-21, both formed interstrand crosslinks in 5'-GATC sequence at higher concentration with no detectable crosslinking in the 5'-GATTC sequence. DRG-16 and ELB-21 had bands just above the single strand lanes at a higher concentration suggesting that there may be formation of mono-alkylated adducts of these drugs instead of interstrand crosslinks. Similar bands of possible monoalkylation were also observed in the previous study of Smellie *et al.* (Smellie *et al.*, 2003). In the present study, n = 3 PBD dimers, SJG-136 and AT-150, showed crosslinking across not only 4 base pairs but also 5 base pairs, although much less intensely. This was not predicted from the molecular modelling studies as it infers that there would be helical distortion on DNA if SJG-136/AT-150 were to crosslink across 5 base pairs. On the other hand, n = 5 PBD dimers, DRG-16 and ELB-21, were found to only crosslink across 4 base pairs under the assay condition, which again was not predicted by the molecular modelling studies. Unfortunately in this assay, a very small % of crosslinks is observed therefore it may not be the optimal assay to observe the efficiency of crosslinking using such small oligonucleotides.

Sites of covalent interaction in a linearised pUC18 plasmid DNA were investigated using the *Taq* polymerase stop assay. Since cisplatin showed binding to the expected sequences and at the doses used previously (Ponti *et al.*, 1991), the assay is proved to be working. However, there was very little evidence of covalent binding for the PBD compounds. This may be due to the PBD-DNA adduct being thermally unstable. High temperature (94 °C for 1 min) is involved in the PCR cycle, which may cause the PBD molecule to dissociate from the DNA. In addition, covalent linkage of the two strands of DNA produced by an interstrand crosslink will prevent separation of the two strands, which is required for the progress of the polymerase. It is therefore not clear how close to an interstrand crosslink the *Taq* polymerase can act. DRG-16 and ELB-21 showed more binding sites and also interaction at lower concentrations compared to SJG-136 or AT-150. This may be because the longer linked dimers are more stable when bound to DNA under the conditions applied. It was shown that DRG-16 and ELB-21 bind to different sites compared to SJG-136 and AT-150. In addition, a different pattern of enhanced cleavage by DNase I is observed between the shorter dimers and the longer dimers, again suggesting different interaction with the DNA.

Both covalent and non-covalent interactions of these compounds with DNA were determined by using a DNase I footprinting technique with a GC-rich region in pUC18 and an AT-rich region in pBR322 DNA fragments. Results showed that DRG-16 and ELB-21 compounds had the same binding sites, with DRG-16 having a much stronger binding affinity. SJG-136 and AT-150 bound with a different selectivity to

DRG-16 and ELB-21 and with lower affinity. There was significantly more interaction in the GC-rich region compared to AT-rich region, which correlates with the known fact that PBDs bind to guanine. There are a few 5'-GATC-3' sequence sites in the pBR322 fragment used. However, only one of the 5'-GATC-3' sequence sites was bound by the PBD dimer compounds, and also with weak intensity. This was unexpected as other reported data of DNase I footprinting studies for SJG-136 using a different DNA plasmid showed binding to 5'-GGATCC-3' with the highest intensity among the other sequences observed (Martin *et al.*, 2005). In addition, since it was 5'-GATCC-3' sequence that the dimers bound, it may be possible that the longer dimers DRG-16 and ELB-21 were crosslinking 5 base pairs instead of 4 base pairs as predicted in the molecular modelling studies. Furthermore, even if the drugs are producing crosslinks it may not be possible to observe such sites because of the high molecular weight of the crosslinked adducts (as observed in Figure 3.20) that are not digested by DNase I. Therefore it could be concluded that the binding sites observed in the footprinting results may be either mono-alkylated adducts, or non-covalent adducts, rather than crosslinking products by the PBD dimers.

In summary, the four dimers tested in this chapter showed highly efficient interstrand crosslinking ability, sequence selectivity, and significant cytotoxicity *in vitro*. The interstrand crosslinks in cells induced by all the dimers were not repaired over 48 hour period. The n = 3 linked dimers, SJG-136 and AT-150, are similar in activity, and since SJG-136 has been selected for clinical trials and shown promising

results so far, the further development of AT-150 *in vivo* is probably not warranted. The n = 5 linked dimers, DRG-16 and ELB-21, were more efficient in interstrand crosslinking and more cytotoxic than the n = 3 linked dimers. The sequence selectivity studies indicated that they may bind to different sites to the n = 3 linked dimers which could infer a different mode of action. Therefore these drugs may be of interest for further pre-clinical development. Indeed, DRG-16 is currently undergoing *in vivo* evaluation and is demonstrating significant antitumour activity *in vivo*.

CHAPTER 4

EVALUATION OF NOVEL PYRROLO [2,1-*c*] [1,4] BENZODIAZEPINE (PBD) COMPOUNDS

4.1 Introduction

In the attempt to obtain drugs with increased cytotoxicity and/or enhanced sequence selectivity, two series of novel PBD dimers and PBD conjugates have been synthesised and the evaluation of biological activity for these compounds will be presented in this chapter. The novel PBD dimers that were synthesised include SJG-428, SJG-570, LCF-178 (Figure 4.1), KG-2, KG-3, SJG-604 and SJG-605 (Figure 4.2). The novel PBD conjugates include a tripyrrole PBD conjugate, a series of aniline mustard PBDs and several novel C2-aryl PBD monomers.

Based on the molecular modelling study of a C-C2/A-C8 linked PBD dimer that is potentially an intra-strand crosslinker, two novel PBD dimers, SJG-428 and SJG-570, were synthesised. Each compound consists of two DC-81 subunits that are tethered through their C-ring and A-ring via an amide linker. These compounds were synthesised in an attempt to examine the biological activity of novel linked dimers beyond the C-C8/C-C8' linked dimers (Chapter 3) and the recently reported C-C2/C-C2' linked dimers (Reddy *et al.*, 2000), although the crosslinking efficiency for the latter compound has not been reported. SJG-428 and SJG-570 differ in that the substituent at A-C7 of the dimer is hydrogen for SJG-428 and a methoxy group for SJG-570.

Similarly, as SJG-428 and SJG-570 are potential intra-strand crosslinking agents, LCF178 with a longer linkage between the two monomer PBD units was synthesised in an attempt to introduce flexibility into the molecule and hence the potential to be an inter-strand crosslinker.

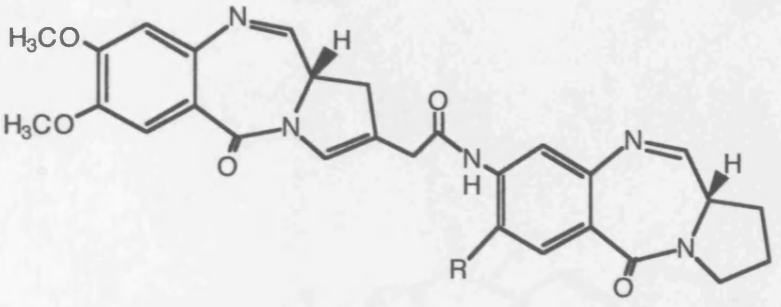

SJG-428 : R = H
SJG-570 : R = OCH_3

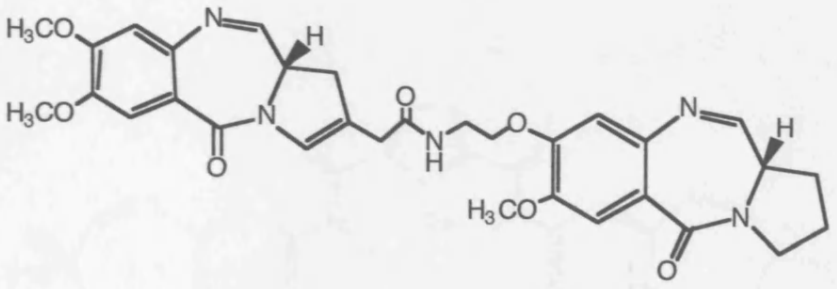

LCF178

Figure 4.1 Structures of C-C2/A-C8 linked dimers.

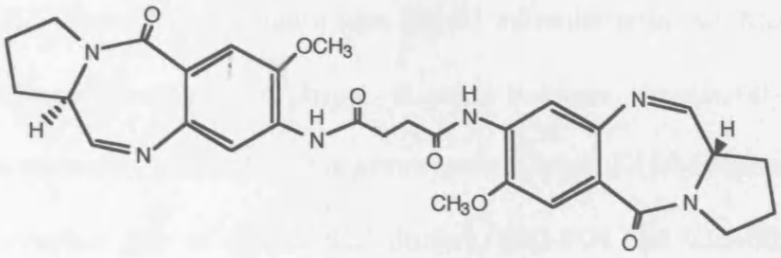

KG-2

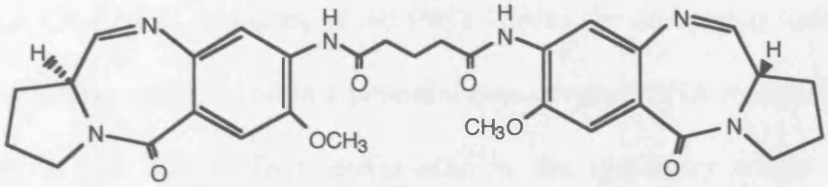

KG-3

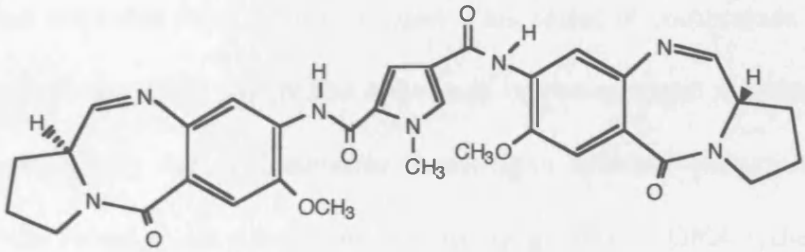

SJG-604

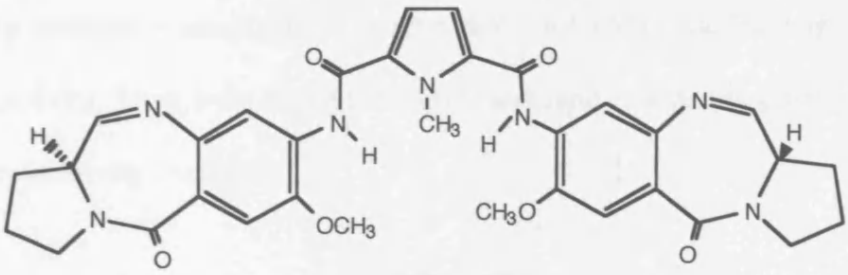

SJG-605

Figure 4.2 Structures of novel A-C8/A'-C8' linked PBD dimers.

KG-2 and KG-3 contain two DC-81 subunits tethered through their A-C8/A'-C8' positions via ethyl- and propyl- diamide linkages, respectively (Figure 4.2). They differ in symmetry where KG-2 is asymmetrical while KG-3 is symmetrical.

Another pair of novel PBD dimers, SJG-604 and SJG-605 (Figure 4.2), was synthesised. They are linked via N-methylpyrrole, which is the distamycin subunit, through the A-C8/A'-C8' positions of the PBD. Unlike the dioxyether linkage of SJG-136 analogues, these dimers contain a potential non-covalent DNA recognition (*i.e.*, AT base) moiety in the linker. They differ also in the symmetry where SJG-604 is asymmetrical and SJG-605 is symmetrical.

A series of novel PBD-aniline mustards (Figure 4.3) have been synthesised and their biological activities have been evaluated. This series of compounds include ones that consist of a single PBD tethered to either one or two nitrogen mustard moieties. It was shown previously that Tallimustine, a nitrogen mustard–polyamide conjugate (Chapter 1) was found to alkylate within the minor groove of DNA rather than in the major groove as found with non-tethered mustards (Broggini *et al.*, 1995). Hence, it was of interest whether a minor groove alkylating PBD combined with a major groove crosslinking nitrogen mustard would behave in a similar way and have any significant biological activity. They were tested for their interstrand crosslinking activity in naked DNA and cytotoxicity evaluated.

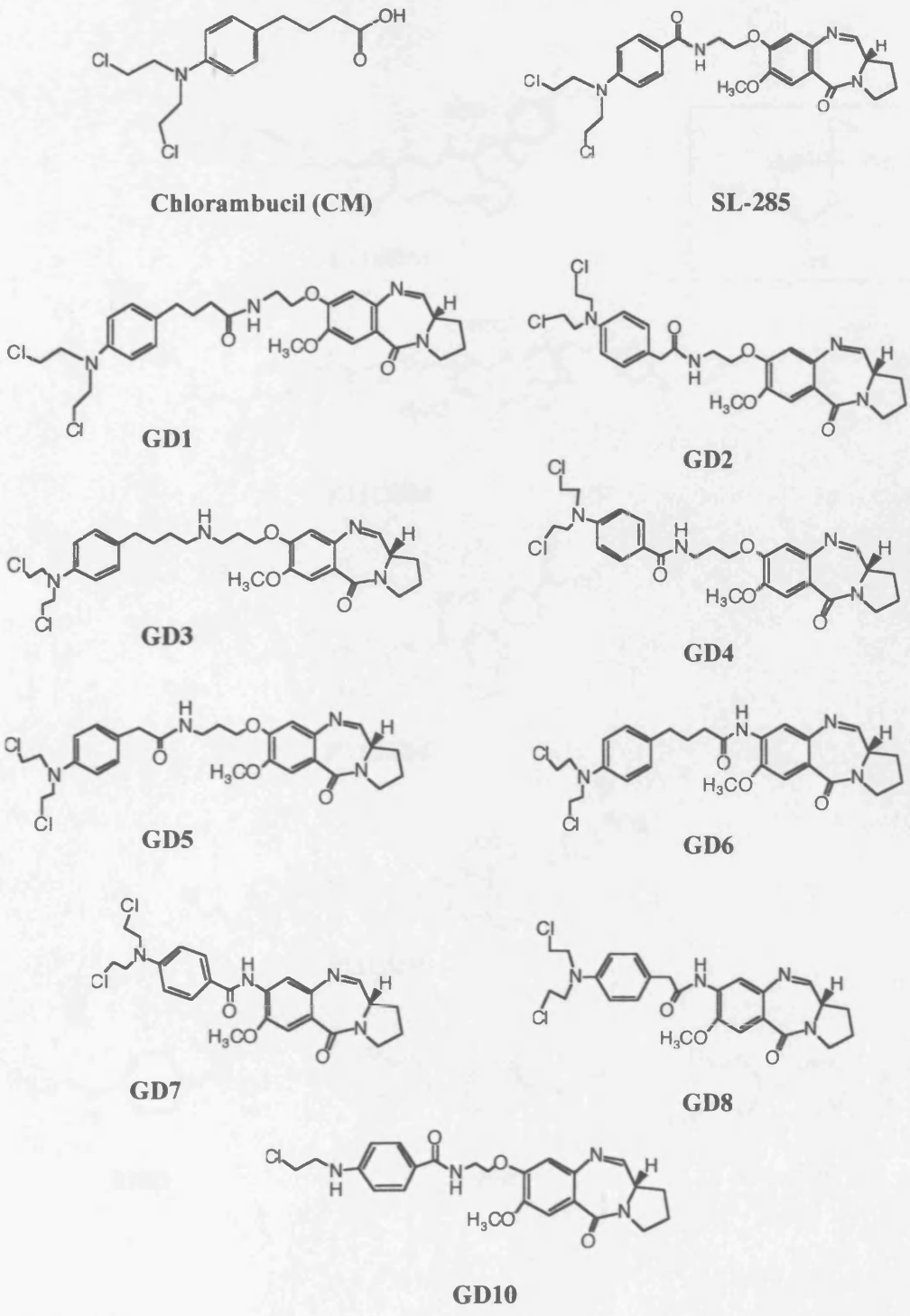

Figure 4.3 Structures of chlorambucil and novel PBD-aniline mustards.

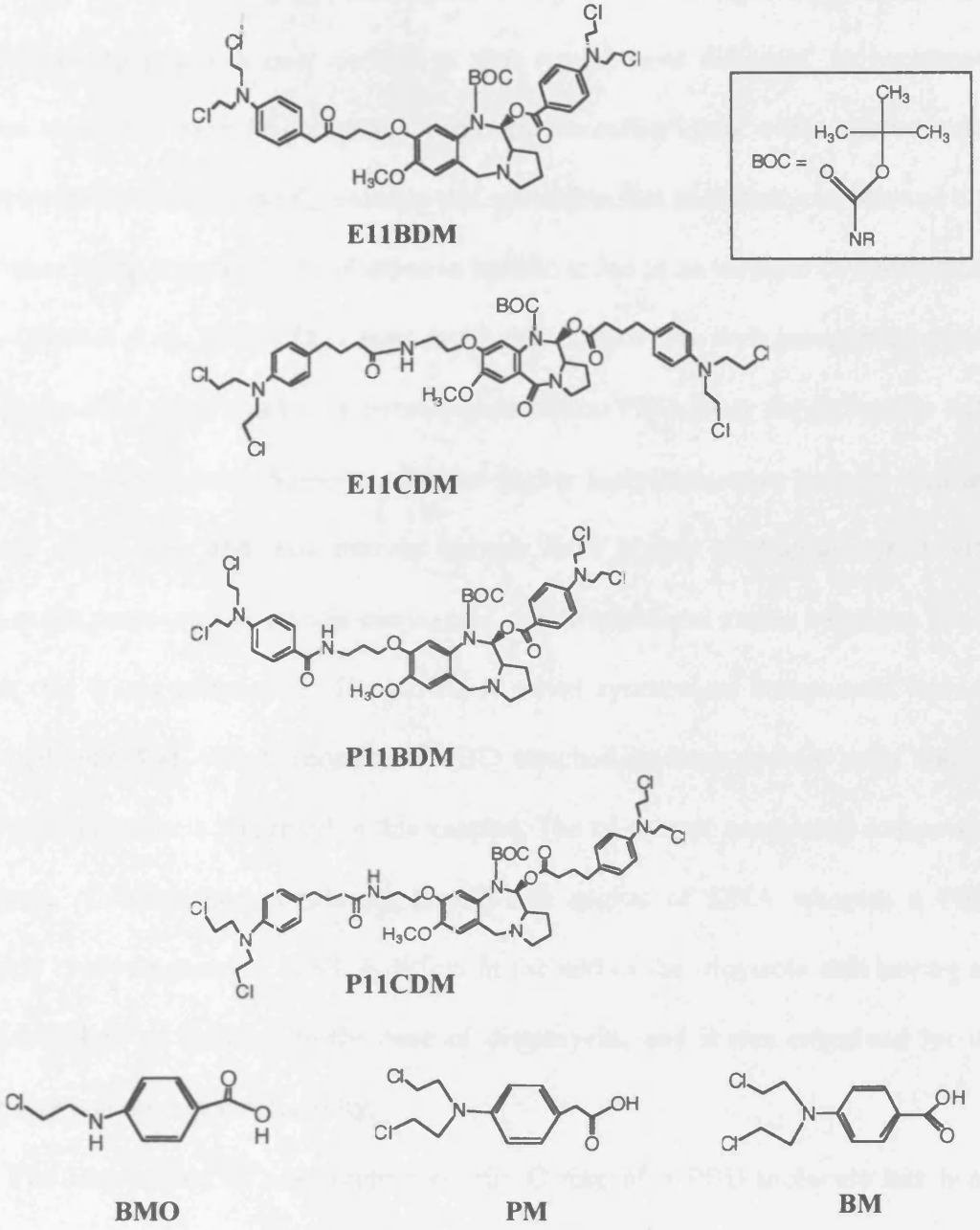

Figure 4.3 (continued) Structures of novel PBD-aniline mustards.

A series of PBD-oligopyrrole amide conjugates was designed and synthesised with the aim to obtain a new derivative that would have different, or increased, sequence selectivity over the component moieties. An earlier study with a similar series of compounds differing in the C-terminus end subunit to that of distamycin, showed that the increase in the length of the polypyrrole backbone led to an increase in cytotoxicity *in vitro* (Baraldi *et al.*, 1999). They were much more active than their parent compounds that contained the same number of pyrrole units but no PBD. Only the molecules with tri- and tetra-pyrrole units, however, showed higher antiproliferative activity than the PBD unit alone. Tri- and tetra-pyrrole hybrids have higher binding affinities with respect to the mono- and di-pyrrole conjugates, due to additional amido hydrogen bonds and van der Waals interaction. The series of novel synthesised compounds include GWL-6 (Figure 4.4), which consists of PBD attached to three pyrrole units and its biological evaluation is presented in this chapter. The tri-pyrrole containing compound, distamycin A, binds non-covalently to AT-rich region of DNA whereas a PBD covalently binds to guanine. GWL-6 differs in the end of the tripyrrole unit having an ester rather than an amidine in the case of distamycin, and it was examined for its cytotoxicity and sequence selectivity.

The importance of unsaturation on the C ring of a PBD molecule has been considered to be a responsible factor for increased cytotoxicity of PBD molecules such as anthramycin, sibiromycin (C2-*endo*/*exo*-unsaturated) and tomaymycin (C2-*exo*-unsaturated) as described in Chapter 1. The explanation for this is that the molecule is able to fit better into the minor groove of DNA without causing steric hindrance

(Puvvada *et al.*, 1993; Gregson *et al.*, 2000). As anthramycin binds to DNA more efficiently, a series of novel PBD-C2-aryl compounds with different aryl groups have been synthesised while retaining the C2-*endo*/*exo*-unstauration of the PBD. Compounds evaluated are NC020, NC048 and NC053 (Figure 4.5), in which the substituent at C2 are toluyl, biphenyl and naphthyl, respectively. These molecules were compared for their cytotoxicity and sequence selectivity.

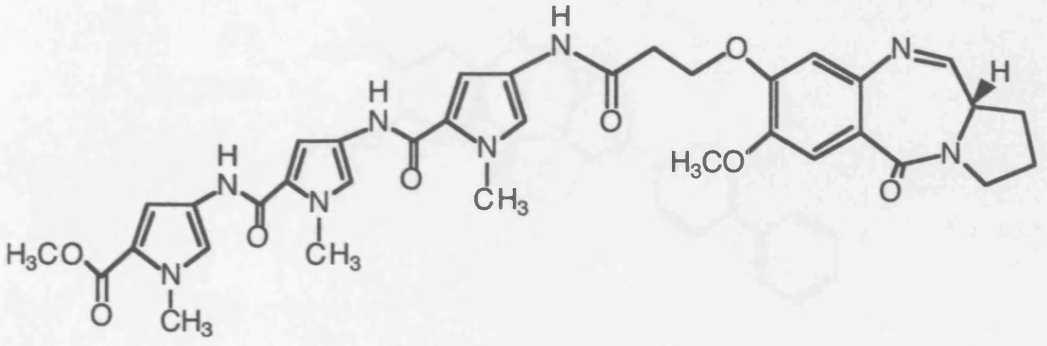

Figure 4.4 Structure of GWL-6.

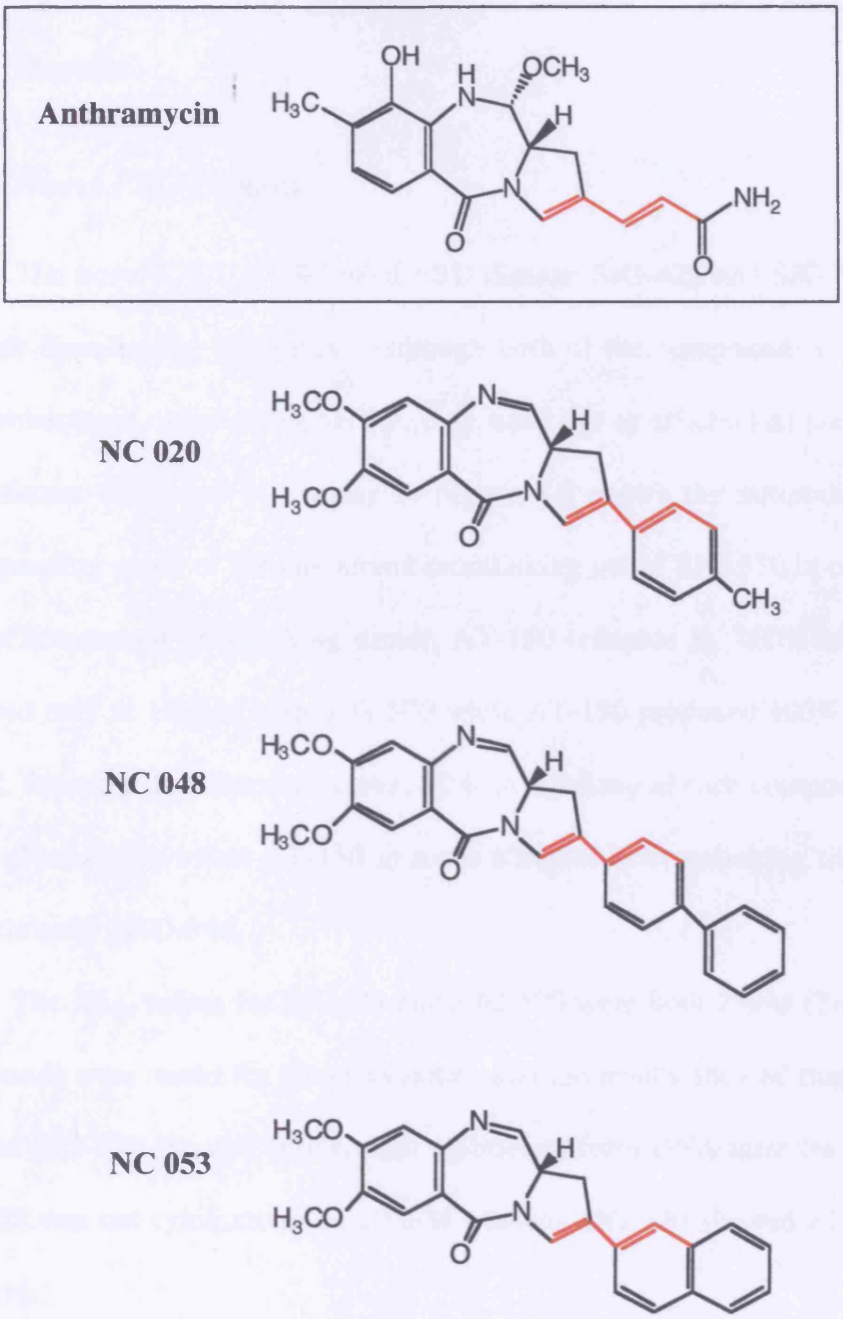

Figure 4.5 Structures of anthramycin and novel PBD-C2-aryl compounds.

4.2 Results

4.2.1 Novel PBD Dimers

The novel C-C2/A-C8 linked PBD dimers, SJG-428 and SJG-570 were tested for their crosslinking efficiency. Although both of the compounds showed a similar DNA interstrand crosslinking ability, they were not as efficient as the C8-C8' linked PBD dimers discussed in chapter 3. Figure 4.6 shows the autoradiograph and its corresponding graph of the interstrand crosslinking gel of SJG-570 in comparison with another interstrand crosslinking dimer, AT-150 (chapter 3). 100% crosslinking was observed only at 100μM with SJG-570 while AT-150 produced 100% crosslinking at 0.1μM. From the dose response curve, 50% crosslinking of each compound is measured and it clearly shows that AT-150 is more efficient in crosslinking than SJG-570 by approximately 1000-fold.

The XL_{50} values for SJG428 and SJG-570 were both 25μM (Table 4.1). These compounds were tested for the cytotoxicity and the results showed that although SJG-428 and SJG-570 showed very similar abilities to form DNA interstrand crosslinking, SJG-428 was not cytotoxic up to 100μM whereas SJG-570 showed a lower IC_{50} value of 75μM.

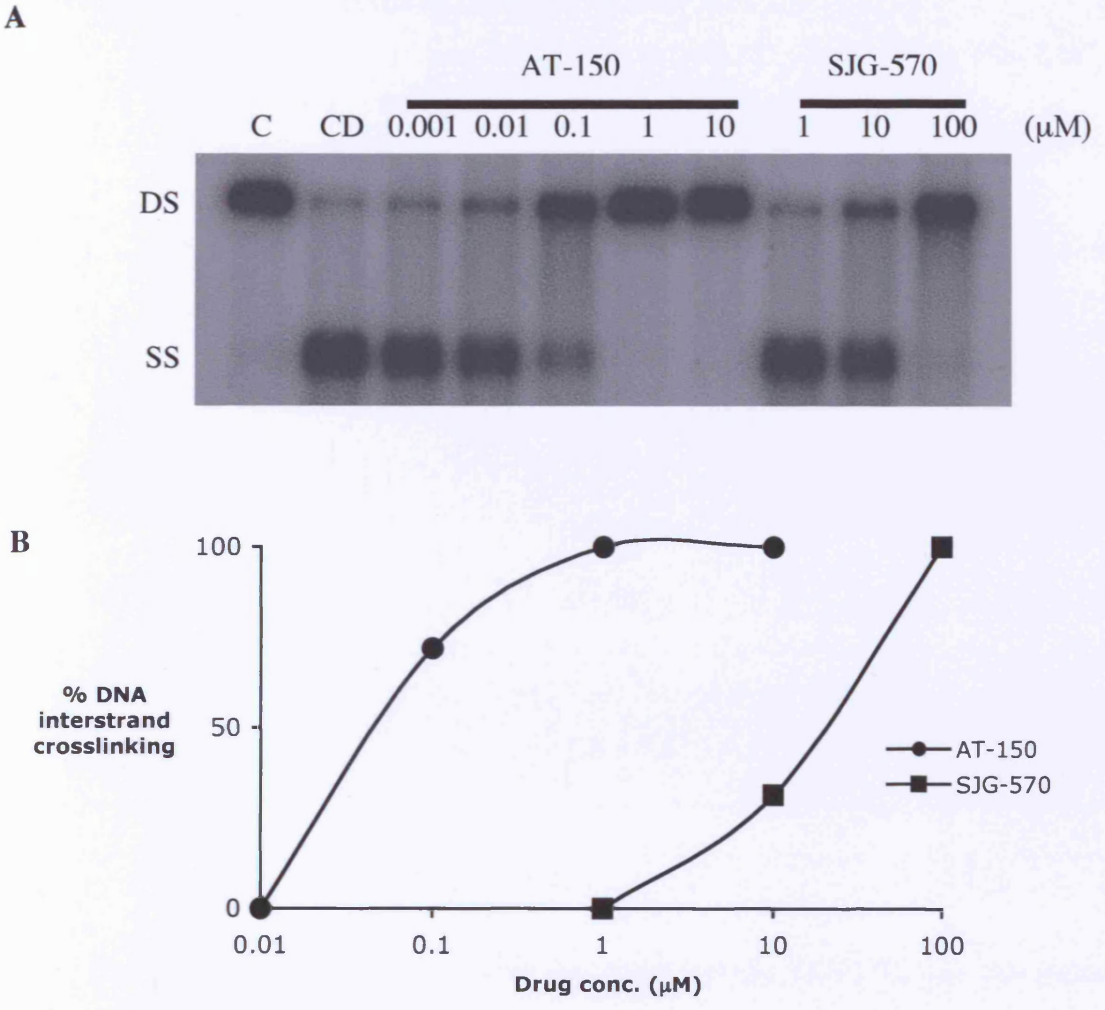

Figure 4.6 (A) Autoradiograph of an agarose gel showing DNA interstrand crosslinking ability of SJG-570 in comparison with AT-150. Drug treatment was for 2 hr at 37°C with pBR322 plasmid DNA.

(B) Dose response graph corresponding to the single experiments shown in (A). Double- (DS) and single- (SS) stranded DNA were quantified by laser densitometry.

Table 4.1 *In Vitro* Cytotoxicity Data in K562 cells after 1 hr incubation at 37°C and DNA Interstrand Crosslinking Data in pBR322 plasmid DNA after 2 hr incubation at 37°C

Compound	IC_{50} (μM)	XL_{50} (μM)
SJG-428	> 100	25 ± 5
SJG-570	75 ± 5	25 ± 1
LCF178	> 100	> 100
KG-2	35 ± 7.5	> 100
KG-3	> 100	> 100
SJG-604	23 ± 5	> 100
SJG-605	1.2 ± 0.4	> 100

The C-C2/A-C8 linked dimer with the longer linkage, LCF178, was also tested for its crosslinking and cytotoxicity activity. It was less efficient at crosslinking compared to the shorter dimers (XL_{50} >100μM, Table 4.1) and also it was not cytotoxic up to 100μM (Table 4.1).

The A-C8/A'-C8' linked dimers, KG-2 and KG-3, also did not show any crosslinking up to 100μM (Table 4.1). However, KG-2 was > 2.8- fold more cytotoxic than KG-3. KG-2 was approximately 2-fold more cytotoxic than SJG-570.

Neither SJG-604 nor SJG-605 showed any interstrand crosslinking up to 100μM (Table 4.1). Figure 4.7 shows the autoradiograph of a typical crosslinking gel of SJG-604 and SJG-605 in which no interstrand crosslinking was observed up to 50μM. Both molecules, however, showed significant cytotoxicity in K562 cells with IC_{50} = 1.2μM for SJG-605 which is 19-fold lower than that of SJG-604 (IC_{50} = 23μM) (Table 4.1).

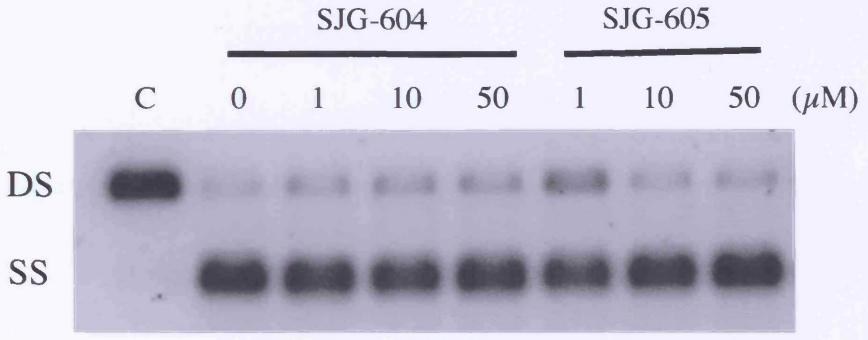

Figure 4.7 Autoradiograph of an agarose gel to examine the DNA interstrand crosslinking ability of SJG-604 and SJG-605. Drug treatment was for 2 hr at 37°C with pBR322 plasmid DNA.

These PBD dimers were also examined for sequence selective interactions by using DNase I footprinting and *Taq* polymerase stop assays in a region of pBR322 DNA. Figure 4.8 shows one example of the footprinting results for SJG-428 and SJG-570, compared to the PBD dimer AT-150 (Chapter 3). No evidence of DNase I

protection was observed up to 100μM with either SJG-428 or SJG-570 (lanes g-l), whereas AT150 clearly showed footprints at a concentration of 10μM (lane d). Using the *Taq* stop polymerase assay, no evidence of DNA interaction was observed up to 100μM with SJG-428 or SJG-570 (data not shown).

Identical analysis of dimer compounds, LCF178, KG-2, KG-3, SJG-604 and SJG-605 similarly gave no evidence of interaction by footprinting and *Taq* polymerase inhibition up to 100μM (data not shown).

4.2.2 Novel PBD-aniline mustards

This series of compounds containing two alkylating moieties, a PBD and a nitrogen mustard (Figure 4.3), were evaluated for cytotoxicity, and DNA interstrand crosslinking activities in naked DNA. The IC_{50} values for these compounds ranged from 0.087 to 65μM (SL-285 to GD10 in Table 4.2). The most cytotoxic compound was GD3 (IC_{50} = 0.087 μM), which was the only one that showed significant crosslinking ability in naked DNA (XL_{50} = 8 μM) under the conditions employed. Figure 4.9 shows the autoradiograph of a typical interstrand crosslinking gel for GD3 and GD4, in which possible loss of DNA with GD4 is observed at 50 μM. The control nitrogen mustard, chlorambucil, had an XL_{50} = 75 μM under the conditions employed (CM in Table 4.2).

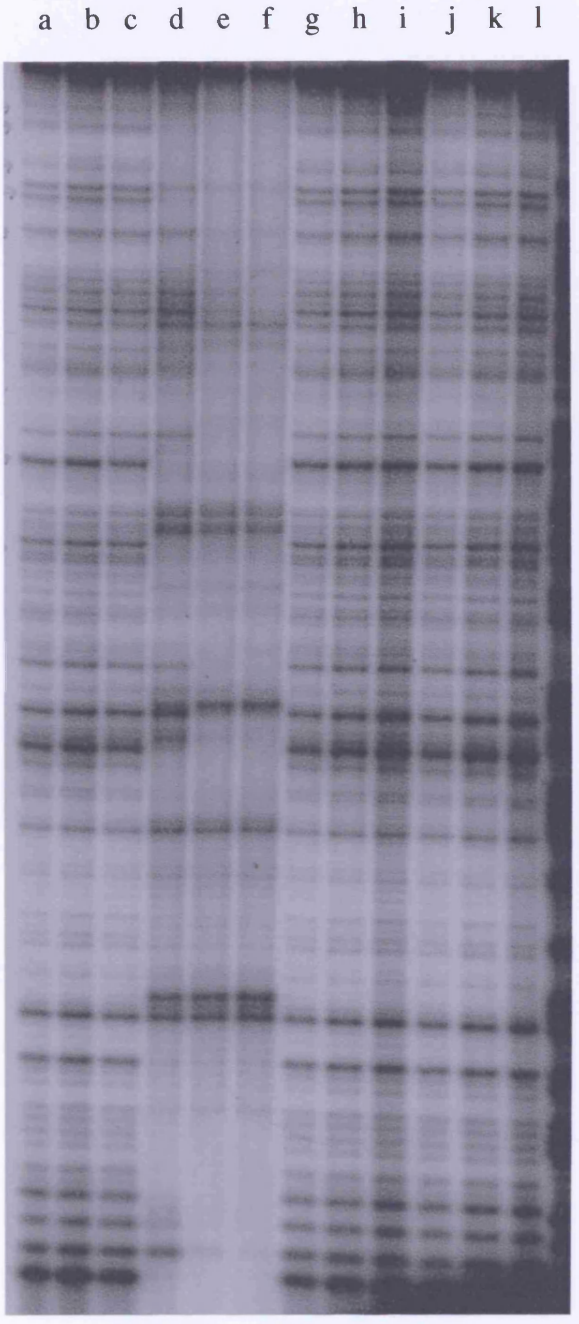

Figure 4.8 Autoradiograph of a gel showing the results of the footprinting assay for AT-150, SJG428 and SJG570 in pBR322 plasmid DNA after 2 hr incubation at 37°C.

a. control
b-f. AT-150 (0.1, 1. 10, 50, 100 μM)
g-i. SJG-428 (1, 10, 50 μM)
j-l. SJG-570 (1, 10, 50 μM)

Table 4.2 *In Vitro* Cytotoxicity Data in K562 cell lines after 1 hr incubation at 37°C and DNA interstrand crosslinking data in pBR322 plasmid DNA after 2 hr incubation at 37 °C.

Compound	IC_{50} (μM)	XL_{50} (μM)
SL285	5 ± 0.74	> 100
GD1	65 ± 5	> 100
GD2	2.45 ± 0.55	> 100
GD3	0.087 ± 0.057	8 ± 1.2
GD4	7 ± 1.53	> 100
GD5	30 ± 6.5	> 100
GD6	0.58 ± 0.16	> 100
GD7	1.5 ± 0.3	> 100
GD8	1.6 ± 0.2	> 100
GD10	4.5 ± 0.35	> 100
E11BDM	>100	>100
E11CDM	>100	>100
P11BDM	>100	>100
P11CDM	>100	>100
BMO	>100	> 100
BM	>100	> 100
PM	16 ± 8	> 100
CM	58.8 ± 4.3	75 ± 5

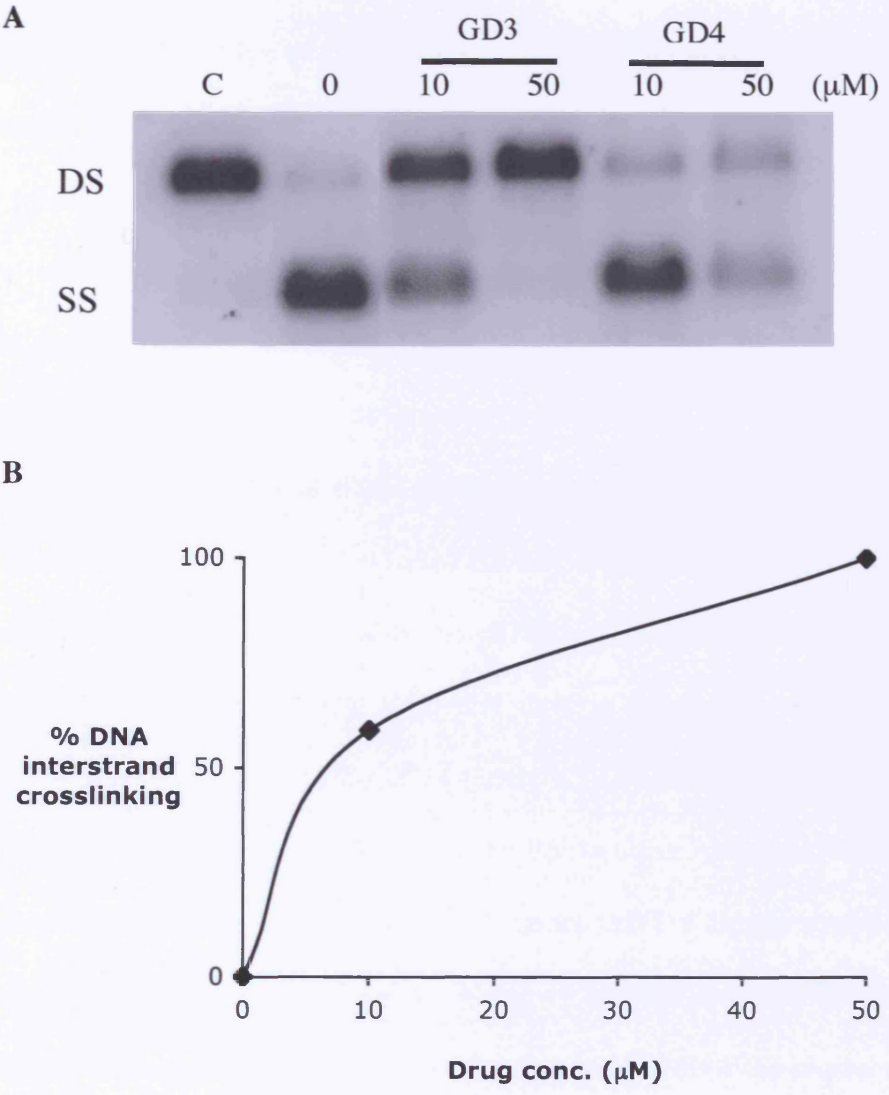

Figure 4.9 (A) Autoradiograph of an agarose gel showing DNA interstrand crosslinking ability of GD3 and GD4. Drug treatment was for 2 hr at 37C with pBR322 plasmid DNA.

(B) Dose response graph of GD3 corresponding to the single experiments shown in (A). Double- (DS) and single- (SS) stranded DNA were quantified by laser densitometry.

Compared to chlorambucil, GD3 was approximately 9-fold more efficient in crosslinking. The IC_{50} value of GD3 was however approximately 675-fold lower than chlorambucil (Table 4.2). None of the PBD-di-aniline mustards showed crosslinking activity up to 100μM (E11BDM to P11CDM in Table 4.2). These compounds did not show any cytotoxicity up to 100μM. The bi-functional chlorambucil analogues (PM and BM) did not produce any crosslinks up to 100μM, however, PM was 3.6-fold more cytotoxic (IC_{50} = 16μM) than chlorambucil (IC_{50} = 58.8μM) (Table 4.2). The monofunctional alkylating agent BMO did not produce any crosslink as expected.

These compounds were also tested for any sequence selectivity using DNase I footprinting and *Taq* polymerase stop assays. Figure 4.10 shows one example of the footprinting result for GD3, GD4, GD5 and GD6 in contrast to the PBD monomer GWL-6 (Section 4.2.2). Except for GD4 (lanes i, j), no strong evidence of DNase I protection was observed up to 100μM with the PBD-aniline mustards (lanes g, h, k-n). GD4 shows weak footprinting at 100μM. In contrast, GWL-6 clearly showed footprints at a concentration of 10μM (lane e). None of the other PBD-mustards or the chlorambucil analogues showed any clear binding sites within the region of pBR322 DNA tested up to 100μM (data not shown). No evidence of DNA covalent interaction of any of the compounds was observed in the *Taq* polymerase stop assay at a dose up to 100μM (data not shown). Taken together these results suggest that the cytotoxicity of the compounds when observed is not due to DNA interaction.

4.2.3 Novel PBD-Tri-Pyrrole Amide

The mono-functional novel compound, GWL-6, showed significant cytotoxicity in the K562 cell line with an IC_{50} value of 0.5 ± 0.058μM. The DNA binding site of GWL-6 was determined by using DNase I footprinting in an AT-rich region of pBR322 DNA. Figure 4.11 shows the autoradiograph of the footprinting result. The compound showed clear footprints at 10μM (lane c). The strongest footprint site is at 5'-^{3199}AGATTAT^{3205}-3' as indicated in the autoradiograph. There is also evidence of enhanced cleavage observed at the concentration of 10μM (as indicated by the arrow in Figure 4.11).

4.2.4 Novel PBD-C2-Aryls

Novel PBD compounds with various C2 aryl substituents; NC020, NC048 and NC053, were investigated (Figure 4.5). As seen in anthramycin, these compounds retain the C2-*endo-exo* unsaturation (coloured red). A summary of cytotoxicity data for these compounds is shown in Table 4.3.

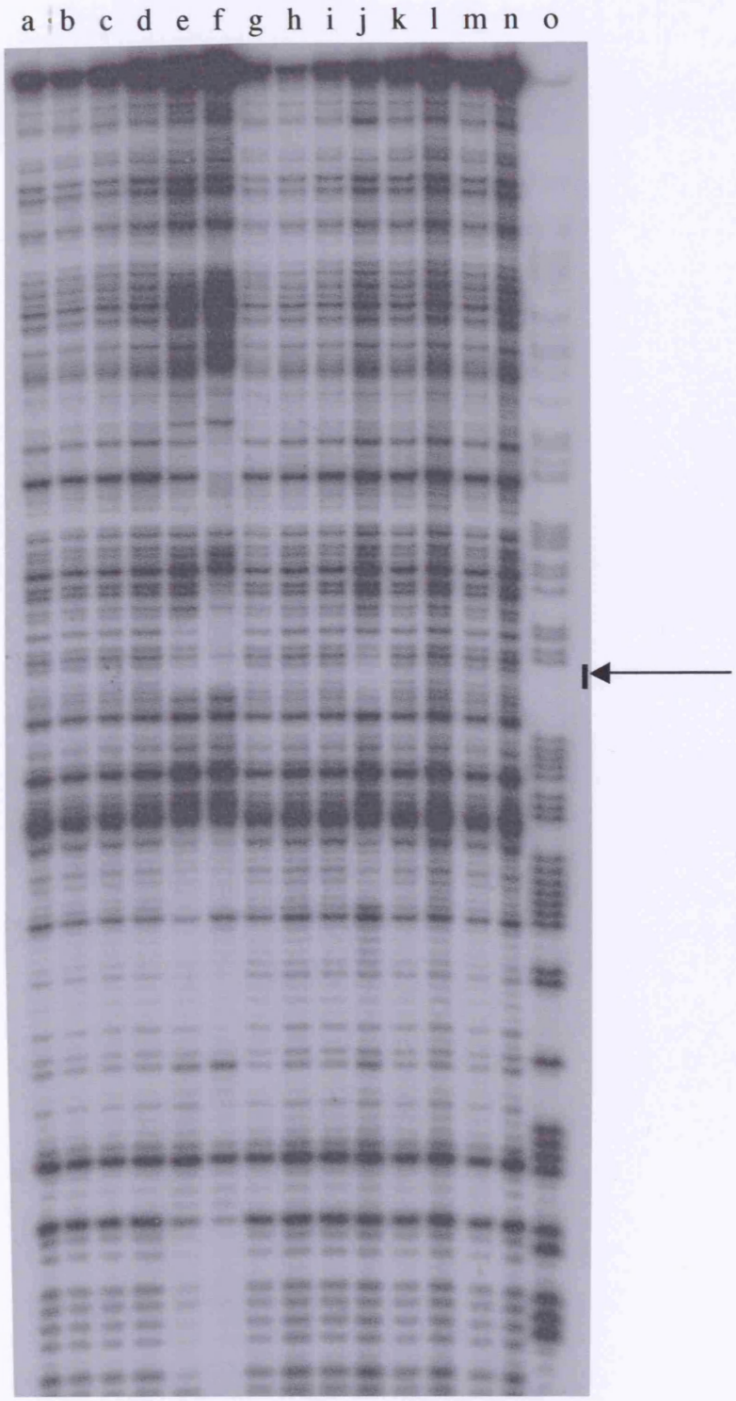

Figure 4.10 Autoradiograph of a gel showing the footprinting results for GWL-6, GD3, GD4, GD5 and GD6 in pBR322 plasmid DNA. Weak footprinting observed with GD4 indicated by an arrow.

a.	control
b-f.	GWL-6 (0.01, 0.1, 1, 10, 100μM)
g-h.	GD3 (50, 100μM)
i-j.	GD4 (50, 100μM)
k-l.	GD5 (50, 100μM)
m-n.	GD6 (50, 100μM)
o.	G+A marker lane

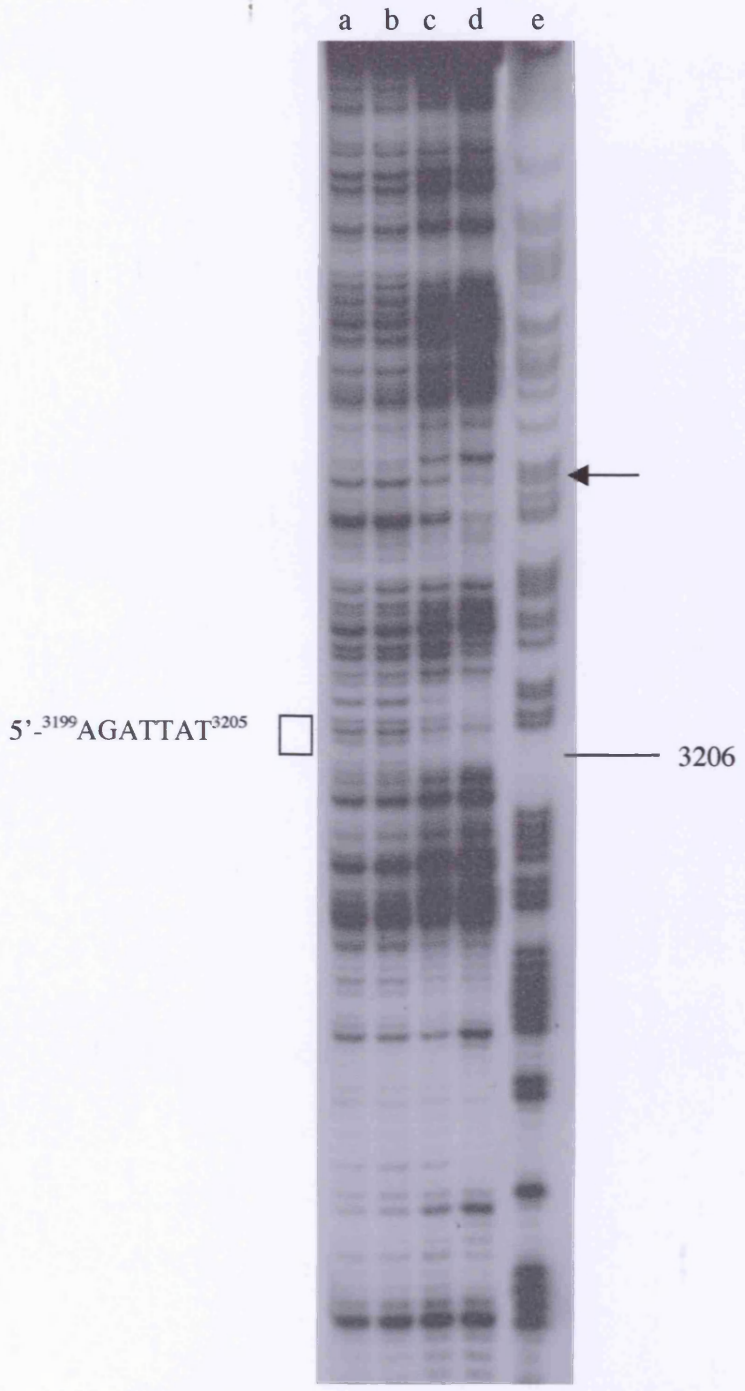

Figure 4.11 Autoradiograph of a gel showing the results of the footprinting assay for GWL-6 in pBR322 plasmid DNA after 2 hr incubation at 37°C. The strongest footprint within this sequence is indicated with a box on the left of the gel. An example of enhanced cleavage is indicated by an arrow on the right of the gel.

a. Control
b. 1
c. 10
d. 100 (μM)
e. G+A marker lane

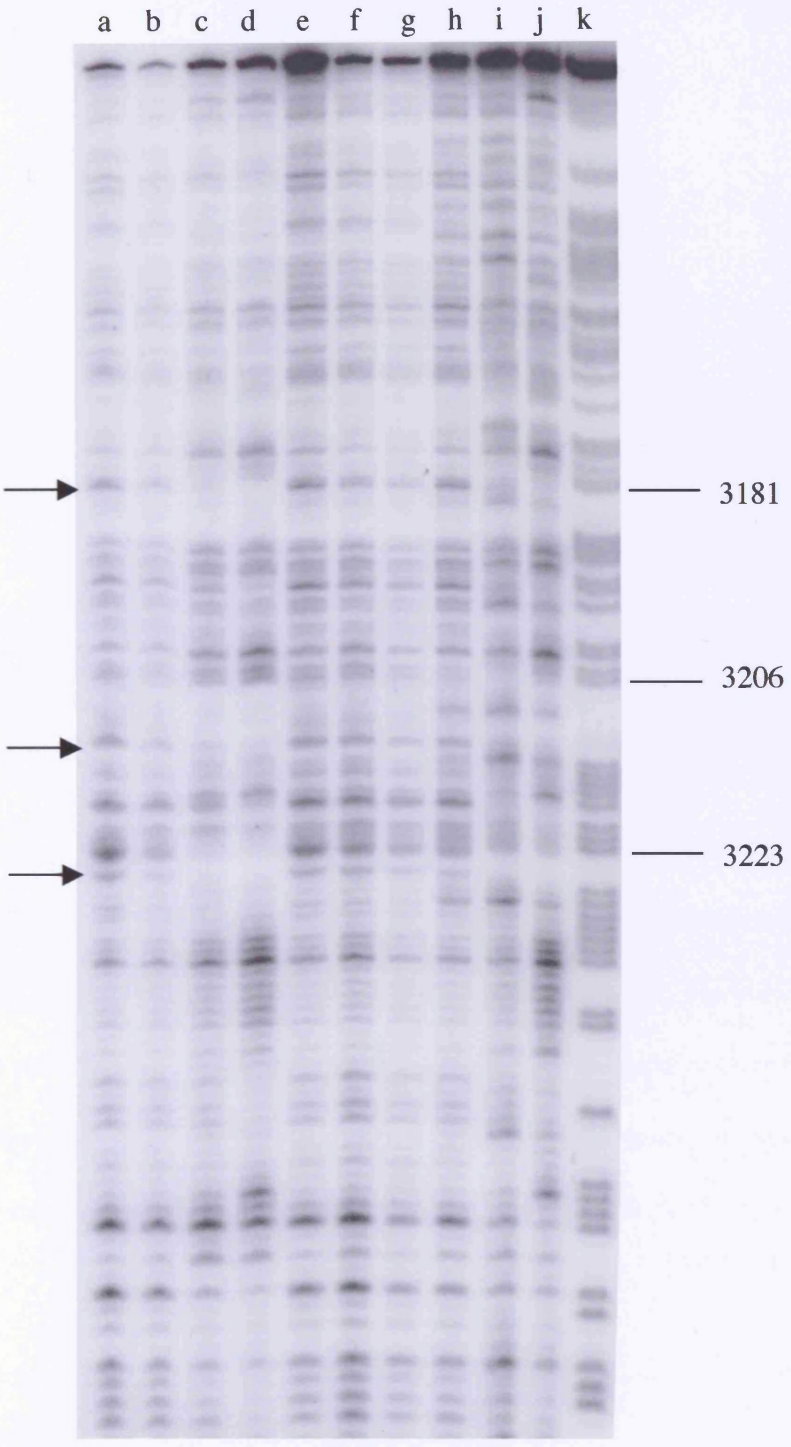

Figure 4.12. Autoradiograph of a gel showing the footprinting results for NC020, NC048 and NC053 in pBR322. The main binding sites are indicated by arrows.

a.	control
b-d.	N020 (1, 10, 50 μM)
e-g.	N048 (1, 10, 50 μM)
h-j.	NC053 (1, 10, 50 μM)
k.	G+A marker lane

Table 4.3 *In Vitro* MTT Cytotoxicity Data for NC020 / NC048 / NC053 in the K562 cell line after 1hr incubation at 37°C.

Compound	IC_{50} (μM)
NC020	0.0475 ± 0.0075
NC048	0.23 ± 0.05
NC053	0.0175 ± 0.0025

Figure 4.12 shows the autoradiograph of the binding sites of these compounds and Figure 4.13 shows the box diagram corresponding to the binding sites in comparison to GWL-6. DNase I footprinting in the AT-rich region of pBR322 DNA showed that all three compounds bound at the same sites indicated by the arrow in the gel. These sites, ^{3183}5'-AGG-3'^{3185}, ^{3211}5'-AGG-3'^{3213} and ^{3224}5'-AGA-3'^{3226}, correspond to known preferred Pu-G-Pu sites for PBD monomer compounds. However, the binding affinities of NC020 and NC053 were higher showing the footprints at 10μM compared to NC048, which only showed very weak footprints at 50μM. This result correlates with the cytotoxicity results where NC020 and NC053 are more potent than NC048.

Figure 4.13 Box diagram showing binding sites of GWL-6, NC020, NC048 and NC053 in pBR322 plasmid DNA.

GWL-6

NC020/NC048/NC053

4.3 Discussion

Among the novel PBD dimers that are asymmetrical C/C2-A'/C8' linked molecules, SJG-428 and SJG-570 showed DNA interstrand crosslinking activity using the gel based assay under the conditions employed. This result was unexpected because SJG-428 and SJG-570 were predicted to be intra-strand crosslinking agents rather than inter-strand crosslinking agents due to the rigid linkages and the molecules being planar. On the other hand, LCF178 has an extra ethyl ether in the linkage and therefore is more flexible and may have the ability to produce inter-strand crosslinking. The lower IC_{50} value of SJG-570 compared to the other two compounds may suggest that the methoxy substituent on the A-ring is more favourable for the cellular pharmacology of the compound. Also SJG-570 may be very efficient at producing intra-strand crosslinking, however, these crosslinks are not measurable using the gel based assay. The same interstrand crosslinking values were obtained for SJG-428 and SJG-570 in naked DNA but as the IC_{50} values of these compounds differed, a comet assay might have shown any differences in the ability of the compounds to form interstrand crosslinks in cells. The results with SJG-570, being more potent, may suggest that this compound may produce more cytotoxic crosslinks in cells.

Unlike the other A/C8-A'/C8'–linked PBD dimer DSB-120 (Chapter 1) which differs in the linkage between the two PBD units, KG-2 and KG-3 did not have any significant interstrand crosslinking activity in naked DNA. Therefore it would suggest that the amide-linkage for this type of dimer is not favourable for DNA interaction.

Although neither of the compounds showed significant crosslinking activity in naked DNA, KG-2, which is an asymmetrical amide-linked dimer, was more potent *in vitro* than the symmetrical KG-3. Hence, the symmetry of the dimer may be important for the cellular pharmacology of the compound. Similarly, another pair of PBD dimers, SJG-604 and SJG-605 that are also A/C8-A'/C8' linked but via a potential non-covalent binding pyrrole moiety, did not show any significant crosslinking ability. Interestingly, however, these molecules showed significant cytotoxicity, which did not correlate with crosslinking in naked DNA. The fact that SJG-605 is 19-fold more cytotoxic than SJG-604 suggests that the symmetry in this type of compounds is important for the activity of the compound. Also SJG-605 being 29-fold more potent than KG-2 suggests that the pyrrole subunit is a better linkage than the di-amide linkage. It is not clear why SJG-605 is significantly cytotoxic without any ability to form DNA interstrand crosslinking.

From the results of the *Taq* polymerase stop and DNase I footprinting assays, it was concluded that none of these dimers showed any significant non-covalent or covalent binding sites within a region of pBR322 plasmid DNA up to the concentration of 100 μM. Although SJG-604 and SJG-605 contain a potential non-covalent DNA interacting moiety and the molecules should span up to seven base pairs, there were no clear footprints observed by these drugs. The results of the *Taq* polymerase stop assay is due to the possibility of the drug-DNA adducts being thermally unstable and therefore the drug falls off the DNA in the high temperature involved during the process. The footprinting results may infer that the lengths of the compounds are not favourable for

high affinity binding to the DNA. Therefore, the cytotoxicity of these dimers may be due to non-DNA interaction mechanisms.

The series of PBD-mono-aniline mustard conjugates (SL285 to GD10 in Figure 4.3) showed a wide range of cytotoxicity values in the K562 cell line under identical conditions. Interestingly, although these compounds have three potential crosslinking moieties (two chloroethyl arms of the mustard unit and N10-C11 of the PBD unit), GD3, which has the longest linkage, was the most potent (IC_{50} = 87nM), and is the only compound to show any significant interstrand crosslinking activity. Compared to the parent nitrogen mustard compound chlorambucil, a significant increase in cytotoxicity for GD3 was observed (approximately 655-fold). Therefore it was possible to obtain a potent interstrand crosslinking agent by combining a nitrogen mustard with a PBD with an appropriate linker length. It has been shown previously with chlorambucil-distamycin conjugates where the conjugate crosslinked in naked and cellular DNA more efficiently than the parent nitrogen mustard chlorambucil (Wyatt *et al.*, 1994). A number of studies have been reported on nitrogen mustard-distamycin conjugates (Broggini *et al.*, 1995; Hartley *et al.*, 1995; Wyatt *et al.*, 1995; 1997a, b; Baraldi *et al.*, 2002a, b). Such compounds include tallimustine (see chapter 1) of which the reported *in vitro* IC_{50} value was ca. 2.4μM (Baraldi *et al.*, 2002a). Similarly, a hairpin polyamide-chlorambucil conjugate was found to be a much more efficient DNA crosslinking agent than chlorambucil (Wang *et al.*, 2003b). It was suggested that this might be due to the more efficient and faster delivery of alkylating groups of chlorambucil to DNA reactive sites as nitrogen mustards alkylate primarily in the major groove and they do not have

any particular affinity for the DNA. This may explain the result with GD3 that the PBD moiety delivers the nitrogen mustard subunit to the minor groove of DNA. As the PBD unit is likely to interact with DNA first followed by the nitrogen mustard moiety, it may suggest that the linker length of GD3 is favourable for such DNA crosslinking.

The PBD-di-aniline mustards (E11CDM to P11BDM in Figure 4.3) did not have any cytotoxic or crosslinking activity up to 100μM. This was interesting because these compounds have four potential crosslinking moieties (2 from each mustard unit) to potentially crosslink the DNA. In these molecules the N10-C11 of the PBD unit is BOC protected, and therefore the PBD moiety would not be able to interact with guanine in the minor groove. The BOC unit was kept attached since the second mustard unit would dissociate if the BOC were to be removed. The chlorambucil analogues BM, PM and BMO (of which BMO is mono-functional), did not show any crosslinking activity up to 100μM. Interestingly, however, PM was 3.6-fold more cytotoxic than chlorambucil (CM), which did show crosslinking.

Apart from GD4, none of the aniline mustard-PBD conjugates, or the chlorambucil analogues showed any evidence of binding within a region of pBR322 plasmid DNA as determined by DNase I footprinting or a *Taq* polymerase stop assay. In the case of GD4 evidence of binding (at 100μM) was observed by footprinting but no evidence of covalent interaction observed using the *Taq* polymerase assay. This would suggest that the interaction is not favourable for alkylation by the mustard group, which

should block the progress of the polymerase. Covalent interaction at guanine-N2 by the PBD portion of the molecule may be occurring but not detected by the *Taq* polymerase assay due to thermal instability of the adduct.

With GD3 it was surprising that no evidence of DNA interactions was indicated by either assay since this molecule was found to be an efficient interstrand crosslinker using the plasmid-based electrophoresis assay. One possibility is that the molecule is relatively selective in its action and that the favourable DNA sequence for crosslinking present in the whole pUC18 plasmid is not represented in the smaller DNA fragment used in the other assays. The fact that no evidence of DNA binding was observed using DNA footprinting would suggest that the PBD moiety is prevented from binding efficiently to its preferred purine-G-purine binding sites. Although the PBD molecule is relatively small and spans only three base pairs it can be detected by footprinting as shown with the C2-aryl compounds (Figure 4.5).

A significant level of alkylation at guanine-N7 or adenine-N3 by the aniline mustard-PBD conjugates is clearly not produced since alkylation at both these sites are known to be detected by the *Taq* polymerase stop assay (Ponti *et al.*, 1991). All of the aniline mustard-PBD conjugates were cytotoxic to the human K562 cell line with IC_{50} values in the low micromolar or sub-micromolar range. The lack of clear evidence of DNA binding in most cases suggests that they do not exert their cytotoxicity through interaction with DNA.

The mono-functional PBD-tripyrrole conjugate, GWL-6, showed significant cytotoxicity in the K562 cell line. The non-covalent binding site of GWL-6 was determined by using DNase I footprinting which showed its binding site at 5'-AGATTAT-3' in a region of pBR322 DNA. This fits with polypyrrole compounds binding to A/T sequences (*eg.* distamycin) and also PBD binding to 5'-pu-G-pu (A-G-A in this case). Interestingly, a previously reported PBD-distamycin conjugate showed a strong binding affinity to GC-rich DNA (Baraldi *et al.*, 1998) suggesting that the sequence selectivity of distamycin towards AT-rich sequences is lost. When a series of PBD-distamycin conjugates with different numbers (n = 1- 4) of polypyrrole backbones of distamycin were evaluated (Baraldi *et al.*, 1999), it showed that the increase in length increased the cytotoxicity of the drugs where all were much more active than the tri-pyrrole distamycin and its four pyrrole analogue. Only n = 3 and 4 retained a higher cytotoxicity compared to the PBD group alone which gave a similar value to DC-81. It was suggested that this was due to additional amido H-bonds and van der Waals interactions as it gives tighter DNA binding which depends on the multiplicity of interactions between the pyrrole carbonyl units and AT-rich sequences of DNA. Therefore, the significant potency and sequence selectivity of GWL-6 may be explained in a similar manner. Later GWL-6 was resynthesised by solid phase synthesis, which will be discussed in chapter 5.

Three PBD-C2-aryl conjugates showed significant cytotoxicity in the order of NC053 > NC020 > NC048 with approximately 13-fold difference between NC053 and

NC048. This correlates with the result of the non-covalent binding intensity determined from DNase I footprinting where NC053 showed clear footprints at much lower concentrations, with the binding sites at 5'-pu-G-pu, within a region of pBR322 DNA. These results are consistent with the previously reported data that the C2-*endo-exo* unsaturation of the PBD plays a significant role in the activity. Two of the best known naturally occurring PBDs, anthramycin and tomaymycin (chapter 1), both have C2-*exo*-unsaturation. However, anthramycin binds to DNA more efficiently (Thurston, 1993) and it is thought to be associated with the C2/C3-*endo* unsaturation of anthramycin. A series of novel C2/C3-*endo*-unsaturated PBDs was synthesised and all the compounds were shown to have enhanced DNA-binding reactivity and *in vitro* cytotoxicity (Gregson *et al.*, 2000).

The different IC_{50} values and binding efficiency of the PBD-C2-aryl conjugates also show that the C2-*endo-exo*-unsaturation of the PBD is dependent on the substituent on the C2 position. Not only the electrophilicity of the C2-substituent is important but also the lipophilicity influences the potency. The fact that NC053 is the most potent compound may suggest that the molecule interacts with the floor of minor groove better as the naphthyl group is lipophilic.

The importance of the electrophilicity of the substituent is explained in previously reported data (Guiotto *et al.*, 1998), where a series of aryl PBD compounds with different substituents on a phenyl ring were evaluated. These compounds were A-

ring substituted rather than on the C-ring of the PBD. These types of compounds were of interest because of the *para* relationship of the A/C7-substituent to the N10 of the DNA-interactive N10-C11 imine moiety. In this series, the cytotoxicity of the compounds was suggested to be an electronic effect of the substituent on the phenyl ring rather than the steric effect. This is because the C7-position of the PBD nucleus is known to point out of the minor groove of DNA. Therefore the substituents can affect the electronic characteristics of the imine, which influences its electrophilicity and ability to interact with DNA.

The novel PBD dimers in this chapter were not very active at DNA interstrand crosslinking, although some had significant cytotoxicity *in vitro*. This may be due to the effect of the linkages of the dimers being not favourable for DNA interstrand crosslinking. None of the A/C8-A'/C8'-linked dimers were more active than the parent dimer DSB-120 and were significantly less potent than molecules in clinical development such as SJG-136. Similarly, the PBD-nitrogen mustard conjugates were not active apart from one compound, GD3. It may be useful to study the molecular modelling and kinetics of the drug-DNA adduct to see if the distance between the PBD and the nitrogen mustard units of GD3 is particularly favourable for the binding and crosslinking in the minor groove. The monofunctional C2-aryl containing PBDs showed promising *in vitro* cytotoxicity. Hence they will be good guides for further investigation of this type of compounds, including novel dimers. The enhanced sequence selectivity

of GWL-6 compared to a PBD alone gives the potential for extended conjugate molecules to cover longer sequences of DNA.

CHAPTER 5

DEVELOPMENT OF SCREENING METHODS FOR SOLID PHASE COMBINATORIAL LIBRARIES

5.1 Introduction

Combinatorial chemistry has become one of the most important tools in drug discovery during the past decade (Song *et al.*, 2003). Synthesis of combinatorial libraries can be used to create new lead compounds for a specific biological target, and also to subsequently optimise these initial leads. Virtually every major pharmaceutical company has adopted this technology for their drug discovery programs. The general approaches in combinatorial peptide library methods include biological libraries, spatially addressable parallel solid phase or solution phase libraries and the 'one-bead one-compound' library method, which results from a split-and-mix strategy. The biological library approach is limited to peptide libraries featuring amino acids. However, the other synthetic approaches can also be utilised in non-peptide oligomer or small molecule libraries (Lam, 1997). The combinatorial isolation of hit compounds consists of three stages: 1) the stepwise generation of a large number of compounds by joining various building blocks together; 2) a high throughput screening method to select for a specific biological property of library members; and 3) identification of active compounds ('hits') by deconvolution methods, or chemical analysis (Lam, 1997).

This chapter is about the development of methods for the screening of a solid phase, 'one-bead, one-compound' library. In such libraries, each bead carries only one type of compound; therefore the entire library can be screened for binding against a tagged acceptor molecule (e.g., receptor, enzyme, antibody, or even small molecules).

An initial combinatorial library was produced, featuring diversity in a peptide chain and N-terminal capping by a PBD moiety (Hardy *et al.*, 2003). Since a PBD is known to bind covalently to guanine bases in DNA (with a preference for 5'-Pu-G-Pu sequences), this interaction combined with the various potential sequence preferences of heterocycles featured in the peptide chain, suggests that such compounds should exhibit different sequence specific DNA binding. Thus, a large number of compounds were synthesised by building up extended molecules on solid support (tentagel bead). Randomised peptide chains containing biological amino acids and aromatic heterocycles were combinatorially synthesised on the surface of tentagel beads and then covalently capped with the PBD group.

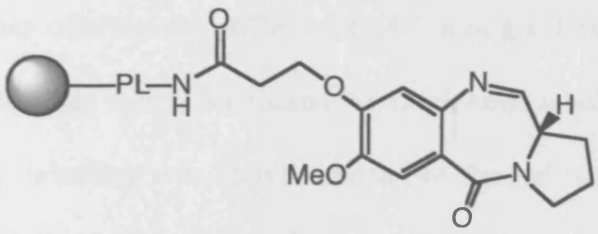

Figure 5.1 An example of resin-bound PBD (PL = photocleavable linker).

An example of resin-bound PBD is shown in Figure 5.1. It was previously proved that such resin-bound PBD selectively binds A-G-A base pair DNA motifs, in the manner of the equivalent solution phase interaction (Hardy *et al.*, 2003). This study was carried out using radiolabelled (isotope ^{32}P) oligonucleotides containing the sequence A-G-A. Two sets of resin were evaluated derived from the same initial batches of Fmoc-protected PBD resin which were then split into two before one half was deprotected. This ensured that the identical PBD species were on the bead, whether the beads were N10-protected or not, allowing the extent of binding to be directly compared. Both sets of resin were incubated with the radiolabelled oligonucleotides followed by washing, then the counts per minute (CPM) of the isotope ^{32}P were measured to indicate the relative binding affinity of the compounds to DNA. The result showed significantly high binding affinity of the unprotected PBD and no binding was observed with the N10-protected PBD (Table 5.1). This important result indicated that PBD attached to the bead surface could interact with DNA after the removal of the N10-Fmoc protecting group during the library synthesis.

In order to further confirm the difference of binding affinity between N10-protected and deprotected PBD resins, an alternative rhodamine label (Figure 5.2) was then used. The rodamine labelling was chosen instead of the radioactivity because of safety considerations and the potential for high throughput fluorescence analysis. As seen with the previous results, a significantly higher value of fluorescence for the N10-deprotected PBD was obtained, indicating the potential to develop sensitive screening procedures based on this strategy (Table 5.2) (Hardy *et al.*, 2003).

Resin-bound compound	CPM (^{32}P)
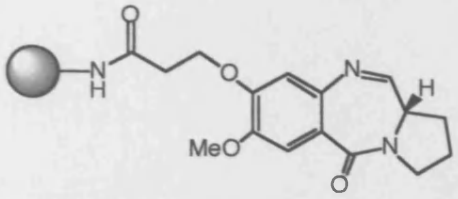	50,304
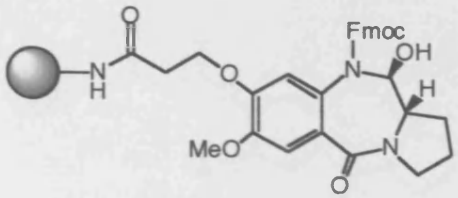	0

Table 5.1 Relative intensity of counts per minute of the isotope ^{32}P indicating the binding affinity of protected and unprotected PBD resin with radiolabelled oligonucleotide containing an AGA sequence (taken from Hardy *et al.*, 2003).

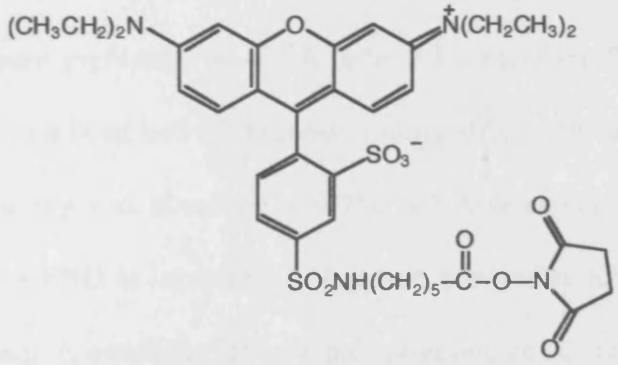

Figure 5.2 Structure of Rhodamine Red ™.

Resin-bound compound	Rhodamine
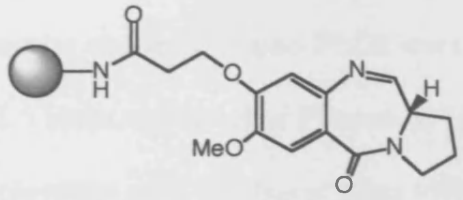	16,539
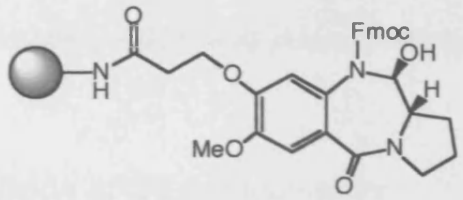	1,122

Table 5.2 Relative intensity of fluorescence indicate the binding affinity of protected and unprotected PBD resin with rhodamine labelled oligonucleotide containing an AGA sequence (taken from Hardy *et al.*, 2003).

Three synthetic oligonucleotides were designed according to the known binding sequence preference of PBDs. They each contained either the A-G-A motif (most preferred), T-G-T (least preferred) or A-I-A (where I = inosine). Previous experiments had showed that PBD on bead had the highest binding affinity towards A-G-A sequence and only residual binding was observed with the A-I-A sequence (Hardy *et al.*, 2003). This confirmed that a PBD is incapable of binding covalently to inosine as it has no exocyclic amino group. A synthetic 20 base pair oligonucleotide containing a single A-G-A sequence and therefore a single PBD covalent binding site was designed (Oligo-1) and was used as a control sequence in subsequent experiments. The sequence of Oligo-1 is 5'- ACACCTAIAGATIAAITCTI –3' where I = inosine.

5.2 Materials and Methods

5.2.1 Materials

Combinatorial libraries and resin bound PBDs were kindly supplied by Dr. P. Howard and Professor D.E. Thurston (School of Pharmacy, University of London).

Synthetic oligonucleotides were purchased from MWG biotech.

Sea plaque agarose was purchased from FMC Bioproducts.

NUNC™ black flat-bottomed 96 well plates were purchased from Fisher.

5.2.2 Hybridisation of Oligonucleotides

Sequences of oligonucleotides were designed according to different target sequences. Each synthetic oligonucleotide was diluted with distilled water to 100pM. To hybridise 50pM of oligonucleotides, rhodamine labelled oligonucleotide was mixed with the same volume of complementary non-labelled strand by heating to 90°C for 2 minutes and then cooling slowly to room temperature. The volume to be used was calculated accordingly for each experiment to give 400μl per 1mg of combinatorial bead library. The duplex was then diluted to 5pM with distilled water prior to incubation with the library.

5.2.3 Screening protocol for resin bound PBD-polypeptide sublibraries (multiple beads per compound)

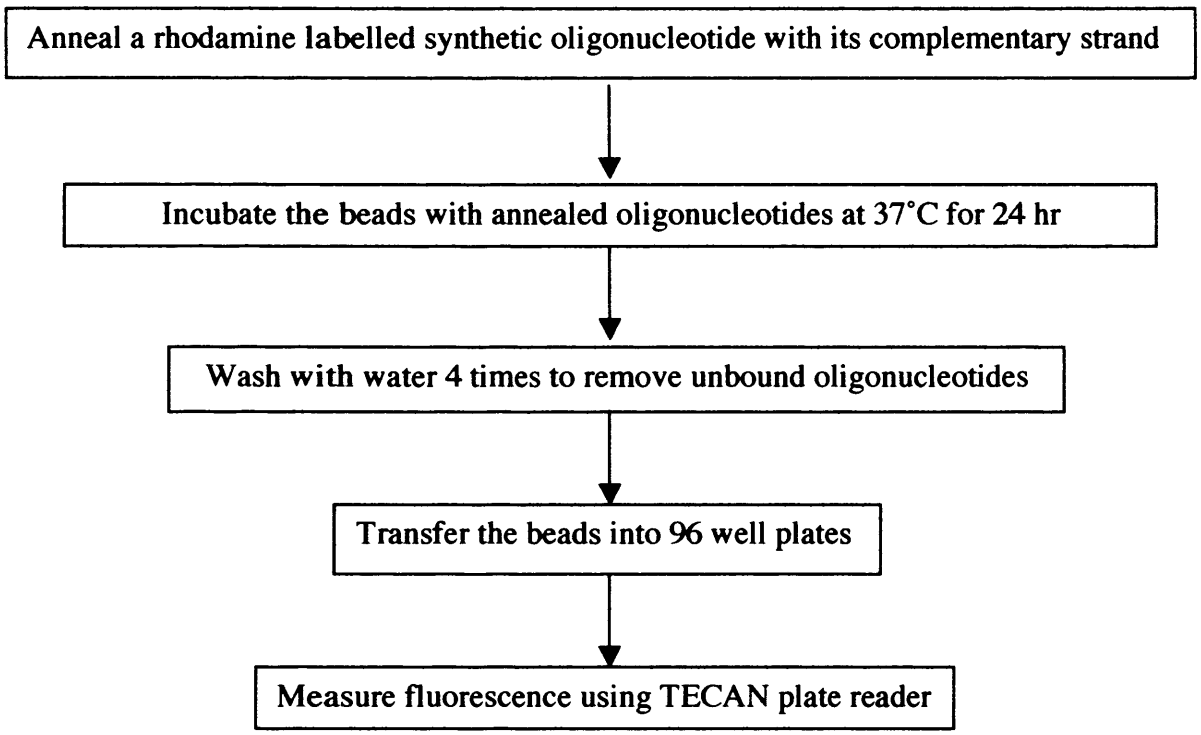

Figure 5.3 Screening methods for libraries containing multiple beads per compound.

In order to measure the fluorescence of the beads that are bound to oligonucleotides and hence compare the binding affinity among the compounds, the following screening protocol was used. Figure 5.3 is the schematic diagram of the protocol. 1mg of each bead library was weighed out and mixed with the duplex rhodamine-labelled-oligonucleotide in an 1ml eppendorf tube at 37°C for 24 hours

followed by washing with distilled water by mixing the tube four times to remove unbound oligonucleotide. The beads were then resuspended in 200µl of distilled water and transferred into a well of a NUNC™ black flat-bottomed 96-well plate using a 1ml tip with a Gilson pipette. Under a light dissecting microscope, the positive beads were visible ranging from pink to dark red as the intensity of the binding increased. To confirm the extent of binding of the dye, the fluorescence of the samples were measured using a TECAN SpectraFlourPlus plate reader. The wavelength used were 485nm for emission and 535nm for excitation.

5.2.4 Screening method of libraries containing one compound per bead

This type of library contained various sublibraries therefore the whole sample was screened at one time to find positive beads. Microscope slides were pre-coated with 500µl of 0.25% sea plaque agarose. Each library were incubated with the annealed rhodamine-labelled oligonucleotide in 1ml eppendorf tube at 37°C for 24 hours with mixing, followed by washing with distilled water four times. The libraries were then mixed with 1ml of 37°C 0.25% sea plaque agarose and layered onto precoated slides, and then allowed to set at room temperature. Each slide containing the beads embedded in the agarose was then hydrolysed with 1ml of water until beads were swollen. The positive beads were visible with the naked eye as red or pink. Under a dissecting light microscope the most positive (red) beads could be removed using a Pasteur pipette. Since the bead was relatively sticky, it stayed on the tip of the pipette to allow transfer of an individual bead into a PCR tube containing 10µl of distilled water. These PCR

tubes containing the positive beads were sent to the Babraham Institute for sequence analysis (Edman Sequencing). Figure 5.4 shows the schematic picture of this screening method.

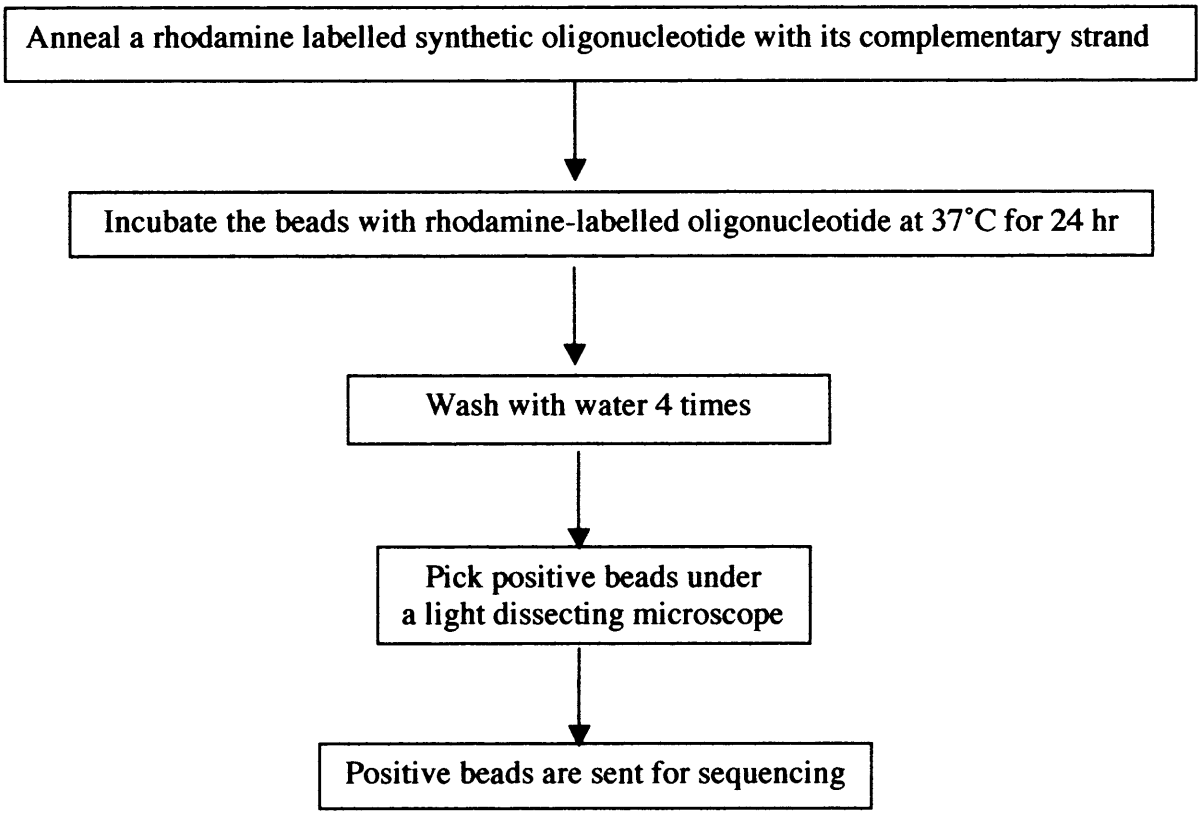

Figure 5.4 Screening method for libraries containing one compound per bead.

5.3 Results

A high throughput screening method was developed to identify compounds from combinatorial libraries that have a high affinity to specific DNA sequences. By mixing beads with rhodamine-labelled target oligonucleotides it was possible to identify interactions between compounds and desired DNA sequences simply by visualising rhodamine-stained beads under light or fluorescent microscopes. The sequence of the peptide chain within each of the interacting compounds was then determined by a direct chemical analysis procedure, where selected rhodamine-stained beads were sent off for Edman sequencing (Lam *et al.*, 1997).

5.3.1 On bead PBD dilactam

It was previously shown that a PBD attached to a bead could bind to its known preferred sequence (AGA) by using this screening method. PMS/42/2 (Figure 5.5) is a PBD dilactam attached to a bead. Therefore as a negative control, this compound was screened against Oligo-1 (see section 5.1). As described previously in Chapter 1, PBD dilactams do not bind covalently to DNA since they lack the N10-C11 electrophilic moiety, which is essential for the covalent binding to the guanine-N2 position. No binding was observed (*i.e.*, no change in bead colour) as expected, indicating that the protocol is applicable as a screening procedure, and does not detect non-specific/non-covalent PBD interactions.

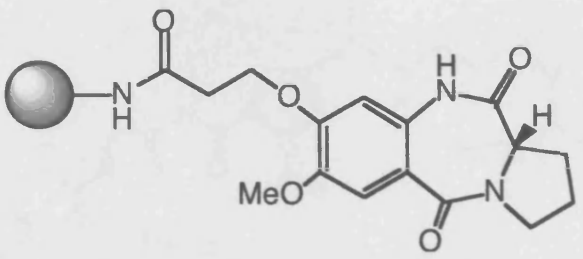

Figure 5.5 MS/42/2

5.3.2 Screening of heterocyclic-PBD libraries

Since the DNA binding characteristics of a PBD and a dilactam on bead are demonstrated as the same as when they are off bead, libraries of longer peptide-PBD conjugates on bead were synthesised in an attempt to obtain a greater sequence selective DNA binding.

5.3.2.1 Sequence selectivity of GWL-6

As presented in Chapter 4, the PBD-polyamide conjugate GWL-6, which consists of three pyrroles attached to a PBD, was found to bind sequence selectively to DNA. The preferred binding sequence of GWL-6 (5'-AGATTAT) was obtained from the footprinting experiments. In order to find if this binding behaviour is retained when the compound is tethered to a solid support, an on-bead-GWL-6 (AH393) was synthesised (Figure 5.6) and screened against several different DNA sequences.

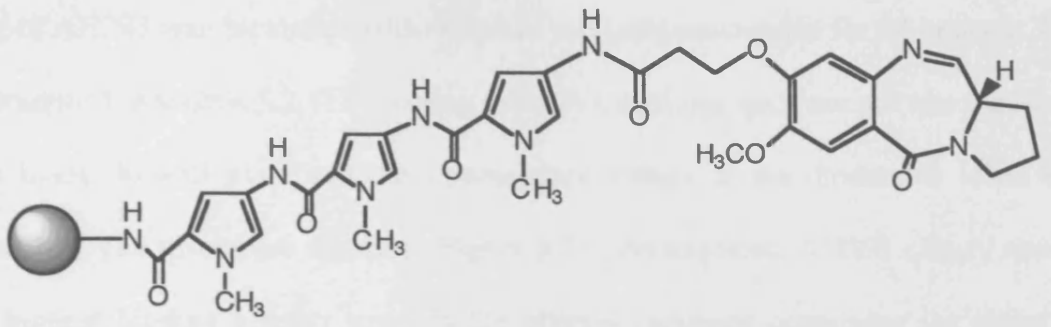

Figure 5.6 Structure of GWL-6 on bead, AH393

Synthetic oligonucleotides were designed according to specific target sequences, *i.e.*, the synthetic oligonucleotide Oligo-2, contains a 20 base pair sequence from the EGFR gene and Oligo-3, a 15 base pair sequence containing an inverted CCAAT box element from the promoter of human topoisomerase IIα gene. As it was shown by footprinting that GWL-6 binds to 5'- AGATTAT-3', a synthetic oligonucleotide containing this sequence was also synthesised (Oligo-4). Sequences of the synthetic oligonucleotides used to screen against various bead libraries are summarised in Table 5.3.

Table 5.3. Sequences of the synthetic oligonucleotides used to screen against libraries.

Oligo-1	5'- ACACCTAIAGATIAAITCTI –3' where I = inosine
Oligo-2	5'- GCACTTTTGAAGATCATTTT-3'
Oligo-3	5'- CTACGATTGGTTCTT –3'
Oligo-4	5'- TGAGATTATCAAAAAG –3'

1mg of AH393 was incubated with 400μl of each oligonucleotide for 24 hours at 37°C as described in section 5.2.4. Following extensive washing, each sample was transferred to a black 96-well plate and the fluorescence values of the rhodamine label were measured. The results are shown in Figure 5.7A. As expected, AH393 clearly showed the highest binding affinity towards the oligo-4 sequence containing the target 5'-AGATTAT sequence while it showed little affinity towards the other sequences, suggesting that the method can detect the sequence selectivity of AH393.

5.3.2.2 Binding affinity and sequence selectivity of heterocyclic compounds

Another set of beads, AH394, that consisted of three consecutive pyrrole units attached to the bead and no PBD capping unit, was synthesised. This compound was also screened against the same four synthetic oligonucleotides in order to examine the influence of a PBD unit on the interaction with the DNA. The fluorescence values observed indicated that the compound had a high binding affinity towards the oligo-4 sequence (Figure 5.7B). The fluorescence value for Oligo-4 was 21-fold higher than that of AH393. AH394 also showed a significant affinity towards Oligo-2 which is approximately 3-fold lower than Oligo-4. The affinity of AH394 towards Oligo-2 is higher than the affinity of AH393 towards Oligo-4 by approximately 7-fold.

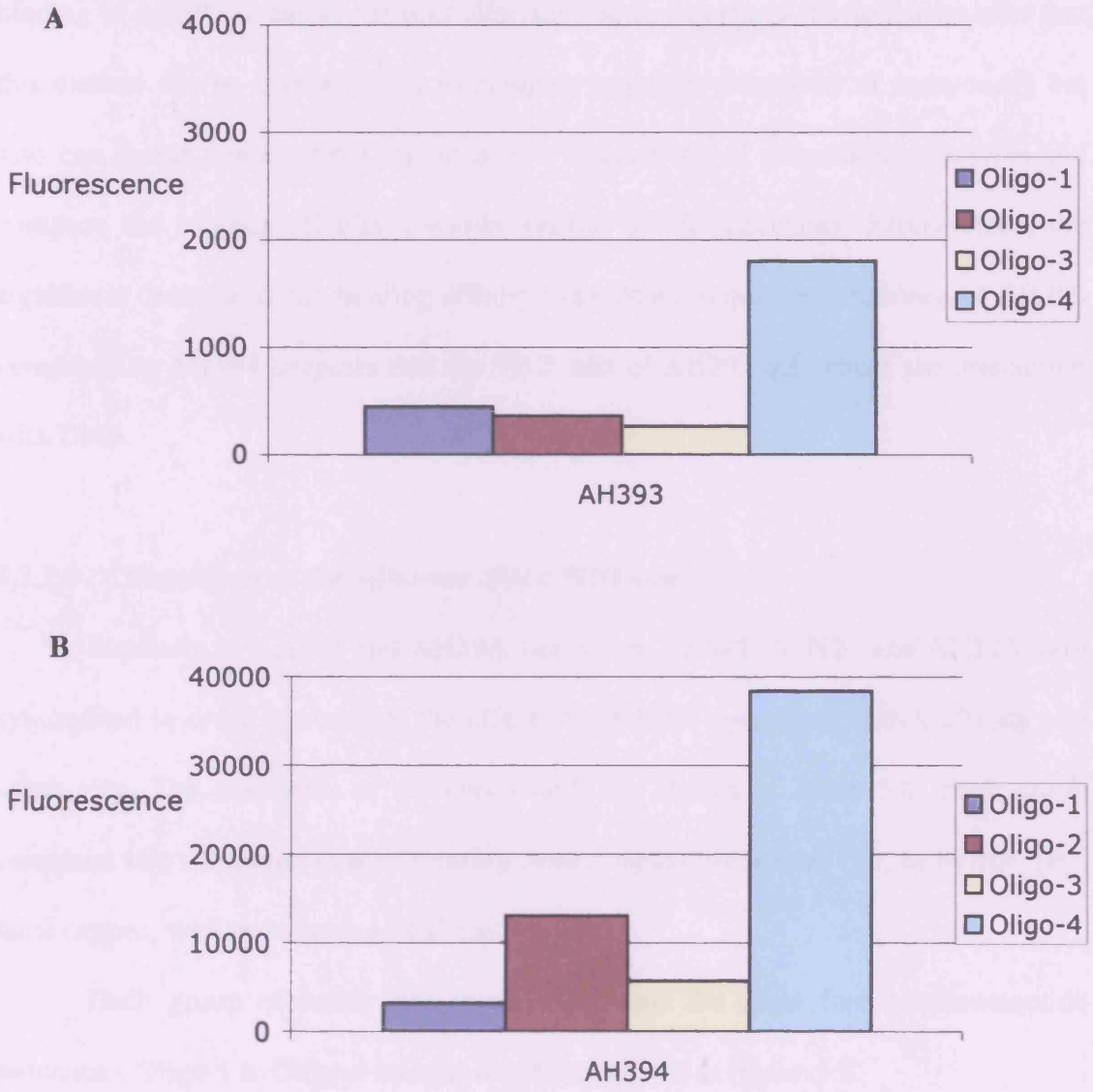

Figure 5.7 Fluorescence measured for (**A**) AH393 and (**B**) AH394 against different sequences from a single experiment.

The binding of AH394 to the least preferred sequence (Oligo-1) was still higher than the binding of AH393 to any of the four oligonucleotide sequences. These results infer that this method can be used not only to compare sequence selectivity of compounds but also can detect non-covalent minor groove interactions of polyamide structures and compare the binding affinity towards various DNA sequences. Furthermore, the significant decrease in the binding affinity towards the sequences examined of AH393 compared to AH394 suggests that the PBD unit of AH393 influences the interaction with DNA.

5.3.2.3 Comparison of the influence of the PBD unit

Similarly to AH393 and AH394, beads sets AH525, AH526 and AH527 were synthesised in order to compare the effect of the PBD towards the DNA affinity and selectivity. The structures of the compounds are shown in Table 5.4. Each group contained two compounds each featuring three coupled imidazoles (Im) or pyrrole (Py) units capped, with or without a PBD unit.

Each group of beads was screened against the same four oligonucleotide sequences, Oligo-1 to Oligo-4 and the results are shown in Figure 5.8.

As observed with the AH393 and AH394 pair, most compounds without a PBD showed higher fluorescence values than the ones with a PBD. However, there was one exception in the group AH525 (three imidazoles) against the Oligo-4 where the compound with a PBD showed higher affinity.

AH525	**a**	TG-Im-Im-Im
	b	TG-Im-Im-Im-PBD
AH526	**a**	TG-Im-Py-Im
	b	TG-Im-Py-Im-PBD
AH527	**a**	TG-Py-Im-Py
	b	TG-Py-Im-Py-PBD

TG = tentagel bead

Table 5.4 Structures of heterocyclic PBD conjugate.

In the AH525 pair (three imidazoles), AH525a had the highest binding affinity towards Oligo-2 followed by Oligo-4. Interestingly, however, AH525b showed the strongest affinity towards Oligo-4, followed by Oligo-2 with much less affinity. This suggests that the DNA affinity of the three imidazoles towards the Oligo-4 sequence is enhanced by the presence of a PBD resulting in an altered sequence selectivity.

Both AH526a and AH527a showed the highest binding affinity towards Oligo-4 followed by Oligo-2, while AH526b and AH527b compounds gave much less intensity to all the sequences.

High fluorescence values were observed for binding to Oligo-2 with AH525a giving the highest binding affinity among the all compounds tested, followed by AH527a > AH526a. Similarly, the values for the Oligo-4 sequence were also high in the order of AH527a > AH525b > AH526a > AH525a.

These fluorescence values were > 4-fold lower than those of AH394, however, higher than those of AH393. Therefore, introducing an imidazole instead of the three consecutive pyrroles influences the DNA interaction and reduces binding affinity towards these sequences compared to AH394. In addition the method clearly shows the sequence selectivity of all the compounds towards different DNA sequences. Importantly, these results indicate that this screening method can discriminate between compounds containing different mixtures of heterocycle unit, with or without a PBD attached to a bead binding to different sequences.

5.4.3 Screening of one compound per bead libraries

5.4.3.1 Peptide-based library

Figure 5.9 shows the structures of the initial libraries screened.

JMB337 was a peptide library with two PBDs, in 17 sublibraries, defined by 17 amino acids.

JMB434 was a peptide only library, in 17 sublibraries, defined by 17 amino acids.

Both of the above libraries were screened against the EGFR sequence (Oligo-2). The most positive beads (average of 15 beads in each library) were picked and sent to Babraham Institute for sequencing.

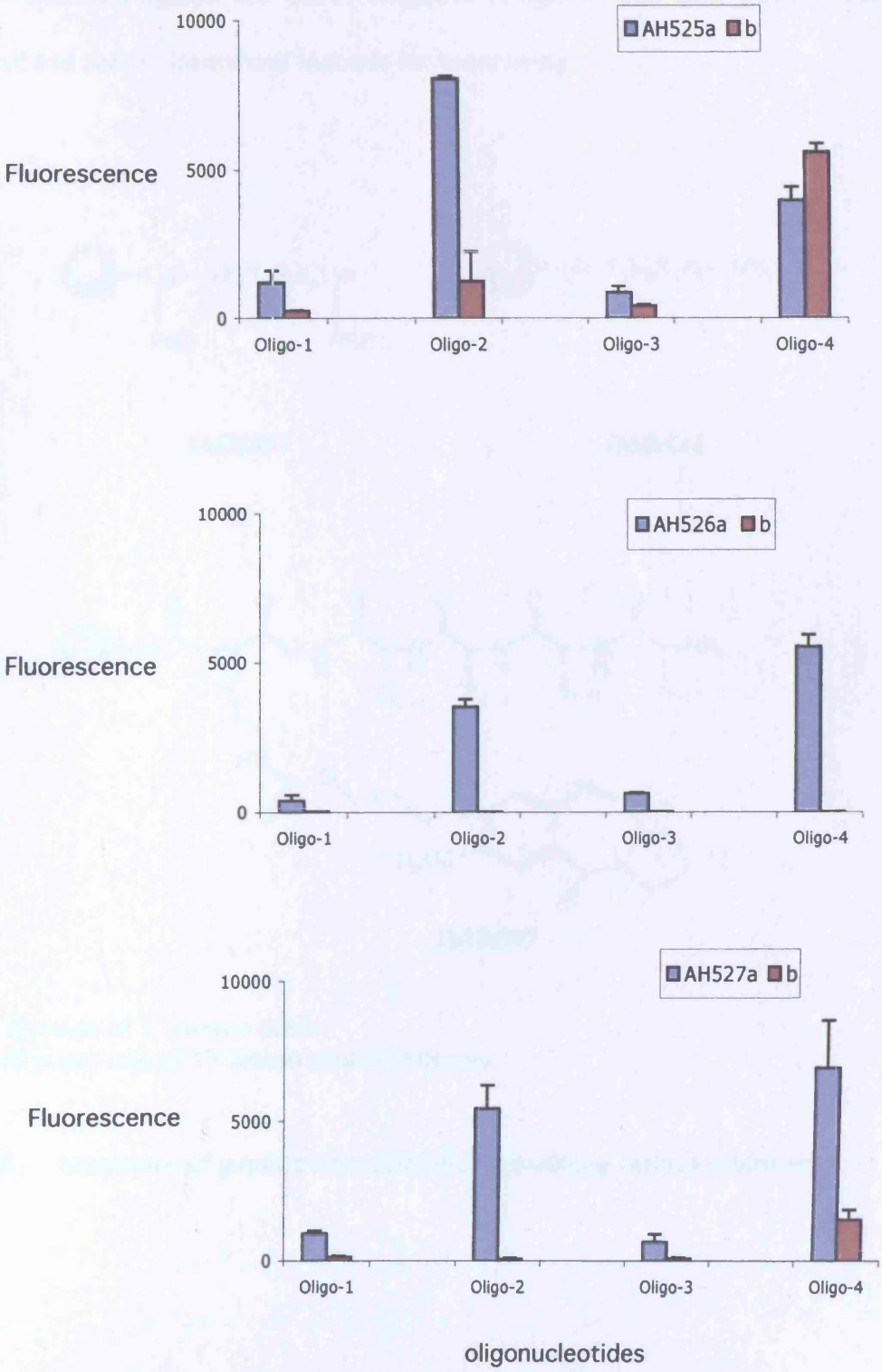

Figure 5.8 Fluorescence values showing differences in binding affinity of heterocyclic compounds.

JMB507 was peptide with PBD in 17 sublibraries defined by 17 different amino acids. They were screened against the CCAT sequence (Oligo-3). The most positive beads were picked and sent to Babraham Institute for sequencing.

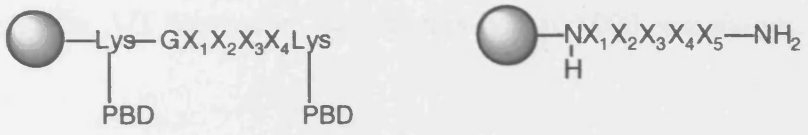

JMB337 **JMB434**

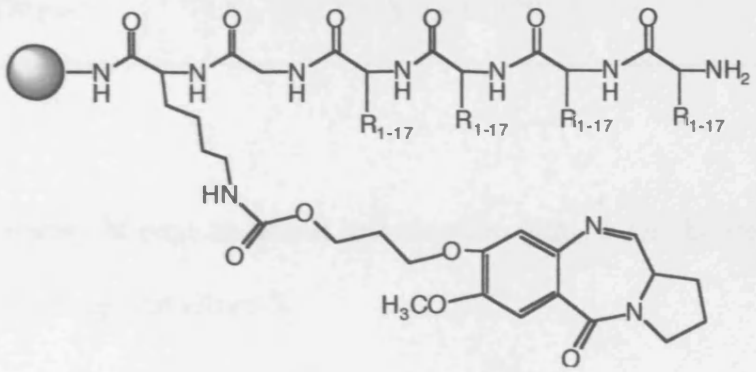

JMB507

X = one of 17 amino acids
R = any one of 17 amino acid side chains

Figure 5.9 Structures of peptide-based libraries containing various sublibraries.

5.3.3.2 PBD-capped heterocycle-based library

A diverse set of heterocycles was chosen based on the concept of naturally occurring AT-rich minor groove binding agents, e.g., N-methylpyrroles in netropsin and distamycin A, in order to increase the variety and selectivity of binding. N-methyl imidazole was included for its ability to tolerate G/C base pairs whereas pyrrole building blocks prefer A/T base pairs. Each library had 100,000 compounds.

Sequences of the synthetic oligonucleotides used in this experiment were Oligo-2 and Oligo-5. Oligo-5 contains a sequence within the bcr-abl oncogene.

Oligo-2	5'- GCACTTTTGAAGATCATTTT-3'
Oligo-5	5'- GACGCAGAAGCCCTT –3'

AH568 was a library of peptide-linked heterocycles with 10 sublibraries (Figure 5.10). They were screened against Oligo-5.

TG14.8 was a library of peptide-linked heterocycles (Figure 5.11). The library featured amino acids side chains assigned randomly to code for each of ten different heterocycles. They were screened against Oligo-2 and Oligo-5.

The positive beads were picked and sent to Babraham Institue for sequencing to find the structure of the libraries that bound to the DNA.

Figure 5.10 AH568 - 100,000 members

X_1-X_2-X_3-X_4-X_5-(C_4)-PBD

10 sub libraries: - final heterocycle known.

Number	Building block	Number	Building block
1	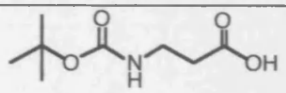	6	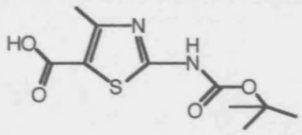
2	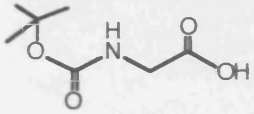	7	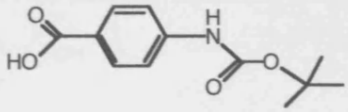
3	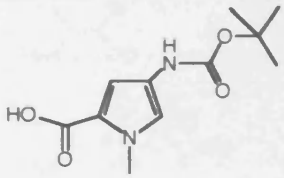	8	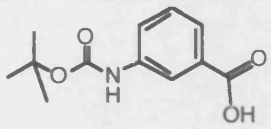
4	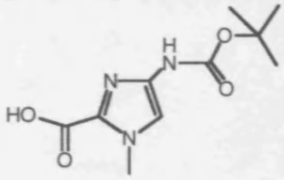	9	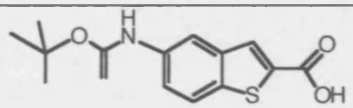
5	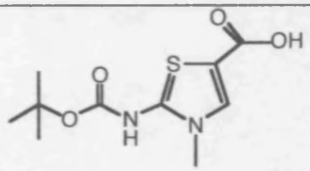	10	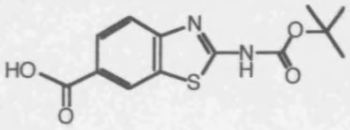

Figure 5.11 TG14.8 - 100,000 members

X_1-X_2-X_3-X_4-X_5-(C_4)-PBD

Coding amino acid (coupled in *N*-FMOC-protected form)		**Corresponding Residue** (coupled in *N*-BOC-protected form)	
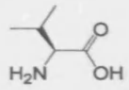	**Val**	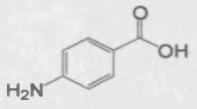	**1**
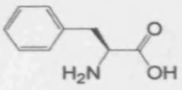	**Phe**	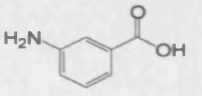	**2**
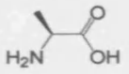	**Ala**	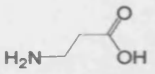	**3**
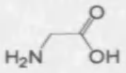	**Gly**	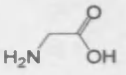	**4**
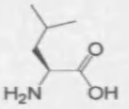	**Leu**	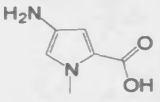	**5**
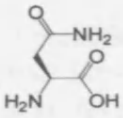	**Asn**	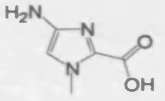	**6**
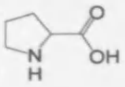	**Pro**	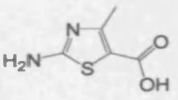	**7**
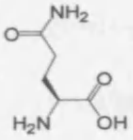	**Gln**	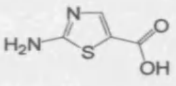	**8**
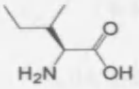	**Ile**	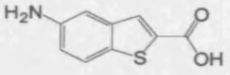	**9**
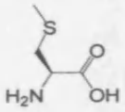	**Met**	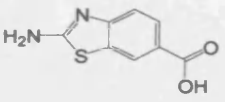	**10**

Figure 5.12 shows an example photograph of a library under a light dissecting microscope where positive beads can be seen to have turned pink.

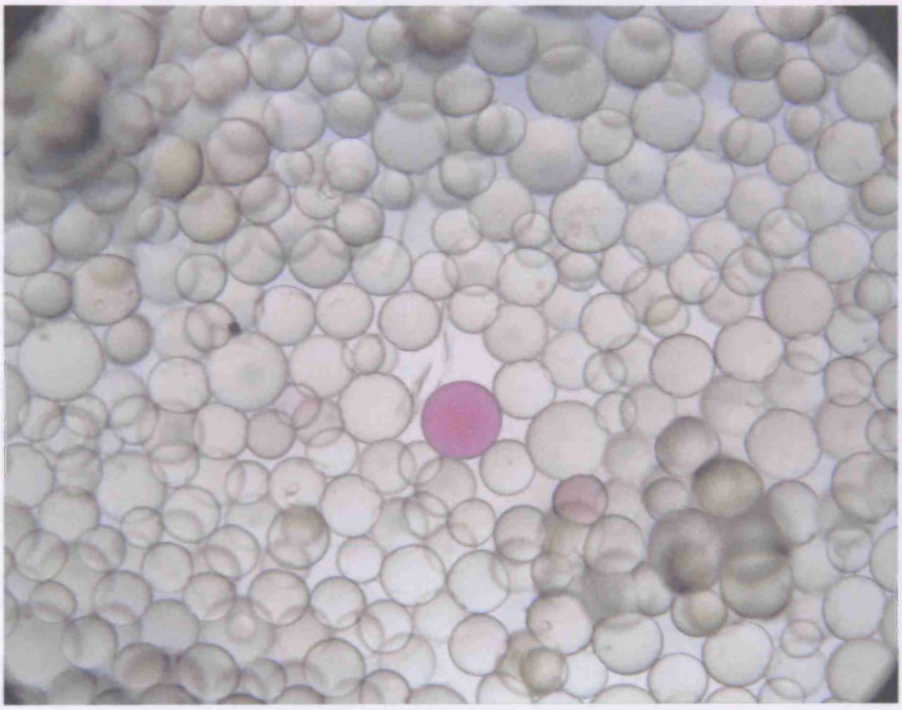

Figure 5.12 A typical image of beads sample after being reacted with synthetic oligos. Incubation at 37°C for 24 hr. The positive beads are shown as pink as the oligos were rhodamine labelled.

One of the positive beads isolated from a library screen against the EGFR sequence (Oligo-2) was successfully sequenced at the Babraham Institute and the compound was resynthesised on bead (JMB471) (Figure 5.13). Screening of this one compound set of beads was re-screened against Oligo-2 and showed strong binding

under a fluorescence microscope, indicating that the method can be used to select out the beads that contain compounds which bind with high affinity to DNA.

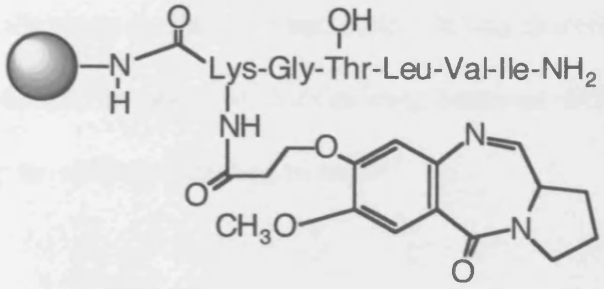

Figure 5.13 Structure of JMB471.

5.4 Discussion

A method for the screening of combinatorial libraries was developed, in order to achieve a high throughput screen for libraries synthesised in the solid phase. The libraries were either one-compound per bead or multiple beads per compound. The TG-resin has a long PEG (polyethylene glycol) coating, and hence the bead is far away from the units added during the combinatorial synthesis and should therefore not interfere with binding to target DNA sequences. In addition, PEG is water missible and so it is suitable for screening in the solution phase.

By reacting the libraries with rhodamine-labelled oligonucleotides of various sequences, it was possible to select specific beads containing compounds that have sequence selective affinity to a specific sequence of DNA. The applicability of the

screening method was initially tested using one-compound per bead and had demonstrated binding of PBD to a single target PuGPu sequence (Hardy *et al.*, 2003). In the present study a PBD dilactam (which is unable to bind covalently to DNA) was found not to bind to the same target oligonucleotide. It was therefore demonstrated that this screening method can be used to discriminate between different compounds on bead in the same way as when unattached to bead.

Further confirmation was obtained by demonstrating that the novel sequence selective agent GWL-6 on bead (AH393) bound with high affinity to the sequence 5'-AGATTATC which was found to be a target sequence by DNA footprinting (Chapter 4). In addition, AH393 bound to this target oligonucleotide (Oligo-4) with higher affinity than to several other oligonucleotide sequences (Oligo 1-3).

A tripyrrole compound but without a PBD unit, AH394, was also found to bind to oligo-4 with the highest affinity among the same four sequences tested. Since the tripyrrole unit is contained in distamycin, which is known to bind preferentially to AT-rich sequences, the strong binding affinity of AH394 to the 5'- AGATTATC sequence (oligo-4) is consistent with the known distamycin sequence selectivity. Between the compounds with tripyrroles (AH394 and AH393), AH394 (without a PBD) showed a stronger binding affinity towards all the sequences than AH393.

In the same manner, three groups of polypeptide compounds on bead with or without a PBD (AH525-AH527) were screened to the same four sequences. The varied fluorescence values for each compound further confirmed that the method could be used to discriminate between the binding affinity of different types of polypeptide with or without a PBD. Therefore, these results demonstrated that this method can be used to measure and compare binding affinity of different compounds towards various DNA sequences, and also to examine sequence selectivity of a compound towards a series of DNA sequences.

In an attempt to develop libraries containing potential DNA binding molecules in large quantity, on-bead heterocycle compounds with PBD were synthesised. These were single compound per bead of 100,000 members in each library. Following the reaction with the labelled oligonucleotides, a range of colour of beads showing from no binding (white) to strong binding (red) was observed and it was possible to isolate the most positive beads. The positive beads were successfully sequenced in a few cases and some of the compounds were resynthesised. JMB471 was a resynthesised compound on bead and it showed strong binding when re-screened against the same oligonucleotide sequence. This confirmed that this screening method is reproducible.

However, the resynthesis stage of the hit compounds encountered problems. One of the problems was ensuring the quality control of the compounds that are synthesised on a bead. Another problem was that coding strands (*e.g.*, TG14.8) on the active bead

were successfully sequenced, however, on attempting to resynthesise larger amounts of the library hits, it became apparent that the heterocycle coupling chemistry was not efficient in all cases. One implication was that during library generation only the coding strand was successfully synthesised to completion and it was these polypeptides that may be binding to the labelled DNA.

Due to these significant problems, small libraries (< 100 compounds) of PBD-containing DNA binding molecules are now being synthesised in solution phase where the quality of libraries can be assured, and also which provide an appropriate environment for the biological screening. Therefore the screening method presented here is no longer applicable. If a better way of controlling the synthesis of large PBD-containing libraries in solid phase is developed in the future, the screening protocol may then be applied.

CHAPTER 6

OVERALL DISCUSSION AND FUTURE WORK

Although cancer research has seen successes in the last two decades, including introduction of new chemotherapy agents such as Herceptin (Harris and Smith, 2002) and Avastin (Ferrara *et al.*, 2004), improvement in terms of tumour response or increased patient survival has largely been dependent on a combination of these new agents with conventional chemotherapy, leading to incremental benefit in survival (Duncan *et al.*, 2005). While an emergence of drug resistance remains a significant problem, it has also become important to discover novel anticancer drugs that are not only cytotoxic to cells but also able to target molecular aberrations that are specific to tumour cells, as described in chapter 1. With the phenomenal progress of molecular mechanism information from genomics and proteomics research, a current large body of research has been focused on the search for low molecular weight anticancer drugs with target selective characteristics. One potential target is specific sequences of DNA with ability to up and down regulate transcription of genes that would have therapeutic activity and limited or no side effects.

This thesis describes an investigation into the interactions of rationally designed novel PBD compounds with DNA *in vitro*. It examines the structural influence of the PBD dimers and the PBD conjugates on the molecular and *in vitro* pharmacological

activity with DNA. This includes the effects of linker length in the case of dimers, C2/C2'-*exo*/*endo*-unsaturation, substituent on the C2 position and different subunit on the conjugates, on the *in vitro* cytotoxicity, DNA interstrand crosslinking in naked DNA and in cells, and affinity and selectivity of binding in the minor groove of DNA. This thesis also describes the development of a screening method for combinatorial libraries where all compounds examined were synthesised in the solid phase.

A comprehensive investigation into the effects of the linker length and C2/C2'-substituents among the four novel PBD dimers that have C2/C'2-*exo*-unsaturation was carried out in Chapter 3. This enabled characterisation of the dimers for cytotoxicity and interstrand crosslinking both in naked DNA and in cells. All these dimers were much more efficient in interstrand crosslinking, and more potent, compared to the dimers with C2/C2'-saturation reported previously (Bose *et al.*, 1992a, b). This proved the importance of C2/C2'-unsaturation of the PBD dimers for efficient interaction with DNA. The presence of the extra methyl at the C2/C2'-substituents of the dimers, however, gave no significant effect on the activity of the drugs. This infers that the extra methyl group in this stereochemistry does not influence the drug to fit any better in the floor of the minor groove.

The investigation of the linker length provided the results that the dimers with five methylene linker (n = 5) showed significantly increased potency and also interstrand crosslinking efficiency compared to equivalent three methylene linked (n =

3) dimers. Interestingly, in a similar comparison reported previously (Smellie *et al.*, 2003) for compounds with C2/C2' saturation, no significantly increased activity of the n = 5 compound was observed. Furthermore, all four dimers examined produced interstrand crosslinks in cells that are not significantly repaired up to 48 hours suggesting that the drugs do not cause perturbation within the minor groove when bound to DNA.

Sequence selectivity of the four novel PBD dimers was also investigated. They showed clear binding to naked DNA as determined by footprinting and *Taq* stop polymerase assays. The binding sites of the n = 3 compounds differed to those of n = 5 compounds suggesting that the DNA interactions are different. Also, the lower concentrations needed to observe the binding sites of n = 5 dimers suggests that they react more efficiently compared to n = 3 dimers.

The importance of interstrand crosslink formation has been well established, however, a number of clinical antitumour drugs such as nitrogen mustards and cisplatin are not only able to form interstrand crosslinks but also they interact with non-DNA macromolecule and other targets. When they interact with DNA, they produce other products such as monoadducts or intrastrand crosslinks which may not contribute to the antitumour activity but contribute to other effects such as toxicity and mutagenesity. Therefore it has been a great interest to develop novel agents that can produce interstrand crosslink lesions much more efficiently in the minor groove of DNA, and

also in a sequence selective manner so that some side effects may be potentially reduced.

Furthermore, the resistance of tumours to currently used antitumour drugs has been one of the major problems in cancer therapeutics. Repair of DNA interstrand crosslinks has been shown to be an important determinant of sensitivity to DNA crosslinking drugs (McHugh *et al.*, 2001) and an important mechanism of clinical drug resistance to nitrogen mustard drugs such as melphalan (Spanswick *et al.*, 2002). The ability of the novel PBD dimers to produce interstrand crosslinks in the minor groove of DNA that are not repaired easily suggests that such compounds may have activity in tumours resistant to clinically used DNA crosslinking drugs. Since one of the four dimers, SJG-136, has been selected for clinical trials and has been shown to be highly efficacious *in vivo* activity in many models including cisplatin-resistant tumours (Hartley *et al.*, 2004), the longer linked analogues of SJG-136 may also be potential candidates as alternative agents as they have different DNA binding sites to SJG-136 and are more potent *in vitro*.

Sequence selectivity of the novel PBD dimers is encouraging for investigation further in this type of compounds, such as increasing the linker length which potentially increases the number of base pairs spanned and hence enhances sequence selectivity. Similarly, novel PBD trimers and tetramers would also potentially have enhanced

sequence selectivity but in different sequences to the dimers as they would involve more than one pair of guanines to be crosslinked.

Different types of novel PBD dimers and novel PBD conjugates were also investigated in Chapter 4. The effect of different linker of PBD dimers was examined for the cytotoxicity and crosslinking ability. None of the dimers produced significant interstrand crosslinks, however, some of them were significantly cytotoxic. A similar trend has been reported recently (Kamal *et al.*, 2005) where the cytotoxicity data for novel piperazine-linked PBD dimers did not correlate with DNA thermal denaturation studies. It is not clear what cellular mechanism of these dimers makes them cytotoxic towards cells without producing interstrand crosslinks. Similarly, among the novel PBD-aniline mustards only one compound, GD3, showed significant interstrand crosslinking although some other closely related compounds were also significantly cytotoxic. Although footprinting and *Taq* polymerase stop assays could not determine the sequence selective binding sites of GD3, this compound may be a good example of a novel PBD-nitrogen mustard conjugates to be developed in the future.

Novel PBD-monomers were also examined in Chapter 4 for cytotoxicity and sequence selectivity. The significant cytotoxicity of a PBD-tripyrrole compound (GWL-6) and the PBD-aryl conjugates correlated to DNA binding affinity. The sequence recognition of the polyamide and PBD moieties of GWL-6 could potentially be enhanced by introducing a longer polyamide chain. For similar compounds, the

evaluation of novel PBD dimers with pyrrole and imidazole polyamide conjugates has recently been reported (Kumar and Lown, 2005). It showed that this type of conjugate in general is potent against many human cancer cell lines although details of the biological evaluation has not been reported yet. Therefore it is a good indication for GWL-6 to be a building block of dimers and trimers of this type of agent.

Development of a high throughput screening method of combinatorial libraries for DNA binding has been carried out in this thesis. A large number of libraries on resin were screened against various designed synthetic oligonucleotides. By using this method, it was possible to select out specific compounds that were bound to DNA, and hence it was demonstrated that the method could be used to discriminate between compounds with different sequence specificities. Although combinatorial libraries synthesised in solid phase on bead continues to be used (Fridkin and Lubell, 2005; Xue and Seto, 2005; Sweeney *et al.*, 2005), the synthesis of heterocycle coupled PBD libraries is no longer continued due to resynthesis and quality control problems encountered. However, screening in the search for compounds with specific sequence affinity continues in solution phase although in much lower throughput.

In conclusion, PBD-based molecules continue to be developed as therapeutic anticancer agents with one of the members (SJG-136) currently in clinical trials. In addition they have potential for use as a component of novel sequence selective agents

to regulate gene expression. The work in this thesis has contributed to the further development of this interesting class of molecule.

Abu-Daya, A., Brown, P. M. & Fox, K. R. (1995) DNA sequence preferences of several AT-selective minor groove binding ligands. *Nucleic Acids Res.* **23**, 3385-92.

Ajani, J. A. (2005) Evolving chemotherapy for advanced gastric cancer. *Oncologist.* **10**, 49-58.

Alberts, S. R., Erlichman, C., Reid, J. M., Sloan, J. A., Ames, M. M., Richardson, R. L. & Goldberg, R. M. (1998) Phase I study of the duocarmycin semisynthetic derivative KW-2189 given daily for five days every six weeks. *Clin Cancer Res.* **4**, 2111-7.

Alcaro, S., Ortuso, F. & Coleman, R. S. (2005) Molecular modeling of DNA cross-linking analogues based on the azinomycin scaffold. *J Chem Inf Model.* **45**, 602-9.

Alexeev, D. G., Lipanov, A. A. & Skuratovskii, I. (1987) Poly(dA).poly(dT) is a B-type double helix with a distinctively narrow minor groove. *Nature.* **325**, 821-3.

Alley, M. C., Hollingshead, M. G., Pacula-Cox, C. M., Waud, W. R., Hartley, J. A., Howard, P. W., Gregson, S. J., Thurston, D. E. & Sausville, E. A. (2004) SJG-136 (NSC 694501), a novel rationally designed DNA minor groove interstrand cross-linking agent with potent and broad spectrum antitumor activity: part 2: efficacy evaluations. *Cancer Res.* **64**, 6700-6.

Ambudkar, S. V., Dey, S., Hrycyna, C. A., Ramachandra, M., Pastan, I. & Gottesman, M. M. (1999) Biochemical, cellular, and pharmacological aspects of the multidrug transporter. *Annu Rev Pharmacol Toxicol.* **39**, 361-98.

Anthoney, D. A. & Kaye, S. B. (1999). Drug resistance. In *Methods in Molecular Medicine: Cytotoxic Drug Resistance mechanisms.* Brown, R. & Boger-Brown, U. (Eds), New Jersey, Humana Press Inc.

Arima, K., Kosaka, M., Tamura, G., Imanaka, H. & Sakai, H. (1972) Studies on tomaymycin, a new antibiotic. I. Isolation and properties of tomaymycin. *J Antibiot (Tokyo).* **25**, 437-44.

Armstrong, R. W., Salvati, M. E. & Nguyen, M. (1992) Novel interstrand cross-links induced by the antitumor antibiotic carzinophilin/azinomycin B. *J. Am. Chem. Soc.* **114**, 3144-5.

Asai, A., Nagamura, S., Saito, H., Takahashi, I. & Nakano, H. (1994) The reversible DNA-alkylating activity of duocarmycin and its analogues. *Nucleic Acids Res.* **22**, 88-93.

Ayi, T. C., Loh, K. C., Ali, R. B. & Li, B. F. (1992) Intracellular localization of human DNA repair enzyme methylguanine-DNA methyltransferase by antibodies and its importance. *Cancer Res.* **52**, 6423-30.

Balcarova, Z., Mrazek, J., Kleinwachter, V. & Brabec, V. (1992) Cleavage by restriction enzymes of DNA modified with the antitumour drug cis-diamminedichloroplatinum(II). *Gen Physiol Biophys.* **11**, 579-88.

Baraldi, P. G., Balboni, G., Cacciari, B., Guiotto, A., Manfredini, S., Romagnoli, R., Spalluto, G., Thurston, D. E., Howard, P. W., Bianchi, N., Rutigliano, C., Mischiati, C. & Gambari, R. (1999) Synthesis, in vitro antiproliferative activity, and DNA-binding properties of hybrid molecules containing pyrrolo[2,1-c][1, 4]benzodiazepine and minor-groove-binding oligopyrrole carriers. *J Med Chem.* **42**, 5131-41.

Baraldi, P. G., Balboni, G., Pavani, M. G., Spalluto, G., Tabrizi, M. A., Clercq, E. D., Balzarini, J., Bando, T., Sugiyama, H. & Romagnoli, R. (2001) Design, synthesis, DNA binding, and biological evaluation of water-soluble hybrid molecules containing two pyrazole analogues of the alkylating cyclopropylpyrroloindole (CPI) subunit of the antitumor agent CC-1065 and polypyrrole minor groove binders. *J Med Chem.* **44**, 2536-43.

Baraldi, P. G., Cacciari, B., Guiotto, A., Leoni, A., Romagnoli, R., Spalluto, G., Mongelli, N., Howard, P. W., Thurston, D. E., Bianchi, N. & Gambari, R. (1998) Design, synthesis and biological activity of a pyrrolo [2,1-c][1,4]benzodiazepine (PBD)-distamycin hybrid. *Bioorg Med Chem Lett.* **8**, 3019-24.

Baraldi, P. G., Romagnoli, R., Giovanna Pavani, M., del Carmen Nunez, M., Bingham, J. P. & Hartley, J. A. (2002a) Benzoyl and cinnamoyl nitrogen mustard derivatives of benzoheterocyclic analogues of the tallimustine: synthesis and antitumour activity. *Bioorg Med Chem.* **10**, 1611-8.

Baraldi, P. G., Romagnoli, R., Guadix, A. E., Pineda de las Infantas, M. J., Gallo, M. A., Espinosa, A., Martinez, A., Bingham, J. P. & Hartley, J. A. (2002b) Design, synthesis, and biological activity of hybrid compounds between uramustine and DNA minor groove binder distamycin A. *J Med Chem.* **45**, 3630-8.

Barkley, M. D., Cheatham, S., Thurston, D. E. & Hurley, L. H. (1986) Pyrrolo[1,4]benzodiazepine antitumor antibiotics: evidence for two forms of tomaymycin bound to DNA. *Biochemistry.* **25**, 3021-31.

Barkley, M. D., Thomas, T. J., Maskos, K. & Remers, W. A. (1991) Steady-state fluorescence and molecular-modeling studies of tomaymycin-DNA adducts. *Biochemistry.* **30**, 4421-31.

Basu, A. K., Hanrahan, C. J., Malia, S. A., Kumar, S., Bizanek, R. & Tomasz, M. (1993) Effect of site-specifically located mitomycin C-DNA monoadducts on in vitro DNA synthesis by DNA polymerases. *Biochemistry.* **32**, 4708-18.

Belitsky, J. M., Leslie, S. J., Arora, P. S., Beerman, T. A. & Dervan, P. B. (2002) Cellular uptake of N-methylpyrrole/N-methylimidazole polyamide-dye conjugates. *Bioorg Med Chem.* **10**, 3313-8.

Best, T. P., Edelson, B. S., Nickols, N. G. & Dervan, P. B. (2003) Nuclear localization of pyrrole-imidazole polyamide-fluorescein conjugates in cell culture. *Proc Natl Acad Sci U S A.* **100**, 12063-8.

Bhuyan, B. K., Smith, K. S., Adams, E. G., Petzold, G. L. & McGovren, J. P. (1992a) Lethality, DNA alkylation, and cell cycle effects of adozelesin (U-73975) on rodent and human cells. *Cancer Res.* **52**, 5687-92.

Bhuyan, B. K., Smith, K. S., Adams, E. G., Wallace, T. L., Von Hoff, D. D. & Li, L. H. (1992b) Adozelesin, a potent new alkylating agent: cell-killing kinetics and cell-cycle effects. *Cancer Chemother Pharmacol.* **30**, 348-54.

Boger, D. L., Boyce, C. W., Garbaccio, R. M. & Goldberg, J. A. (1997) CC-1065 and the Duocarmycins: Synthetic Studies. *Chem Rev.* **97**, 787-828.

Boger, D. L. & Johnson, D. S. (1995) CC-1065 and the duocarmycins: unraveling the keys to a new class of naturally derived DNA alkylating agents. *Proc Natl Acad Sci U S A.* **92**, 3642-9.

Boger, D. L., Johnson, D. S. & Yun, W. (1994) (+)- and ent-(-)-Duocarmycin SA and (+)- and ent-(-)-N-BOC-DSA DNA Alkylation Properties.Alkylation Site Models That Accommodate the Offset AT-Rich Adenine N3 Alkylation Selectivity of the Enantiomeric Agents. *J. Am. Chem. Soc.* **116**, 1635 - 1656.

Boger, D. L., Stauffer, F. & Hedrick, M. P. (2001) Substituent effects within the DNA binding subunit of CBI analogues of the duocarmycins and CC-1065. *Bioorg Med Chem Lett.* **11**, 2021-4.

Bontemps, J., Houssier, C. & Fredericq, E. (1975) Physico-chemical study of the complexes of "33258 Hoechst" with DNA and nucleohistone. *Nucleic Acids Res.* **2**, 971-84.

Borst, P., Evers, R., Kool, M. & Wijnholds, J. (2000) A family of drug transporters: the multidrug resistance-associated proteins. *J Natl Cancer Inst.* **92**, 1295-302.

Bose, D. S., Thompson, A. S., Ching, J., Hartley, J. A., Berardini, M. D., Jenkins, T. C., Neidle, S., Hurley, L. H. & Thurston, D. E. (1992a) Rational design of a highly efficient irreversible DNA interstrand cross-linking agent based on the pyrrolobenzodiazepine ring system. *J. Am. Chem. Soc.* **114**, 4939 – 4941.

Bose, D. S., Thompson, A. S., Smellie, M., Berardini, M. D., Hartley, J. A., Jenkins, T. C., Neidle, S. & Thurston, D. E. (1992b) Effect of linker length on DNA-binding affinity, crosslinking efficiency and cytotoxicity of C8-linked pyrrolobenzodiazepine dimers. *J Chem Soc Chem Commun.* **14**, 1518-20.

Boyd, F. L., Cheatham, S. F., Remers, W., Hill, G. C. & Hurley, L. H. (1990a) Characterization of the structure of the anthramycin-d(ATGCAT)2 adduct by NMR and molecular modeling studies. Determination of the stereochemistry of the covalent linkage site, orientation in the minor groove of DNA, and effect on local DNA structure. *J. Am. Chem. Soc.* **112**, 3279-3289.

Boyd, F. L., Stewart, D., Remers, W. A., Barkley, M. D. & Hurley, L. H. (1990b) Characterization of a unique tomaymycin-d(CICGAATTCICG)2 adduct containing two drug molecules per duplex by NMR, fluorescence, and molecular modeling studies. *Biochemistry.* **29**, 2387-403.

Boyer, M. J. & Tannock, I. F. (1998). Cellular and molecular basis of chemotherapy. In *The Basic Science of Oncology.* Tannock, I. F. & Hill, R. P. (Eds), New York, McGraw-Hill Health Professions Division, 350-369.

Brabec, V. & Balcarova, Z. (1993) Restriction-enzyme cleavage of DNA modified by platinum(II) complexes. *Eur J Biochem.* **216**, 183-7.

Brazhnikova, M. G., Konstantinova, N. V. & Mesentsev, A. S. (1972) Sibiromycin: isolation and characterization. *J Antibiot (Tokyo).* **25**, 668-73.

Brendel, M. & Ruhland, A. (1984) Relationships between functionality and genetic toxicology of selected DNA-damaging agents. *Mutat Res.* **133**, 51-85.

Broggini, M., Coley, H. M., Mongelli, N., Pesenti, E., Wyatt, M. D., Hartley, J. A. & D'Incalci, M. (1995) DNA sequence-specific adenine alkylation by the novel antitumor drug tallimustine (FCE 24517), a benzoyl nitrogen mustard derivative of distamycin. *Nucleic Acids Res.* **23**, 81-7.

Brosh, R. M., Jr., Majumdar, A., Desai, S., Hickson, I. D., Bohr, V. A. & Seidman, M. M. (2001) Unwinding of a DNA triple helix by the Werner and Bloom syndrome helicases. *J Biol Chem.* **276**, 3024-30.

Burden, D. A. & Osheroff, N. (1998) Mechanism of action of eukaryotic topoisomerase II and drugs targeted to the enzyme. *Biochim Biophys Acta.* **1400**, 139-54.

Carbone, G. M., McGuffie, E., Napoli, S., Flanagan, C. E., Dembech, C., Negri, U., Arcamone, F., Capobianco, M. L. & Catapano, C. V. (2004) DNA binding and antigene activity of a daunomycin-conjugated triplex-forming oligonucleotide targeting the P2 promoter of the human c-myc gene. *Nucleic Acids Res.* **32**, 2396-410.

Carter, C. A., Waud, W. R., Li, L. H., DeKoning, T. F., McGovren, J. P. & Plowman, J. (1996) Preclinical antitumor activity of bizelesin in mice. *Clin Cancer Res.* **2**, 1143-9.

Casely-Hayford, M. A., Pors, K., James, C. H., Patterson, L. H., Hartley, J. A. & Searcey, M. (2005) Design and synthesis of a DNA-crosslinking azinomycin analogue. *Org Biomol Chem.* **3**, 3585-9.

Chaires, J. B. (1998) Drug--DNA interactions. *Curr Opin Struct Biol.* **8**, 314-20.

Chaires, J. B., Leng, F., Przewloka, T., Fokt, I., Ling, Y. H., Perez-Soler, R. & Priebe, W. (1997) Structure-based design of a new bisintercalating anthracycline antibiotic. *J Med Chem.* **40**, 261-6.

Chang, S. M., Theodosopoulos, P., Lamborn, K., Malec, M., Rabbitt, J., Page, M. & Prados, M. D. (2004) Temozolomide in the treatment of recurrent malignant glioma. *Cancer.* **100**, 605-11.

Cheatham, S., Kook, A., Hurley, L. H., Barkley, M. D. & Remers, W. (1988) One- and two-dimensional 1H NMR, fluorescence, and molecular modeling studies on the tomaymycin-d(ATGCAT)2 adduct. Evidence for two covalent adducts with opposite orientations and stereochemistries at the covalent linkage site. *J Med Chem.* **31**, 583-90.

Chen, A. Y., Yu, C., Bodley, A., Peng, L. F. & Liu, L. F. (1993a) A new mammalian DNA topoisomerase I poison Hoechst 33342: cytotoxicity and drug resistance in human cell cultures. *Cancer Res.* **53**, 1332-7.

Chen, A. Y., Yu, C., Gatto, B. & Liu, L. F. (1993b) DNA minor groove-binding ligands: a different class of mammalian DNA topoisomerase I inhibitors. *Proc Natl Acad Sci U S A.* **90**, 8131-5.

Chen, C. J., Chin, J. E., Ueda, K., Clark, D. P., Pastan, I., Gottesman, M. M. & Roninson, I. B. (1986) Internal duplication and homology with bacterial transport proteins in the mdr1 (P-glycoprotein) gene from multidrug-resistant human cells. *Cell.* **47**, 381-9.

Chiang, S. Y., Welch, J., Rauscher, F. J., 3rd & Beerman, T. A. (1994) Effects of minor groove binding drugs on the interaction of TATA box binding protein and TFIIA with DNA. *Biochemistry.* **33**, 7033-40.

Chu, E. & Allegra, C. (1996). Antifolates. In *Cancer chemotherapy and biotherapy: principles and practice.* Chabner, B. A. & Longo, D. L. (Eds), Philadelphia, Lippincott-Raven, 109-148.

Chun, E. H., Gonzales, L., Lewis, F. S., Jones, J. & Rutman, R. J. (1969) Differences in the in vivo alkylation and cross-linking of nitrogen mustard-sensitive and -resistant lines of Lettre-Ehrlich asites tumors. *Cancer Res.* **29**, 1184-94.

Clingen, P. H., De Silva, I. U., McHugh, P. J., Ghadessy, F. J., Tilby, M. J., Thurston, D. E. & Hartley, J. A. (2005) The XPF-ERCC1 endonuclease and homologous recombination contribute to the repair of minor groove DNA interstrand crosslinks in mammalian cells produced by the pyrrolo[2,1-c][1,4]benzodiazepine dimer SJG-136. *Nucleic Acids Res.* **33**, 3283-91.

Cole, R. S. (1973) Repair of DNA containing interstrand crosslinks in Escherichia coli: sequential excision and recombination. *Proc Natl Acad Sci U S A.* **70**, 1064-8.

Coleman, R. S., Perez, R. J., Burk, C. H. & Navarro, A. (2002) Studies on the mechanism of action of azinomycin B: definition of regioselectivity and sequence selectivity of DNA cross-link formation and clarification of the role of the naphthoate. *J Am Chem Soc.* **124**, 13008-17.

Coll, M., Frederick, C. A., Wang, A. H. & Rich, A. (1987) A bifurcated hydrogen-bonded conformation in the d(A.T) base pairs of the DNA dodecamer d(CGCAAATTTGCG) and its complex with distamycin. *Proc Natl Acad Sci U S A.* **84**, 8385-9.

Colvin, O. M. (2001). Antitumour alkylating agents. In *Cancer: Principles and Practice of Oncology.* De Vita Jr, V. T., Hellman, S. & Rosenberg, S. A. (Eds), Philadelphia, Lippincott-Williams & Wilkins, 363-375.

Comess, K. M. & Lippard, S. J. (1993). Molecular Aspects of Platinum-DNA Interactions. In *Molecular Aspects of Anticancer Drug - DNA Interactions. Volume 1.* Neidle, S. & Waring, M. J. (Eds), London, Macmillan Press, 134-168.

Cozzi, P. (2003) The discovery of a new potential anticancer drug: a case history. *Farmaco.* **58**, 213-20.

Crooke, S. T. (1999) Molecular mechanisms of action of antisense drugs. *Biochim Biophys Acta.* **1489**, 31-44.

Crooke, S. T. (2000) Potential roles of antisense technology in cancer chemotherapy. *Oncogene.* **19**, 6651-9.

Crowley, K. S., Phillion, D. P., Woodard, S. S., Schweitzer, B. A., Singh, M., Shabany, H., Burnette, B., Hippenmeyer, P., Heitmeier, M. & Bashkin, J. K. (2003) Controlling the intracellular localization of fluorescent polyamide analogues in cultured cells. *Bioorg Med Chem Lett.* **13**, 1565-70.

Cuvier, O. & Hirano, T. (2003) A role of topoisomerase II in linking DNA replication to chromosome condensation. *J Cell Biol.* **160**, 645-55.

D'Incalci, M. (2001). Vinca alkaloids, taxanes, and podophyllotoxins. In *Oxford Textbook of Oncology.* Souhami, R. L., Tannock, I. F., Hohenberger, P. & Horiot, J. C. (Eds), New York, Oxford University Press, 729-738.

D'Incalci, M. & Sessa, C. (1997) DNA minor groove binding ligands: a new class of anticancer agents. *Expert Opin Investig Drugs.* **6**, 875-84.

Dallas, A. & Vlassov, A. V. (2006) RNAi: A novel antisense technology and its therapeutic potential. *Med Sci Monit.* **12**, RA67-74.

Darnell, J. E., Jr. (2002) Transcription factors as targets for cancer therapy. *Nat Rev Cancer.* **2**, 740-9.

de Jong, S., Mulder, N. H. & de Vries, E. G. E. (2001). Mechanisms of drug resistance. In *Oxford Textbook of Oncology*. Souhami, R. L., Tannock, I. F., Hohenberger, P. & Horiot, J. C. (Eds), New York, Oxford University Press, 755-772.

De Silva, I. U., McHugh, P. J., Clingen, P. H. & Hartley, J. A. (2000) Defining the roles of nucleotide excision repair and recombination in the repair of DNA interstrand cross-links in mammalian cells. *Mol Cell Biol.* **20**, 7980-90.

Dean, N. M. & Bennett, C. F. (2003) Antisense oligonucleotide-based therapeutics for cancer. *Oncogene.* **22**, 9087-96.

Dervan, P. B. (1986) Design of sequence-specific DNA-binding molecules. *Science.* **232**, 464-71.

Dervan, P. B. & Edelson, B. S. (2003) Recognition of the DNA minor groove by pyrrole-imidazole polyamides. *Curr Opin Struct Biol.* **13**, 284-99.

Dickinson, L. A., Burnett, R., Melander, C., Edelson, B. S., Arora, P. S., Dervan, P. B. & Gottesfeld, J. M. (2004) Arresting cancer proliferation by small-molecule gene regulation. *Chem Biol.* **11**, 1583-94.

Dickinson, L. A., Gulizia, R. J., Trauger, J. W., Baird, E. E., Mosier, D. E., Gottesfeld, J. M. & Dervan, P. B. (1998) Inhibition of RNA polymerase II transcription in human cells by synthetic DNA-binding ligands. *Proc Natl Acad Sci U S A.* **95**, 12890-5.

Doroshow, J. H. & Longo, D. L. (1996). Anthracyclines. In *Cancer chemotherapy and biotherapy: Principles and practice.* Chabner, B. A. & Longo, D. L. (Eds), Philadelphia, Lippincott-Raven, 409-434.

Dronkert, M. L. & Kanaar, R. (2001) Repair of DNA interstrand cross-links. *Mutat Res.* **486**, 217-47.

Dudouet, B., Burnett, R., Dickinson, L. A., Wood, M. R., Melander, C., Belitsky, J. M., Edelson, B., Wurtz, N., Briehn, C., Dervan, P. B. & Gottesfeld, J. M. (2003) Accessibility of nuclear chromatin by DNA binding polyamides. *Chem Biol.* **10**, 859-67.

Duncan, R., Vicent, M. J., Greco, F. & Nicholson, R. I. (2005) Polymer-drug conjugates: towards a novel approach for the treatment of endrocine-related cancer. *Endocr Relat Cancer.* **12**, 189-199.

Ebbinghaus, S. W. (2003) Site-selective DNA binding drugs. *Chem Biol.* **10**, 895-7.

Farmer, J. D., Jr., Gustafson, G. R., Conti, A., Zimmt, M. B. & Suggs, J. W. (1991) DNA binding properties of a new class of linked anthramycin analogs. *Nucleic Acids Res.* **19**, 899-903.

Farmer Jr, J. D., Rudnicki, S. M. & Suggs, J. W. (1988) Synthesis and dna crosslinking ability of a dimeric anthramycin analogue. *Tetrahedron Letters.* **29**, *5105-5108.*

Ferrara, N., Hillan, K. J., Gerber, H. P. & Novotny, W. (2004) Discovery and development of bevacizumab, an anti-VEGF antibody for treating cancer. *Nat Rev Drug Discov.* **3**, 391-400.

Fossella, J. A., Kim, Y. J., Shih, H., Richards, E. G. & Fresco, J. R. (1993) Relative specificities in binding of Watson-Crick base pairs by third strand residues in a DNA pyrimidine triplex motif. *Nucleic Acids Res.* **21**, 4511-5.

Fox, E., Curt, G. A. & Balis, F. M. (2002) Clinical trial design for target-based therapy. *Oncologist.* **7**, 401-9.

Frank-Kamenetskii, M. D. & Mirkin, S. M. (1995) Triplex DNA structures. *Annu Rev Biochem.* **64**, 65-95.

Fratini, A. V., Kopka, M. L., Drew, H. R. & Dickerson, R. E. (1982) Reversible bending and helix geometry in a B-DNA dodecamer: CGCGAATTBrCGCG. *J Biol Chem.* **257**, 14686-707.

Fridkin, G. & Lubell, W. D. (2005) Deazapurine solid-phase synthesis: combinatorial synthesis of a library of N3,N5,C6-trisubstituted pyrrolo[3,2-d]pyrimidine derivatives on cross-linked polystyrene bearing a cysteamine linker. *J Comb Chem.* **7**, 977-86.

Friedberg, E. C., Walker, G. C. & Siede, W. (1995). DNA repair and mutagenesis.In Book DNA repair and mutagenesis Editor, (Ed.^Eds),Washington DC, ASM Press, Pages.

Garrett, M. D. & Workman, P. (1999) Discovering novel chemotherapeutic drugs for the third millennium. *Eur J Cancer.* **35**, 2010-30.

Gerlach, J. H., Endicott, J. A., Juranka, P. F., Henderson, G., Sarangi, F., Deuchars, K. L. & Ling, V. (1986) Homology between P-glycoprotein and a bacterial haemolysin transport protein suggests a model for multidrug resistance. *Nature.* **324**, 485-9.

Gibbs, J. B. (2000) Mechanism-based target identification and drug discovery in cancer research. *Science.* **287**, 1969-73.

Gilman, A. & Philips, F. S. (1946) The Biological Actions and Therapeutic Applications of the B-Chloroethyl Amines and Sulfides. *Science*, 409-436.

Goldstein, L. J., Galski, H., Fojo, A., Willingham, M., Lai, S. L., Gazdar, A., Pirker, R., Green, A., Crist, W., Brodeur, G. M. & et al. (1989) Expression of a multidrug resistance gene in human cancers. *J Natl Cancer Inst.* **81**, 116-24.

Gottesfeld, J. M., Neely, L., Trauger, J. W., Baird, E. E. & Dervan, P. B. (1997) Regulation of gene expression by small molecules. *Nature.* **387**, 202-5.

Gottesman, M. M. (2002) Mechanisms of cancer drug resistance. *Annu Rev Med.* **53**, 615-27.

Gottesman, M. M., Mickisch, G. H. & Pastan, I. (1994) In vivo models of P-glycoprotein-mediated multidrug resistance. *Cancer Treat Res.* **73**, 107-28.

Graves, D. E., Pattaroni, C., Krishnan, B. S., Ostrander, J. M., Hurley, L. H. & Krugh, T. R. (1984) The reaction of anthramycin with DNA. Proton and carbon nuclear magnetic resonance studies on the structure of the anthramycin-DNA adduct. *J Biol Chem.* **259**, 8202-9.

Graves, D. E., Stone, M. P. & Krugh, T. R. (1985) Structure of the anthramycin-d(ATGCAT)2 adduct from one- and two-dimensional proton NMR experiments in solution. *Biochemistry.* **24**, 7573-81.

Green, J. A., Robertson, L. J. & Clark, A. H. (1993) Glutathione S-transferase expression in benign and malignant ovarian tumours. *Br J Cancer.* **68**, 235-9.

Gregson, S. J., Howard, P. W., Barcella, S., Nakamya, A., Jenkins, T. C., Kelland, L. R. & Thurston, D. E. (2000a) Effect of C2/C3-endo unsaturation on the cytotoxicity and DNA-binding reactivity of pyrrolo[2,1-c][1,4]benzodiazepines. *Bioorg Med Chem Lett.* **10**, 1849-51.

Gregson, S. J., Howard, P. W., Corcoran, K. E., Barcella, S., Yasin, M. M., Hurst, A. A., Jenkins, T. C., Kelland, L. R. & Thurston, D. E. (2000b) Effect of C2-exo unsaturation on the cytotoxicity and DNA-binding reactivity of pyrrolo[2,1-c][1,4]benzodiazepines. *Bioorg Med Chem Lett.* **10**, 1845-7.

Gregson, S. J., Howard, P. W., Corcoran, K. E., Jenkins, T. C., Kelland, L. R. & Thurston, D. E. (2001a) Synthesis of the first example of a C2-C3/C2'-C3'-endo unsaturated pyrrolo[2,1-c][1,4]benzodiazepine dimer. *Bioorg Med Chem Lett.* **11**, 2859-62.

Gregson, S. J., Howard, P. W., Gullick, D. R., Hamaguchi, A., Corcoran, K. E., Brooks, N. A., Hartley, J. A., Jenkins, T. C., Patel, S., Guille, M. J. & Thurston, D. E. (2004) Linker length modulates DNA cross-linking reactivity and cytotoxic potency of C8/C8' ether-linked C2-exo-unsaturated pyrrolo[2,1-c][1,4]benzodiazepine (PBD) dimers. *J Med Chem.* **47**, 1161-74.

Gregson, S. J., Howard, P. W., Hartley, J. A., Brooks, N. A., Adams, L. J., Jenkins, T. C., Kelland, L. R. & Thurston, D. E. (2001b) Design, synthesis, and evaluation of a novel pyrrolobenzodiazepine DNA-interactive agent with highly efficient cross-linking ability and potent cytotoxicity. *J Med Chem.* **44**, 737-48.

Gregson, S. J., Howard, P. W., Jenkins, T. C., Kelland, L. R. & Thurston, D. E. (1999) Synthesis of a Novel C2/C2'-exo Unsaturated Pyrrolobenzodiazepine Cross-linking Agent with Remarkable DNA Binding Affinity and Cytotoxicity. *Journal of the Chemical Society Chemical Communication.* **9**, 797-798.

Gregson, S. J., Howard, P. W. & Thurston, D. E. (2003) Synthesis of the first examples of A-C8/C-C2 amide-Linked pyrrolo[2,1-c][1,4]benzodiazepine dimers. *Bioorg Med Chem Lett.* **13**, 2277-80.

Grem, J. L. (1996). 5-Fluoropyrimidines. In *Cancer chemotherapy and biotherapy: principles and practice.* Chabner, B. A. & Longo, D. L. (Eds), Philadelphia, Lippincott-Raven, 149-212.

Grunberg, E., Prince, H. N., Titsworth, E., Beskid, G. & Tendler, M. D. (1966) Chemotherapeutic properities of anthramycin. *Chemotherapy.* **11**, 249-60.

Guchelaar, H. J., Vermes, A., Vermes, I. & Haanen, C. (1997) Apoptosis: molecular mechanisms and implications for cancer chemotherapy. *Pharm World Sci.* **19**, 119-25.

Guiotto, A., Howard, P. W., Baraldi, P. G. & Thurston, D. E. (1998) Synthesis of novel C7-aryl substituted pyrrolo[2,1-c][1,4]benzodiazepines (PBDs) via pro-N10-Troc protection and Suzuki coupling. *Bioorg Med Chem Lett.* **8**, 3017-8.

Hanahan, D. & Weinberg, R. A. (2000) The hallmarks of cancer. *Cell.* **100**, 57-70.

Hande, K. R. (1998) Clinical applications of anticancer drugs targeted to topoisomerase II. *Biochim Biophys Acta.* **1400**, 173-84.

Hanka, L. J., Dietz, A., Gerpheide, S. A., Kuentzel, S. L. & Martin, D. G. (1978) CC-1065 (NSC-298223), a new antitumor antibiotic. Production, in vitro biological activity, microbiological assays and taxonomy of the producing microorganism. *J Antibiot (Tokyo).* **31**, 1211-7.

Hara, M., Tamaoki, T., Yoshida, M., Morimoto, M. & Nakano, H. (1988) DC 102, a new glycosidic pyrrolo(1,4)benzodiazepine antibiotic produced by Streptomyces sp. *J Antibiot (Tokyo).* **41**, 702-4.

Hardy, A., Berry, J. M., Brooks-Turner, N., Howard, P. W., Hartley, J. A. & Thurston, D. E. (2003). The Generation and DNA-Interaction of PBD and CBI Libraries. In *Small Molecule DNA and RNA Binders.* Demeunynck, M., Bailly, C. & Wilson, W. D. (Eds), Weinheim, Wiley-VCH Verlag GmbH, 697-710.

Harris, J. M. & Chess, R. B. (2003) Effect of pegylation on pharmaceuticals. *Nat Rev Drug Discov.* **2**, 214-21.

Harshman, K. D. & Dervan, P. B. (1985) Molecular recognition of B-DNA by Hoechst 33258. *Nucleic Acids Res.* **13**, 4825-35.

Hart, I. R. (2001). Metastasis. In *Oxford Textbook of Oncology.* Souhami, R. L., Tannocl, I. F., Hohenberger, P. & Horiot, J. C. (Eds), New York, Oxford University Press, 103-114.

Hartley, J. A. (1993). Selectivity in Alkylating Agent-DNA Interactions. In *Molecular Aspects of Anticancer Drug - DNA Interactions. Volume 1.* Neidle, S. & Waring, M. J. (Eds), London, Macmillan Press, 1-22.

Hartley, J. A. (2001). Alkylating agents. In *Oxford Textbook of Oncology.* Souhami, R. L., Tannocl, I. F., Hohenberger, P. & Horiot, J. C. (Eds), New York, Oxford University Press, 639-654.

Hartley, J. A., Berardini, M. D. & Souhami, R. L. (1991) An agarose gel method for the determination of DNA interstrand crosslinking applicable to the measurement of the rate of total and "second-arm" crosslink reactions. *Anal Biochem.* **193**, 131-4.

Hartley, J. A., Preti, C. S., Wyatt, M. D. & Lee, M. (1995) Design, synthesis and biological evaluation of benzoic acid mustard derivatives of imidazole-containing and C-terminal carboxamide analogues of distamycin. *Drug Des Discov.* **12**, 323-35.

Hartley, J. A., Spanswick, V. J., Brooks, N., Clingen, P. H., McHugh, P. J., Hochhauser, D., Pedley, R. B., Kelland, L. R., Alley, M. C., Schultz, R., Hollingshead, M. G., Schweikart, K. M., Tomaszewski, J. E., Sausville, E. A., Gregson, S. J., Howard, P. W. & Thurston, D. E. (2004) SJG-136 (NSC 694501), a novel rationally designed DNA minor groove interstrand cross-linking agent with potent and broad spectrum antitumor activity: part 1: cellular pharmacology, in vitro and initial in vivo antitumor activity. *Cancer Res.* **64**, 6693-9.

Herman, D. M., Baird, E. E. & Dervan, P. B. (1999) Tandem Hairpin Motif for Recognition in the Minor Groove of DNA by Pyrrole-Imidazole Polyamides. *Chemistry - A European Journal.* **5**, 975-983.

Hertzberg, R. P., Hecht, S. M., Reynolds, V. L., Molineux, I. J. & Hurley, L. H. (1986) DNA sequence specificity of the pyrrolo[1,4]benzodiazepine antitumor antibiotics. Methidiumpropyl-EDTA-iron(II) footprinting analysis of DNA binding sites for anthramycin and related drugs. *Biochemistry.* **25**, 1249-58.

Hill, R. P. & Tannock, I. F. (1998). Introduction to cancer biology.In Book Introduction to cancer biology Editor, (Ed.^Eds),New York, McGraw-Hill Health Professions Division, Pages.

Hochlowski, J. E., Andres, W. W., Theriault, R. J., Jackson, M. & McAlpine, J. B. (1987) Abbeymycin, a new anthramycin-type antibiotic produced by a streptomycete. *J Antibiot (Tokyo).* **40**, 145-8.

Hoeijmakers, J. H. (2001) Genome maintenance mechanisms for preventing cancer. *Nature.* **411**, 366-74.

Huang, J., Wu, L., Tashiro, S., Onodera, S. & Ikejima, T. (2005) Bcl-2 up-regulation and P-p53 down-regulation account for the low sensitivity of murine L929 fibrosarcoma cells to oridonin-induced apoptosis. *Biol Pharm Bull.* **28**, 2068-74.

Humbert, O., Fiumicino, S., Aquilina, G., Branch, P., Oda, S., Zijno, A., Karran, P. & Bignami, M. (1999) Mismatch repair and differential sensitivity of mouse and human cells to methylating agents. *Carcinogenesis.* **20**, 205-14.

Hurley, L. H. (1977) Pyrrolo(1,4)benzodiazepine antitumor antibiotics. Comparative aspects of anthramycin, tomaymycin and sibiromycin. *J Antibiot (Tokyo).* **30**, 349-70.

Hurley, L. H., Gairola, C. & Zmijewski, M. (1977) Pyrrolo(1,4)benzodiazepine antitumor antibiotics. In vitro interaction of anthramycin, sibiromycin and tomaymycin with DNA using specifically radiolabelled molecules. *Biochim Biophys Acta.* **475**, 521-35.

Hurley, L. H. & Petrusek, R. (1979) Proposed structure of the anthramycin-DNA adduct. *Nature.* **282**, 529-31.

Hurley, L. H., Reck, T., Thurston, D. E., Langley, D. R., Holden, K. G., Hertzberg, R. P., Hoover, J. R., Gallagher, G., Jr., Faucette, L. F., Mong, S. M. & et al. (1988) Pyrrolo[1,4]benzodiazepine antitumor antibiotics: relationship of DNA alkylation and sequence specificity to the biological activity of natural and synthetic compounds. *Chem Res Toxicol.* **1**, 258-68.

Hurley, L. H., Reynolds, V. L., Swenson, D. H., Petzold, G. L. & Scahill, T. A. (1984) Reaction of the antitumor antibiotic CC-1065 with DNA: structure of a DNA adduct with DNA sequence specificity. *Science.* **226**, 843-4.

Itoh, J., Watabe, H., Ishii, S., Gomi, S., Nagasawa, M., Yamamoto, H., Shomura, T., Sezaki, M. & Kondo, S. (1988) Sibanomicin, a new pyrrolo[1,4]benzodiazepine antitumor antibiotic produced by a Micromonospora sp. *J Antibiot (Tokyo).* **41**, 1281-4.

Jamieson, E. R. & Lippard, S. J. (1999) Structure, Recognition, and Processing of Cisplatin-DNA Adducts. *Chem Rev.* **99**, 2467-98.

Japanese Patent, JP 58,180,487 (1983). Antibiotic DC-81. [83,180,487] (CI.CO7D487/04) Kyowa Hakko Kogyo Co. Ltd, Jpn Kokai Tokkyo Koho, Appl. 21 Oct 1983, 82/63, 16 Apr 1982. *Chem. Abstr.* (1984), **100**, 173150k

Jenkins, T. C., Hurley, L. H., Neidle, S. & Thurston, D. E. (1994) Structure of a covalent DNA minor groove adduct with a pyrrolobenzodiazepine dimer: evidence for sequence-specific interstrand cross-linking. *J Med Chem.* **37**, 4529-37.

Jones, G. B., Davey, C. L., Jenkins, T. C., Kamal, A., Kneale, G. G., Neidle, S., Webster, G. D. & Thurston, D. E. (1990) The non-covalent interaction of pyrrolo[2,1-c][1, 4] benzodiazepine-5, 11-diones with DNA. *Anticancer Drug Des.* **5**, 249-64.

Judson, I. & Kelland, L. R. (2001). Cisplatin and analogues. In *Oxford Textbook of Oncology*. Souhami, R. L., Tannock, I. F., Hohenberger, P. & Horiot, J. C. (Eds), New York, Oxford University Press, 655-662.

Juliano, R. L. & Ling, V. (1976) A surface glycoprotein modulating drug permeability in Chinese hamster ovary cell mutants. *Biochim Biophys Acta.* **455**, 152-62.

Kamal, A., Devaiah, V., Reddy, K. L. & Kumar, M. S. (2005) Synthesis and biological activity of fluoroquinolone-pyrrolo[2,1-c][1,4]benzodiazepine conjugates. *Bioorg Med Chem.* **13**, 2021-9.

Kamal, A., Laxman, N., Ramesh, G., Srinivas, O. & Ramulu, P. (2002a) Synthesis of C-8 alkylamino substituted pyrrolo[2,1-c][1,4]benzodiazepines as potential anti-cancer agents. *Bioorg Med Chem Lett.* **12**, 1917-9.

Kamal, A., Ramesh, G., Ramulu, P., Srinivas, O., Rehana, T. & Sheelu, G. (2003) Design and synthesis of novel chrysene-linked pyrrolo[2,1-c][1,4]-benzodiazepine hybrids as potential DNA-binding agents. *Bioorg Med Chem Lett.* **13**, 3451-4.

Kamal, A., Ramesh, G., Srinivas, O., Ramulu, P., Laxman, N., Rehana, T., Deepak, M., Achary, M. S. & Nagarajaram, H. A. (2004a) Design, synthesis, and evaluation of mixed imine-amine pyrrolobenzodiazepine dimers with efficient DNA binding affinity and potent cytotoxicity. *Bioorg Med Chem.* **12**, 5427-36.

Kamal, A., Ramu, R., Khanna, G. B., Saxena, A. K., Shanmugavel, M. & Pandita, R. M. (2004b) Pyrrolo[2,1-c][1,4]benzodiazepine-anthraquinone conjugates. Synthesis, DNA binding and cytotoxicity. *Bioorg Med Chem Lett.* **14**, 4907-9.

Kamal, A., Ramulu, P., Srinivas, O., Ramesh, G. & Kumar, P. P. (2004c) Synthesis of C8-linked pyrrolo[2,1-c][1,4]benzodiazepine-benzimidazole conjugates with remarkable DNA-binding affinity. *Bioorg Med Chem Lett.* **14**, 4791-4.

Kamal, A., Reddy, B. S., Reddy, G. S. & Ramesh, G. (2002b) Design and synthesis of C-8 linked pyrrolobenzodiazepine-naphthalimide hybrids as anti-tumour agents. *Bioorg Med Chem Lett.* **12**, 1933-5.

Kamal, A., Reddy, P. S., Reddy, D. R. & Laxman, E. (2006) DNA binding potential and cytotoxicity of newly designed pyrrolobenzodiazepine dimers linked through a piperazine side-armed-alkane spacer. *Bioorg Med Chem.* **14**, 385-94.

Kamal, A., Reddy, P. S., Reddy, D. R., Laxman, E. & Murthy, Y. L. (2004d) Synthesis of fluorinated analogues of SJG-136 and their DNA-binding potential. *Bioorg Med Chem Lett.* **14**, 5699-702.

Kamal, A., Srinivas, O., Ramulu, P., Ramesh, G. & Kumar, P. P. (2004e) Synthesis of C8-linked pyrrolo[2,1-c][1,4]benzodiazepine-acridone/acridine hybrids as potential DNA-binding agents. *Bioorg Med Chem Lett.* **14**, 4107-11.

Kamal, A., Srinivas, O., Ramulu, P., Ramesh, G., Kumar, P. P. & Kumar, M. S. (2004f) Synthesis and DNA binding affinity of novel A-C8/C-C2-exo unsaturated alkoxyamido-linked pyrrolo[2,1-c][1,4]benzodiazepine dimers. *Bioorg Med Chem.* **12**, 4337-50.

Kanaar, R., Hoeijmakers, J. H. & van Gent, D. C. (1998) Molecular mechanisms of DNA double strand break repair. *Trends Cell Biol.* **8**, 483-9.

Kartner, N., Riordan, J. R. & Ling, V. (1983) Cell surface P-glycoprotein associated with multidrug resistance in mammalian cell lines. *Science.* **221**, 1285-8.

Kelly, J. J., Baird, E. E. & Dervan, P. B. (1996) Binding site size limit of the 2:1 pyrrole-imidazole polyamide-DNA motif. *Proc Natl Acad Sci U S A.* **93**, 6981-5.

Kers, I. & Dervan, P. B. (2002) Search for the optimal linker in tandem hairpin polyamides. *Bioorg Med Chem.* **10**, 3339-49.

Khanna, K. K. & Jackson, S. P. (2001) DNA double-strand breaks: signaling, repair and the cancer connection. *Nat Genet.* **27**, 247-54.

Kielkopf, C. L., Baird, E. E., Dervan, P. B. & Rees, D. C. (1998a) Structural basis for G.C recognition in the DNA minor groove. *Nat Struct Biol.* **5**, 104-9.

Kielkopf, C. L., Bremer, R. E., White, S., Szewczyk, J. W., Turner, J. M., Baird, E. E., Dervan, P. B. & Rees, D. C. (2000) Structural effects of DNA sequence on T.A recognition by hydroxypyrrole/pyrrole pairs in the minor groove. *J Mol Biol.* **295**, 557-67.

Kielkopf, C. L., White, S., Szewczyk, J. W., Turner, J. M., Baird, E. E., Dervan, P. B. & Rees, D. C. (1998b) A structural basis for recognition of A.T and T.A base pairs in the minor groove of B-DNA. *Science.* **282**, 111-5.

Kobayashi, E., Okamoto, A., Asada, M., Okabe, M., Nagamura, S., Asai, A., Saito, H., Gomi, K. & Hirata, T. (1994) Characteristics of antitumor activity of KW-2189, a novel water-soluble derivative of duocarmycin, against murine and human tumors. *Cancer Res.* **54**, 2404-10.

Kohn, K. W., Ewig, R. A. G., Erickson, L. C. & Zwelling, L. A. (1981). Measurement of strand breaks and crosslinks in DNA by alkaline elution. In *DNA Repair: A Laboratory Manual of Research Techniques.* Friedberg, E. C. & Hanawalt, P. C. (Eds), New York, Marcel Dekker, 379-404.

Kohn, K. W., Glaubiger, D. & Spears, C. L. (1974) The reaction of anthramycin with DNA. II. Studies of kinetics and mechanism. *Biochim Biophys Acta.* **361**, 288-302.

Kohn, K. W. & Spears, C. L. (1970) Reaction of anthramycin with deoxyribonucleic acid. *J Mol Biol.* **51**, 551-72.

Konishi, M., Ohkuma, H., Naruse, N. & Kawaguchi, H. (1984) Chicamycin, a new antitumor antibiotic. II. Structure determination of chicamycins A and B. *J Antibiot (Tokyo).* **37**, 200-6.

Kopka, M. L., Yoon, C., Goodsell, D., Pjura, P. & Dickerson, R. E. (1985a) Binding of an antitumor drug to DNA, Netropsin and C-G-C-G-A-A-T-T-BrC-G-C-G. *J Mol Biol.* **183**, 553-63.

Kopka, M. L., Yoon, C., Goodsell, D., Pjura, P. & Dickerson, R. E. (1985b) The molecular origin of DNA-drug specificity in netropsin and distamycin. *Proc Natl Acad Sci U S A.* **82**, 1376-80.

Kreidberg, J. A. & Natoli, T. A. (2001). Animal models for tumour suppressor genes. In *Tumour Suppressor Genes in Human Cancer.* Fisher, D. E. (Ed). New Jersey, Humana Press Inc., 3-28.

Krowicki, K. & Lown, J. W. (1987) Synthesis of novel imidazole-containing DNA minor groove binding oligopeptides related to the antiviral antibiotic netropsin. *J. Org. Chem.* **52**, 3493 - 3501.

Krugh, T. R., Graves, D. E. & Stone, M. P. (1989) Two-dimensional NMR studies on the anthramycin-d(ATGCAT)2 adduct. *Biochemistry.* **28**, 9988-94.

Kumar, R. & Lown, J. W. (2003a) Recent developments in novel pyrrolo[2,1-c][1,4]benzodiazepine conjugates: synthesis and biological evaluation. *Mini Rev Med Chem.* **3**, 323-39.

Kumar, R. & Lown, J. W. (2003b) Synthesis and antitumor cytotoxicity evaluation of novel pyrrolo[2,1-c][1,4]benzodiazepine imidazole containing polyamide conjugates. *Oncol Res.* **13**, 221-33.

Kumar, R. & Lown, J. W. (2005) Design, synthesis and in vitro cytotoxic studies of novel bis-pyrrolo[2,1][1,4] benzodiazepine-pyrrole and imidazole polyamide conjugates. *Eur J Med Chem.* **40**, 641-54.

Kumar, S., Lipman, R. & Tomasz, M. (1992) Recognition of specific DNA sequences by mitomycin C for alkylation. *Biochemistry.* **31**, 1399-407.

Kunimoto, S., Masuda, T., Kanbayashi, N., Hamada, M., Naganawa, H., Miyamoto, M., Takeuchi, T. & Umezawa, H. (1980) Mazethramycin, a new member of anthramycin group antibiotics. *J Antibiot (Tokyo).* **33**, 665-7.

Kurreck, J. (2003) Antisense technologies. Improvement through novel chemical modifications. *Eur J Biochem.* **270**, 1628-44.

Kutyavin, I. V., Gamper, H. B., Gall, A. A. & Meyer, R. B. (1993) Efficient, specific interstrand cross-linking of double-stranded DNA by a chlorambucil-modified, triplex-forming oligonucleotide. *J. Am. Chem. Soc.* **115**, 9303-9304.

Lam, K. S. (1997) Application of combinatorial library methods in cancer research and drug discovery. *Anticancer Drug Des.* **12**, 145-67.

Lam, K. S., Lebl, M. & Krchnak, V. (1997) The "One-Bead-One-Compound" Combinatorial Library Method. *Chem Rev.* **97**, 411-448.

Lazo, J. S. & Chabner, B. A. (1996). Bleomycin. In *Cancer chemotherapy and biotherapy. Principles and practice.* Chabner, B. A. & Longo, D. L. (Eds), Philadelphia, Lippincott-Raven, 379-394.

Leber, J. D., Hoover, J. R., Holden, K. G., Johnson, R. K. & Hecht, S. M. (1988) A revised structure of sibiromycin. *J. Am. Chem. Soc.* **110**, 2992 - 2993.

Lee, M., Krowicki, K., Shea, R. G., Lown, J. W. & Pon, R. T. (1989) Molecular recognition between oligopeptides and nucleic acids. Specificity of binding of a monocationic bis-furan lexitropsin to DNA deduced from footprinting and 1H NMR studies. *J Mol Recognit.* **2**, 84-93.

Leimgruber, W., Batcho, A. D. & Schenker, F. (1965a) The structure of anthramycin. *J Am Chem Soc.* **87**, 5793-5.

Leimgruber, W., Stefanovic, V., Schenker, F., Karr, A. & Berger, J. (1965b) Isolation and characterization of anthramycin, a new antitumor antibiotic. *J Am Chem Soc.* **87**, 5791-3.

LePla, R. C., Landreau, C. A., Shipman, M., Hartley, J. A. & Jones, G. D. (2005) Azinomycin inspired bisepoxides: influence of linker structure on in vitro cytotoxicity and DNA interstrand cross-linking. *Bioorg Med Chem Lett.* **15**, 2861-4.

Letai, A. G., Palladino, M. A., Fromm, E., Rizzo, V. & Fresco, J. R. (1988) Specificity in formation of triple-stranded nucleic acid helical complexes: studies with agarose-linked polyribonucleotide affinity columns. *Biochemistry.* **27**, 9108-12.

Li, L. H., DeKoning, T. F., Kelly, R. C., Krueger, W. C., McGovren, J. P., Padbury, G. E., Petzold, G. L., Wallace, T. L., Ouding, R. J., Prairie, M. D. & et al. (1992) Cytotoxicity and antitumor activity of carzelesin, a prodrug cyclopropylpyrroloindole analogue. *Cancer Res.* **52**, 4904-13.

Li, L. H., Kelly, R. C., Warpehoski, M. A., McGovren, J. P., Gebhard, I. & DeKoning, T. F. (1991) Adozelesin, a selected lead among cyclopropylpyrroloindole analogs of the DNA-binding antibiotic, CC-1065. *Invest New Drugs.* **9**, 137-48.

Liu, Y. Y., Han, T. Y., Giuliano, A. E. & Cabot, M. C. (2001) Ceramide glycosylation potentiates cellular multidrug resistance. *Faseb J.* **15**, 719-30.

Lodish, H., Berk, A., Zipursky, S. L., Matsudaira, P., Baltimore, D. & Darnell, J. (2000) *Molecular Cell Bioloby.* New York, W. H. Freeman & Co.

Longley, D. B., Harkin, D. P. & Johnston, P. G. (2003) 5-fluorouracil: mechanisms of action and clinical strategies. *Nat Rev Cancer.* **3**, 330-8.

Loontiens, F. G., Regenfuss, P., Zechel, A., Dumortier, L. & Clegg, R. M. (1990) Binding characteristics of Hoechst 33258 with calf thymus DNA, poly[d(A-T)], and d(CCGGAATTCCGG): multiple stoichiometries and determination of tight binding with a wide spectrum of site affinities. *Biochemistry.* **29**, 9029-39.

Loudon, G. M. (1995) *Organic Chemistry.* CA, The Benjamin/Cummings Company, Inc.

Lowe, S. W., Ruley, H. E., Jacks, T. & Housman, D. E. (1993) p53-dependent apoptosis modulates the cytotoxicity of anticancer agents. *Cell.* **74**, 957-67.

Lown, J. W. & Joshua, A. V. (1979) Molecular mechanism of binding of pyrrolo(1,4)benzodiazepine antitumour agents to deoxyribonucleic acid--anthramycin and tomaymycin. *Biochem Pharmacol.* **28**, 2017-26.

Lown, J. W., Krowicki, K., Bhat, U. G., Skorobogaty, A., Ward, B. & Dabrowiak, J. C. (1986) Molecular recognition between oligopeptides and nucleic acids: novel imidazole-containing oligopeptides related to netropsin that exhibit altered DNA sequence specificity. *Biochemistry.* **25**, 7408-16.

Markovic, S. N., Suman, V. J., Vukov, A. M., Fitch, T. R., Hillman, D. W., Adjei, A. A., Alberts, S. R., Kaur, J. S., Braich, T. A., Leitch, J. M. & Creagan, E. T. (2002) Phase II trial of KW2189 in patients with advanced malignant melanoma. *Am J Clin Oncol.* **25**, 308-12.

Marky, L. A. & Breslauer, K. J. (1987) Origins of netropsin binding affinity and specificity: correlations of thermodynamic and structural data. *Proc Natl Acad Sci U S A.* **84**, 4359-63.

Martin, C., Ellis, T., McGurk, C. J., Jenkins, T. C., Hartley, J. A., Waring, M. J. & Thurston, D. E. (2005) Sequence-selective interaction of the minor-groove interstrand cross-linking agent SJG-136 with naked and cellular DNA: footprinting and enzyme inhibition studies. *Biochemistry.* **44**, 4135-47.

Maruyama, I. N., Tanaka, N., Kondo, S. & Umezawa, H. (1981) Fluorospectrometric studies on neothramycin and its reaction with DNA. *J Antibiot (Tokyo).* **34**, 427-35.

Masterson, L. A., Croker, S. J., Jenkins, T. C., Howard, P. W. & Thurston, D. E. (2004) Synthesis and biological evaluation of pyrrolo[2,1-c][1,4]benzodiazepine (PBD) C8 cyclic amine conjugates. *Bioorg Med Chem Lett.* **14**, 901-4.

Mattes, W. B., Hartley, J. A., Kohn, K. W. & Matheson, D. W. (1988) GC-rich regions in genomes as targets for DNA alkylation. *Carcinogenesis.* **9**, 2065-72.

McGovren, J. P., Clarke, G. L., Pratt, E. A. & DeKoning, T. F. (1984) Preliminary toxicity studies with the DNA-binding antibiotic, CC-1065. *J Antibiot (Tokyo).* **37**, 63-70.

McHugh, M. M., Kuo, S. R., Walsh-O'Beirne, M. H., Liu, J. S., Melendy, T. & Beerman, T. A. (1999) Bizelesin, a bifunctional cyclopropylpyrroloindole alkylating agent, inhibits simian virus 40 replication in trans by induction of an inhibitor. *Biochemistry.* **38**, 11508-15.

McHugh, P. J., Spanswick, V. J. & Hartley, J. A. (2001) Repair of DNA interstrand crosslinks: molecular mechanisms and clinical relevance. *Lancet Oncol.* **2**, 483-90.

Meister, G. & Tuschl, T. (2004) Mechanisms of gene silencing by double-stranded RNA. *Nature.* **431**, 343-9.

Middleton, M. R. & Margison, G. P. (2003) Improvement of chemotherapy efficacy by inactivation of a DNA-repair pathway. *Lancet Oncol.* **4**, 37-44.

Miyamoto, M., Kondo, S., Naganawa, H., Maeda, K. & Ohno, M. (1977) Structure and synthesis of neothramycin. *J Antibiot (Tokyo).* **30**, 340-3.

Mohamed, H. E., Asker, M. E., Ali, S. I. & el-Fattah, T. M. (2004) Protection against doxorubicin cardiomyopathy in rats: role of phosphodiesterase inhibitors type 4. *J Pharm Pharmacol.* **56**, 757-68.

Moore, M. J. & Erlichman, C. (1998). Pharmacology of anticancer drugs. In *The Basic Science of Oncology.* Tannock, I. F. & Hill, R. P. (Eds), New York, McGraw-Hill Health Professions Division, 370-391.

Morris, S. J., Thurston, D. E. & Nevell, T. G. (1990) Evaluation of the electrophilicity of DNA-binding pyrrolo[2,1-c][1,4]benzodiazepines by HPLC. *J Antibiot (Tokyo).* **43**, 1286-92.

Moscow, J. A., Swanson, C. A. & Cowan, K. H. (1993) Decreased melphalan accumulation in a human breast cancer cell line selected for resistance to melphalan. *Br J Cancer.* **68**, 732-7.

Mrksich, M. & Dervan, P. B. (1994) Design of a Covalent Peptide Heterodimer for Sequence-Specific Recognition in the Minor Groove of Double-Helical DNA. *J. Am. Chem. Soc.* **116**, 3663-3664.

Mrksich, M., Parks, M. E. & Dervan, P. B. (1994) Hairpin Peptide Motif. A New Class of Oligopeptides for Sequence-Specific Recognition in the Minor Groove of Double-Helical DNA. *J. Am. Chem. Soc.* **116**, 7983-7988.

Mrksich, M., Wade, W. S., Dwyer, T. J., Geierstanger, B. H., Wemmer, D. E. & Dervan, P. B. (1992) Antiparallel side-by-side dimeric motif for sequence-specific recognition in the minor groove of DNA by the designed peptide 1-methylimidazole-2-carboxamide netropsin. *Proc Natl Acad Sci U S A.* **89**, 7586-90.

Nagatsugi, F. & Sasaki, S. (2004) Chemical tools for targeted mutagenesis of DNA based on triple helix formation. *Biol Pharm Bull.* **27**, 463-7.

Needham-VanDevanter, D. R., Hurley, L. H., Reynolds, V. L., Theriault, N. Y., Krueger, W. C. & Wierenga, W. (1984) Characterization of an adduct between CC-1065 and a defined oligodeoxynucleotide duplex. *Nucleic Acids Res.* **12**, 6159-68.

Neidle, S. (2001) DNA minor-groove recognition by small molecules. *Nat Prod Rep.* **18**, 291-309.

Neidle, S., Puvvada, M. S. & Thurston, D. E. (1994) The relevance of drug DNA sequence specificity to anti-tumour activity. *Eur J Cancer.* **30A**, 567-8.

Nelson, H. C., Finch, J. T., Luisi, B. F. & Klug, A. (1987) The structure of an oligo(dA).oligo(dT) tract and its biological implications. *Nature.* **330**, 221-6.

Newlands, E. S., Stevens, M. F., Wedge, S. R., Wheelhouse, R. T. & Brock, C. (1997) Temozolomide: a review of its discovery, chemical properties, pre-clinical development and clinical trials. *Cancer Treat Rev.* **23**, 35-61.

Nishioka, Y., Beppu, T., Kosaka, M. & Arima, K. (1972) Mode of action of tomaymycin. *J Antibiot (Tokyo).* **25**, 660-7.

O'Connor, P. M. & Kohn, K. W. (1990) Comparative pharmacokinetics of DNA lesion formation and removal following treatment of L1210 cells with nitrogen mustards. *Cancer Commun.* **2**, 387-94.

Oehlke, J., Birth, P., Klauschenz, E., Wiesner, B., Beyermann, M., Oksche, A. & Bienert, M. (2002) Cellular uptake of antisense oligonucleotides after complexing or conjugation with cell-penetrating model peptides. *Eur J Biochem.* **269**, 4025-32.

Pardridge, W. M. & Boado, R. J. (1991) Enhanced cellular uptake of biotinylated antisense oligonucleotide or peptide mediated by avidin, a cationic protein. *FEBS Lett.* **288**, 30-2.

Pelton, J. G. & Wemmer, D. E. (1989) Structural characterization of a 2:1 distamycin A.d(CGCAAATTGGC) complex by two-dimensional NMR. *Proc Natl Acad Sci U S A.* **86**, 5723-7.

Pepper, C. J., Hambly, R. M., Fegan, C. D., Delavault, P. & Thurston, D. E. (2004) The novel sequence-specific DNA cross-linking agent SJG-136 (NSC 694501) has potent and selective in vitro cytotoxicity in human B-cell chronic lymphocytic leukemia cells with evidence of a p53-independent mechanism of cell kill. *Cancer Res.* **64**, 6750-5.

Peters, G. I. & Jansen, G. (2001). Antimetabolites. In *Oxford Textbook of Oncology.* Souhami, R. L., Tannock, I. F., Hohenberger, P. & Horiot, J. C. (Eds), New York, Oxford University Press, 663-714.

Petrusek, R. L., Anderson, G. L., Garner, T. F., Fannin, Q. L., Kaplan, D. J., Zimmer, S. G. & Hurley, L. H. (1981) Pyrrol[1,4]benzodiazepine antibiotics. Proposed structures and characteristics of the in vitro deoxyribonucleic acid adducts of anthramycin, tomaymycin, sibiromycin, and neothramycins A and B. *Biochemistry.* **20**, 1111-9.

Ponti, M., Forrow, S. M., Souhami, R. L., D'Incalci, M. & Hartley, J. A. (1991) Measurement of the sequence specificity of covalent DNA modification by antineoplastic agents using Taq DNA polymerase. *Nucleic Acids Res.* **19**, 2929-33.

Portugal, J. & Waring, M. J. (1987) Comparison of binding sites in DNA for berenil, netropsin and distamycin. A footprinting study. *Eur J Biochem.* **167**, 281-9.

Pullman, A. & Pullman, B. (1981) Molecular electrostatic potential of the nucleic acids. *Q Rev Biophys.* **14**, 289-380.

Puvvada, M. S., Forrow, S. A., Hartley, J. A., Stephenson, P., Gibson, I., Jenkins, T. C. & Thurston, D. E. (1997) Inhibition of bacteriophage T7 RNA polymerase in vitro transcription by DNA-binding pyrrolo[2,1-c][1,4]benzodiazepines. *Biochemistry.* **36**, 2478-84.

Puvvada, M. S., Hartley, J. A., Jenkins, T. C. & Thurston, D. E. (1993) A quantitative assay to measure the relative DNA-binding affinity of pyrrolo[2,1-c] [1,4]benzodiazepine (PBD) antitumour antibiotics based on the inhibition of restriction endonuclease BamHI. *Nucleic Acids Res.* **21**, 3671-5.

Quintana, J. R., Lipanov, A. A. & Dickerson, R. E. (1991) Low-temperature crystallographic analyses of the binding of Hoechst 33258 to the double-helical DNA dodecamer C-G-C-G-A-A-T-T-C-G-C-G. *Biochemistry.* **30**, 10294-306.

Radhakrishnan, I. & Patel, D. J. (1994) DNA triplexes: solution structures, hydration sites, energetics, interactions, and function. *Biochemistry.* **33**, 11405-16.

Rao, K. E., Krowicki, K., Burckhardt, G., Zimmer, C. & Lown, J. W. (1991) Molecular recognition between oligopeptides and nucleic acids: DNA binding selectivity of a series of 1,2,4-triazole-containing lexitropsins. *Chem Res Toxicol.* **4**, 241-52.

Rao, K. E., Shea, R. G., Yadagiri, B. & Lown, J. W. (1990) Molecular recognition between oligopeptides and nucleic acids: DNA sequence specificity and binding properties of thiazole-lexitropsins incorporating the concepts of base site acceptance and avoidance. *Anticancer Drug Des.* **5**, 3-20.

Rao, S. N. & Remers, W. A. (1990) All atom molecular mechanics simulations on covalent complexes of anthramycin and neothramycin with deoxydecanucleotides. *J Med Chem.* **33**, 1701-7.

Rao, S. N., Singh, U. C. & Kollman, P. A. (1986) Molecular mechanics simulations on covalent complexes between anthramycin and B DNA. *J Med Chem.* **29**, 2484-92.

Reddy, B. S., Sondhi, S. M. & Lown, J. W. (1999) Synthetic DNA minor groove-binding drugs. *Pharmacol Ther.* **84**, 1-111.

Reed, J. C. (1994) Bcl-2 and the regulation of programmed cell death. *J Cell Biol.* **124**, 1-6.

Remers, W. A., Mabilia, M. & Hopfinger, A. J. (1986) Conformations of complexes between pyrrolo[1,4]benzodiazepines and DNA segments. *J Med Chem.* **29**, 2492-503.

Reynisson, J., Schuster, G. B., Howerton, S. B., Williams, L. D., Barnett, R. N., Cleveland, C. L., Landman, U., Harrit, N. & Chaires, J. B. (2003) Intercalation of trioxatriangulenium ion in DNA: binding, electron transfer, x-ray crystallography, and electronic structure. *J Am Chem Soc.* **125**, 2072-83.

Reynolds, V. L., Molineux, I. J., Kaplan, D. J., Swenson, D. H. & Hurley, L. H. (1985) Reaction of the antitumor antibiotic CC-1065 with DNA. Location of the site of thermally induced strand breakage and analysis of DNA sequence specificity. *Biochemistry.* **24**, 6228-37.

Rosenberg, B., Vancamp, L. & Krigas, T. (1965) Inhibition Of Cell Division In Escherichia Coli By Electrolysis Products From A Platinum Electrode. *Nature.* **205**, 698-9.

Rothenberg, M. L. (1997) Topoisomerase I inhibitors: review and update. *Ann Oncol.* **8**, 837-55.

Rowinsky, E. & Donehower, R. (1996). Antimicrotubule agents. In *Cancer chemotherapy and biotherapy: principles and practice.* Chabner, B. A. & Longo, D. L. (Eds), Philadelphia, Lippincott-Raven, 263-296.

Sagnou, M. J., Howard, P. W., Gregson, S. J., Eno-Amooquaye, E., Burke, P. J. & Thurston, D. E. (2000) Design and synthesis of novel pyrrolobenzodiazepine (PBD) prodrugs for ADEPT and GDEPT. *Bioorg Med Chem Lett.* **10**, 2083-6.

Schabel, F. M., Jr., Johnston, T. P., Mc, C. G., Montgomery, J. A., Laster, W. R. & Skipper, H. E. (1963) Experimental evaluation of potential anticancer agents VIII. Effects of certain nitrosoureas on intracerebral L1210 leukemia. *Cancer Res.* **23**, 725-33.

Sehouli, J., D. Stengel, et al. (2003) A new therapeutical approach: topotecan plus gemcitabine in the treatment of patients with relapsed ovarian cancer after failure of first-line chemotherapy with paclitaxel and platinum. *J Obstet Gynaecol Res.* **29**, 123-31.

Seidman, M. M. & Glazer, P. M. (2003) The potential for gene repair via triple helix formation. *J Clin Invest.* **112**, 487-94.

Shimizu, K., Kawamoto, I., Tomita, F., Morimoto, M. & Fujimoto, K. (1982) Prothracarcin, a novel antitumor antibiotic. *J Antibiot (Tokyo).* **35**, 972-8.

Shoemaker, R. H. & Sausville, E. A. (2001). New drug development. In *Oxford Textbook of Oncology*. Souhami, R. L., Tannock, I. F., Hohenberger, P. & Horiot, J. C. (Eds), New York, Oxford University Press, 781-788.

Smellie, M., Bose, D. S., Thompson, A. S., Jenkins, T. C., Hartley, J. A. & Thurston, D. E. (2003) Sequence-selective recognition of duplex DNA through covalent interstrand cross-linking: kinetic and molecular modeling studies with pyrrolobenzodiazepine dimers. *Biochemistry.* **42**, 8232-9.

Smellie, M., Kelland, L. R., Thurston, D. E., Souhami, R. L. & Hartley, J. A. (1994) Cellular pharmacology of novel C8-linked anthramycin-based sequence-selective DNA minor groove cross-linking agents. *Br J Cancer.* **70**, 48-53.

Soderlind, K. J., Gorodetsky, B., Singh, A. K., Bachur, N. R., Miller, G. G. & Lown, J. W. (1999) Bis-benzimidazole anticancer agents: targeting human tumour helicases. *Anticancer Drug Des.* **14**, 19-36.

Song, A., Zhang, J., Lebrilla, C. B. & Lam, K. S. (2003) A novel and rapid encoding method based on mass spectrometry for "one-bead-one-compound" small molecule combinatorial libraries. *J Am Chem Soc.* **125**, 6180-8.

Souhami, R. L. (2002). Oxford textbook of oncology.In Book Oxford textbook of oncology Editor, (Ed.^Eds),Oxford, Oxford University Press, Pages.

Spanswick, V. J., Craddock, C., Sekhar, M., Mahendra, P., Shankaranarayana, P., Hughes, R. G., Hochhauser, D. & Hartley, J. A. (2002) Repair of DNA interstrand crosslinks as a mechanism of clinical resistance to melphalan in multiple myeloma. *Blood.* **100**, 224-9.

Spanswick, V. J., Hartley, J. M., Ward, T. H. & Hartley, J. A. (1999). Measurement of drug-induced DNA interstrand crosslinking using the single-cell gel electrophoresis (Comet) assay. In *Methods in Molecular Medicine: Cytotoxic Drug Resistance Mechanisms.* Vol 28. Brown, R. & Boger-Brown, U. (Eds), Totowa, NJ, Humana Press Inc, 143-145.

Stacey, D. W., Hitomi, M. & Chen, G. (2000) Influence of cell cycle and oncogene activity upon topoisomerase IIalpha expression and drug toxicity. *Mol Cell Biol.* **20**, 9127-37.

Staker, B. L., Hjerrild, K., Feese, M. D., Behnke, C. A., Burgin, A. B., Jr. & Stewart, L. (2002) The mechanism of topoisomerase I poisoning by a camptothecin analog. *Proc Natl Acad Sci U S A.* **99**, 15387-92.

Sumner, W., 2nd & Bennett, G. N. (1981) Anthramycin inhibition of restriction endonuclease cleavage and its use as a reversible blocking agent in DNA constructions. *Nucleic Acids Res.* **9**, 2105-19.

Sun, D. & Hurley, L. H. (1993) Analysis of the monoalkylation and cross-linking sequence specificity of bizelesin, a bifunctional alkylation agent related to CC-1065. *J. Am. Chem. Soc.* **115**, 5925-5933.

Sunters, A., Springer, C. J., Bagshawe, K. D., Souhami, R. L. & Hartley, J. A. (1992) The cytotoxicity, DNA crosslinking ability and DNA sequence selectivity of the aniline mustards melphalan, chlorambucil and 4-[bis(2-chloroethyl)amino] benzoic acid. *Biochem Pharmacol.* **44**, 59-64.

Sweeney, M. C., Wavreille, A. S., Park, J., Butchar, J. P., Tridandapani, S. & Pei, D. (2005) Decoding protein-protein interactions through combinatorial chemistry: sequence specificity of SHP-1, SHP-2, and SHIP SH2 domains. *Biochemistry.* **44**, 14932-47.

Synold, T. W., Dussault, I. & Forman, B. M. (2001) The orphan nuclear receptor SXR coordinately regulates drug metabolism and efflux. *Nat Med.* **7**, 584-90.

Takeuchi, T., Miyamoto, T., Ishizuka, M., Naganawa, H. & Kondo, S. (1976) Neothramycins A and B, new antitumor antibiotics. *J Antibiot (Tokyo).* **29**, 93-6.

Tannock, I. F. & Goldenberg, G. G. (1998). Drug resistance and experimental chemotherapy. In *The Basic Science of Oncology*. Tannock, I. F. & Hill, R. P. (Eds), New York, McGraw-Hill Health Professions Division, 392-419.

Thurston, D. E. (1993). Advances in the Study of Pyrrolo(2,1-c)(1,4)Benzodiazepine (PBD) Antitumour Antibiotics. In *Molecular Aspects of Anticancer Drug - DNA Interactions. Volume 1.* Neidle, S. & Waring, M. J. (Eds), London, Macmillan Press, 54-88.

Thurston, D. E. (1999) Nucleic acid targeting: therapeutic strategies for the 21st century. *Br J Cancer.* **80** Suppl 1, 65-85.

Thurston, D. E. & Bose, D. S. (1994) Synthesis of DNA-interactive pyrrolo[2.1-c][1,4]benzodiazepines. *Chem Rev.* **94**, 433-465.

Thurston, D. E., Bose, D. S., Howard, P. W., Jenkins, T. C., Leoni, A., Baraldi, P. G., Guiotto, A., Cacciari, B., Kelland, L. R., Foloppe, M. P. & Rault, S. (1999) Effect of A-ring modifications on the DNA-binding behavior and cytotoxicity of pyrrolo[2,1-c][1,4]benzodiazepines. *J Med Chem.* **42**, 1951-64.

Thurston, D. E., Bose, D. S., Thompson, A. S., Howard, P. W., Leoni, A., Croker, S. J., Jenkins, T. C., Neidle, S., Hartley, J. A. & Hurley, L. H. (1996) Synthesis of Sequence-Selective C8-Linked Pyrrolo[2,1-c][1,4]benzodiazepine DNA Interstrand Cross-Linking Agents. *J Org Chem.* **61**, 8141-8147.

Thurston, D. E. & Hurley, L. H. (1983) A rational basis for development of antitumour agents in the pyrrolo[1,4]benzodiazepine group. *Drugs of the future.* **8**, 957-971.

Timur, M., Akbas, S. H. & Ozben, T. (2005) The effect of Topotecan on oxidative stress in MCF-7 human breast cancer cell line. *Acta Biochim Pol.* **52**, 897-902.

Tomasz, M. (1993). The Mitomycins: Natural Cross-Linkers of DNA. In *Molecular Aspects of Anticancer Drug-DNA Interactions.* Waring, M. J. & Neidle, S. (Eds), London, Macmillan Press, 312-349.

Tomasz, M. (1995) Mitomycin C: small, fast and deadly (but very selective). *Chem Biol.* **2**, 575-9.

Tomasz, M., Lipman, R., Chowdary, D., Pawlak, J., Verdine, G. L. & Nakanishi, K. (1987) Isolation and structure of a covalent cross-link adduct between mitomycin C and DNA. *Science.* **235**, 1204-8.

Tong, W. P., Kirk, M. C. & Ludlum, D. B. (1982) Formation of the cross-link 1-[N3-deoxycytidyl),2-[N1-deoxyguanosinyl]ethane in DNA treated with N,N'-bis(2-chloroethyl)-N-nitrosourea. *Cancer Res.* **42**, 3102-5.

Trauger, J. W., Baird, E. E. & Dervan, P. B. (1996) Recognition of DNA by designed ligands at subnanomolar concentrations. *Nature.* **382**, 559-61.

Tsunakawa, M., Kamei, H., Konishi, M., Miyaki, T., Oki, T. & Kawaguchi, H. (1988) Porothramycin, a new antibiotic of the anthramycin group: production, isolation, structure and biological activity. *J Antibiot (Tokyo).* **41**, 1366-73.

Turner, P. R. & Denny, W. A. (2000) The genome as a drug target: sequence specific minor groove binding ligands. *Curr Drug Targets.* **1**, 1-14.

Twentyman, P. R. & Luscombe, M. (1987) A study of some variables in a tetrazolium dye (MTT) based assay for cell growth and chemosensitivity. *Br J Cancer.* **56**, 279-85.

Ueda, K., Pastan, I. & Gottesman, M. M. (1987) Isolation and sequence of the promoter region of the human multidrug-resistance (P-glycoprotein) gene. *J Biol Chem.* **262**, 17432-6.

Valkov, N. I. & Sullivan, D. M. (2003) Tumor p53 status and response to topoisomerase II inhibitors. *Drug Resist Updat.* **6**, 27-39.

van Maanen, J. M., Retel, J., de Vries, J. & Pinedo, H. M. (1988) Mechanism of action of antitumor drug etoposide: a review. *J Natl Cancer Inst.* **80**, 1526-33.

Vidal, L., Blagden, S., Attard, G. & de Bono, J. (2005) Making sense of antisense. *Eur J Cancer.* **41**, 2812-8.

Wade, W. S., Mrksich, M. & Dervan, P. B. (1992) Design of peptides that bind in the minor groove of DNA at 5'-(A,T)G(A,T)C(A,T)-3' sequences by a dimeric side-by-side motif. *J. Am. Chem. Soc.* **114**, 8783-8794.

Walton, M. I., Goddard, P., Kelland, L. R., Thurston, D. E. & Harrap, K. R. (1996) Preclinical pharmacology and antitumour activity of the novel sequence-selective DNA minor-groove cross-linking agent DSB-120. *Cancer Chemother Pharmacol.* **38**, 431-8.

Wang, J. C. (1991) DNA topoisomerases: why so many? *J Biol Chem.* **266**, 6659-62.

Wang, Y., Li, L., Ye, W., Tian, Z., Jiang, W., Wang, H., Wright, S. C. & Larrick, J. W. (2003a) CC-1065 analogues bearing different DNA-binding subunits: synthesis, antitumor activity, and preliminary toxicity study. *J Med Chem.* **46**, 634-7.

Wang, Y. D., Dziegielewski, J., Chang, A. Y., Dervan, P. B. & Beerman, T. A. (2002) Cell-free and cellular activities of a DNA sequence selective hairpin polyamide-CBI conjugate. *J Biol Chem.* **277**, 42431-7.

Wang, Y. D., Dziegielewski, J., Wurtz, N. R., Dziegielewska, B., Dervan, P. B. & Beerman, T. A. (2003b) DNA crosslinking and biological activity of a hairpin polyamide-chlorambucil conjugate. *Nucleic Acids Res.* **31**, 1208-15.

Warren, A. J., Maccubbin, A. E. & Hamilton, J. W. (1998) Detection of mitomycin C-DNA adducts in vivo by 32P-postlabeling: time course for formation and removal of adducts and biochemical modulation. *Cancer Res.* **58**, 453-61.

Warren, A. J., Mustra, D. J. & Hamilton, J. W. (2001) Detection of mitomycin C-DNA adducts in human breast cancer cells grown in culture, as xenografted tumors in nude mice, and in biopsies of human breast cancer patient tumors as determined by (32)P-postlabeling. *Clin Cancer Res.* **7**, 1033-42.

Wellenzohn, B., Loferer, M. J., Trieb, M., Rauch, C., Winger, R. H., Mayer, E. & Liedl, K. R. (2003) Hydration of hydroxypyrrole influences binding of ImHpPyPy-beta-Dp polyamide to DNA. *J Am Chem Soc.* **125**, 1088-95.

Weyermann, P. & Dervan, P. B. (2002) Recognition of ten base pairs of DNA by head-to-head hairpin dimers. *J Am Chem Soc.* **124**, 6872-8.

White, S., Szewczyk, J. W., Turner, J. M., Baird, E. E. & Dervan, P. B. (1998) Recognition of the four Watson-Crick base pairs in the DNA minor groove by synthetic ligands. *Nature.* **391**, 468-71.

Wilson, S. C., Howard, P. W., Forrow, S. M., Hartley, J. A., Adams, L. J., Jenkins, T. C., Kelland, L. R. & Thurston, D. E. (1999) Design, synthesis, and evaluation of a novel sequence-selective epoxide-containing DNA cross-linking agent based on the pyrrolo[2, 1-c][1,4]benzodiazepine system. *J Med Chem.* **42**, 4028-41.

Wong, E. T. & Berkenblit, A. (2004) The role of topotecan in the treatment of brain metastases. *Oncologist.* **9**, 68-79.

Workman, P. (2001) Paul Workman--at the cutting edge of drug discovery (interview by Dorothy Bonn). *Lancet Oncol.* **2**, 113-8.

Woynarowski, J. M. (2002) Targeting critical regions in genomic DNA with AT-specific anticancer drugs. *Biochim Biophys Acta.* **1587**, 300-8.

Wurtz, N. R. & Dervan, P. B. (2000) Sequence specific alkylation of DNA by hairpin pyrrole-imidazole polyamide conjugates. *Chem Biol.* **7**, 153-61.

Wyatt, M. D., Garbiras, B. J., Haskell, M. K., Lee, M., Souhami, R. L. & Hartley, J. A. (1994) Structure-activity relationship of a series of nitrogen mustard- and pyrrole-containing minor groove-binding agents related to distamycin. *Anticancer Drug Des.* **9**, 511-25.

Wyatt, M. D., Lee, M., Garbiras, B. J., Souhami, R. L. & Hartley, J. A. (1995) Sequence specificity of alkylation for a series of nitrogen mustard-containing analogues of distamycin of increasing binding site size: evidence for increased cytotoxicity with enhanced sequence specificity. *Biochemistry.* **34**, 13034-41.

Wyatt, M. D., Lee, M. & Hartley, J. A. (1997a) Alkylation specificity for a series of distamycin analogues that tether chlorambucil. *Anticancer Drug Des.* **12**, 49-60.

Wyatt, M. D., Lee, M. & Hartley, J. A. (1997b) The sequence specificity of alkylation for a series of benzoic acid mustard and imidazole-containing distamycin analogues: the importance of local sequence conformation. *Nucleic Acids Res.* **25**, 2359-64.

Xue, F. & Seto, C. T. (2005) Selective inhibitors of the serine protease plasmin: probing the S3 and S3' subsites using a combinatorial library. *J Med Chem.* **48**, 6908-17.

Yoshida, M., Banville, D. L. & Shafer, R. H. (1990) Structural analysis of d(GCAATTGC)2 and its complex with berenil by nuclear magnetic resonance spectroscopy. *Biochemistry.* **29**, 6585-92.

Zakrzewska, K. & Pullman, B. (1986) A theoretical investigation of the sequence specificity in the binding of the antitumor drug anthramycin to DNA. *J Biomol Struct Dyn.* **4**, 127-36.

Zhilina, Z. V., Ziemba, A. J., Trent, J. O., Reed, M. W., Gorn, V., Zhou, Q., Duan, W., Hurley, L. & Ebbinghaus, S. W. (2004) Synthesis and evaluation of a triplex-forming oligonucleotide-pyrrolobenzodiazepine conjugate. *Bioconjug Chem.* **15**, 1182-92.

Zhou, B. B. & Elledge, S. J. (2000) The DNA damage response: putting checkpoints in perspective. *Nature.* **408**, 433-9.

Ziemba, A. J., Reed, M. W., Raney, K. D., Byrd, A. B. & Ebbinghaus, S. W. (2003) A bis-alkylating triplex forming oligonucleotide inhibits intracellular reporter gene expression and prevents triplex unwinding due to helicase activity. *Biochemistry.* **42**, 5013-24.

PUBLICATION ASSOCIATED WITH THIS THESIS

Gregson, S. J., Howard, P. W., Gullick, D. R., Hamaguchi, A., Corcoran, K. E., Brooks, N. A., Hartley, J. A., Jenkins, T. C., Patel, S., Guille, M. J. & Thurston, D. E. (2004) Linker length modulates DNA cross-linking reactivity and cytotoxic potency of C8/C8' ether-linked C2-exo-unsaturated pyrrolo[2,1-c][1,4]benzodiazepine (PBD) dimers. *J Med Chem.* **47**, 1161-74.

Linker Length Modulates DNA Cross-Linking Reactivity and Cytotoxic Potency of C8/C8′ Ether-Linked C2-*exo*-Unsaturated Pyrrolo[2,1-*c*][1,4]benzodiazepine (PBD) Dimers

Stephen J. Gregson,[†] Philip W. Howard,[†] Darren R. Gullick,[†] Anzu Hamaguchi,[‡] Kathryn E. Corcoran,[†] Natalie A. Brooks,[‡] John A. Hartley,[‡] Terence C. Jenkins,[§] Sejal Patel,[∥] Matthew J. Guille,[∥] and David E. Thurston*,[†]

10.1021/jm0308971 CCC: $27.50
Published on Web 01/30/2004